Design and Syntheses of Potential Drugs Based on $GABA_A$ Receptor Pharmacophores

Ella Chow Clement

Dissertation submitted to the Faculty of the Virginia Polytechnic Institute
and State University in partial fulfillment of the requirements
for the Degree of

Doctor of Philosopy
in
Chemistry

Dr. Paul R. Carlier, Chairman
Dr. Jeffrey R. Bloomquist
Dr. Richard D. Gandour
Dr. David G. I. Kingston
Dr. James M. Tanko

June 28, 2005
Blacksburg, Virginia

Keywords: $GABA_A$ receptor, Partial/full agonists, Superagonist, Antagonists, Non-zwitterionic GABA amide homodimers and heterodimers, $^{36}Cl^-$ Flux assay, [^{3}H]Muscimol binding, ZAPA, PEG, Memory of Chirality

Design and Syntheses of Potential Drugs Based on $GABA_A$ Receptor Pharmocophores

Ella Chow Clement

ABSTRACT

Numerous previous studies of $GABA_AR$ ligands have suggested that $GABA_AR$ agonists must be zwitterionic and feature an intercharge separation similar to that of GABA (approx. 4.7-6.0 Å). We have demonstrated that monomeric, homodimeric and heterodimeric non-zwitterionic GABA amides are partial, full, or superagonists at the murine $GABA_A$ receptor ($GABA_AR$). The agonism of these GABA amides is comparable to that of THIP, as shown by *in vitro* assay results. The assay data indicate that the agonism of GABA amides is tether length-dependent. Optimum agonism is achieved with a tether length of four methylenes in GABA amide dimers and in GABA amides bearing pendant amide or amino groups. We have further investigated the structure-activity relationship for GABA amides on the $GABA_AR$ by performing structural modifications to both the superagonist **2c** and the agonist **6c**. Synergism and [^{3}H]muscimol binding experiments show that **2c** binds to the same sites as GABA. Structural modification of **2c** demonstrated that partial rigidification of the tether eliminated agonism and caused ligands to behave as weak competitive antagonists. We have also investigated the agonism of four ZAPA derivatives in $^{36}Cl^-$ uptake functional assay. Two of them are found to be as potent as GABA.

In our studies of 1,4-benzodiazepines, our goal was to synthesize three different subtypes of quaternary 1,4-benzodiazepines by use of the memory of chirality (MOC)

strategy. Disappointingly, most of the deprotonation/alkylations failed, due to various reasons. The failure of the reactions of (*S*)-alanine-derived tetrahydro-1,4-benzodiazepin-3-ones was probably due to either the unexpected side reactions or the steric hindrance of enolate alkylation. In the case of tetrahydro-1,4-benzodiazepin-2-ones, computational studies suggested that steric hindrance by both the benzo ring and N4-allyl group might retard deprotonation at C3 by bulky bases like KHMDS or LDA. Finally, (*S*)-serine-derived 1,4-benzodiazepin-2-ones and their elimination products (α-methylene benzodiazepines) were prepared. These proved unreactive towards deprotonation/alkylations and conjugate additions, respectively. The low reactivity of the α-methylene benzodiazepines towards nucleophiles was attributed to highly delocalized LUMOs that failed to direct nucleophiles to the β-carbons.

Acknowledgements

First of all, I would like to thank my advisor, Dr. Paul Carlier, for giving me the opportunity to come with him and study at Virginia Tech. I would also like to thank Dr. Carlier for his guidance and financial support during my Ph.D. study. Secondly, I would like to thank Dr. Jeffrey Bloomquist for his help and support in doing bioassay experiments. Thirdly, I would like to thank my committee members for their assistance in fulfilling departmental requirements. I would also like to thank Mr. Tom Glass and Mr. Bill Bebout for their analytical services, and my group members for sharing lab responsibility.

I would like to thank Mrs. Kay Castagnoli and Dr. Emre Isin for their friendship and support. I also like to thank friends, especially Dr. Mary Dean Coleman, Miss Amy Fletcher, Miss Jennifer Farris, and Ms. Mary Billings from the Graduate Christian Fellowship for their prayers and support.

I would like to thank my family for their love and support during my study. I would like to especially thank my father, who has gone to be with the Lord, for his great influence in my life. Finally, I would like to thank my husband Jason for his love, help, and support in every aspect of my studies and life.

Table of Contents

List of Figures

List of Schemes

List of Tables

Chapter 1 Introduction and Background of $GABA_A$ Receptors

1.1 Background and Significance of the $GABA_A$ Receptor

Gamma-aminobutyric acid (GABA) is the major inhibitory neurotransmitter in the mammalian central nervous system (CNS). It is found mainly in the brain,[1] and is an agonist at three receptor subtypes.[2] Altered GABAergic function (GABA-activated neurotransmission) in the brain is believed to responsible for the development of some neurological and psychiatric disorders in humans such as Huntington's chorea and schizophrenia.[1,3,4]

GABA, which was first discovered in the brain by Roberts and Awapara in 1950, functions as an inhibitory neurotransmitter in the CNS, as suggested by electrophysiological studies between 1950 and 1965.[4] Since then, the complicated mechanisms that contribute to GABA-mediated neurotransmission have been studied extensively using electrophysiological, pharmacological, and molecular biological techniques.[5] Generally, GABA serves as an inhibitory neurotransmitter that decreases neuronal excitability by increasing the conductance of post-synaptic membranes to Cl^- ion.[6-8] Its inhibitory effect plays an important role in all central neurons, and it has been suggested that 30% or more of central neurons may use GABA as a neurotransmitter.[1]

GABA plays a part in the regulation of physiological mechanisms, including the secretion of hormones such as prolactin and growth hormone. GABA is also involved in the control of cardiovascular functions and pain processes. The synaptic mechanisms associated with anxiety, and with feeding and aggressive behavior are also believed to be under control of GABA.[1] In addition, GABA also has physiological functions in the

peripheral nervous system (PNS). GABA receptors have been detected in the endocrine glands, smooth muscles, and the female reproductive system.[7]

1.2 Classification of Three GABA Receptor Subtypes

GABA (**1**) is important for the overall balance between neuronal inhibition and excitation, and is an agonist at three receptor subtypes: $GABA_A$, $GABA_B$, and $GABA_C$ receptors.[2, 9] The notion of $GABA_A$ and $GABA_B$Rs were introduced by Hill and Bowery in 1981, based on the discovery of difference between GABA-mediated activation of bicuculline-sensitive chloride channels and GABA-mediated activation of cation channels. These two receptors are pharmacologically, electrophysiologically and biochemically different.[2,4] The $GABA_A$R is a ligand-gated chloride ion channel (Figure 1.1),[10, 11] and has a number of binding sites for other ligands, including benzodiazepines, barbiturates, convulsants such as picrotoxinin (**2**) (Scheme 1), some general anesthetics, neurosteroids, and perhaps ethanol.[2, 10, 12]

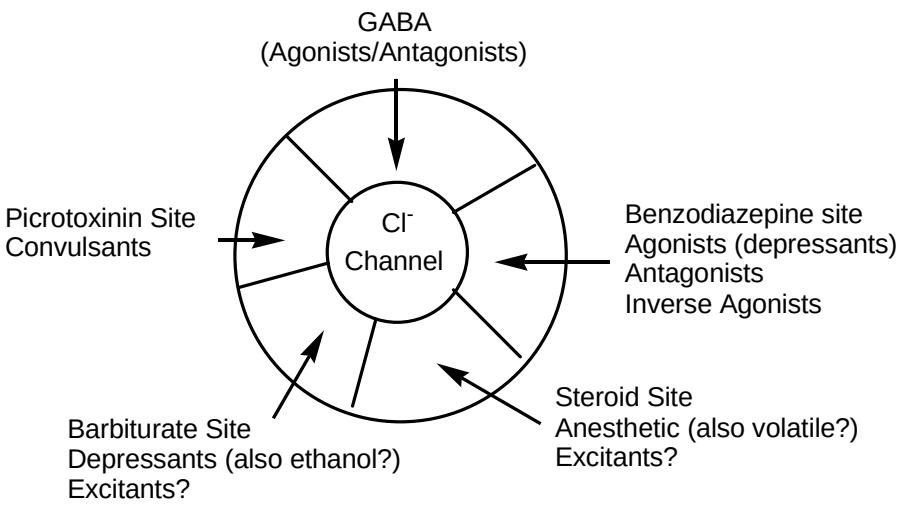

Figure 1.1 A highly simplified illustration of the $GABA_AR$. Picture is adapted from Ref. 10

The $GABA_AR$ is a member of the ligand-gated ion channel (LGIC) superfamily, that consists of the glycine receptor, the nicotinic acetylcholine receptor (nAChR), glutamate receptor, and the serotonin type 3 receptor ($5\text{-}HT_3$).[8, 13] The GABA binding site of the $GABA_AR$ is the site directly responsible for the Cl^- channel opening. $GABA_A$ agonists, including muscimol (**3**), isoguvacine (**4**), 4,5,6,7-tetrahydroisoxazolo [5,4-*c*] pyrindin-3-ol (THIP) (**5**), and 3-aminopropane sulfonic acid (3-APS) (**6**) (Scheme 1) bind to the same site and induce GABA-like responses.[4] The potent and specific $GABA_AR$ agonist muscimol is one of the most useful GABA analogs, and has been used extensively for both pharmacological and radioligand binding studies.[4] The binding of GABA to the $GABA_AR$ is blocked by the competitive antagonist, bicuculline (**7**) (Scheme 1.1). Non-competitive antagonists of the $GABA_AR$ are also known; these compounds (e.g., picrotoxinin)[2] bind to another site but effectively block channel gating.

Scheme 1.1 $GABA_AR$, $GABA_BR$ and $GABA_CR$ Agonists and Antagonists

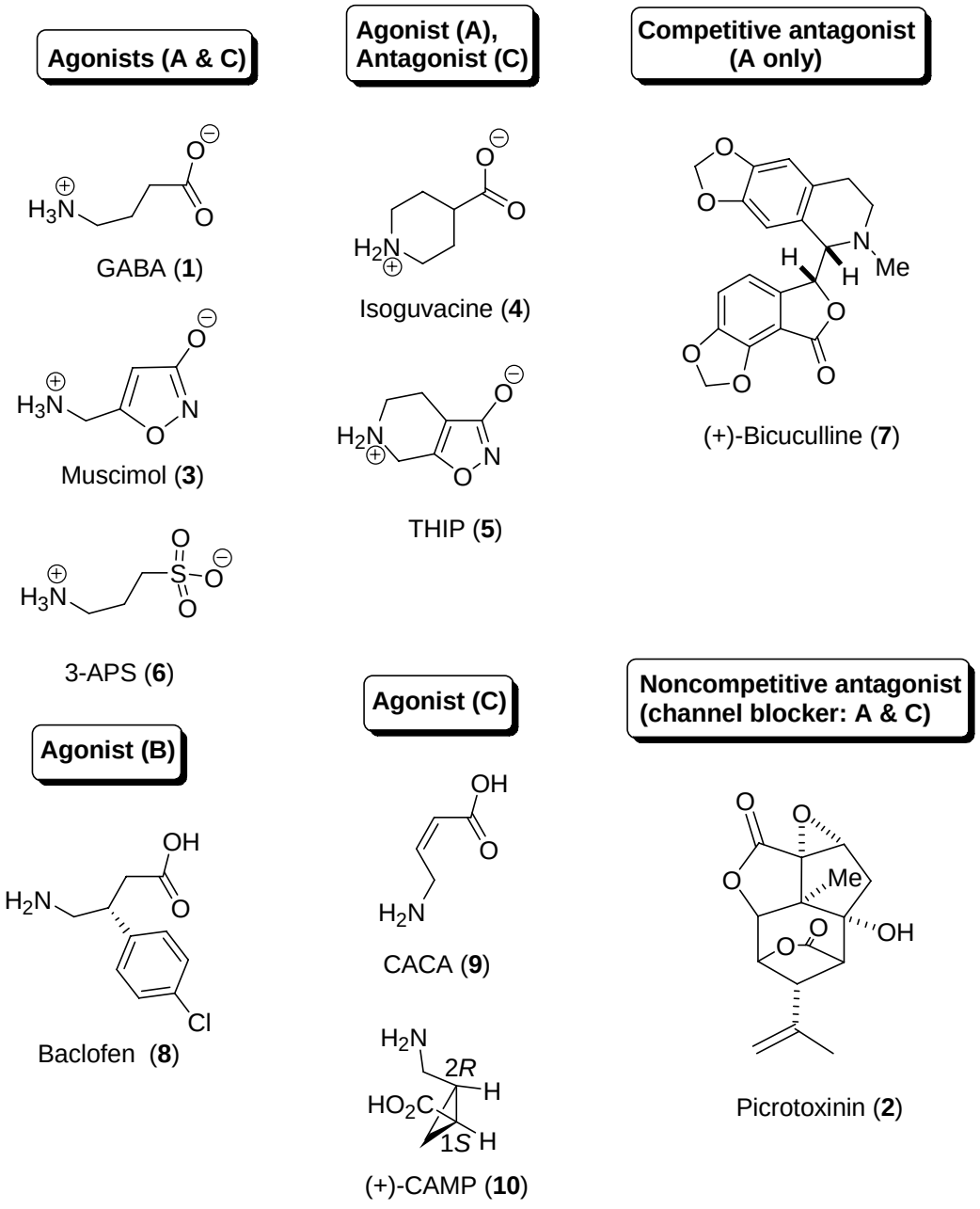

$GABA_B$ receptors, which are 7-transmembrane domain spanning G-protein coupled receptors, are associated with a second messenger system, and coupled to Ca^{2+} and K^+ channels.[2, 4, 9, 14] The $GABA_BR$ is insensitive to the $GABA_A$ antagonist

bicuculline, and to the $GABA_A$ agonists isoguvacine, THIP, and 3-APS.[4] The $GABA_B$Rs are found on dopaminergic and glutamatergic neurons in the ventral tegmental area. The systematic administration of $GABA_B$R agonist baclofen **8** has shown to decrease the firing rate and bursting firing of ventral tegmental dopaminergic neurons as well as reducing extracellular dopamine levels in the nucleus accumbens, suggesting the inhibitory role of the $GABA_B$R in the mesolimbic circuitry.[15] Clinical and preclinical data also suggest the importance of the $GABA_B$R in therapeutic drug action. The $GABA_B$R agonists such as baclofen have shown to demonstrate muscle relexant and analgesic properties, reduce the craving for alcohol and nicotine consumption as well as abuse of drugs such as cocaine, heroin, opiate and methamphetamine.[15,16,17] In addition, the data suggest that these agonists may be useful in treatment of gastrointestinal disorders, asthma and overactive bladder. In the case of $GABA_B$R antagonists, animal studies indicate that these antagonists display antiepileptic, neuroprotectant, cognition enhancement and antidepressant properties.[16,18,19]

The $GABA_C$ receptor also gates a Cl^- ion channel, which led to its initially being classified as a subspecies of the $GABA_A$R.[2] However, unlike the $GABA_A$R, the $GABA_C$R is not widely distributed in the CNS; it appears principally in the vertebrate retina.[5] The $GABA_C$R is insensitive to the $GABA_B$ agonist-baclofen (**8**) (Scheme 1.1), and the $GABA_A$ antagonist-bicuculline, as first identified by Johnston and colleagues in 1984. The $GABA_C$ receptor has been further identified by its response to agonist CACA (*cis*-4-amino-crotonic acid) (**9**) and selective agonist (+)-CAMP (1*S*, 2*R*-2-(aminomethyl)cyclopropanecarboxylic acid (**10**) (Scheme 1), to which the $GABA_A$R is insensitive.[2, 9, 20] $GABA_C$ receptors are either homooligomers of ρ (ρ1-3) subunits or

pseudohomooligomers ($\rho1\rho2$),[2] and cloning studies have shown that $\rho1$ shares some homology with the α and β subunits of $GABA_AR$ (vide infra).[5] The $GABA_AR$ and $GABA_CR$ share structural and functional features with other members of the LGIC superfamily. However, many details of the physiology and pharmacology of $GABA_CR$ remain unknown.[2, 5, 20]

1.3 $GABA_A$ Receptor Physiology and Pharmacology

1.3.1 Current Models for the Structure and Function of the $GABA_A$ Receptors

$GABA_ARs$ are chloride channel proteins, which are opened by the binding of GABA agonists. $GABA_ARs$, like nicotinic acetylchlorine receptors (nAChRs), are 70 Å-wide heteropentameric glycoproteins with a central water-filled pore,[21] as suggested by electron microscopic studies. Many $GABA_AR$ subunits have been identified by cDNA cloning and sequencing (α_{1-6}, β_{1-4}, γ_{1-3}, δ, ε, ρ_{1-2},θ and π).[22, 23] The predominant native isoforms (60%) of $GABA_A$ receptors consist of $2\alpha_1$, $2\beta_2$, and one γ_2 subunit (Figure 1.2),[14, 24, 25] as suggested by protein chemistry, antibody separations and site-directed mutagenesis.[26] The isoforms of each subunit class share 70 percent sequence identity, and the subunits have approximately 20-30 percent sequence identity between classes.[2, 4, 12, 27] Each individual subunit is about 50-60 kDa, which includes a large N-terminal extracellular domain (ECD), a transmembrane domain (TMD) with four α-helical segments (TM1-TM4), and a large intracellular domain.[23, 28] The combination of α, β and γ subunits is necessary to reconstitute the full pharmacological functions of the native receptor, including sigmoidal dose-response to GABA and benzodiazepine

potentiation.[29-31] The importance of the α subunit has been further suggested by Sigel *et al.*,[32] who has studied the point mutation of α1-Phe64 to Leu and found that α1-Phe64 is essential for GABA dependent channel gating. Substitution of Phe64 by Leu dramatically decreases the GABA agonism: the EC_{50} value (concentration of agonists that elicits half-maximal ion flux)[33] increases from 6 μM to 1260 μM.

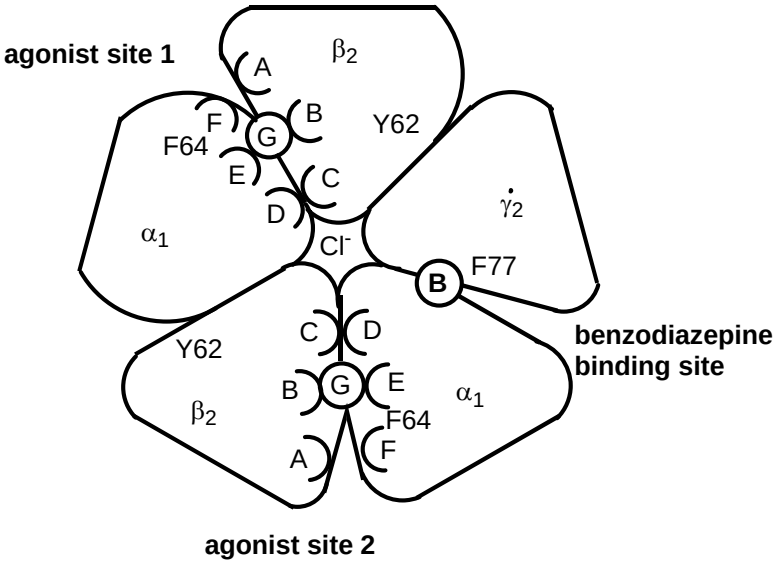

Figure 1.2 Proposed $GABA_AR$ structure showing the two functional agonist sites (G) and the benzodiazepine binding site (B). Letters A-F are designated as six discontinous polypeptide loops that are participated in the formation of agonist binding pocket. Picture is adapted from Ref 23 and 34

In 2000, when we started this project, evidence suggested that there exist two distinct classes of binding sites on the $GABA_AR$: high- and low affinity agonist sites, which differ by up to three orders of magnitude in their affinities for agonists.[35-37] Channel-gating is proposed to be the consequence of agonist binding to the low affinity sites, since micromolar concentrations are required to activate the chloride channel. In contrast, radioligand binding studies have been used to identify the existence of high

affinity sites, since displacement of radiolabeled agonist from the high affinity sites occurs at nanomolar concentrations.[5,35] For instance, [^{3}H]muscimol can be displaced from membranes with nanomolar concentrations of muscimol or GABA. What possible reasons are there for the observation of these two classes of sites? One possibility is that the difference in apparent affinities is due to the fact that functional and binding assays involve quite different measurements. That is, there is in fact only one type of agonist binding site that exhibits high affinity under some conditions, and low affinity under other conditions. The second possibility is that the high- and low- affinity sites are structurally distinct. In 1989, Dunn[36] reported characterization of both nanomolar and micromolar binding of [^{3}H]muscimol in the same membrane preparations. Dunn was the first to use equilibrium binding studies to demonstrate a biphasic binding curve, and concluded that the $GABA_AR$ contains structurally distinct low and high affinity sites.[36] Her conclusions influenced our earlier thinking of the structure of the $GABA_AR$, as will be discussed in chapter 2. In line with this view, based on the photoaffinity [^{3}H]muscimol labeling studies in the bovine $GABA_AR$ α1- subunit, Olsen *et al.*[29] suggest that the high- and low-affinity sites may be differently located, but the data propose a location for low affinity agonist binding that agrees with Sigel mutagenesis studies. The amino acid residue which is labeled with [^{3}H]muscimol was identified Olsen *et al.*[29] as Phe65. However, this Phe65 residue is the bovine homolog to Phe64 in the rat α1-subunit, which was previously identified by the mutageneis studies of Sigel *et al.*[32] as possibly involving the functional GABA binding site.

Dunn's demonstration of two classes of binding sites is an important break-through, but does not take into consideration the fact that a typical binding assay

membrane preparation is very different from a functional assay membrane preparation. Functional assays (e.g., measurement of the uptake of $^{36}Cl^-$ into vesicles) are generally carried out under approximately physiological conditions; typically with synaptoneurosomes (which bear intact membranes) at 30 °C and pH 7.4. However, binding assays (radioligand displacement studies of agonists from the high affinity sites) are carried out under optimal ligand binding conditions.[38] Typical binding assays are done with frozen-thawed, well-washed, lysed membranes.[36] Perhaps the preparation of the membranes for a binding experiment actually creates high affinity sites that were not there to begin with. In support of this idea, both Schwartz *et al.*[38] and Brown *et al.*[39] have done binding studies under conditions that more closely approximate functional assays, and found only micromolar binding of [^{3}H]muscimol. Their perhaps suggest that high affinity sites are an artifact of the binding assay membranes preparation method.

In order to further test the theory of two distinct classes of binding site in the $GABA_AR$. Dunn *et al.*[35] have expressed single receptor isoforms in HEK (human embryonic kidney)-293 cells and characterized both micromolar and nanomolar concentration binding of [^{3}H]muscimol in 2000. Interestingly, Dunn's published study does not address or offer any explanation to Schwartz's results. On the other hand, Dunn[35] has also studied the effect of mutation of tyrosine residues at positions 62 and 74 to phenylalanine or serine on both [^{3}H]muscimol binding in HEK-293 cells, and ion channel activation in *Xenopus* oocytes, and found that Y62S mutation (mutation of tyrosine to serine) completely eliminates high affinity binding in HEK-293 cells without affecting low affinity binding, E_{max}, or benzodiazepine potentiation; however, both mutations (Y62S and Y74F) increase the EC_{50} channel activation, 6- and 2-fold

respectively. Since disruption of the high affinity site does not have a significant effect on receptor function, Dunn and coworkers suggest that the high affinity sites may play a role in receptor desensitization (closed state of the receptor).[35] In line with this idea, Dunn *et al.*[37] later on studied the effect of mutations of both Y62S and Y74F on the desensitization of the $GABA_AR$ in *Xenopus* oocytes, and suggested that high affinity sites stabilize the desensitized state of the receptor, based on the voltage clamp results. At low concentration, the desensitization characteristics measured in Y74F mutant receptor is similar to those of wild-type receptor; but the Y62S mutant receptor recovers from desensitization even in the continued presence of GABA.

Based on Dunn's experiments, it is reasonable to believe that there are distinct high and low affinity agonist sites on intact individual receptors, and that only the low affinity sites are involved in channel gating. However, Sigel *et al.*[40] in 2003 published a study that challenged the idea of independent high- and low-affinity sites on a single receptor. Sigel and co-worker investigated the effect of point mutation of α_1F64L and the similar mutation of β_2Y62L on binding and receptor function. The data show that α_1F64L mutation strongly affects the channel activation (38-fold increase in EC_{50} value) and desensitization by GABA; it also causes the maximum binding of [^{3}H]muscimol to drop dramatically. On the other hand, mutation of β_2Y62L has little effect on binding properties, channel activation (3.4-fold increase in EC_{50} value) and desensitization, as compared with the wild-type receptor. The shift of 3.4-fold in EC_{50} value upon mutation of β_2Y62L is comparable to the shifts of 2- and 6-fold for β_2Y62F and β_2Y62S mutations that are reported by Dunn *et al.*[35] Apparently, mutation of α_1F64L causes complete loss of the high affinity sites and the channel activation to be affected strongly, but the

changes are not significant with the β_2Y62L mutation. Therefore, Siegel *et al.* argue that high- and low-affinity sites are probably structural identical.[40]

α_1F64 has been previously shown to be important in channel activation, and is photoaffinity labeled by [^{3}H]muscimol.[29, 32] This is consistent with Siegel's recent published data.[40] However, the significant discrepancies between Siegel's and Dunn's results require a good explanation. It is believed that the dissociation constant (K_D) of high affinity binding sites for $GABA_AR$ agonists is 10-30 nM, whereas that for low affinity sites is 0.1-1.0 μM. Dunn has shown that β_2Y62S mutation shifts K_D of [^{3}H]muscimol to 300 nM in HEK293 cell, and this result leads Dunn and coworker to believe the importance of β_2Y62 in high affinity site binding.[35] However, Siegel et al. claim that K_D values in the 100 nM range (150-300 nM) are difficult to measure due to two reasons. Firstly, fast dissociation rates of [^{3}H]muscimol lead to a significant loss of observed binding. Secondly, non-specific binding becomes significant as compared with specific binding at higher ligand concentrations. Thus Dunn's data and conclusions are subject to question.[40] Siegel *et al.* also challenge the role of β_2Y62 in the process of desensitization. They believe that the voltage clamp measurements that were performed by Dunn and co-worker[37] have not been done in a classical way, which describes the time-dependent current decay in the presence of the agonist. On the other hand, Siegel and co-worker observe that β_2Y62L mutation does not have significant effect on the time course of desensitization after exposure to 1-10 mM GABA. In contrast, mutation of α_1F64L changes the current decay properties greatly.[40] Based on these results, Siegel *et al.* conclude that high-and low-affinity sites are structurally identical and these are the two classes of site that are in equilibrium conformations during agonist binding. After

reviewing Sigel's works and criticism of Dunn's experiments, we also believe that high- and low-affinity sites are interconvertible sites on the $GABA_AR$. That is, these sites are identically located and exhibit different affinities towards agonist binding.

Figure 1.2 shows a hypothetical model of the $GABA_A$ receptor with the agonist and modulatory site at subunit interface. In the $GABA_AR$, low affinity sites are proposed to be located between α and β subunit interfaces, while both photoaffinity radiolabeling experiments and site-directed mutagenesis studies suggest that the modulatory benzodiazepine binding site is located between the α and γ subunits.[28,35] Based on structural notation of the binding loops of X-ray crystal structure of AChBP and more detailed analyses of the $GABA_AR$ binding sites, six discontinuous polypeptide loops designated A-F at the α and β subunit interfaces are identified to take part in the formation of the agonist binding pocket of the $GABA_AR$ (Figure 1.2).[23] The charged residues in the TM1-TM2 are believed to form the ion channel "gate" in the $GABA_AR$.[28] As we mentioned previously, $GABA_AR$ and nAChR belong to the same super family, and share structural and functional features. AChBP (acetylcholine-binding protein) is a structural and functional homologue of the extracellular portion of the α-subunit of nAChR.[41] Therefore, it is relevant to use structural notation of the binding loops of X-ray crystal structure of AChBP in assigning the binding loops for the $GABA_AR$.

Patch-clamp[8] studies demonstrate that the dose-response curves of GABA typically have a Hill slope of 2, implying that there are two low affinity binding sites (agonist site 1 and 2, Figure 1.2) in the $GABA_AR$ and at least two agonist molecules (one to each low affinity agonist site) are bound to these sites before the Cl^- ion channel opens.[32,42,43] A proposed gating scheme is given in Figure 1.3.[33]

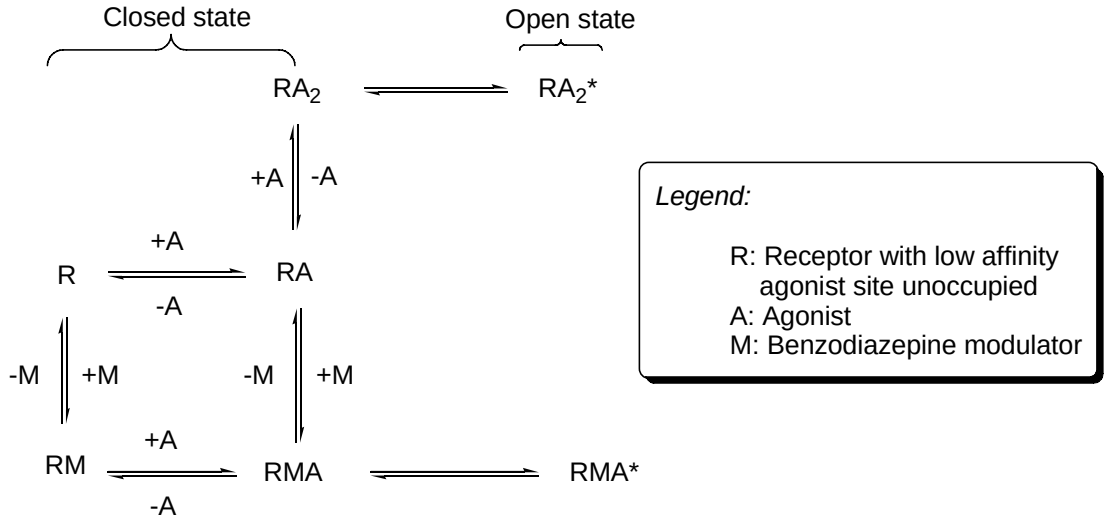

Figure 1.3 A proposed gating scheme for the $GABA_AR$ in the presence of agonist and benzodiazepine modulators; * represents activated receptor.

Within a few seconds of reversible channel gating, the receptor becomes desensitized[8] at this point the channel will remain closed until the agonist concentration is made very low. The rapid desensitization of $GABA_AR$ upon exposure to agonists also indicates that chloride ion is transported into brain membrane vesicles quickly. Although Siegel *et al.*[40] have recently reported that α_1F64 is involved in channel desensitization, the exact mechanism of desensitization still remains unknown.

1.3.2 Benzodiazepine Binding Sites of The $GABA_A$ Receptors

The $GABA_AR$ is the target of a variety of clinically and pharmacologically important drugs such as anxiolytic benzodiazepines (e.g., diazepam (**11**)). The benzodiazepine binding site is believed to be located at the $\alpha_1(+)/\gamma_2$ (-) subunit interface, and the amino acid Phe77 residue has been identified to participate in the formation of the benzodiazedine binding site (Figure 1.2).[40] Benzodiazepines, which were first introduced in the 1960s as sleeping pills, are agonistic modulators of the $GABA_AR$.[44] Agonistic modulators by definition, are ligands that bind to an allosteric site on the $GABA_AR$, and enhance the agonistic effect of GABA. Benzodiazepines such as diazepam and flurazepam (**12**) have a sedative, anxiolytic, muscle relaxant, hypnotic and anticonvulsant action.[45] Therefore, benzodiazepine sites are significant therapeutic targets of the $GABA_AR$ within the brain.[12,46] Benzodiazepines such as chlordiazepoxide and midazolam enhance the $GABA_AR$ function by increasing the apparent potency of GABA.[46,47] However, benzodiazepines cannot open the ion channel in the absence of agonist. How do benzodiazepines exert this action on the $GABA_AR$? Serfozo *et al.* propose that benzodiazepines enhance chloride flux by introducing another gating mechanism: only one agonist molecule is required to open the chloride channel with one benzodiazepine bound.[47] (As shown in Figure 1.3)

Many studies have demonstrated that benzodiazepine agonists such as Ro 11-6896 [$B_{10}(+)$] (**13**) (Scheme 2), diazepam, clonazepam and flurazepam, shift the GABA agonist (GABA, muscimol) concentration-response curves shift to the left, indicating that benzodiazepines potentiate GABAergic function by decreasing the agonist EC_{50} (Figure 1.4) with no effect on the maximal response induced by GABA.[12, 48, 49, 50] Studies of

[^{3}H]muscimol binding to low affinity sites by Schwartz *et al.* also suggest that benzodiazepines do not increase the affinity of the receptor for the agonist.[38] The rank of order of potentiation of these agonists was [B_{10}(+)] > diazepam > clonazepam > flurazepam using 1 μM of each drug. However, these benzodiazepines have no effect on $^{36}Cl^-$ uptake in the absence of GABA agonist.

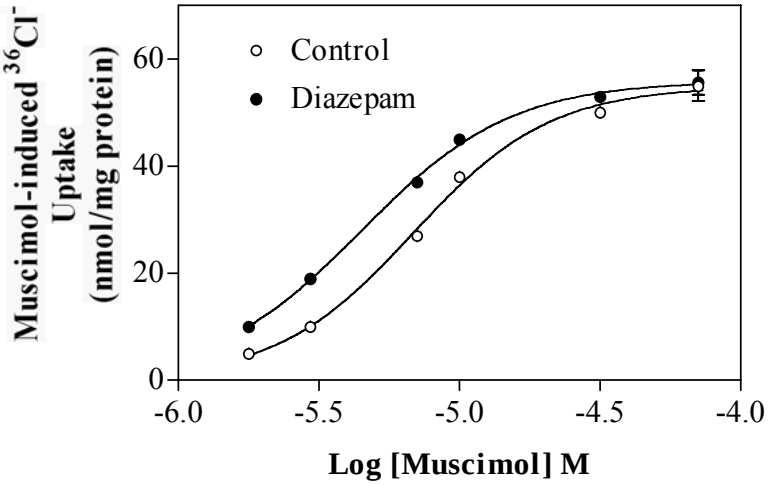

Figure 1.4 Enhancement of muscimol-induced $^{36}Cl^-$ uptake by diazepam. Picture is modified from Ref. 41
(o) Synaptoneurosomes were preincubated with buffer,
(●) Synaptoneurosomes were preincubated with 10 μM diazepam.

Benzodiazepines increase the chloride channel opening frequency, but they do not alter single channel currents or channel opening burst duration of $GABA_AR$[50,51] ("bursts"[51] are defined as an opening or a group of openings separated by a relatively long closed period). The effect of diazepam (20-1000 nM) on $GABA_AR$ single channel currents has been studied by Macdonald *et al.* Their patch-clamp studies show that GABA-mediated channel opening frequencies and bursts are increased with increasing concentrations of diazepam up to 50 nM.[51] However, the magnitudes of the increase in

channel opening and burst frequencies are decreased at higher concentration of diazepam (250 nM). Macdonald *et al*.[51] proposes that perhaps the rate of $GABA_AR$ channel desensitization is increased with higher concentration of diazepam since the frequency of bursts of channel openings is increased. In contrast, the mean $GABA_AR$ single-channel current amplitudes are decreased by inverse agonists (ligands that exert a negative allosteric effect on GABA agonism), such as methyl-6,7-dimethyoxyl-4-ethyl-β-carboline-3-carboxylate (DMCM).[51]

1.3.3 Barbiturates, Picrotoxinin and Steroid Anesthetic Binding Sites in the $GABA_AR$

The $GABA_AR$ is also the target of action of depressant and sedative-hypnotic barbiturates (e.g., pentobarbital, PB, **14**), and anesthetics such as etomidate (**15**), propoflo, and alfaxalone (**16**) (Scheme 1.2).[11] Electrophysiological studies have demonstrated that at a 50-200 μM concentration range, barbituates such as pentobarbital enhance GABAergic neurotransmission by increasing the mean channel open time to chloride ion, but without affecting the channel opening frequency.[52] The single-channel bursting inward currents from spinal cord neurons of mice induced by both GABA (2 μM) and GABA plus PB (50 μM) have been studied by Macdonald *et al.*, and they have found that PB increases the mean open time of $GABA_AR$ from 3.5 ms (with GABA only) to 8.3 ms (GABA plus PB).[52]

Scheme 1.2 Important drugs and modulators for $GABA_AR$

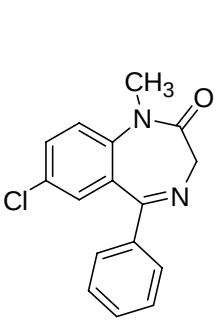

Diazepam (**11**)

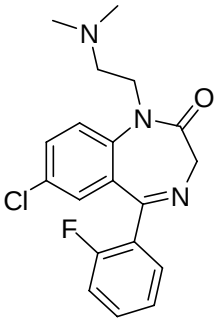

Flurazepam (**12**)

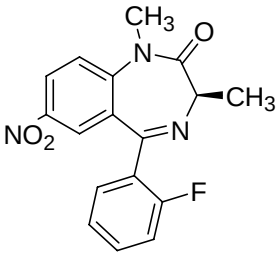

Ro 11-6896 [B_{10}(+)] (**13**)

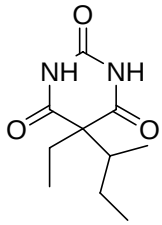

PB (**14**)

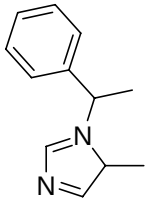

Etomidate (**15**)

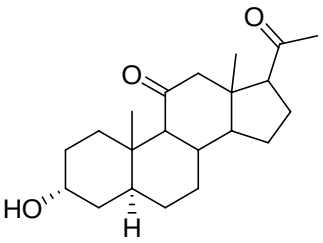

Alphaxolone (**16**)

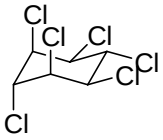

Lindane (**17**)

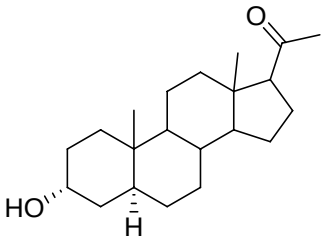

3a-OH-DHP (**18**)

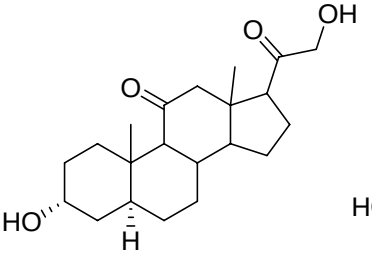

5a-THDOC (**19**)

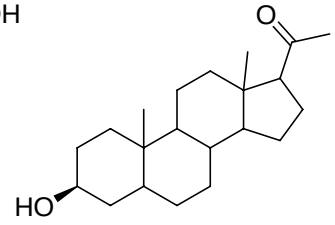

PRE (**20**)

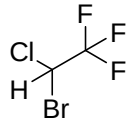

Halothane (**21**)

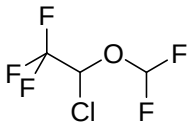

Isoflurane (**22**)

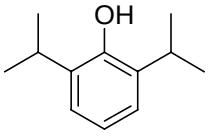

Propofol (**23**)

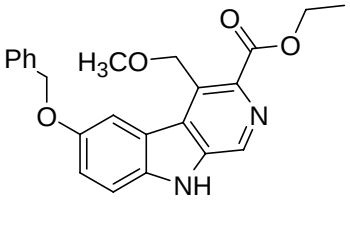

ZK 93423 (**24**)

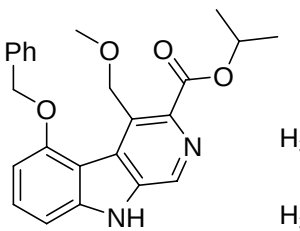

Abecarnil (**25**)

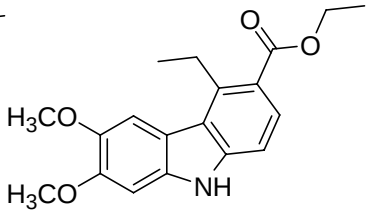

DMCM (**26**)

Pentobarbital (50 μM) enhances the muscimol-mediated $^{36}Cl^-$ uptake by shifting the muscimol concentration response curve to the left, decreasing the EC_{50} value from 7.0 μM to 2.5 μM.[6] At higher concentrations (100-500 μM), barbituates are able to elicit Cl^- conductance in the absence of GABA, with a maximal response at 500 μM.[14, 53] However, at concentrations higher than 500 μM, pentobarbital causes the functional desensitization of the $GABA_AR$. Higashi and Nishi[54] propose that barbiturates at high concentrations may induce a conformational change in the receptor complex, thereby causing blockade of Cl^- channels.[6]

Convulsant neurotoxicants such as picrotoxinin, and insecticides such as lindane, (**17**)[55] are channel blockers. The picrotoxinin site is located on or closely associated with the chloride ion channel,[56] and picrotoxinin inhibits the GABA-activated chloride influx by causing a decrease in mean channel open time and stabilizing closed channel states.[11, 57]

The hypnotic neurosteroids such as 3α-OH-DHP (**18**) and 5α-THDOC (**19**) (Scheme 1.2), are among the most potent known steroid modulators of $GABA_ARs$.[14, 58] The synthetic anesthetic steroids such as pregnanolone (PRE, **20**),[59] ethanol, volatile gas anesthetics halothane[60] (**21**) and isoflurane (**22**),[61] and propofol (**23**), also enhance $GABA_AR$ chloride channel function and modulate binding *in vitro.* PRE is a "barbituate-like modulator" of the $GABA_AR$, which increases the average chloride channel open time at low concentration (100 nM to 1 μM) and decreases the prolongation of the average open duration at higher concentration (10 μM), (as shown in Table 1.1), indicating that GABA-mediated chloride channel is blocked by PRE, the reason is that PRE at high concentrations may also cause conformational change in the receptor complex. The

modulating effects of ethanol on $GABA_AR$ is also concentration-dependent, at relatively low concentration (subanesthetic concentration, 20 mM). Ethanol has sedative and motor-uncoordinating effects, and at high concentration (anesthetic concentrations, 50-400 mM), it has an anesthetic effect, suggesting that the $GABA_AR$ may play important roles in the actions of ethanol and in alcoholism.

Table 1.1 PRE regulation of $GABA_AR$ open properties*

	GABA (2 μM)	+ PRE (100 nM)	+ PRE (1 μM)	+ PRE (10 μM)
Average open duration (ms)	3.92	5.07	5.59	5.33

* GABA and GABA + PRE induced bursting single-channel currents in patch-clamp recordings from spinal cord neurons of mouse held at –75 mV.

The anxiolytic β-carbolines such as 6-benzyloxy-4-methoxymethyl-β-carboline-3-carboxylate ethyl ester (ZK 93423) (**24**), and Abecarhil (**25**), (Scheme 1.2) are a potent positive, and a partial positive allosteric modulator for $GABA_AR$, respectively.[14] The anxiogenic β-carboline, DMCM (**26**) however, is a very potent negative modulator for $GABA_AR$.[14]

With such a therapeutically relevant and rich pharmacology, the $GABA_AR$ has been extensively studied by molecular biologists and medicinal chemists.[5, 14, 44] In particular there is increasing interest in separating the anxiolytic, muscle relaxant, sedative, and antiepileptic properties of benzodiazepines, with respect to both receptor isoform specificity[62] and drug structure.[63] Due to their potential therapeutic use for

treatment of anxiety disorders,[7] epilepsy,[3, 5] pain,[5] and insomnias,[64] design of novel $GABA_AR$ agonists and partial agonists is also of considerable interest.

1.4 $GABA_A$ Receptor-Agonists and Partial Agonists

$GABA_AR$ agonists are compounds that induce GABA-gated chloride channel opening. Channel opening is proposed to result from binding to the low affinity agonist sites of $GABA_AR$. The inhibitory nature of the GABA in the CNS encouraged the design and development of various structural types of GABA agonists.[5] In the past, based on the conformational restriction of different parts of the GABA molecule and bioisosteric replacements of the functional groups of this amino acid, a diverse group of specific $GABA_A$ agonists have been developed. Some of these agonists have played an important role in the development of the $GABA_AR$ pharmacology.[5, 20]

1.4.1 Structure and Conformation of Active GABA Analogs (Exogenous $GABA_A$ agonists)

GABA is a flexible molecule, which can exist in several conformations, ranging from "fully extended, partially folded, to fully folded," as shown in Figure 1.5.[20, 65] There is great interest in determining which comformation GABA adopts when bound to the receptor. If only staggered conformations (i.e. energy minima) are allowed, 9 conformers must be considered. Of course, the receptor bound agonist may exist in other conformations (e.g. eclipsed conformations) not described in Figure 1.5. The different efficacies of enantiomers of (*RS*)-dihydromuscimol (DHM)[66] suggest that GABA may adopt a chiral conformation on binding. (*S*)-DHM (**27**) is the most potent

$GABA_A$ agonist described so far. It is 40 times more potent than GABA, suggesting that (*S*)-DHM may closely mimic the receptor bound conformation of GABA.

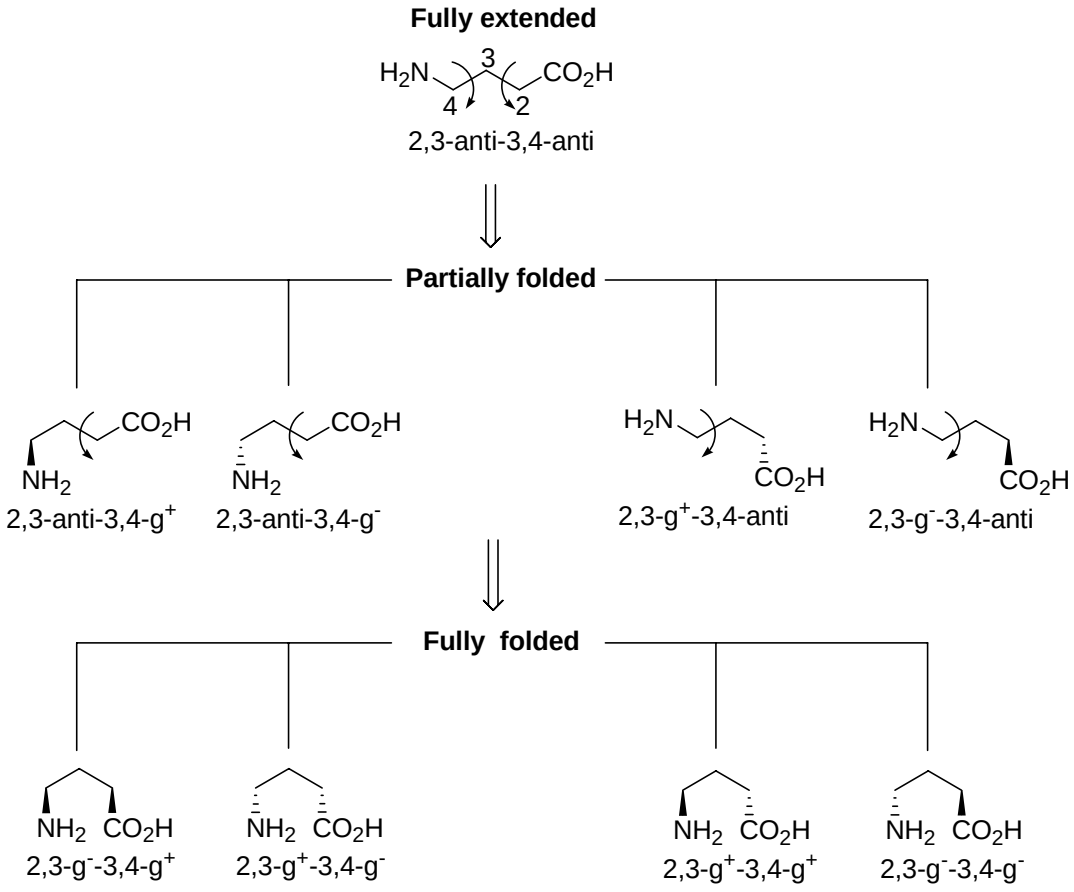

Figure 1.5 Potential conformational energy minima of GABA[17]

On the basis of the possibility of different interactions of these different GABA conformations with various receptors, enzymes, and transporters, medicinal chemists have developed GABA analogs that feature various geometric constraints. The introduction of double bonds into the GABA backbone, incorporation of the backbone atoms into a ring structure, and addition of bulky substituents have all been explored, as illustrated in Scheme 1.3.

Scheme 1.3 Conformationally restricted GABA analogs in their ionized and unionized forms

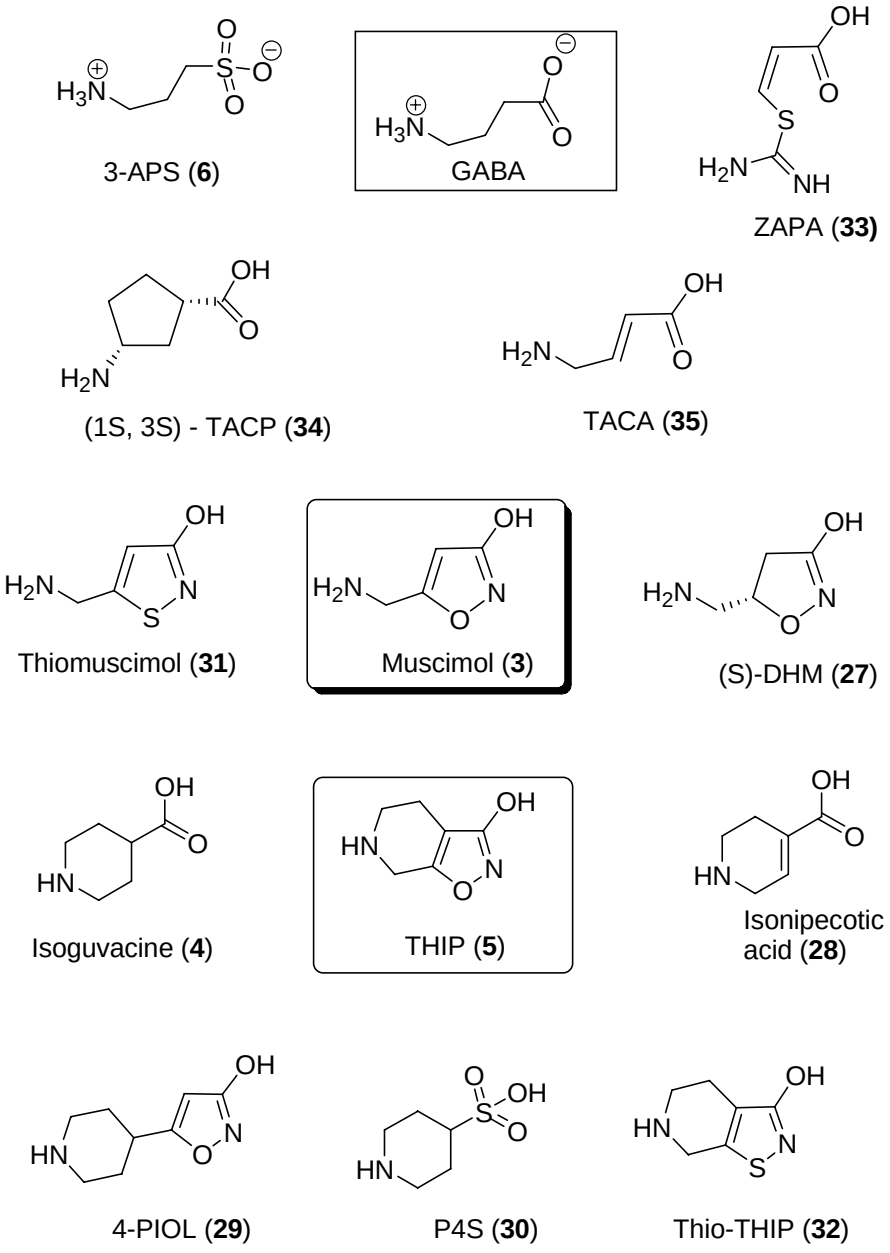

Muscimol (**3**), which was first introduced in 1968 as a conformationally restricted GABA analog, is a psychoactive natural product from *Amanita muscaria* mushrooms.[20, 67] It is a more potent $GABA_AR$ agonist than GABA, with an EC_{50} value of 7.3 ± 0.5 μM,

compared with 10 μM of GABA.[6] However, muscimol is toxic and it will be metabolized after peripheral administration, so it is not clinically useful.[1, 3] The relatively rigid muscimol analog, THIP (**5**), is a partial $GABA_AR$ agonist, and it has some selectivity for particular β-subunits of the $GABA_A$ receptor.[68] THIP is less potent than musicmol, but it is comparatively non-toxic in rats and dogs, and also, it can penetrate the blood brain barrier (BBB) very easily after systematic administration.[3,65] THIP is a proven antinociceptive agent-it can be as effective as morphine. Its analgesic action therefore highlights the possible importance of GABA mechanisms in pain.[65, 69] However its side effects, including sedation, dizziness, and blurred vision, prevent it from being a useful therapeutic agent.[14, 20] Based on the structure of THIP, several specific monoheterocyclic $GABA_A$ agonists have been developed, including isoguvacine (**4**), isonipecotic acid (**28**), 5-(4-piperidyl)isoxazol-3-ol (4-PIOL, **29**) and piperidine-4-sulfonic acid (P4S, **30**). Isoguvacine (**5**) is approximately as potent as GABA in competing for the binding of [^{3}H]GABA, but it is slightly less potent than GABA in mediating chloride flux.[5, 70] 4-PIOL is a partial agonist with an EC_{50} of 91 μM at $GABA_A$ receptor, and it is approximately 200 times less potent than isoguvacine as an agonist.[15, 71]

Both thiomuscimol (**31**) and DHM are derived from muscimol. The $GABA_A$ agonism of muscimol is not lost upon certain minor structural modifications. Thiomuscimol is approximately equipotent with muscimol as a $GABA_A$ agonist, whereas "(*S*)-DHM (**27**) is the most potent $GABA_A$ agonist so far described", as demonstrated in both functional and binding assays. However, replacement of oxygen in the iosoxazole moiety in THIP by sulphur to give thio-THIP (**32**), is less potent than its parent

compound. Likewise, the sulfonic acid analog of GABA, 3-aminopropane sulfonic acid (APS, **6**) is less potent than GABA at inducing $^{36}Cl^-$ influx.[42] However, 3-APS is twice as potent as GABA in competing for the binding of [^{3}H]GABA.[72] This result highlights the fact that agonist potency may not always track well with high-affinity binding.

(*Z*)-3-[(Aminoiminomethyl)thio]prop-2-enoic acid (ZAPA, **33**), an isothiouronium analog of GABA of restricted conformation, is more potent than GABA on low-affinity GABA binding sites, with EC_{50} of 10.3 ± 0.7 μM, while the EC_{50} of GABA is 12.8 ± 0.4 μM.[14, 73] The Hill slopes of the concentration-dependent curve of ZAPA are 2, indicating that 2 ZAPA molecules are needed to activate $GABA_AR$.[74] The cyclopentane analogue of GABA, (1*S*, 3*S*)-(+)-*trans*-3-aminocyclopentane-1-carboxylic acid ((+)-TACP, **34**), is also a potent $GABA_A$ agonist.[5, 14] The conformationally restricted analog of isoguvacine and GABA, *trans*-4-aminocrotonic acid (TACA, **35**), is an agonist at $GABA_AR$.

1.4.2 Endogenous Agonists

GABA itself is the most significant endogenous agonist, the other agonists include imidazole-4-acetic acid (IAA, **36**), taurine (**37**) and β-alanine (**38**).[14] IAA, the histamine metabolite, is present in the mammalian CNS, and is a comparatively potent $GABA_A$ agonist. It has hypnotic and analgesic effects, however, few studies have been done to determine its pharmacological and clinical potential.[1, 5, 14] Taurine, β-amino sulfonic acid, is a weak $GABA_AR$ agonist, being 68-fold less potent than GABA.[75] Taurine is also a partial $GABA_A$ agonist in activating benzodiazepine binding.[14] β-Alanine is a much weaker agonist, being 230 times less potent than GABA in stimulating

$GABA_AR$.[14] Finally, the synthetic dipeptide, GABA-taurine (**39**) has no effect on $GABA_AR$.[76]

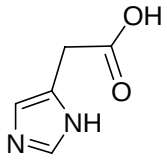

IAA (**36**)

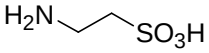

Taurine (**37**)

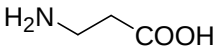

β-Alanine (**38**)

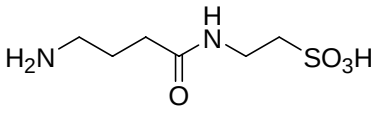

GABA-Taurine (**39**)

1.5 $GABA_A$ Agonist-Receptor Interactions

Based on structure-activity analyses, the $GABA_A$ receptor can tolerate some bioisosteric alteration of the functional groups of GABA. For example, we have already discussed the agonistic potency of muscimol, DHM, TACA and ZAPA. Surprisingly, however minor structural modification of a particular agonist molecule usually results in the loss of $GABA_A$ agonism.[5, 74] Generally, the presence of negatively and positively charged groups (zwitterionic) is essential, but not major for $GABA_A$ agonist activity. The $GABA_AR$ agonism is maintained or enhanced if the GABA analogs resemble one of the possible comformations of GABA. All of the potent $GABA_A$ agonists described so far are structurally related to GABA.

At least three aspects of agonist structure affect $GABA_A$ agonism, including electronic factors, structural and conformational factors, and stereochemical factors.[77] We will also review the work on current agonist binding model of the $GABA_AR$.

1.5.1 Electronic Factors

Prior to our work, it was believed that a zwitterionic structure of GABA analogs is necessary for $GABA_AR$ agonism. In addition, on the basis of structure-activity analysis, a high degree of delocalization of the positive charges reduces both $GABA_A$ agonism and inhibition of $GABA_AR$ binding. IAA (**36**) is a good example. IAA is less potent than GABA in both functional and binding assays. [77] As shown below, IAA features more delocalization of positive charge than GABA. However, ZAPA is an exceptional case, as we mentioned earlier, ZAPA is more potent than GABA as $GABA_AR$ agonist.

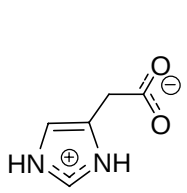

IAA (**36**)

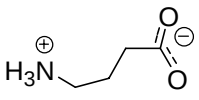

GABA (**1**)

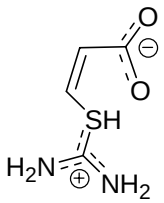

ZAPA (**28**)

On the other hand, Wermuth *et al.*[78] suggested that the delocalization of cationic charge is important for improving $GABA_A$ antagonist activity. *N*-Pyridazinyl derivatives of GABA (e.g. **SR 95531**), muscimol, and thiomuscimol[79] are very potent antagonists.

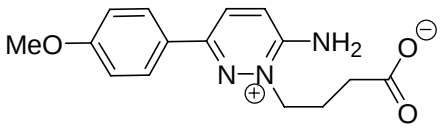

Gabazine (**SR 95531**)

1.5.2 Structural and Conformational Factors.

As we have mentioned before, it is important to have a "GABA structural element" for the interaction of $GABA_A$ agonists with the $GABA_AR$. But within certain

limits, the primary amino group of GABA can be substituted by other functional groups without significant loss of $GABA_A$ agonism. ZAPA is a good example. However, an incorporation of substituents onto the terminal amino groups of $GABA_A$ agonists normally results in a significant or complete loss of $GABA_A$ agonism.[5,77, 80] *N*-Methyl-GABA[81] is almost inactive, *N, N*-dimethyl- and *N, N,N*-trimethyl-GABA are completely inactive. The *N*-methyl derivatives of muscimol[82] and thiomuscimol are only weak $GABA_AR$ agonists.[77, 83]

1.5.3 Stereochemical Factors

Structure-activity analysis studies have demonstrated that $GABA_AR$ is stereoselective. (*S*)-DHM, is 50 times more potent than its (*R*)-isomer for gating the $GABA_AR$.[66] ZAPA (**33**) and TACA (**35**) are both conformationally restricted analogues of GABA. The *trans*-isomer of **33** is inactive at $GABA_AR$, while **33** is more potent at the $GABA_AR$ than GABA and muscimol.[73] Likewise, TACA is a $GABA_AR$ agonist, but its isomer, CACA (**9**) is a $GABA_CR$ agonist.[20] (*S*)-4-Me-TACA is also a $GABA_A$ agonist, but its (*R*)-isomer has no effect on $GABA_AR$.[66] 5'-Me-muscimol has been studied in the binding assay, the *S*-(-)-isomer has found to have a 31-fold higher binding affinity than the *R*-(+)-isomer at binding assays.[78]

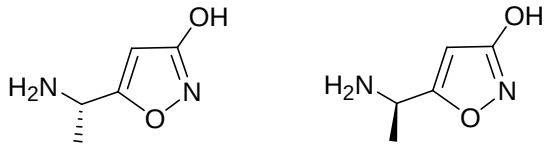

S- (-) - *R*- (+) -

5'-Me-muscimol

1.5.4 Current Agonist Binding model of the $GABA_A$ Receptor

To date, direct structural determination of the $GABA_AR$ has been a challenge due to its low abundance (pmol/mg of protein) and heterogeneous nature, in addition to the difficulties of isolating and purifying whole membrane proteins. Many indirect but useful methods such as site-directed mutagenesis, chemical modification and molecular modeling were therefore used to provide insight into receptor structure and function.[23] Photoaffinity labeling, site-directed mutagenesis and SCAM (substituted cysteine accessibility method) have been used to identify many amino acid residues that participate in agonist binding (Table 1.2).[13, 23, 84-85] Many of these studies assayed in how mutation affects GABA dose-response curves in both agonism and gating.

Table 1.2 Residues lining the $GABA_AR$ agonist binding pocket

Binding loop notation*	**A**	**B**	**C**	**D**	**E**	**F**
Residues of α_1 subunits	-	-	-	Phe64, Phe65, Arg66, Arg67, Ser68, Ser69, Gln67, Trp69	Thr129, Arg131	Arg176, Val178, Val180, Asp183
Residues of β_2 subunits	Tyr97, Leu99	Tyr198, Tyr200, Tyr157	Thr244, Tyr247, Thr202, Tyr205, Ser204, Arg207, Ser209	-	-	-

*Binding loop notations are depicted in Figure 1.2.

SCAM has been used to identify pore-lining residues in the binding pocket of nicotinic and GABA receptors. This method is based on how the modification of the substituted cysteine (selected amino acids were mutated to cysteine) by a reactive water-soluble sulfhydryl compound (MTSEA-biotin: *N*-biotinylaminoethyl methanethiosulfonate) could affect the receptor function. If the modification takes part in a binding domain of the receptor, it is likely to cause a change in the functional properties of the receptor. There are two factors that affect the rate of reaction of MTSEA-biotin with introduced cysteine: ionization of the sulfhydryl side chain and steric hindrance. Ionization of cysteine side chain is more likely to occur in aqueous environment. MTS reacts 10^9-10^{10} times faster with ionized sulfhydryl side than they do with protonated sulfhydryls. Steric hindrance reflects how easy or difficult it is for MTS to physically access and interact with the sulfhydryl group. Therefore, whether the substituted cysteine can be accessed by MTS and how quickly cysteine can react with MTS provide useful information about the structure and the environment of the receptor.[13] Based on the accessibility pattern and the results of MTSEA-biotin reaction rates from G203C-S209C, Czajkowski *et al.*[13] have proposed that β_2 loop C is a coil and the $GABA_AR$ binding pocket is a narrow cleft that is located in both a hydrophobic environment and a sterically hindered region. The results also suggest that the binding site constrict during gating due to the movement of α_1 and β_2 domains of the GABA binding sites toward each other.

A flexible binding-site model has been used by Jones *et al.*[86] to explain the binding behavior of the $GABA_A$ agonists. They propose that the binding site behaves like a pair of movable "arms" attached to rigid "anchor" sites by spring-like tethers, which are separated by a distance. Binding induces movement of the arms to “hold” the

agonist molecule. Such process involves activation energy, which is consistent with the idea that the gating of the ion channel is initiated by agonist-triggered movements within the ligand binding site.[87] On the other hand, Czajkowski *et al.*'s have proposed that the binding site constricts during gating due to the movement of α_1 and β_2 domains of the GABA binding site toward each other. Three arginine residues at the α_1 and β_2 domains (β_2-Arg207, α_1-Arg66 and α_1-Arg131) have been identified to directly stabilize GABA during binding by electrostatic interaction between the positively charged guanido group at the end of the arginine side chain and the negatively charged carboxylate group on the GABA molecule. Czajkowski *et al.*[87] propose that these three arginines form a triangle of positive charge that collaborate to accommodate the negatively charged carboxylate group of the GABA molecule. Since the GABA binding pocket is narrow, this "crown of arginine" arrangement would have implied that GABA molecule is situated vertically within the binding pocket, with the positively charged amino group pointing away from the arginine crown.

Figure 1.6 is a simple description of receptor occupancy and gating of the $GABA_AR$. Basically, the agonists activate the Cl^- channel of the $GABA_AR$ by interacting with the agonist-binding sites, triggering a conformational change in the receptor (structural transition from closed state, A_2R to open state, A_2R^*) that results in the opening of the ion channel. This process, which also known as gating happens quickly and reversibly, but the exact mechanism involved in structural rearrangement, was not well understood.[28,88] Recently, several workers have studied the nature of the coupling agonist binding to channel gating, and identified four amino acids in loop C α_1 domain

and the charged residues located in flexible loops of either α_1 or β_2 subunits are involved in coupling agonist binding to channel gating.[13,28, 89]

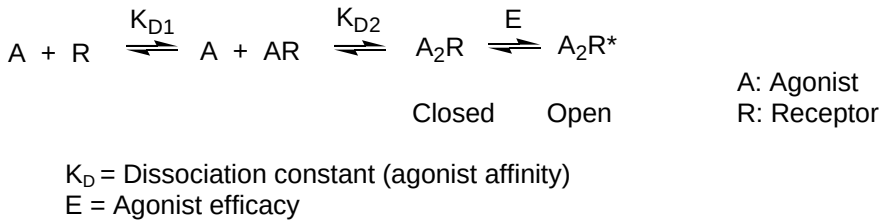

Figure 1.6 Schematic description of receptor occupancy and gating of $GABA_AR$

Based on SCAM, Wagner and Czajkowski[13] have proposed that the residues Phe200, Ser201, Tyr202 and Gly203 in loop C α_1 subunit are involved in mediating GABA binding. Three of the residues (Phe200 to Tyr202) appear to be outside the binding pocket and buried in membrane lipid. Gly203 has been shown to be at the mouth of the binding pocket. Harrison *et al.*[89] show that electrostatic interactions between negatively charged Asp57 and Asp149 in the flexible loops 2 and 7 in the extracellular domain, and positively charged Lys279 in the short transmembrane linker (TM2-3L) region of the $GABA_AR$-α_1 subunit are involved in the process of receptor activation. Apparently, Asp149 and Lys279 move closer together during gating. In line with the results of this view, Kash *et al.*[28] also obtained the same observations using site-directed mutagenesis. They identified the acidic residue Asp 146 in loop 7 of β_2 subunit and basic residue Lys215 in pre-transmembrane domain–1 are involved in coupling agonist binding to the gating of channel through electrostatic interactions.

The studies described previously are based on how mutation changed the EC_{50} values of GABA. The question is how we can determine whether the amino residues

involved in mutation studies are related to coupling agonist binding to channel gating or binding directly. The amino acid residues in Table 1 were identified lining the binding pocket. Both site-directed mutagensis and SCAM have found that mutation of these residues causes a large increase in EC_{50} values of GABA; there is no doubt that these residues are directly involved in agonist binding and the subsequent opening of ion channel. However, the residues like Phe200, Ser201, Tyr202, Gly203, Asp57, Asp 149, Lys279, Asp 146 and Lys215 are identified either in extracellular domains or in transmembrane domains. Mutation of these residues causes an increase in EC_{50} values of the $GABA_AR$ agonists, especially partial agonist like P4S with a decrease in agonist efficacy. Such decrease in agonist efficacy suggests that mutated amino residues are involved in gating.

1.6 Traditional Assays for Agonists

Functional assays, such as patch-clamp and $^{36}Cl^-$ flux, provide functional measurement of actions of GABA agonists and antagonists.[90] Due to the unique pharmacological and clinical importance of $GABA_AR$, there is considerable interest in studying the factors that would affect the functional assays of the $GABA_A$ agonists. As regards $^{36}Cl^-$ flux, the first factor is the incubation time of agonists; generally, GABA-mediated $^{36}Cl^-$ flux was complete within 15 seconds of incubation.[42] Prolonged incubation time results in a higher absolute chloride uptake, and therefore decreases the EC_{50} of GABA, as listed in Table 1.3.[90, 91] Longer incubation time also enhances the modulatory effect of pentobarbital, indicating that the potentiation effect of pentobarbital on GABA-activated $^{36}Cl^-$ flux takes place only after GABA has bound to the binding

sites.[90] Prolonged incubation time also demonstrated that GABA-dependent $^{36}Cl^-$ uptake was slowly recovered in the presence of GABA antagonists, picrotoxinin, endrin and TBPS.[42]

Table 1.3 Correlation of incubation time on GABA-mediated chloride flux and EC_{50}

Incubation time (msec)	24	50	500	3000
EC_{50} (μM)	100	59	42	22

The second factor is the temperature effect; the GABA-induced $^{36}Cl^-$ uptake depends on temperature slightly, as indicated by little change in GABA-stimulated chloride flux within the range 20 to 40 °C. This result also suggests that the GABA-dependent chloride transport is passive rather than active.[43, 90] However, the action of ethanol on GABA-activated chloride uptake is temperature dependent. At 34 or 37 °C, ethanol shows potentiation effect on $^{36}Cl^-$ uptake but not at 30 or 32 °C.[92] Rapid desensitization of the GABA receptor-coupled chloride ion channel is the third factor that affects the functional assay.[8, 43, 90] The duration of GABA-mediated chloride channel opening is of the order of 1-10 ms, followed by rapid desensitization induced by GABA or muscimol at higher concentration.[42, 90, 93] However, the exact mechanism of desensitization remains unknown.

1.7 Pharmacokinetic Aspects and Prodrugs

All $GABA_AR$ agonists described so far have zwitterionic structures; however, only non-ionized neutral molecules can penetrate the BBB. The inadequate ability of $GABA_AR$ agonists to penetrate the BBB reflects the difficulties in developing such agonists with satisfactory pharmacokinetics properties.[5,77] The ratio between the concentrations of ionized and unionized molecules (*I/U* ratio) indicates the ability of $GABA_AR$ agonists to penetrate the BBB. This *I/U* ratio is a function of the difference between the pK_a^I and pK_a^{II} values.[52,94] Figure 1.7 shows an illustration of the determination of the *I/U* ratio for isoguvacine in aqueous solution. Basically, the *I/U* ratio of neutral isoguvacine can be calculated in two ways, as the ratio between the intrinsic constants K_a and K_b or between K_d and K_c. The approximate values of K_a and K_c are measured by titration of isoguvacine. Species **i** will be the predominant form below pH 4, species **ii** will predominate at pH 5-9, and species **iii** will predominate at pH>10. The values of K_b and K_d can not be determined by titration directly, since species **iv** will not predominate at any pH, they are thus estimated indirectly by titration of appropriate derivatives of isoguvacine, in which either the acid or the basic function, respectively, has been blocked, as shown in Figure 1.7. From the values of K_a, K_c, K_N, and K_E, two similar *I/U* ratios were calculated for isoguvacine. Values of pK_a, and *I/U* ratios of some $GABA_AR$ agonists and their ability to penetrate the BBB are shown in Table 1.4.[67] In general, the higher the *I/U* ratio, the smaller the fractions of un-ionized molecules will be present in the solution, and the lower the ability of $GABA_AR$ agonists to penetrate the BBB.[1, 5, 53, 67]

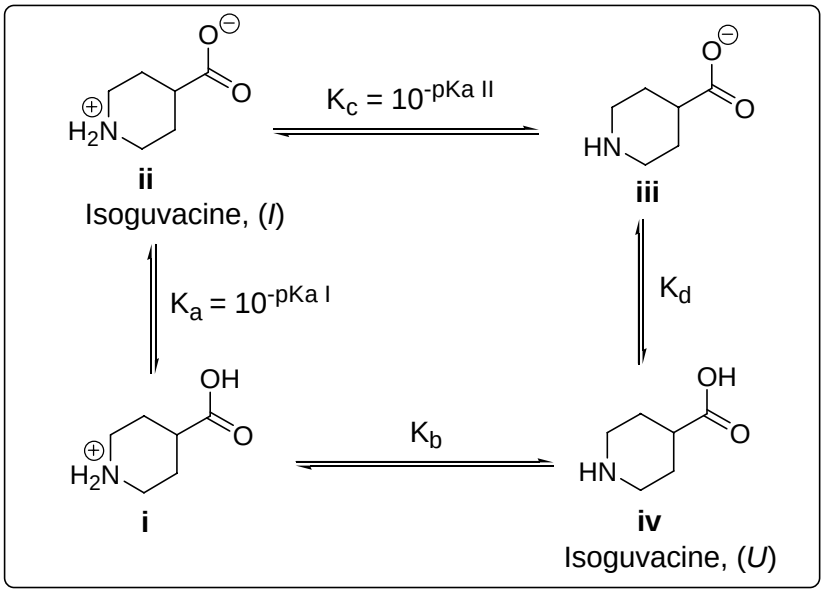

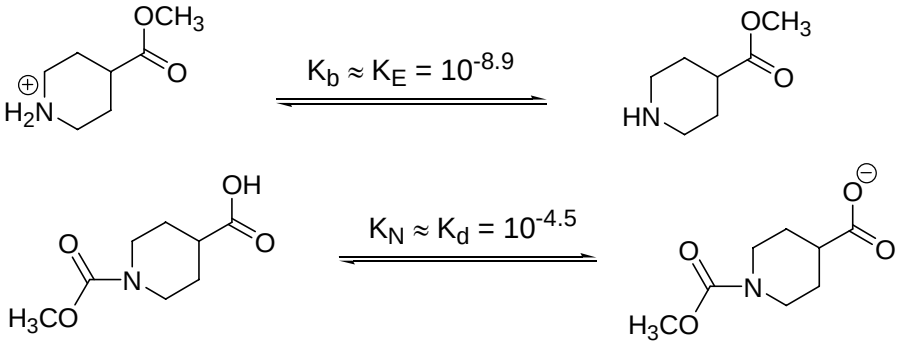

$$\frac{\text{[Zwitterionic isoguvacine]}}{\text{[Unionized isoguvacine]}} = \textit{I/U}\text{ ratio} = \frac{K_a}{K_b} \approx \frac{K_a}{K_E} = \frac{10^{-3.6}}{10^{-8.9}} = 200{,}000$$

$$= \frac{K_d}{K_c} \approx \frac{K_N}{K_c} = \frac{10^{-4.5}}{10^{-9.8}} = 220{,}000$$

Figure 1.7 An illustration of the determination of the I/U ratio for Isoguvacine in aqueous solution

Table 1.4 pK_a values, and *I/U* ratios of some $GABA_AR$ agonists and their ability to penetrate the BBB[67]

$GABA_AR$ agonists	pK_a values (I; II)	*I/U* ratio*	Penetration of the BBB
GABA	4.0; 10.7	800,000	No
(*RS*)-DHM	5.8; 9.3	630	Yes
Muscimol	4.8; 8.4	900	Yes
Thiomuscimol	6.1; 8.5	16	Yes
THIP	4.4; 8.5	1,500	Yes
Isoguvacine	3.6; 9.8	200,000	No
4-PIOL	5.2; 10.2	31, 000	No
P4S	<1; 10.3	>1,000,000	No

Both muscimol and THIP can penetrate the BBB, however, muscimol is toxic and it will be easily metabolized after systemic administration; THIP has analgesic effects, but its side effects such as sedation and blurred vision prevent it to be clinical useful. (*RS*)-DHM can also penetrate the BBB, however, pharmacological data of animal behavioral studies is not available.[66]

Because most of the $GABA_A$ agonists do not penetrate the BBB, the prodrug approach would be a useful strategy to convert zwitterionic $GABA_A$ agonists into clinically useful CNS agents. An ideal prodrug is the derivative of the biologically active compound that can be easily converted into parent compound in the CNS without formation of toxic by-products, and also it should have a long half-life.[53] Important GABA prodrugs include progabide (**40**) and (**41**) (Figure 1.8).[1, 5, 53, 95] The

pharmacological data of (**40**) show that it has anticonvulsant effects in diverse types of epilepsy, and no potential toxicity of the benzophenone moiety has been reported so far.[1] (**41**), like (**40**) which decomposes in the brain to give GABA and increases GABA level, and shows continual anticonvulsant effects in rats.[1] The acyloxymethyl esters (**42**) and (**43**) are systemically active prodrugs of isoguvacine.[1, 53] Their half-lives are about 10 minutes and 6 hours respectively under approximate physiological conditions *in vitro*.[53]

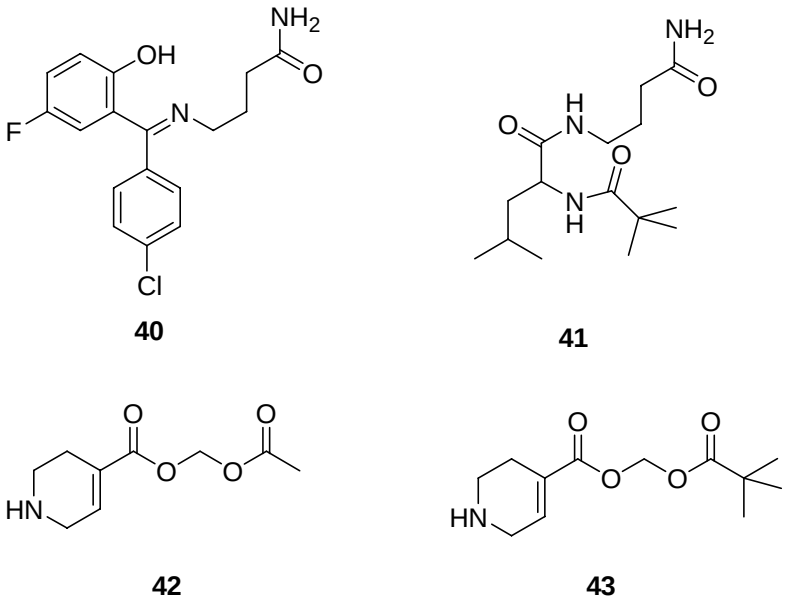

Figure 1.8 $GABA_A$ agonists prodrugs

Compound **40** is a benzophenone imine derivative of GABA. It is believed that (**40**) is partially metabolized into the corresponding carboxylic acid *in vivo* by oxidative deamination or transamination, which is then hydrolyzed to give GABA and orthohydroxy-benzophenone (path **A** to **B** to **D**). The corresponding carboxylic acid (**SL 75102**) is a $GABA_A$ agonist,[96] being 33-fold less potent than GABA.[96] An alternative possibility is that (**40**) is converted into GABA-amide by cleavage of imine bond, which

is subsequently hydrolyzed to provide GABA (path **A** to **C** to **D**),[1, 95] as illustrated in Scheme 1.4. Path (**A** to **B** to **D**) is believed to the preferred pathway.[95]

Scheme 1.4 Proposed mechanisms for the hydrolysis of progabide (**40**)

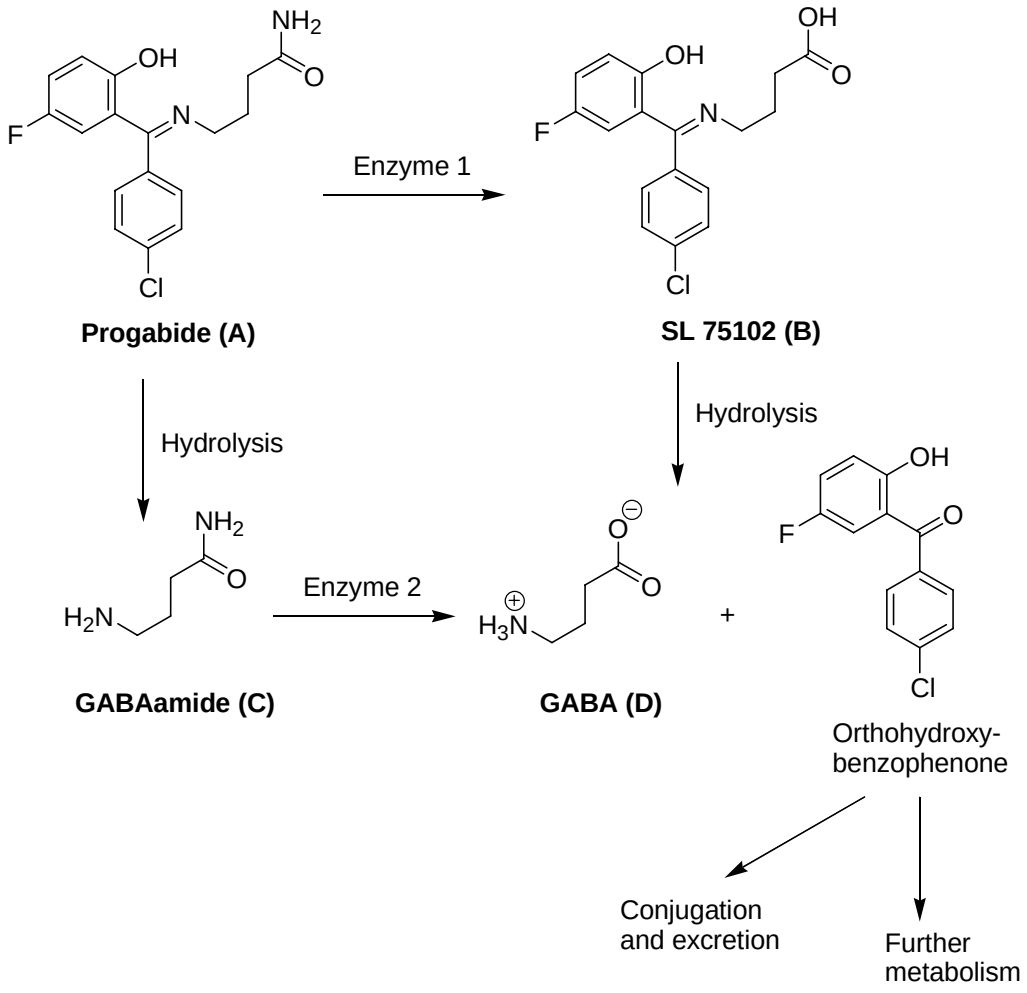

References for chapter 1

1 Krogsgaard-Larsen, P. Amino Acid Receptors. *Comp. Med. Chem. Vol .3*, 493-531.

2 Bormann, J. The 'ABC' Of GABA receptors. *Trends Pharmacol. Sci.* **2000**, *21*, 13.

3 Krogsgaard-Larsen, P.; Roldskov-Christiansen, T. GAGA Agonists. Synthesis and Structure-activity Studies on Analogues of Isoguvacine and THIP. *Eur. J. Med. Chem. - Chim Ther*. **1979**, *14*, 157-164.

4 Sigel, G. J. In *Basic Neurochemistry*. Timothey, M. Delorey; Richard W. Olsen. Raven Press, Ltd, New York. **1994**, 389-399.

5 Krogsgaard-Larsen, P.; Hround, B.; Jrogensen, S. F.; Schousboe, A. $GABA_A$ Receptor Agonists, Partial Agonists, and Antagonists. Design and Therapeutic Propects. *J. Med. Chem.* **1994**, *37* (16), 2489-2505.

6 Schwartz, D. R.; Suzdak, P. D.; Paul, S. M. γ - Aminobutyric Acid (GABA)- and Barbiturate-Mediated Cl^- Uptake in Rate Brain Synaptoneurosomes: Evidence for Rapid Desensitization of the GABA Receptor-Coupled Chloride Ion Channel. *Mol. Pharmacol.* **1986**, *30*, 419-426.

7 Smart, T. G. In *Amino Acid Neurotransmission*; F. Anne Stephenson; A. J. Turner, Eds.; Portland Press, Ltd, London. 1998, 37-63.

8 Bormann, J.; Clapham, D. E. γ–Aminobutyric acid receptor channels in adrenal chromaffin cells: A patch-clamp study. *Proc. Natl. Acad. Sci. USA.* **1985**, *82*, 2168-2172.

9 Chebib, M.; Johnston, G. A. R. GABA-activated Ligand Gated Ion Channels: Medicinal Chemistry and Molecular Biology. *J. Med. Chem*. **2000**, *43*, 1427-1447.

10 Macdonald R. L.; Olsen, R. W. $GABA_A$ Receptor Channels. *Annu. Rev. Neurosci.* **1994,** *17,* 569-602.

11 Sieghart, W. $GABA_A$ receptors: ligand-gated Cl^- ion channels modulated by multiple drug-binding sites. *Trends Pharmacol. Sci.* **1992**, *13*, 446-450.

12 Delorey, T. M.; Olsen, R. W. γ–Aminobutyric $Acid_A$ Receptor Structure and Function. *J. Biol. Chem.* **1992,** *267,* 16747-16750.

13 Wagner, D. A.; Czajkowski, C. Structure and Dynamics of the GABA Binding Pocket: A Narrowing Cleft that Constricts during Activation. *J. Neuroscience* **2001**, *21*, 67-74.

14 Johnston G. A. R. $GABA_A$ receptor pharmacology. *Pharmacol. Ther.* **1996**, *69*, 173-198.

15 Paterson, N. E.; Froestl, W.; Markows, A. Repeated Administration of the $GABA_B$ Receptor Agonist CGP44532 Decreased Nicotine Self-Administration, and Acute Administration Decreased Cue-Induced Reinstatement of Nicotine-Seeking in Rats. *Neuropsychopharmacol.* **2005,** *30,* 119-128.

16 Enna, S. J.; Bowery, N. G. $GABA_B$ receptor alterations as indicators of physiological and pharmacological function. Biochemical Pharmacology. *Biochem. Pharmacol.* **2004,** *68,* 1541-1548.

17 Capasso, A. $GABA_B$ receptors are involved in the control of acute opiate withdrawal in isolated tissue. *Prog. Neuro-pshychopharmacol. Biol. Psychiat.* **1999,** *23,* 289-299.

18 Xiong, Z.-Q.; Stringer, J. L. Effects of postsynaptic $GABA_B$ receptor activation on epileptiform activity in hippocampal slices. *Neuropharmacol.* **2001,** *40,* 131-138.

19 Snead III, O. C. Antiabsence seizure activity of specific $GABA_B$ and γ-hydroxybutyric acid receptor antagonist. *Pharmacol. Biochem. Behavior.* **1996,** *53,* 73-79.

20 Martin, D. L.; Olsen, R. W. In *GABA in the Nervous System: The View at Fifty Years.* Lippincott Williams & Wilkins **2000,** 65-80.

21 Nayeem, N.; Green, T. P.; Martin, I. L.; Barnard, E. A. Quaternary Structure of the Native $GABA_A$ Receptor Determined by Electron Microscopic Image Analysis. *J. Neurochem.* **1994**, *62*, 815-818.

22 Boileau, A. J.; Evers, R. A.; Davis, A. F.; Czajkowski, C. Mapping the Agonist Binding Site of the $GABA_A$ Receptor: Evidence for a β-Strand. *J. Neurosci.* **1999**, *19*, 4847-4854.

23 Kash, T. L.; Trudell, J. R.; Harrison, N. L. Structural elements involved in activation of the γ-aminobutryic acid type A ($GABA_A$) receptor. *Biochem. Soc. Trans.* **2004,** *32,* 540-546.

24 Smith, G. B.; Olsen, R. W. Functional domains of $GABA_A$ receptors. *Trends Pharmacol. Sci.* **1995,** *16,* 162-168.

25 Mohler, H.; Rudolph, U. Selective $GABA_A$ circuits for novel CNS drugs. *Drug Discovery Today: Ther. Strategies.* **2004,** *1,* 117-123.

26 Chang, Y.; Wang, R.; Barot, S.; Weiss D. S. Stoichemistry of a recombinant $GABA_A$ receptor. *J. Neurosci.* **1996,** *16,* 5415-5424.

27 Smart T. G. In *Amino Acid Neurotransmission*; F. Anne Stephenson; A. J. Turner, Eds.; Portland Press, Ltd, London. **1998**, 65-92.

28 Kash, T. L.; Dizon, M.-J. F.; Trudell, J. R.; Harrison, N. L. Charged Residues in the β2 Subunit Involved in $GABA_A$ Receptor Activation. *J. Bio. Chem.* **2004,** *279,* 4887-4893.

29 Smith, G. B.; R. Olsen W. Identification of a [^{3}H] Musicmol Photoaffinity Substrate in the Bovine γ-Aminobutyric Acid$_A$ Receptor α Subunit. *J. Biol. Chem.* **1994**, *269*, 20380-20387.

30 Luddens, H.; Korpi, E. R.; Seeburg, P. H. GABA$_A$/Benzodiazepine Receptor Heterogeneity Neurophysiological Implications. *Neuropharmacol*. **1995**, *34*, 245-254.

31 Pritchett, D. B.; Sontheimer, H.; Shivers, B. D.; Ymer, S.; Kettenmann, H.; Shofield, P. R.; Seeburg, P. H. Importance of a novel GABA$_A$ receptor subunit for benzodiazepine pharmacology. *Nature* **1989,** *338,* 582-585.

32 Sigel, E.; Baur, R.; Kellenberger, S.; Malherbe, P. Point mutations affecting antagonist affinity and agonist dependent gating of GABA$_A$ receptor channels. *EMBO J.* **1992,** *11,* 2017-2023.

33 Colquhoun, D. Binding, gating, affinity and efficacy: The Interpretation of structure-activity relationships for agonists and of the effects of mutating receptors. *Br. J. Pharmacol.* **1998,** *125,* 924-947.

34 Baumann, S. W.; Baur, R.; Sigel, E. Individual properties of the two functional agonist sites in GABA$_A$ receptors. *J. Neurosci.* **2003,** *23,* 11778.

35 Newell, J. G.; Davies, M.; Bateson, A. N.; Dunn, S. M. J. Tyrosine 62 of the γ-Aminobutyric Acid Type A Receptor β2 Subunit Is an Important Determinant of High Affinity Agonist Binding. *J. Biol. Chem.* **2000**, *275*, 14198-14204.

36 Agey, M. W.; Dunn, S. M. J. Kinetics of [^{3}H]Muscimol Binding to the GABA$_A$ Receptor in Bovine Brain Membranes. *Biochemistry***, 1989,** *28,* 4200-4208.

37 Newell, J. G.; Dunn, S. M. J. Functional Consequences of the Loss of High Affinity Agonist Binding to γ-Aminobutyric Acid Type A Receptors. *J. Bio. Chem.* **2002,** *277,* 21423-21430.

38 Edgar, P. P.; Schwartz, R. D. Functionally Relevant γ–Aminobutyric Acid$_A$ Receptors: Equivalence between Receptor Affinity (K_d) and Potency (EC_{50})? *Mol. Pharmacol.* **1992,** *41*, 1124-1129.

39 DeLorey, T. M.; Brown, G. B. γ-Aminobutyric acid$_A$ Receptor Pharmacology in Rat Cerebral Cortical Synaptoneurosomes. J. Neurochem. 1992, 58, 2162-2169.

40 Baur, R.; Sigel, E. On high- and low-affinity agonist sites in GABA$_A$ Receptor. *J. Neurosci.* **2003,** *87,* 325-332.

41 Brejc, K.; Van Dijk, W. J.; Klaassen, R. V.; Schuurmans, M.; Van der Oost, J.; Smit, A. B.; Sixma, T. K. Crystal structure of the an ACh-binding protein reveals the ligand-binding domain of nicotinic receptors. *Nature,* **2001,** *411,* 269-276.

42 Cupello, A.; Hyden, H. Binding experiment K_d values and physiologically active GABA concentrations: an only apparent contradiction? *Int. J. Neurochem.* **1986,** *30,* 297-301.

43 Amin, J.; Welss, D. S. Binding experiment K_d values and physiologically active GABA concentrations: an only apparent contradiction? *Nature* , **1993,** *366,* 565-569.

44 Lancel, M.; Steiger, A. Sleep and Its Modulation by Drugs That Affect $GABA_A$ Receptor Function. *Angew. Chem. Int. Ed.* **1999**, *111*, 2852-2864.

45 Fryer, R. I. Ligand Interactions at the Benzodiazepine Receptor. *Comp. Med. Chem.*3, 540-543.

46 Olsen, R. W.; Venter, J. C. In the Benzodiazepine/GABA Receptors and Chloride Channels: Structural and Functional Properties. Alan R. Liss, Inc. New York 1986, 97.

47 Serfozo, P.; Cash, D. Effect of benzodiazepine (chlordiazepoxide) on a $GABA_A$ Receptor from rat brain: Requirement of only one bound GABA molecule for channel opening. *FEBS. J.* **1992,** *310,* 55-59.

48 Harris, R. A.; Allan, A. M. Functional Coupling of γ–Aminobutyric Acid Receptors to Chloride Channels in Brain Membranes. *Science* **1985,** *228,* 1108-1110.

49 Morrow, A. L.; Paul, S. M. Benzodiazepine Enhancement of γ–Aminobutyric Acid-Mediated Chloride Ion Flux in Rat Brain Synaptoneurosomes. *J. Neurochem.* **1988,** *50,* 302-306.

50 Vicini, S.; Mienville, J.-M.; Costa, E. Actions of Benzodiazepine and β-Carboline Derivatives on γ–Aminobutyric Acid-Activated Cl^- Channels Recorded from Membrane Patches of Neonatal Rat Cortical Neurons in Culture. *J. Pharmaco. Exp. Ther.* **1987,** *243,* 1195-1201.

51 Rogers, C. J.; Twyman, R. E.; Macdonald, R. L. Benzodiazepine and β-carboline regulation of single $GABA_A$ receptor channels of mouse spinal neurons in culture. *J Physiol.* **1994,** *475,* 69-82.

52 Macdonald, R. L.; Rogers, C. J.; Twyman, R. E. Barbiturate regulation of kinetic properties of the $GABA_A$ receptor channel of mouse spinal neurons in culture. *J Physiol.* **1989,** *417,* 486-500.

53 Krogsgaard-Larsen, P. In *Amino Acid Receptors*. Comp. Med. Chem. *Vol 3*, 388-409.

54 Higashi, H.; Nishi, S. Effect of barbiturates on the GABA receptor of rat primary afferent neurons. *J. Physiol.(Lond.)* **1982,** *332,* 299-314.

55 Bloomquist, J. R. Ion Channels as Targets for Insecticides. *Ann Rev. Entomol.* **1996,** *41,*163-190.

56 Bloomquist, J. R. Intrinsic Lethality of Chloride Channel-Directed Insecticides and Convulsants in Mammals. *Toxicol. Lett.* **1992,** *60,* 289-298.

57 Bloomquist, J. R.; Jackson, J. L.; Karr, L. L.; Ferguson, H. J.; Gajewski, R. P. A new chemical class of insecticide acting upon the GABA receptor/chloride ionophore complex. *Pesticide Sci*. **1993**, *39*, 185-192.

58 Lan, N. C.; Gee, K. W.; Bolger, M. B; Chen, J. S. Differential Responses of Expressed Recombinant Human γ–Aminobutyric $Acid_A$ Receptors to Neurosteroids. *J. Neurochem.* **1991,** *57,* 1818-1821.

59 Twyman, R. E.; Macdonald, R. L. Neurosteroid regulation of $GABA_A$ receptor channel kinetic properties of mouse spinal neurons in culture. *J Physiol.* **1992,** *456,* 215-245.

60 Longoni, B.; Demontis, G. C.; Olsen, R. W. Enhancement of γ–Aminobutyric $Acid_A$ Receptor Function and Binding By the Volatile Anesthetic Halothane. *J. Pharmacol. Exp. Ther.* **1993,** *266,* 153-159.

61 Quinlan, J. J.; Firestone, S.; Firestone, L. L. Isoflurane's enhancement of Chloride Flux through Rat Brain gama-Aminobutyric Acid Type A Receptors Is Stereoselective. *Anesthesiology,* **1995**, *83,* 611-615.

62 McKernan, R. M.; Rosahl, T. W.; Reynolds, D. S.; Sur, C.; Wafford, K. A.; Atack, J. R.; Farrar, S.; Myers, J.; Cook, G.; P. Ferris; Garrett; L. B.; Marshall, G.; Macauley, A.; Brown, N.; Howell, O.; Moore, W. K.; Carling, R. W.; Street, L. J.; Castro, J. L.; Ragan, C. I.; Dawson, G. R.; Whiting, P. J. Sedative but not anxiolytic properties of benzodiazepines are mediated by the $GABA_A$ receptor α1 subtype. *Nature Neurosci.* **2000,** *3,* 587-592.

63 Huang, Q.; He, X.; Ma, C.; Liu, R.; Yu, S.; Dayer, C. A.; Wenger, G. R.; Mckernan, J. M. Pharmacophore GABAA/Receptor Models for /BzR Subtypes (α1β3γ2, α5β3γ2 and α6β3γ2) via a Comprehensive Ligand-Mapping Approach. *J. Med. Chem.* **2000**, *43*, 71-95.

64 Martin, D. L.; Olsen, R. W. In the *GABA in the Nervous System: The View at Fifty Years.* Lippincott Williams & Wilkins **2000,** 97.

65 Johnston, G. A. R.; Allan, R. D.; Kennedy, S. M. E.; Twitchin B. Systematic Study of GABA Analogues of Restricted Conformation. In *GABA- Neuro-Transmitters;* Krogsgaard-Larsen, P.; Scheel-Kruger, J.; Kofod, H.; Eds.; Munkgaard: Copenhagen, **1979**, 149-164.

66 Krogsgaard-Larsen, P.; Nielsen, L.; Falch, E.; Curtis, D. R. GABA Agonist. Resolution, Absolute Stereochemistry, and Enantioselectivity of (*S*)-(+)- and (*R*)-(-)-Dihydromuscimol. *J. Med. Chem.* **1985,** *28,* 1612-1617.

67 Krogsgaard-Larsen, P.; Honoré, T.; Thysssen, K.. In *GABA- Neuro-Transmitters;* P. Krogsgaard-Larsen; J. Scheel-Kruger; H. Kofod, Eds.; Munkgaard: Copenhagen, **1979**, 201-216.

68 Bureau, M.; Olsen, R. W. Multiple distinct subunits of the γ–aminobutyric $acid_A$ receptor protein show different ligand binding properties. *Mol. Pharmacol.* **1990,** *37,* 497-502.

69 Krogsgaard-Larsen, P.; Falch, E. The Binding of the GABA Agonist [^{3}H] THIP to Rat Brain Synaptic Membranes. *J. Neurochem.* **1982,** *38,* 1123.

70 Bloomquist, J. R.; Grubs, R. E.;.Soderlund, D. M.; Knipple, D. C. Prolonged exposure to GABA activates GABA-gated chloride channels in the presence of channel-blocking convulsants. *Comp. Biochem. Physiol.* **1991,** *99C,* 397-402.

71 Kristiansen, U.; Lambert, J. D. C.; Falch, E.; Krogsgaard-Larsen, P. Electrophysiological studies of the $GABA_A$ receptor ligand, 4-PIOL, on cultured hippocampal neurons. *Br. J. Pharmacol.* **1991,** *104,* 85-90.

72 Breckenridge, R. J.; Nicholson, S. H.; Nicol, A. J.; Suckling, C. J.; Leigh, B.; Iversen L. Inhibition of [^{3}H] GABA Binding to Postsynaptic Recetors in Human Cerebellar Synaptic Membranes by Carboxyl and Amino Derivatives of GABA. *J Neurochem.* **1981**,*37*, 837-844.

73 Allan ,R. D.; Dickenson, H. W.; Hiern G. B. P.; Johnston, A. R.; Kazlauskas, R. Isothiouronium compounds as γ–aminobutyric acid agonists. *Br. J. Pharmacol.* **1986,** *88,* 379-387.

74 Holden-Dye, L.; Walker, R. J. ZAPA, *Z*-3-[(aminoiminomethyl)thio]prop-2penoic acid hydrochloride, a potent agonist at GABA-receptors on the *Ascaris* muscle cell. *Br. J. Pharmacol.* **1988,** *95,* 3-5.

75 Luu, M. D.; Morrow, A. L.; Paul, S. M.; Schwartz, R. D. Characterization of $GABA_A$ Receptor-mediated 36Chloride Uptake in Rat Brain Synaptosomes. *Life Sci***. 1987,** *41, 1277-1287.*

76 Varga, V.; Kontro, P.; Oja, S. S. Modulation of GABAergic Neurotransmission in the Brain by Dipetides. *Neurochem. Res.* **1988,** *13,* 1027-1034.

77 Olsen, R. W.; Venter, J. C. In the Benzodiazepine/GABA Receptors and Chloride Channels: Structural and Functional Properties. Alan R. Liss, Inc. New York **1986,** 73.

78 Wermuth, C. G.; Biziere, K. Pyridazyl-GABA derivatives: a new class of synthetic GABAA antagonists. *Trends Pharm. Sci.* **1986,** *7,* 721-724.

79 Melikian, A.; Schlewer, G.; Chambon, J. P.; Wermuth, C. G. Condensation of Muscimol or Thiomuscimol with Aminopyridazines Yields GABA-A Antagonists. *J. Med. Chem.* **1992,** *35,* 4092-4097.

80 Krogsgaard-Larsen, P.; Johnston, G. A. R.; Curtis, D. R.; Game, C. J. A.; McCullonch, R. M. Structure and Biological Activity of A Series of Conformationally Restricted Analogues of GABA. *J. Neurochem.* **1975**, *25*, 803-809.

81 Falch, E.; Krogsgaard-Larsen, P.; Jacobsen, P.; Engesgaard, A.; Braestrup, C.; Crutis, D. R. Synthesis, GABA agonist activity and effects on GABA and diazepam binding of some *N*-substituted analogues of GABA. *Eur. J. Med. Chem. - Chim Ther*. **1985**, *20*, 447-453.

82 Frey, M.; Jager, V. Synthesis of *N*-Substituted Muscimol Derivatives Including N-Glycylmuscimol. *Synthesis, 1985*. 1100-1104.

83 Aprison, M. H.; Lipkowitz, K. B. Muscimol and *N,N*-Dimethylmuscimol: From a GABA Agonist to a Glycine Antagonist. *J. Neurosci. Res.* **1992**, *31*, 166-174.

84 Bollan, K.; King, D.; Robertson, L. A.; Brown, K.; Taylor, P. M.; Moss, S. J.; Connolly, C. N. $GABA_A$ Receptor Composition Is Determined by Distinct Assembly Signals within α and β Subunits. *J. Bio. Chem.* **2003,** *278,* 4747-4755.

85 Sedelnikova, A.; Smith, C. D.; Zakharkin, S. O.; Davis, D.; Weiss, D. S.; Chang, Y. Mapping the ρ1 $GABA_C$ Receptor Agonist Binding Pocket. *J. Bio. Chem.* **2005,** *280,* 1535.

86 Jones, M. V.; Sahara, Y.; Dzubay, J. A.; Westbrook, G. L. Defining affinity with the $GABA_A$ receptor. *J. Neurosci.* **1998**, *18*, 8590-8604.

87 Wagner, D. A.; Czajkowski, C.; Jone, M. V. An Arginine Involved in GABA Binding and Unbinding But Not Gating of the $GABA_A$ Receptor. *J. Neurosci.* **2004,** *24,* 2733-2741..

88 Jones, M. V.; Jonas, P.; Sahara, Y.; Westbrook, G. L. Microscopic Kinetics and Energetics Distinguish $GABA_A$ Receptor Agonists and Antagonists. *Biophys. J.* **2001,** *81,* 2660-2670.

89 Kash, T. L.; Jenkins, A.; Kelley, J. C.; Trudell, J. R.; Harrison, N. L. Coupling of angonist binding to channel gating in the $GABA_A$ receptor. *Nature,* **2003,** *421,* 272-275.

90 Mihic, S. J.; Berckel V. B. N. M.; Wu, P. H.; Kalant, H. GABA and pentobarbital potentiation of chloride influx into microsacs is influenced by incubation time. *Brain Research*, **1993**, *619*, 319-323.

91 Kardos, J.; Cash, D. J. Transmembrane $^{36}Cl^-$ Flux Measurements and Desensitization of the γ-Aminobutyric $Acid_A$ Receptor. *J. Neurochem.* **1990,** *55,* 1095-1099.

92 McQuilkin S. J.; Harris R. A. Factors affecting actions of ethanol on GABA-activated Chloride channels. *Life Sci.* **1990***, 46,* 527-541.

93 Mihic, S. J.; Wu, P. H.; Kalant, H. Potentiation of γ–Aminobutyric Acid-Mediated Chloride Flux by Pentobarbital and Diazepam but Not Ethanol. *J. Neurochem* **1992,** *58,* 745-751.

94 Krogsgaard-Larsen, P.; Mikkelsen, H.; Jacobsen, P.; Falch E.; Curtis, D. R.; Peet, M. J.; Leah, J. D. 4,5,6,7-Tetrahydroisothiazolo[5,4-*c*]pyridin-3-ol and Related Analogues of THIP. Sysnthesis and Biological Activity. *J. Med. Chem.* **1983,** *26,* 895-900.

95 Worms, P.; Depoortere, H.; Durand, A.; Morselli, P. L.; Lloyd, K. G.; Bartholini G. γ–Aminobutyric Acid (GABA) Receptor Stimulation. I. Neuropharmacological Profiles of Progabide (SL 76002) and SL 75102, with Emphasis on Their Anticonvulsant Spectra. *J Pharmacol. Exp. Ther.* **1982,** *220,* 660.

96 Desarmenien, M.; Feltz, P.; Headley, P.M.; Santangelo, F. SL 75102 as a γ–Aminobutyric Acid agonist: experiments on dorsal root ganglion neurones *in vitro. Br. J. Pharmac.* **1981***, 72,* 355-364.

Chapter 2 Syntheses of $GABA_A$ receptor analogs

Numerous previous studies of $GABA_A$ receptor ($GABA_AR$) ligands have suggested that $GABA_AR$ agonists must be zwitterionic and feacture an intercharge separation similar to that of GABA (approx. 4.7-6.0 Å).[1,2] GABA amides were studied relatively early in the development of $GABA_AR$ pharmacology, and received little attention thereafter. Suckling reported that **1a-d** were 5,000-11,000-fold less potent that GABA to displace [^{3}H]GABA from human cerebellum membranes; however, no functional assay data on these compounds were reported[3] (Scheme 2.1). More recently, GABA dipeptides such as GABA-His and GABA-Gly were studied.[4] Chloride flux assay at 0.1 and 1 mM showed that these compounds were not agonists.[5] Taken together, these published studies provided little motivation to further explore GABA amides. However, because of our interest in developing tethered $GABA_AR$ agonists,[6,7] and because functionalization of the GABA carboxyl is one of the few conceivable ligation strategies, we were motivated to synthesize three series of new GABA amides and re-examine a small collection of known GABA amides in a functional assay. We have published the synthesis and evaluation of some of these GABA amides in 2002.[8] With eventual goal of developing bivalent ZAPA agonists, we also examined one of the $GABA_AR$ analogs, ZAPA and its derivatives in the same functional assay.

Scheme 2.1 GABA amides examined previously by other workers

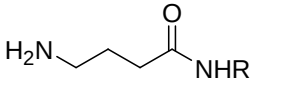

1a R = H (gabamide)
1b R = *n*-Bu
1c R = Ph
1d R = *n*-$C_{12}H_{25}$

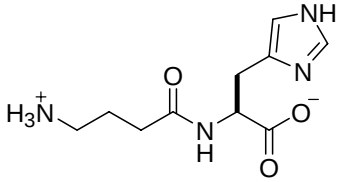

GABA-His

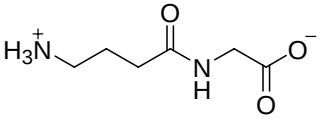

GABA-Gly

2.1 Syntheses and Evaluation of homodimeric $GABA_A$ receptor analogs

GABA amide homodimers **2a-i** were prepared from *N*-Boc-2-pyrrolidone, which was in turn synthesized from Boc anhydride and 2-pyrrolidone according to the literature method[9] (Scheme 2.2). Ring-opening with diamines afforded the corresponding N-Boc GABA amide dimer derivatives, and either HCl or trifluoroacetic acid (TFA) deprotection provided **2a-i** in moderate to good yields.

Scheme 2.2 Synthesis of GABA amide homodimers

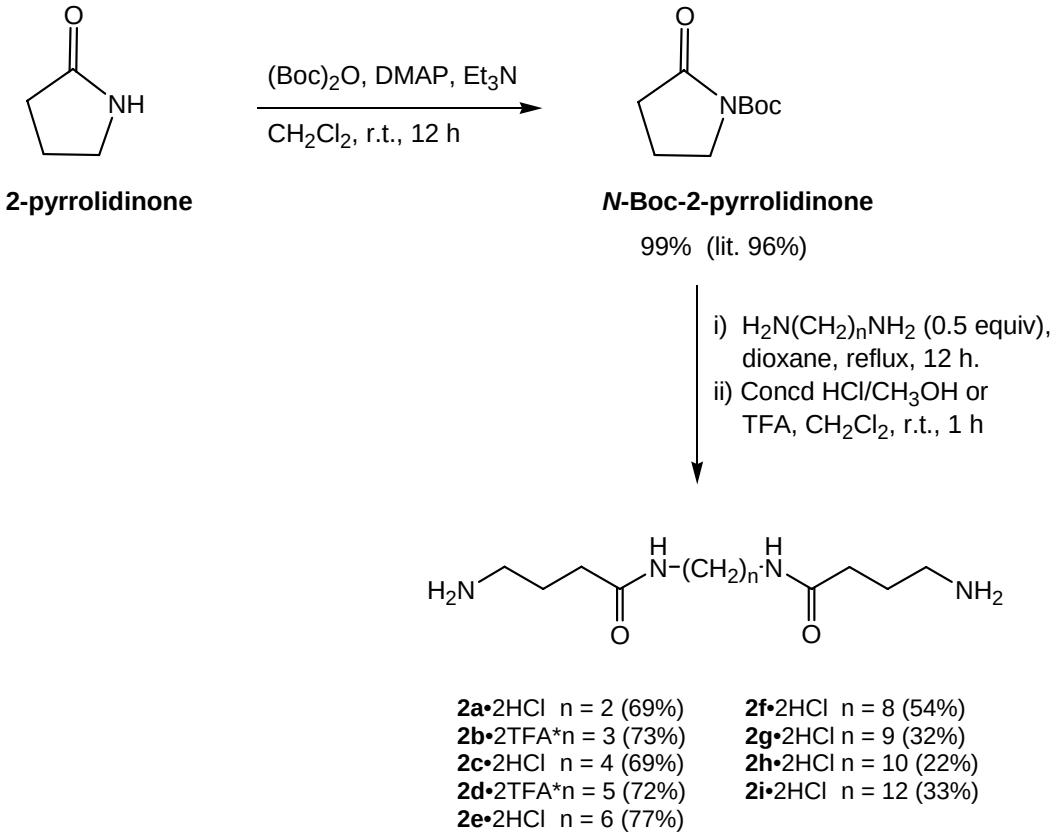

2a•2HCl n = 2 (69%)
2b•2TFA*n = 3 (73%)
2c•2HCl n = 4 (69%)
2d•2TFA*n = 5 (72%)
2e•2HCl n = 6 (77%)
2f•2HCl n = 8 (54%)
2g•2HCl n = 9 (32%)
2h•2HCl n = 10 (22%)
2i•2HCl n = 12 (33%)

*Compounds **2b** and **2d** were synthesized by Yiqun Zhang. Bioassay experiments were performed by the author.

2.1.1 Bioassay Results of New GABA amide homodimers

The new GABA amide dimers were screened for their activity as $GABA_AR$ agonists using a standard $^{36}Cl^-$ flux assay in mouse brain synaptoneurosomes.[10] Prior to assay, the amide homodimers that are hydrochloride salts were analyzed by HPLC using a modification of Sallers' procedure (assay of the dansyl sulfonamide derivatives),[11] to confirm that they were free from trace GABA impurities (<0.1 wt%). Details of the HPLC analysis are discussed in section 2.5.

These GABA amide homodimers were first screened for their activity at 1 mM. The results showed that the agonism by these dimers was tether length dependent (Figure 1.1). As can be seen, chloride uptake increased as the tether length increased from 2 to 4 methylenes; the uptake then gradually declined to the background level from four methylenes to nine methylenes. Chloride uptake above background was statistically significant ($p<0.05$, *t*-test) only for tether lengths of 2-6 methylenes (**2a-e**); at longer tether lengths (8, 9,10, and 12 methylenes) uptake was indistinguishable from background. At this point the optimum tether length appeared to be four methylenes. Dose-response curves were also obtained for GABA amide dimers **2a-e**; compound **2c** proved to be the most potent (Figure 2.2, Table 2.1). The Hill slopes for all of these GABA amide dimers were in the range of 1.3-2.1, consistent with the idea that two agonists must bind in order to gate the $GABA_AR$. The dose-response curves displaced differing degrees of agonism for different tether lengths.

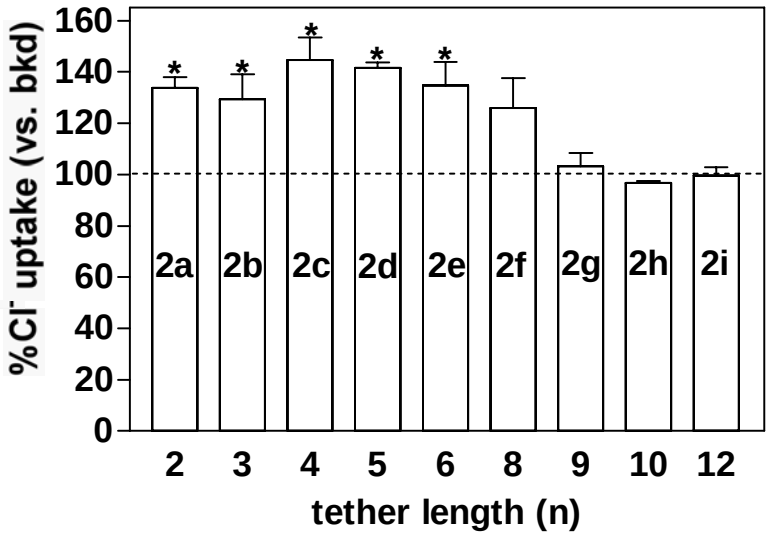

Figure 2.1 Effect of tether length of GABA amide dimers (n = number of methylenes) on $^{36}Cl^-$ flux (at 1 mM drug) in mouse brain synaptoneurosomes, expressed as % uptake versus background (bkd, 100%, dotted line). An asterisk signifies that uptake is significantly different than background ($p<0.05$, *t*-test)

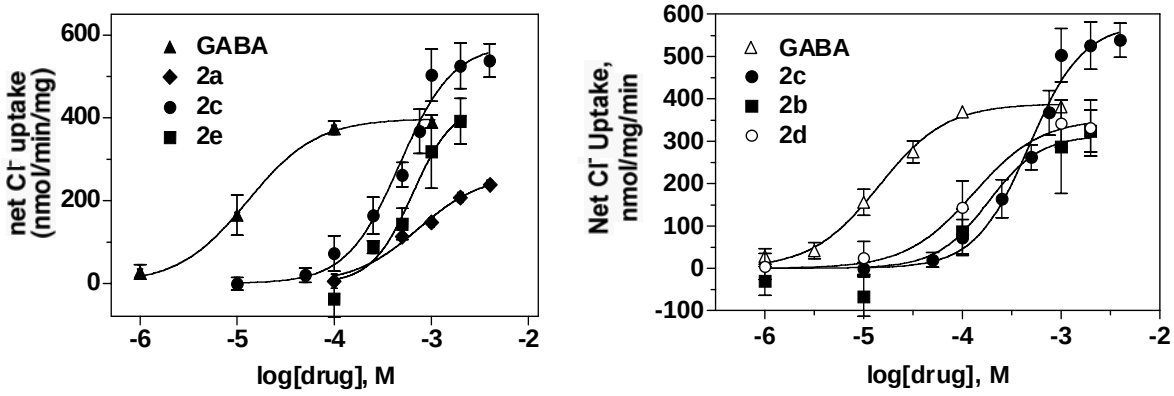

Figure 2.2 Dose-response relationship of Cl^- uptake and drug (GABA and **2a-e**) concentrations in mouse brain synaptoneurosomes

Table 2.1 $GABA_AR$ agonism (E_{max}), chloride uptake (EC_{50} values) and Hill slope of GABA amides and controls

Compound	Chloride uptake EC_{50}, μM	Agonism (E_{max})	Hill Slope
2a•2HCl	733±1.3	Partial (264±36)	1.3
2b•2TFA	184±3.5	Full (314±100)	1.7
2c•2HCl	475±1.1	Super (578±40)	1.6
2d•2TFA	130±1.3	Full (353±25)	1.3
2e•2HCl	643±1.4	Full (433±94)	2.1
GABA	14.3±1.1	Full (389±12)	1.3
GABA + **2c**•2HCl	6.01±2.6	Super (530±48)	1.4
GABA + **3b**•2TFA	30.4±1.4	Full (362±36)	1.2

Although **2c** is 33-fold less potent than GABA, it is a 'superagonist' because its maximal uptake (E_{max}) is 49% higher than that achieved by GABA (Figure 2.2, Table 2.1). To establish that the superagonism of **2c** was not an artifact, we took steps to determine whether GABA active transport during the assay casued a sub-optimal GABA E_{max}. The GABA transport inhibitor nipecotic acid (100 μM)[12] was added to chloride flux experiments containing 13 μM and 1 mM GABA. In neither case did addition of nipecotic acid give additional ion flux (Figure 2.3), indicating that GABA transport did not limit GABA E_{max}, confirming the 'superagonist' status of **2c**.

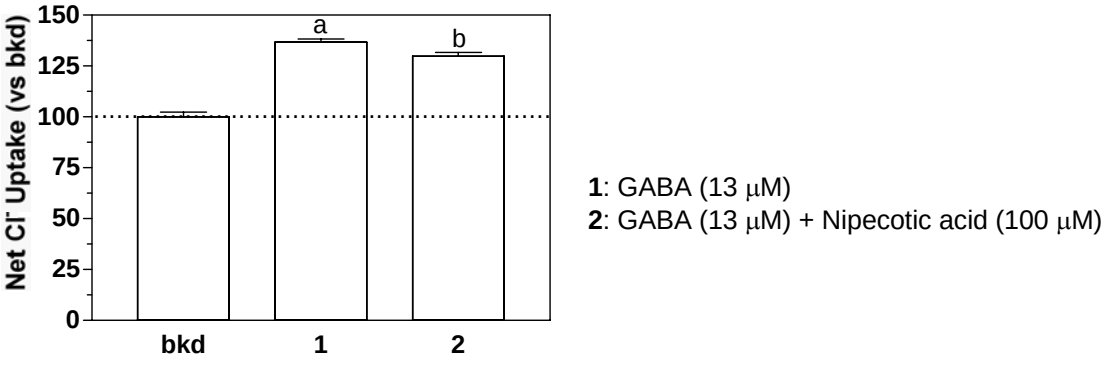

Figure 2.3 Effect of nipecotic acid (100 μM) on GABA-induced Cl^- uptake. Letters a and b signify that uptake is significantly different than background ($p<0.05$, *t*-test); and the uptake of experiment 1is not significantly different than that of experiment 2

To confirm that the effects of **2c** on chloride uptake were indeed mediated by the $GABA_AR$, control experiments were performed (Figure 2.4). Picrotoxinin (a $GABA_AR$ non-competitive antagonist) blocked the stimulating effects of **2c** on $^{36}Cl^-$ uptake, confirming that the observed uptake was mediated by the $GABA_AR$ and not another chloride channel. Additional controls with bicuculline (a $GABA_AR$ competitive antagonist) also showed the antagonism of chloride uptake by **2c**, confirming that observed **2c** bound to the same $GABA_AR$ agonist site as GABA.

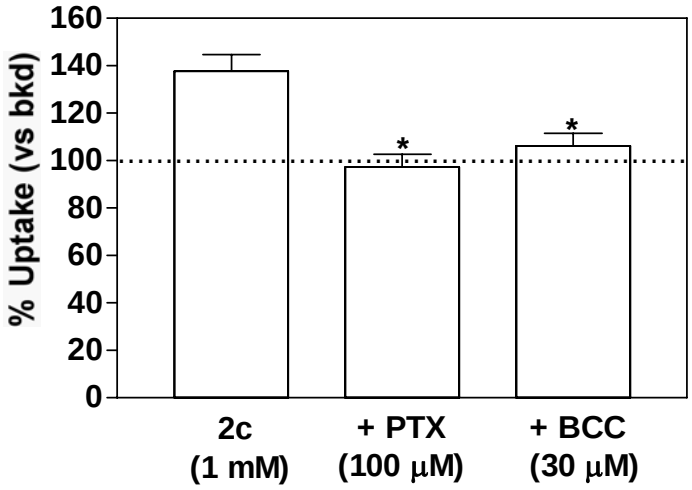

Figure 2.4 Effect of non-competitive (picrotoxinin, PTX) and competitive (bicuculline, BCC) inhibitors on $^{36}Cl^-$ ion flux elicited by **2c** (1 mM) in mouse brain synaptoneurosomes; bkd represents background uptake in the absence of agonist. Asterisks indicate that the aonist-induced uptake in the presence of blocker significantly less than that observed with 1 mM **2c** alone ($p<0.05$, *t*-test)

Compound **2c** is a 'superagonist' and also the best homodimer among the GABA amides that we have evaluated so far. In order to determine whether GABA and **2c** might show synergism with each other, we conducted a dose-response experiment of GABA in the presence of 250 μM **2c** (Figure 2.5). At lower concentrations of GABA (<1 μM), the net Cl^- uptake in the co-application experiment was due to the presence of 250 μM **2c** alone. As the concentration of GABA increased from 1μM to 100 μM, the dose-response curve of GABA in the presence of 250 μM **2c** did not level off at the E_{max} of GABA, but

rather reached the approximate E_{max} of **2c**. However, further increase in GABA concentration caused the net Cl^- uptake to decrease, suggesting that GABA dominated the binding at the $GABA_AR$ at higher concentrations (≥1 mM); and the effect of **2c** on receptor activation was no longer significant. Therefore, these data indicate that GABA and **2c** bind to the same site. At GABA concentration <1 μM, 250 μM **2c** competes with GABA for binding to the receptor and an additive effect of the two agonists is seen. However, above 1 mM, GABA out-competes 250 μM **2c** for binding to the receptor and a typical GABA E_{max} is seen.

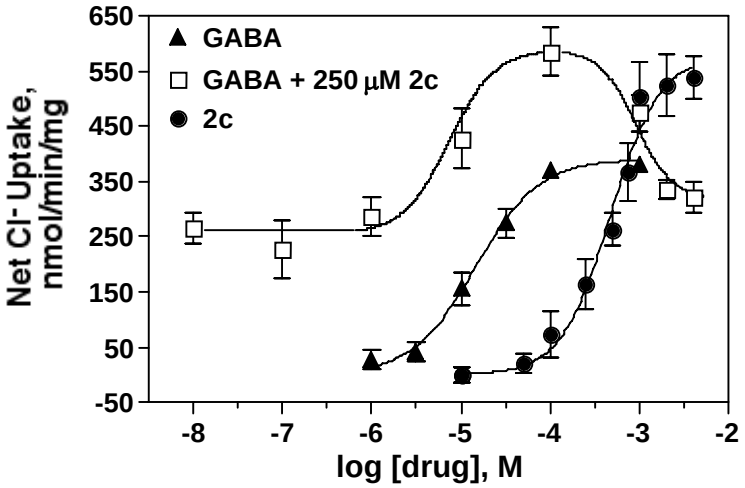

Figure 2.5 Co-incubation experiment of (dose-response curve of GABA + 250 μM **2c**) GABA and **2c**

2.1.2 Synthesis of Derivatives of 'Superagonist' Dimer 2c (4a-h)

We have discussed the role of tether length on agonism by the GABA amide dimers and shown that the optimum activity achieved by dimer with four methylenes. However, the distance imparted by this tether could be spanned with other linkers. It is possible that dimers that are structurally similar to **2c** will show greater potency or agonism than **2c**. In addition, flexible methylene tethers suffer from a higher entropic

penalty upon binding when compared to relatively rigid tethers. Partial rigidification of the tether can reduce the entropic penalty of binding, and hence improve efficacy or potency of GABA amide agonists. Thus, as part of our investigation of the structural requirements for optimal binding of GABA amide homodimers to the low-affinity sites on the $GABA_AR$, we replaced the tether length of four methylenes of **2c** with a more rigid framework **A** and that imparts approximately the same distance between N_1 and N_2 (Scheme 2.3).

Scheme 2.3 Design of derivatives of **2c** (**4a-h**)

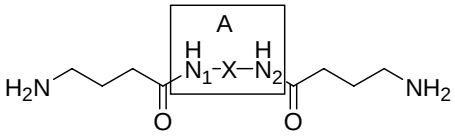

2c·2HCl
X = $CH_2CH_2CH_2CH_2$ (superagonist)

Compound	Framework A	Distance (Å)	Compound	Framework A	Distance (Å)
4a·2TFA	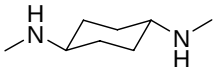	5.7	4e·2TFA	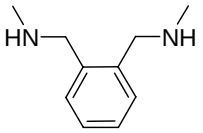	4.0
4b·2TFA	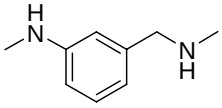	5.4	4f·2TFA	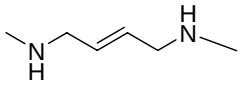	5.7
4c·2TFA	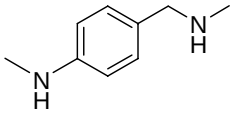	6.4	4g·2TFA	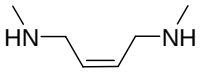	3.5
4d·2TFA	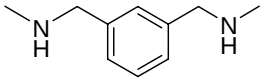	5.8	4h·2TFA	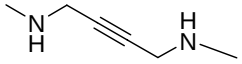	5.8

*N_1-N_2 distances of equilibrium geometries of **4a-h** in the fully extended conformation are measured at MM/MMFF, using Spartan'04 windows

Note that attempts to synthesize **4a** and **4b** from *N*-Boc-2-pyrrolidinone by refluxing in dioxane were unsuccessful. This was probably due to the steric crowding around the amine groups in *trans*-1,4-cyclohexanediamine which might inhibit formation

of the tetrahedral intermediate needed for reactivity with *N*-Boc-2-pyrrolidinone. On the other hand, 3-aminobenzylamine was less reactive because it is an aniline derivative, which makes it less nucleophilic. Both compounds are thus less reactive than the primary amines that were used in the synthesis of **2a-i**. Therefore, new GABA amide homodimers **4a-h** were prepared from *N*-Boc-GABA (**3**), which was synthesized according to the literature method in quantitative yield.[13] Coupling of diamines or hydrochloride salts of diamine with *N*-Boc-GABA in the presence of EDCI and DMAP in CH_2Cl_2 afforded the corresponding *N*-Boc GABA derivatives, and subsequent trifluoroacetic acid (TFA) deprotection provided **4a-h** as TFA salts in moderate to good yields (31-97%, Scheme 2.4). Et_3N (4.0 equiv.) was added to the coupling reaction when the HCl salts of diamine were used.

Scheme 2.4 Synthetic scheme of derivatives of **2c** (**4a-h**)

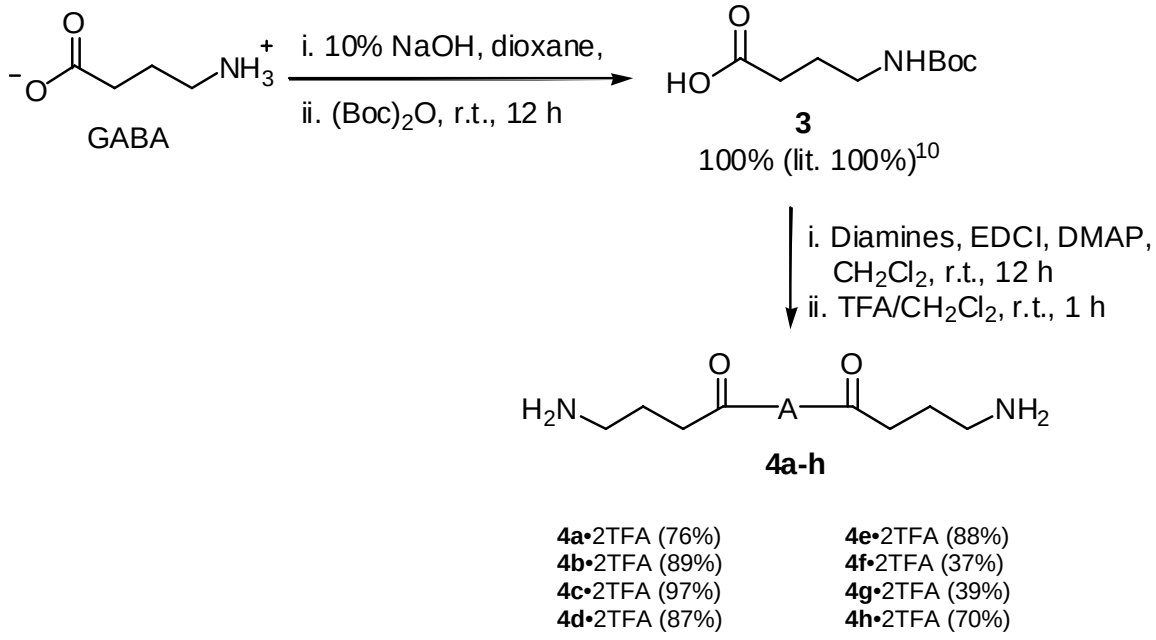

4a•2TFA (76%)
4b•2TFA (89%)
4c•2TFA (97%)
4d•2TFA (87%)
4e•2TFA (88%)
4f•2TFA (37%)
4g•2TFA (39%)
4h•2TFA (70%)

Four of the diamines that are used in the coupling reactions in Scheme 4 are not commercially available. These diamines include *o*-xylylenediamine, *trans/cis*-1,4-diaminobut-2-ene dihydrochlorides and 1,4-diaminobut-2-yne dihydrochloride, which are

in turn synthesized from corresponding dihalides according to the modified literature method (Scheme 2.5).[14] The synthesis of *o*-xylylenediamine has been reported previously, but the other three diamines are new compounds.

Scheme 2.5 Synthesis of dihydrochloride salts of diamine

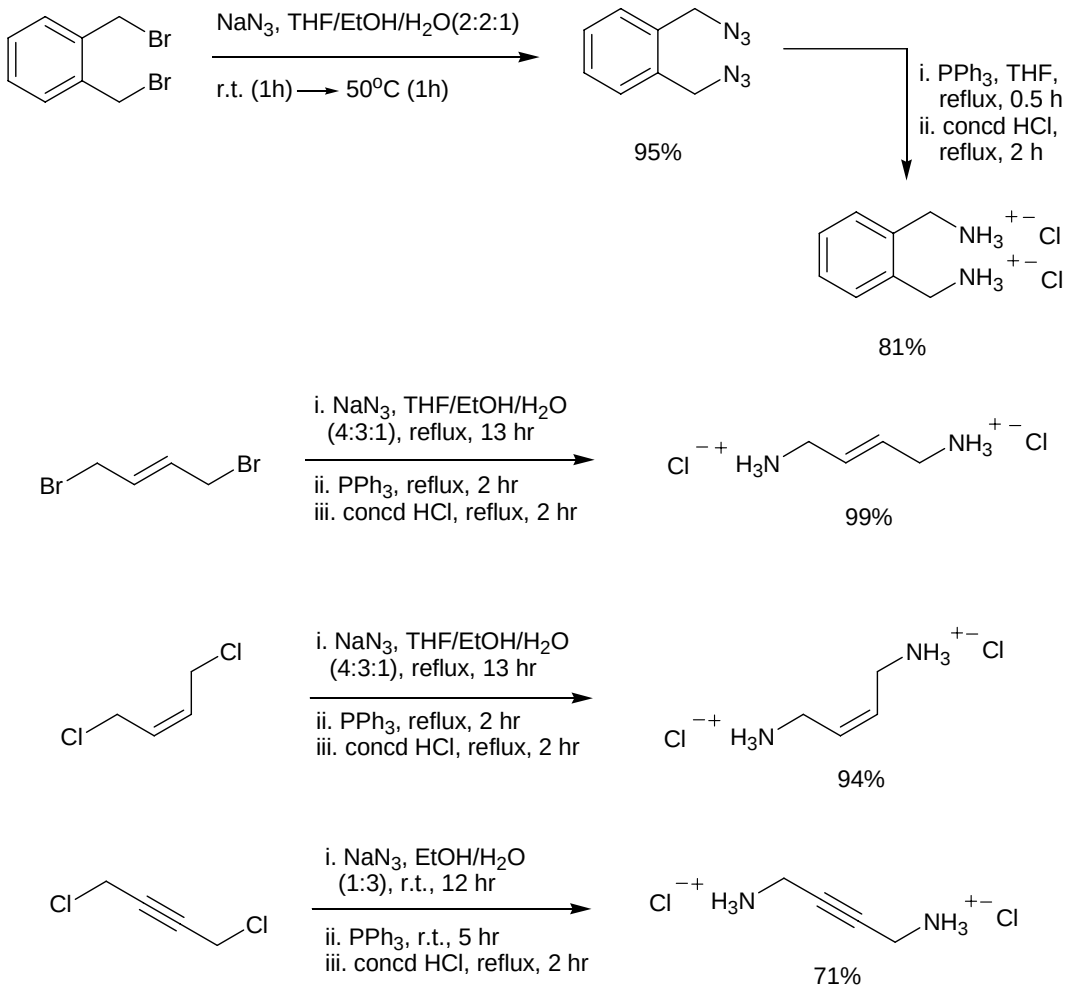

2.1.3 Bioassay Results of the Derivatives (4a-h)

All of these new analogues of **2c** derivatives were screened for their activity as $GABA_AR$ agonist. To our surprise, none of the new homodimer analogs **4a-h** elicited any net chloride uptake at the highest concentration tested (1mM). Apparently, partial rigidification of tethers of these new amide dimers caused the loss of activity, which indicates that flexible tethers (methylene chains) are important for agonism of GABA amide agonists. As agonists must bind to the receptor in both closed and open conformations, flexibility may be required to trigger a conformational change of the receptor and eventually the gating of the chloride channel.

In order to test the possibility that agonism, not binding, is diminished in the partially rigidified analogues, we screened these new amide dimers for their ability to block the stimulating effect of GABA on $^{36}Cl^-$ uptake.[15] Six of the new GABA amide dimers (**4b-g**) were found to inhibit the chloride ion flux elicited by GABA (Figure 2.6). As can be seen, the GABA-induced uptake in the presence of blockers (**4b-g**) were significantly less than that observed with 100 μM GABA alone ($p < 0.05$, *t*-test). Since all six of these new dimer analogs, which contain rigid double bonds, were not agonists but were antagonists, it was likely that partial rigidification caused these amide dimers to lose activity and antagonize GABA-induced channel activation.

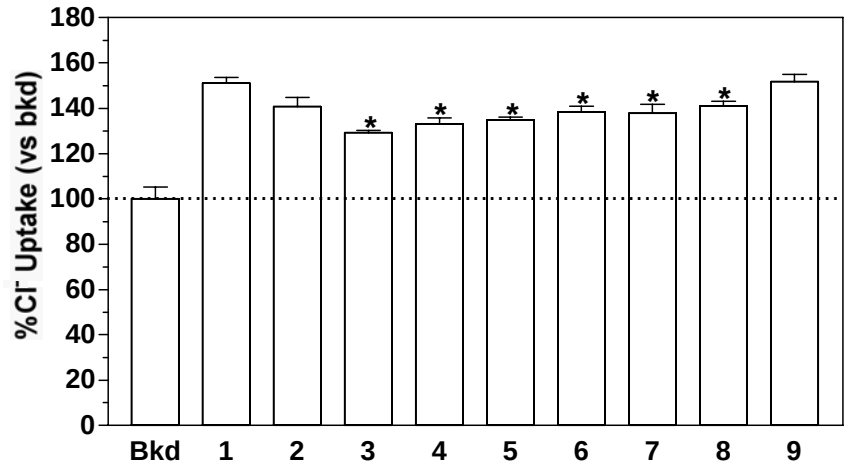

Figure 2.6 Effects of GABA amide dimer derivatives **4a-h** on ion flux elicited by GABA (0.1 mM); bkd represents background, uptake in the absence of agonist. Asterisks indicate that the GABA-induced uptake in the presence of the blocker at 1mM is significantly less than that observed with 0.1 mM GABA alone ($p < 0.05$, *t*-test)

We also performed the dose-response experiment of GABA in the presence of one of these antagonists, **4b**, in order to determine whether compounds **4b-g** are competitive or non-competitive antagonists. The result showed that the dose-response curve of GABA in the presence of **4b** was shifted parallel to the right (Figure 2.7). The potency of GABA was decreased by about 2-fold (Table 2.1), but E_{max} remained about the same as that of GABA alone. This experiment demonstrated that **4b** (and by extension **4c-g**) can compete with agonist for binding, but cannot gate the receptor.

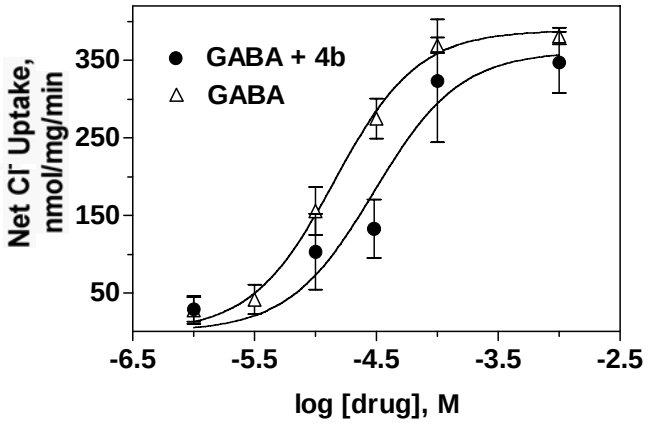

Figure 2.7 Inhibitory effect of **4b** on concentration dependent chloride uptake by GABA in mouse brain synaptoneurosomes

2.1.4 [^{3}H]Muscimol Binding Experiments

The inhibitory effect of these partial rigidified homodimers (**4b-h**) was further examined in the binding experiments. The ability of GABA, **2c** or **4b** to displace [^{3}H]muscimol from binding sites were tested in two different assays (filtration and centrifugation assays). Typical binding assays ([^{3}H]muscimol or [^{3}H]GABA) were done with frozen-thawed, well-washed, lysed membranes to optimize the binding.[16] However, these studies generated little information regarding low affinity binding associated with the channel gating in functional assay. In order to address this issue, both DeLorey and Brown (filtration assay) and Schwartz *et al.*[17] (centrifugation assay) have done binding studies under conditions that more closely approximate functional assays, and found only micromolar binding of [^{3}H]muscimol (1.9 μM [16] and 2.0 μM[17] respectively). Based on Brown's literature method, we carried out [^{3}H]muscimol (70 nM) binding experiments in the presence of three unlabeled ligands (1 mM GABA, **2c** and **4b** respectively). The specific [^{3}H]muscimol binding in the presence of 1 mM GABA or **2c** was about 50% of total binding. This value was comparable to the value that reported (40%) by DeLorey

and Brown.[16] However, specific [^{3}H]muscimol binding in the presence of the weak antagonist **4b** was indistinguishable from background (Figure 2.8). One possible reason for the apparent lack of binding by **4b** is the rapid washing and filtering used in the filtration assay. Since **4b** is a low potency antagonist, the wash and filtration may have facilitated the dissociation of **4b** from the binding sites; thus no binding was detected.

The centrifugation assay is better at detecting low affinity binding since no rapid wash and filtration are required as in the filtration assay. Thus, dissociation of weakly bound ligands to the binding sites should be minimal in the centrifugation assay. We therefore conducted [^{3}H]muscimol (70 nM) binding experiments in the presence of three unlabeled ligands (1 mM GABA, **2c** and **4b** respectively) based on Schwartz's method.[17] Unlabeled mucimol (1 μM) was also added to each experiment to ensure the measurement of low affinity-site binding. In the presence of 1 mM GABA or **2c**, the specific [^{3}H]muscimol binding was about 40% (Figure 2.8). This result again indicated that **2c** bound to the same sites as GABA. The specific [^{3}H]muscimol binding in the presence of the weak antagonist **4b** was only about 15%; however this result was statistically significant. The result of **4b** also shows that the centrifugation method is a better technique for weak agonist or antagonist binding. In general, these results were in good agreement with Schwartz's published data (56 to 67% specific [^{3}H]muscimol binding in the presence of 1 mM GABA).[17]

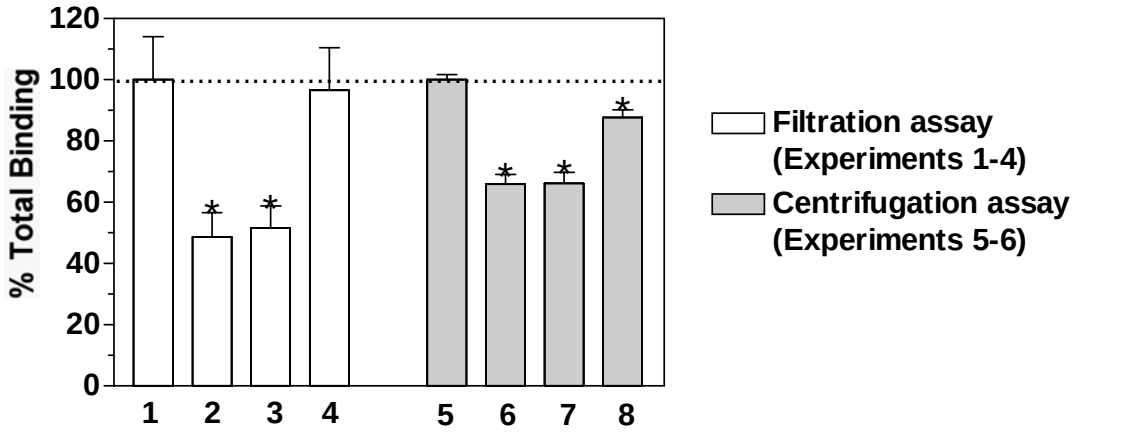

1: 70 nM [^{3}H]muscimol
2: 70 nM [^{3}H]muscimol + 1 mM GABA
3: 70 nM [^{3}H]muscimol + 1 mM **2c**
4: 70 nM [^{3}H]muscimol + 1 mM **4b**
5: 70 nM [^{3}H]muscimol + 1 μM muscimol
6: 70 nM [^{3}H]muscimol + 1 μM muscimol + 1 mM GABA
7: 70 nM [^{3}H]muscimol + 1 μM muscimol + 1 mM **2c**
8: 70 nM [^{3}H]muscimol + 1 μM muscimol + 1 mM **4b**

Figure 2.8 % Total binding of [^{3}H]muscimol in the presence of unlabeled ligands and other unlabeled ligands in mouse brain synaptoneurosomes. An asterisk indicates that the binding is significantly different than from treatment 1 ($p < 0.05$, *t*-test)

Despite the fact that we have conducted the [^{3}H]muscimol binding experiments in two completely different assays, the values of specific [^{3}H]muscimol binding (in the presence of 1 mM GABA or **2c**) generated from the centrifugation assay (micromolar concentration measurements) were not significantly different ($p > 0.05$, *t*-test) than the results that obtained from the filtration assay (nanomolar concentration measurements). A similar observation has also been made by Brown *et al.* In both assays, synaptoneurosomes and the ligands were co-incubated for 20 to 30 minutes, which allowed the tissue and ligands to equilibrate before filtration or centrifugation.

Note that since we have not performed any dose-response binding experiments, we are not able to determine the actual K_d of either GABA or **2c** to displace [^{3}H]muscimol. All we can say is that these compounds do displace [^{3}H]muscimol under conditions optimized to assess low affinity binding.

2.2 Syntheses and Evaluation of heteromeric $GABA_A$ receptor analogs

Simple GABA amide heterodimers **1a-b**, and **5a-e** were also prepared from *N*-Boc-2 pyrrolidinone (Scheme 2.6). In the case of **5a-e**, excess corresponding amines were used in order to obtain good yield of heteromers instead of dimers. In order to prepare GABA amides with a pendant acetyl group, acetylation of the terminal amino group was carried out before acidic deprotection, to afford **6a-e** in moderate to good yields (Scheme 2.7). In general, HCl deprotection provided crystalline products; in case where the HCl salts were not crystalline, the trifluoroacetic acid salts were prepared.

Scheme 2.6 Synthetic scheme for simple GABA amides

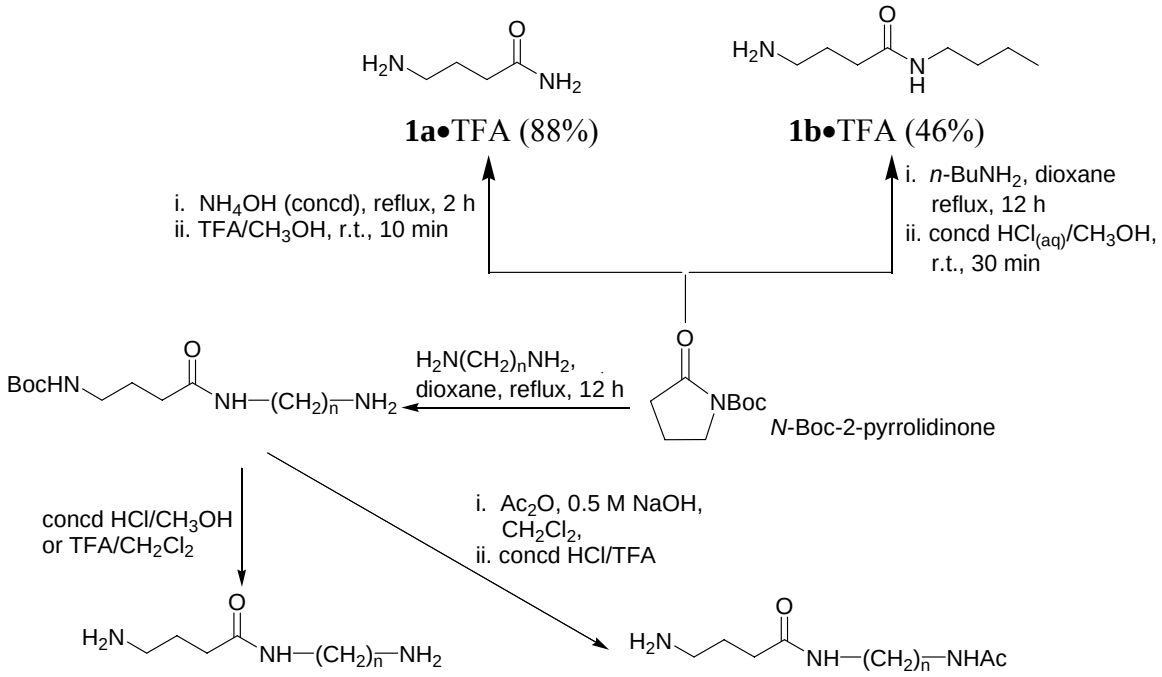

5a•2TFA n = 2 (80%) **5d**•2TFA n = 5 (74%)
5b•2TFA n = 3 (51%) **5e**•2TFA n = 6 (92%)
5c•2HCl: n = 4 (77%)

6a•TFA: n = 2 (48%) **6d**•TFA: n = 5 (95%)
6b•TFA: n = 3 (85%) **6e**•TFA: n = 6 (83%)
6c•HCl: n = 4 (61%)

Attempts to synthesize **1c** in the same method as other simple GABA amides failed (Scheme 2.7). Thus compound **1c** was prepared from aniline and *N*-Boc-GABA using the EDCI/ DMAP coupling method in excellent yield (Scheme 2.7).

Scheme 2.7 Synthesis of **1c** under two different conditions

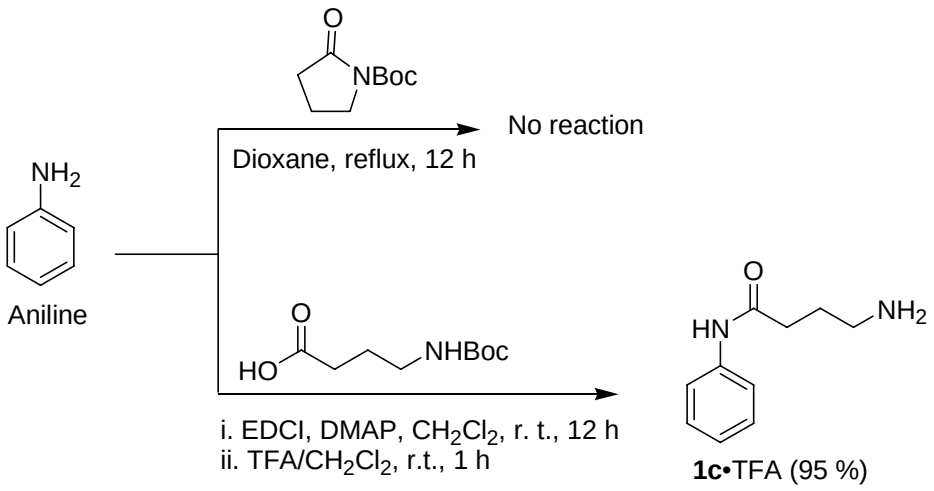

2.2.1 Bioassay Results of the Amide Heterodimers

All of these amide heteromers were also screened for their activity as $GABA_AR$ agonists using the same functional assay that we employed previously. As in the case of dimers, two of these heterodimers (**5c•**2HCl and **6c•**2HCl) were also analyzed by HPLC prior to assay to make sure that they were free trace of GABA contamination (<0.1 wt%). In fact, compounds **5a** and **6a** were first synthesized as hydrochloride salts, which turned out to be contaminated with GABA (>0.1 wt%). Compounds **1a-b** were reported by other workers to be inactive in a high affinity [^{3}H]GABA binding assay, and were shown to be partial and full agonists respectively (Figure 2.9, Table 2.2). However, compound **1c** was inactive in the functional assay. As we mentioned in chapter 1, THIP is shown to be a $GABA_AR$ partial agonist and a potent antinociceptive agent[18]. As can be seen in

Figure 2.9, the EC_{50} values and degree of agonism of compounds **1a** and **1b** were comparable to that of THIP.

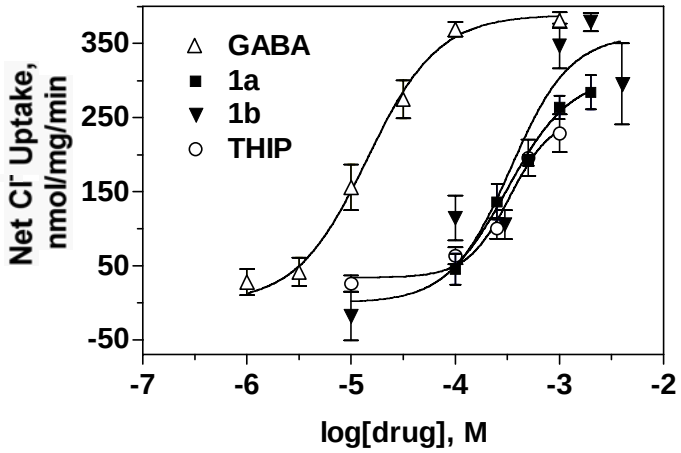

Figure 2.9 Dose-response relationship of Cl^- uptake and drug (GABA, **1a-b** and THIP) concentrations in mouse brain synaptoneurosomes

Both series of compounds **5a-e** and **6a-e** were first tested for their ability to elicit Cl^- uptake at 1mM (Figures 2.10). As can be seen, in the series of **5a-e**, chloride uptake above background was significant only for tether length of 4 and 6 methylenes (**5c** and **5e**,); neither **5a** nor **5b** was active at 1 mM, however, activity seemed to increase as the tether length increased from 2 to 4 methylenes. It appeared that agonism of this series of compounds was also tether length dependent, as in the case of amide dimers (**2a-i**). We also observed the same tether length dependence trend for compounds **6a-e**. Chloride uptake above background was significant for tether length of 3 to 5 methylenes (**6b-d**), but not for **6a** and **6e**. In both compounds **5** and **6** series, the optimum tether appeared to be four methylenes, which is consistent with the optimum tether length that we observed in the amide dimer series.

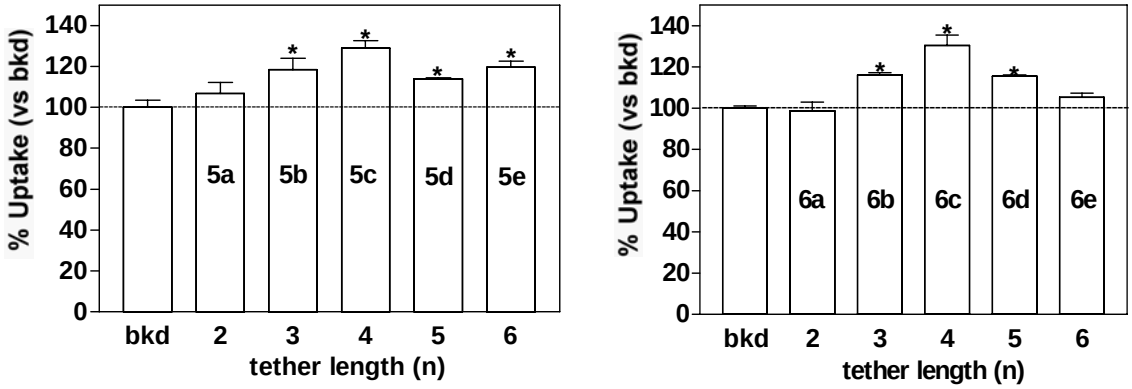

Figure 2.10 Effect of tether length of GABA amides (n = number of methylenes) on chloride flux (at 1 mM drug) in mouse brain synaptoneurosomes, expressed as % uptake versus background. An asterisk indicates that the uptake is significantly different than background ($p < 0.05$, *t*-test)

Table 2.2 $GABA_AR$ agonism by GABA amides and controls

Compound	Chloride uptake EC_{50}, μM	Agonism (E_{max})	Hill Slope
1a•TFA	313±1.1	Partial (307±19)	1.4
1b•2HCl	336±1.9	Full (361±81)	1.5
5c•2HCl	1137±1.4	Full (497±76)	1.5
6c•2HCl	422±1.3	Full (549±40)	1.7
7a•TFA	317±1.1	Partial (188±8)	1.0
THIP	643±1.4	Partial (252±20)	2.1

We have also obtained the EC_{50} values of both compounds **5c** and **6c** from dose-response curves (Figure 2.11, Table 2.2). Both of these compounds are full agonists, but less potent than GABA. Since within experimental error the E_{max} values of **5c** and **6c** match that of GABA. Based on the agonism of **5c** and **6c**, the pendant amide group (**6c**) appears to be superior to the ammonium group (**5c**). This suggests that proximal to the agonist binding site there exist a site that can weakly bind the pendant amide group. The superior activity of **6c** to **5c** (note these differ only in that **6c** has an additional acetyl group) must be due to another complementary binding interaction of the acetyl group in **6c**.

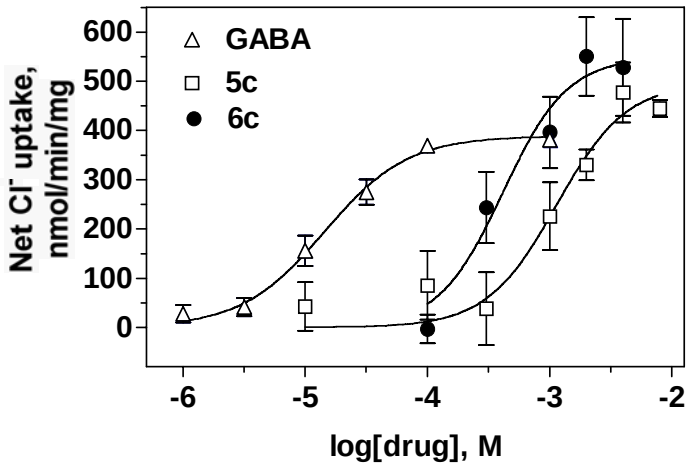

Figure 2.11 Dose-response relationship of Cl^- uptake and drug (GABA, **5c** and **6c**) concentrations in mouse brain synaptoneurosomes

Four methylenes appear to be the optimum tether length for these two series of amide heterodimers; however, only two pendant groups (acetamide and amino groups) have been explored so far, it is too early to conclude that the acetamide group is the best pendant group among the amide heterodimers with four methylenes. Moreover, the binding preferences of the proximal subsite are unknown. Therefore, as part of structural investigation for this kind of compounds, we optimized the pendant group (Y) based on the structure of **6c** (Scheme 2.8).

Scheme 2.8 Design of derivatives of **6c** (**7a-i**)

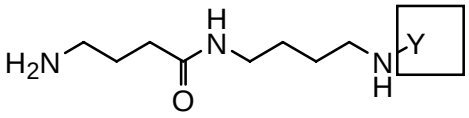

6c·2HCl

Y = $COCH_3$ (full agonist)

Compounds	Pentant groups	Compounds	Pentant groups
7a·TFA	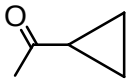	**7f**·TFA*	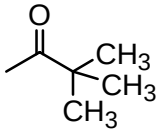
7b·TFA	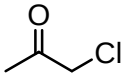	**7g**·HCl*	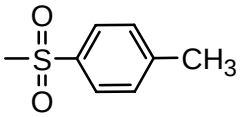
7c·HCl*	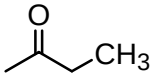	**7h**·TFA*	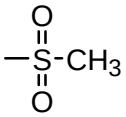
7d·HCl*	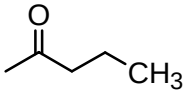	**7i**·TFA*	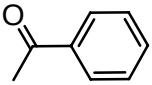
7e·TFA*	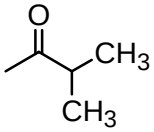		

*Compounds **7c-i** were synthesized by Yiqun Zhang; bioassay experiments were performed by the author.

Based on the structure of **6c**, nine compounds (Scheme 2.8, **7a-i**) were synthesized by varing the pendant groups Y. All of these compounds were synthesized in good yields according to the procedures that we used for the sythesis of **6c**, with the exception that pyridine or Et_3N was used as base (instead of 0.5 M NaOH) in some cases. The bioassay results for this series of compounds reveal a significant loss of activity when compared with the original compound (**6c**). Only two out of these nine compounds are active at the highest concentration tested (1mM). Compound **7a** is a partial agonist (Table 2.2, dose-response curve is not shown), and though **7c** induces chloride uptake significantly above the background at 1 mM, the potency of **7c** is too weak to be

determined. All of these nine compounds are structurally similar to **6c**; however, replacing the acetamide group with either the bulkier amide groups or sulfonamide groups caused a loss of activity. These results suggest the important role of the actamide group in investigated bioactivity. These results also suggested that the proximal binding site for the pendant amide is small.

2.3 Syntheses and Evaluation of ZAPA and its derivatives

2.3.1 Synthesis of ZAPA and its derivatives

As mentioned in chapter 1, ZAPA (*Z*-3-[(aminoiminomethyl)thio]prop-2-enoic acid), an isothiouronium analog of GABA (γ-aminobutyric acid), is a potent $GABA_AR$ agonist, which is a potentially therapeutic agent for anxiety, epilepsy, and pain.[19] ZAPA has also shown good antidiabetic activity in animal models of non-insulin diabetes mellitus (NIDDM).[20] Interestingly, the *E*-isomer of ZAPA has been shown to be inactive at the $GABA_AR$.[21] A structure-activity relationship study of ZAPA have been reported by Allan *et al.*[22] in 1997 in a guinea pig ileum contraction assay, which tested the ability of ZAPA and its derivatives to produce GABA-like contractions in the guinea pig ileum. Most of the ZAPA derivatives studied by these authors produced GABA-like agonism, but all of them were less potent than either GABA or ZAPA.[22] However, none of the derivatives that studied by Allan and co-workers have been tested in a standard $^{36}Cl^-$ flux or electrophysiological functional assay. Due to our interest in preparing ZAPA linked bivalent agonists that can be tethered to other drug sites, we synthesized two new and two known ZAPA derivatives and the tested these derivatives in the standard $^{36}Cl^-$ flux functional assay for the first time.

ZAPA derivatives were prepared from the corresponding primary *N*-alkylthioureas and propiolic acid. The traditional syntheses of primary or *N*, *N*'-disubstituted thioureas usually involved a two-step process, which often required vigorous conditions to cleave the benzoyl group from thiourea.[22, 23 -27] We employed several modified methods that were reported in the literature for the synthesis of *n*-alkylthioureas. Most of the methods that we tried were unsuccessful. Prolonged heating and use of strong bases led to the formation of side product *n*-alkylurea. Detailed syntheses were shown in Table 2.3.

Table 2.3 Two-step synthesis of *n*-alkylthioureas

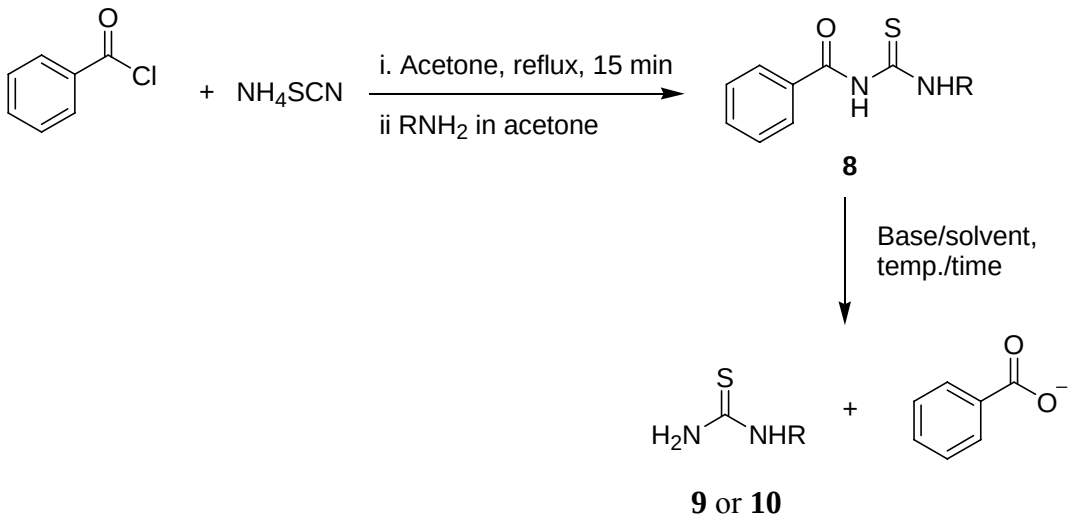

Entry	Base/solvent	Temp/time	Remarks	R
1	4.0 eq. KOH/ EtOH	Heated in a pressurized bottle/10 h	Isolated 30% yield of thiourea and 24% yield of side product urea	*n*-butyl
2	2.0 eq. KOH/ 1-pentanol	Reflux/1 h	Observed 8 spots on TLC; no pure product isolated	*n*-pentyl
3	4.0 eq. KOH/ 1-pentanol	Reflux/1 h	Recovered *n*-pentyl amine and isolated 26% yield of urea	*n*-pentyl
4	4.0 eq. KOH/ 1-pentanol	Heated in a pressurized bottle/10 h	Recovered *n*-pentyl amine	*n*-pentyl
5	4.0 eq Na/ EtOH	r.t. to reflux/15min	Isolated 42% yield of product	*n*-pentyl
6	4.0 eq KOH/ EtOH	Reflux/2 h	Isolated 77% yield of product	*n*-pentyl
7	2.0 eq K_2CO_3/ MeOH-H_2O	Reflux/2 h	Isolated 84% yield of product	*n*-pentyl
8	10% NaOH/ MeOH	Reflux/2 h	Isolated 83% yield of product	*n*-pentyl

Due to initial unsuccessful attempts to synthesize *N*-alkylthioureas from the two-step method described above, we explored other reaction conditions at the same time. Eventually, we found that compound **9** and **10** could be synthesized from a simple one-step synthesis of *n*-alkylthioureas from respective *n*-alkylamines and 1,1'-thiocarbonyldiimidazole, using the modified literature method in good yields (74-89%, Scheme 2.9).[28] The corresponding ZAPA derivatives **11** and **12** were prepared from respective primary *n*- alkylthioureas (**9** and **10**) and propiolic acid (Scheme 2.9). ZAPA was prepared as an off-white crystalline hydrochloride salt based on the literature method.[29]

Scheme 2.9 Synthesis of ZAPA derivatives

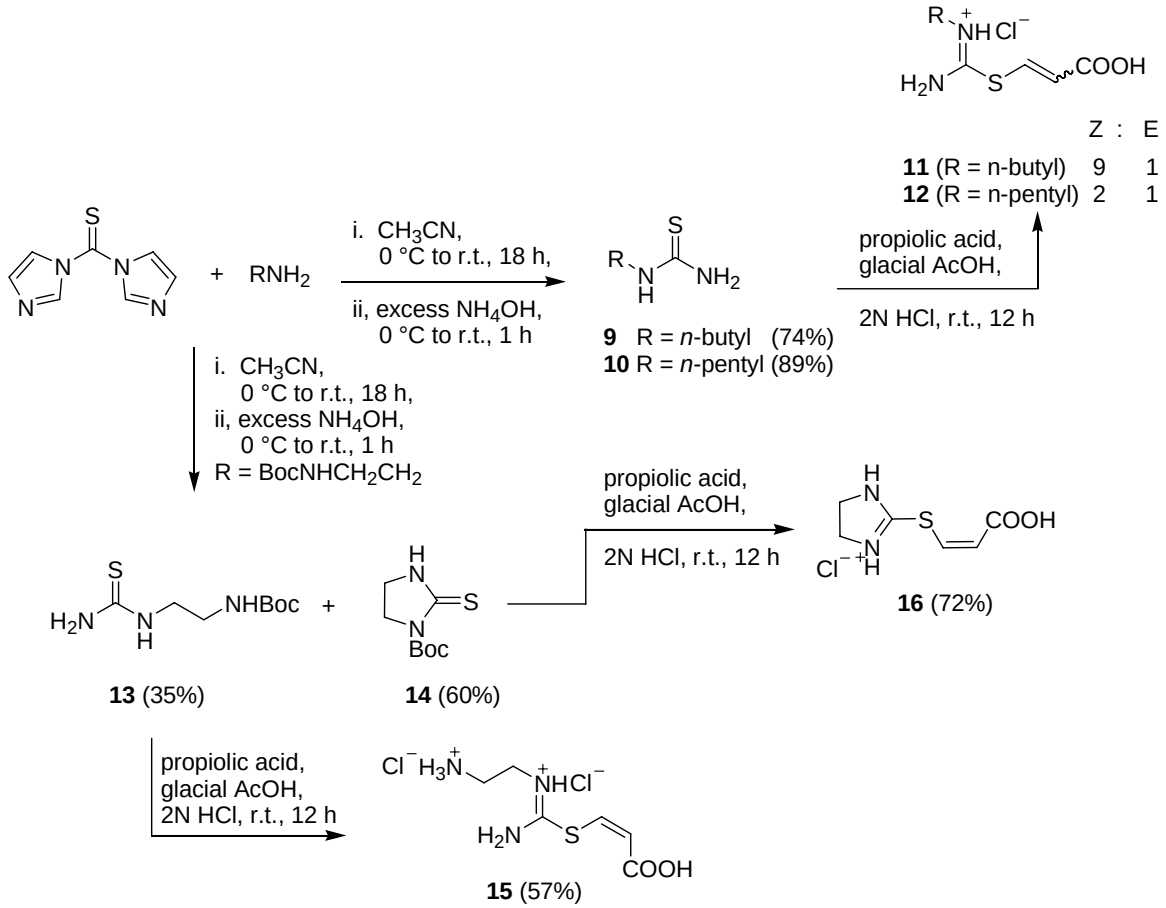

The corresponding two *N*-alkylZAPA analogs (**11** and **12**), as reported by Allan *et al.*,[22] were prepared as mixtures of *Z* and *E* isomers (Scheme 2.9), which were difficult to separate due to their non-crystalline nature. The synthesis of compound **12** was previously reported by Allan *et. al*, but compound **11** was not previously known. An attempted to synthesize *N*-ethyl-3-(aminoiminomethyl)thiourea **13** yielded a mixture of compounds, with compound **14** being the major product. Apparently compound **13** underwent an intramolecular nucleophilic addition and eliminated NH_3 from the reaction (Scheme 2.10). Both compounds **13** and **14** reacted with propiolic acid under acidic conditions to afford pure *Z*-isomers (**15** and **16** respectively) after crystallization.

Scheme2.10 Proposed mechanism for the formation of compound **13**

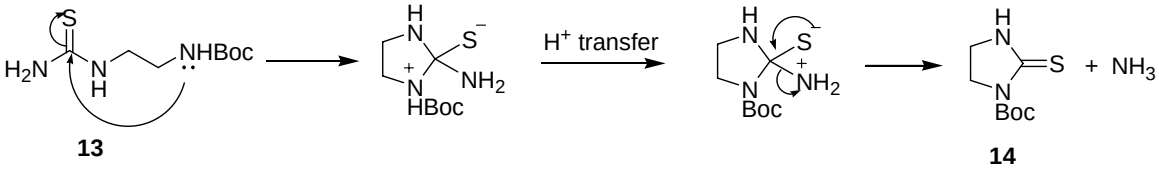

2.3.2 Bioassay Results of ZAPA and its derivatives

We tested all four of these ZAPA derivatives (**11**, **12**, **15**, **16**) in the $^{36}Cl^-$ flux functional assay. As mentioned in earlier section, compounds **12** and **16** were previously tested in guinea pig ileum, but not in a neuronal $^{36}Cl^-$ flux assay. Compounds **11** and **12** were tested as a mixture of *Z/E* isomers (**11**: *Z/E* 9:1; **12**: *Z/E* 2:1) in the standard $^{36}Cl^-$ functional assay. Allan *et al.*[22] have reported that *Z/E* mixture of *n*-pentyl ZAPA (**12)** was 2.5 times less potent than GABA; however, we found that the potencies of both **11** and **12** were comparable to that of GABA (Figure 2.12, Table 3.3). In fact, compound **12** (*n*-pentyl ZAPA, 12.4 μM) was in fact slightly more potent than GABA (14.3 μM).

Compound **15** was also found to be a $GABA_AR$ agonist with a EC_{50} value of 95.6 μM (Figure 2.12, Table 2.4). Interestingly, the net chloride uptake of compound **15** did not reach down to zero as other two ZAPA derivatives at the lowest concentration tested (1μM).

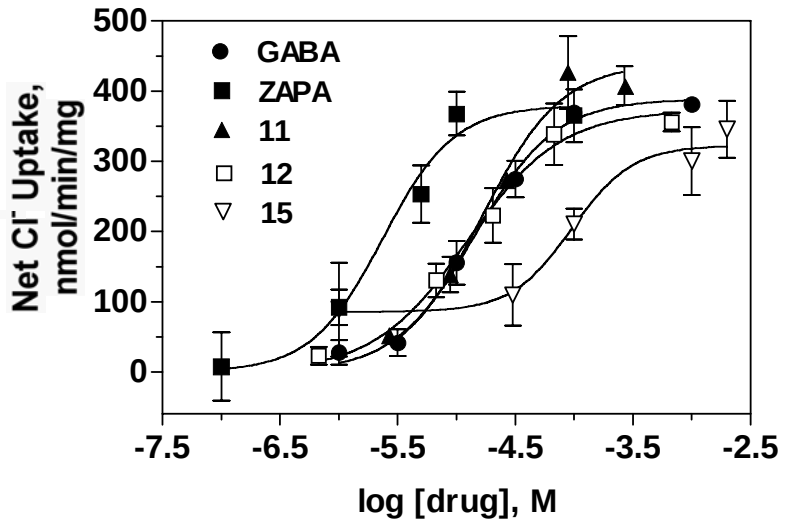

Figure 2.12 Dose-response relationship of Cl^- uptake and drug (GABA, ZAPA, compound **11**, **12** and **15**) concentrations in mouse brain synaptoneurosomes

Both compounds (**11** and **12**) were about 6 to 7-fold less potent than ZAPA (Table 2.3). Since the *E*-isomer of ZAPA has been shown to be inactive at the $GABA_AR$,[21] we calculated the EC_{50} values of **11** and **12** in terms of the concentrations of *Z*-isomers only. Attempts to recrystallize pure *Z*-isomer from *Z/E* mixture of **12** yielded mainly its *E*-isomer (97:3 *E/Z*) as a white solid. We conducted a dose-response experiment (1 μM to 2 mM) on this 97% pure *E*-isomer. When the concentrations were ≥1mM, the chloride uptake induced by this 97:3 *E/Z* mixture were significantly different than background ($p < 0.05$, *t*-test, Figure 2.13); however, when concentrations were ≤ 100 μM, the chloride uptake elicited by this compound were indistinguishable from the background. Thus the activity of the 97:3 *E/Z* mixture at both 1 mM and 2 mM is likely due to the presence of a

small amount (3%) of the *Z*-isomer. This experiment further confirmed that *E*-isomers of ZAPA and its derivatives were indeed inactive at the $GABA_AR$.

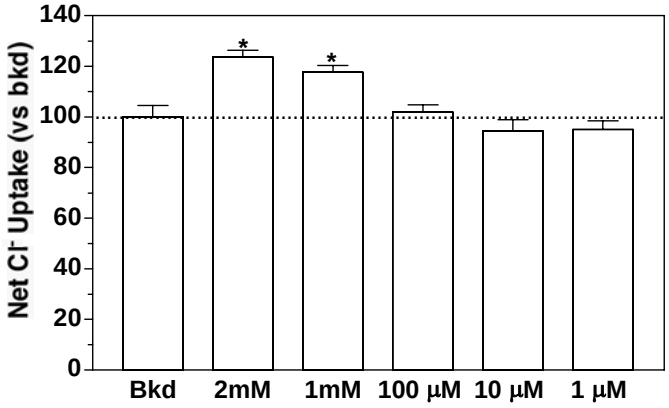

Figure 2.13 Ion flux elicited by 97% pure *E*-isomer (with 3% *Z*-isomer) of compound **12** in mouse brain synaptoneurosomes, expressed as % uptake versus background. An asterisk indicates that the uptake is significantly different than background ($p < 0.05$, *t*-test)

Table 2.4 $GABA_AR$ agonism, EC_{50} values and Hill slopes of GABA, ZAPA and ZAPA derivatives

Compound	Chloride uptake EC_{50}, μM	Agonism (E_{max})	Hill Slope
11•HCl	16.4±1.3	Full (440±36)	1.4
12•HCl	12.4±1.2	Full (373±23)	1.3
ZAPA	2.4±1.3	Full (379±28)	1.4
15•2HCl	95.6±1.4	Full (323±34)	1.7
GABA	14.3±1.1	Full (389±12)	1.3

Compound **16** may be viewed as a restricted conformer of *N*-ethyl-3-[(aminoiminomethyl)thio]prop-2-enoic acid (**15**) and it was shown to be 30-fold less potent than GABA in producing GABA-like contraction activity in guinea pig ileum.[22] However, when we tested **16** in the functional assay; it did not show any agonism at the highest concentration (2 mM) tested (Figure 2.14).

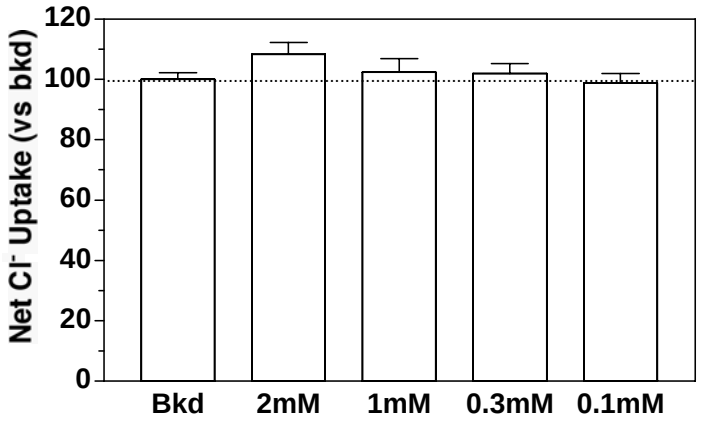

Figure 2.14 Ion flux elicited by 4 different concentrations of compound 15 in mouse brain synaptoneurosomes, expressed as % uptake versus background

Allan and co-workers discovered that the GABA-like contraction activity of *N*-substituted ZAPA derivatives increased significantly when the size of alkyl group increased from methyl to hexyl, with maximum activity obtained by *N*-hexyl and pentyl derivatives. No clear explanation has been reported for the activity changes as the alkyl group became longer. From the assay results of these four ZAPA derivatives (**11**, **12**, **15** and **16**) that we tested, we also observed that the activities of these compounds increased as the alkyl chain became longer and the potency was greatly enhanced as the alkyl group changed from hydrophilic group (**15**) to hydrophobic alkyl groups (**11** and **12**). We propose that there are two main factors that affected the strength of *N*-substituted ZAPA derivative- $GABA_AR$ interactions: steric compensation and desolvation penalty. Steric compensation is the steric effect that changes the shape of both agonist and the receptor in order to allow binding of the agonist to the receptor. The desolvation penalty is the desolvation energy of both the receptor and the ligand that must be overcome before a charged ligand (*N*-substituted ZAPA derivative) can either bind to a hydrophobic host ($GABA_AR$, Figure 2.15) or activate the receptor. In our case, the desolvtion penalty effect outweighed the steric effect. The more hydrophobic the ligand, the less

desolvation penalty would be, as reflected in the agonism of compounds **11**, **12**, **15** and **16**.

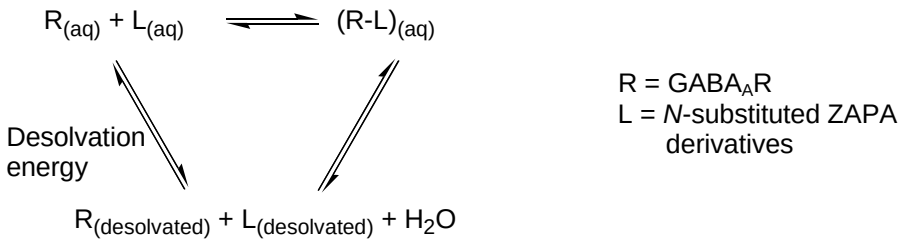

Figure 2.15 A schematic diagram of desolvation penalty effect in ligand-receptor interaction

2.4 Syntheses and Evaluation of PEG-linked $GABA_A$ receptor analogs

2.4.1 Synthesis of PEG-linked GABA amide dimers

This part of the GABA project involves design of bivalent agonists to test models of $GABA_AR$ structure and function. It has been shown in the literature that $GABA_AR$ has two low affinity agonist sites.[30,31] How far are these agonist binding sites on the $GABA_AR$? To date, no estimates have been published and within this superfamily, most is known about nAChR. During the course of our research, the leading theories on the location of these sites underwent major change. Electron microscopy of the nicotinic acetylcholine receptor (nAChR), although at low resolution, suggests a 70 Å-wide heteropentameric transmembrane structure ($(\alpha_1)_2\beta\gamma\delta$) with an approximate 30 Å-wide central, water-filled pore.[32] On the basis of microscopy,[33,34] and fluorescence resonance energy transfer (FRET)[35] of the intact nAChR receptor, the agonist (ACh) binding sites were proposed to be located at the bottom of 20 Å deep channels on the extracellular face of the receptor. This proposed localization would result in a through-space distance between two agonist binding sites on the nAChR of 40-50 Å.

However, Sixma *et al.*[36] published an X-ray crystal structure of a related protein, the acetylcholine binding protein (AChBP), that revealed the same general gross structure features. AChBP is a soluble homopentameric protein found in the nail *Lymnaea stagnalis*. AChBP is not a functional protein, and it does not possess the transmembrane and intracellular portions of the nAChR. However, the primary sequence of the AChBP and the extracellular portion of the α-subunit of the nAChR are highly similar. In addition, the AChBP binds nAChR agonists and antagonists such as acetylcholine and nicotine. Five HEPES (*N*-2-hydroxyethylpiperazine-*N'*-2-ethanesulphonic acid) surfactants are also found to bind at residues corresponding to those proposed to line the agonist binding sites in the nAChR. HEPES contains a positively charged quaternary ammonium group, and thus it is similar to some known nicotinic receptor ligands. For these reasons, the AChBP likely provides the clearest picture to date of the nAChR.

The ligand-binding sites in the AChBP structure are proposed to be at subunit junctions on the external cylindrical portion of the receptor, approximately 22 Å below the extracellular face (Figure 2.16). Figure 2.16 shows the homopentameric structure of the AChBP and presence of 5 identical ligand binding sites at the subunit junctions.

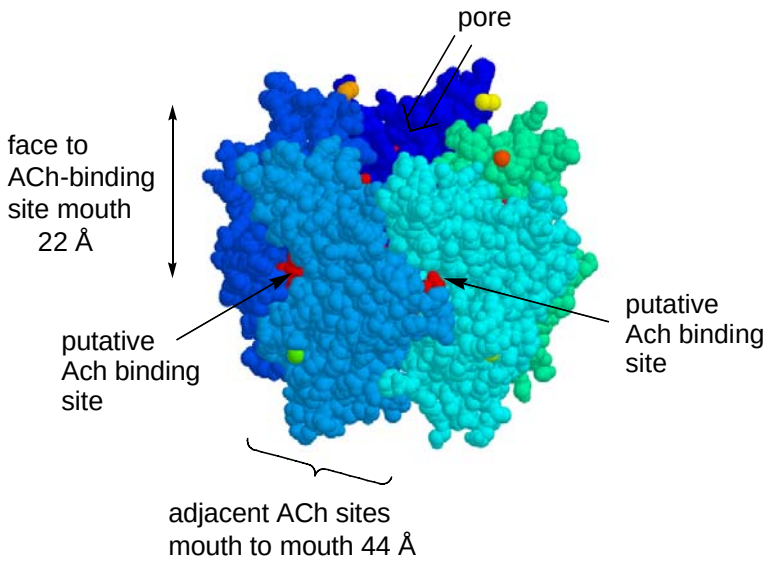

Figure 2.16 Side view of X-ray crystal structure of the AChBP (pdb code 1I9B, graphic created with RasMol Molecular Graphics). HEPES ligands (red) represent the putative ACh binding sites

As mentioned previously, the nAChR and $GABA_AR$ belong to the same ligand-gated ion channel (LGIC) superfamily, and share similar structural and functional features.[37] By assuming that there is a high degree of homology between the $GABA_AR$ and nAChR, we can estimate a mouth-to-mouth distance of 40-50 Å between two low affinity agonist sites on the $GABA_AR$ based on nAChR-like facial model, and a "as the crow flies distance" distance (through space distance) of 88 Å (Figure 2.17) between these two sites based on AChBP-like structural model (cf. Figure 2.16).

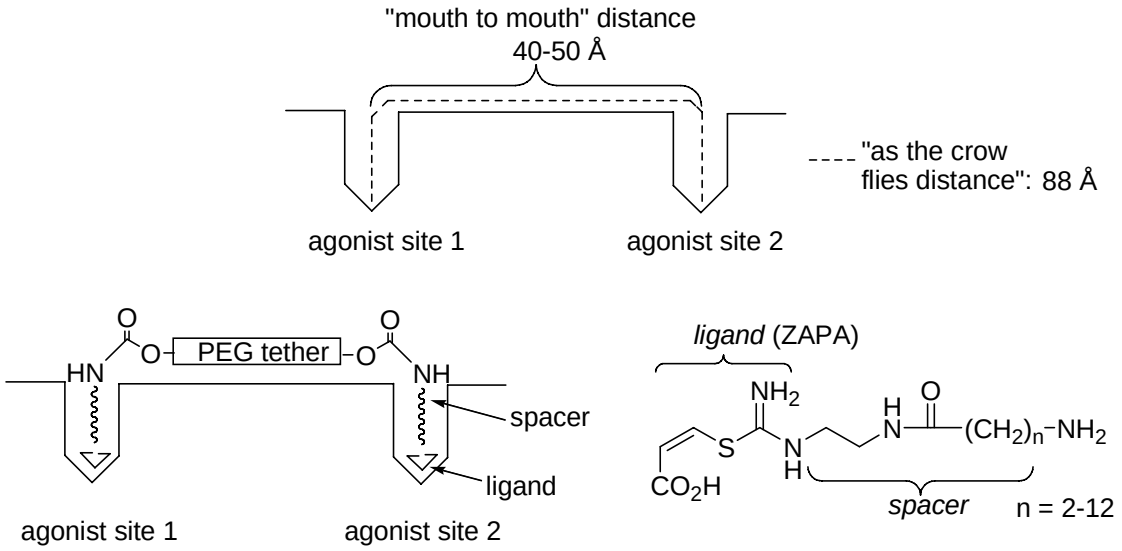

Figure 2.17 A simplified schematic diagram of mouth-to-mouth distance between two agonist binding sites of on the $GABA_AR$ (top), and a bivalent ligand designed to span the sites (bottom, with an example of liagand (ZAPA in this case) and spacer)

How can we span the distances between the relevant binding sites? One strategy is to synthesize homodimers that can span such long distances; this can be achieved by linking $GABA_A$ agonists with poly(ethylene glycol) (PEG) derived tethers (Figure 2.17, bottom right). Kramer and Karpen,[38] and Fan[39] have demonstrated that bi- and multivalent binding at distances of 15-45 Å can be achieved successfully by use of these tethers. Carlier and Pang have also demonstrated that dual-site binding enhances the inhibition of acetylcholinesterase (Scheme 2.11).[40,41] In the case of bis(*n*)-tacrine, the best dimer is bis(7)-tacrine with a AChE IC_{50} value of 1.5 ± 0.3 nM. The IC_{50} values are tether-length dependent, AChE IC_{50} values increase dramatically when the tether is shorter than 5 methylenes. The dimer potency reaches to the IC_{50} value of mononer (tacrine) when the tether lengths are 3 or 4 methylenes, indicating that dual-site binding is no longer significant. (*S*,*S*)-(-)-**17** is another good example of dual-site binding that improves the potency of bivalent drug significantly. (-)-Huperzine A is a potent and selective reversible inhibitor of AChE, but simplified fragment (±)-**18** has almost no

inhibition potency. However, the potency of bivalent drug (*S*,*S*)-(-)-**17** is improved greatly by dimerizing **18**, optimizing the tether length, and selecting the proper enantiomer.

Scheme 2.11 Selected successful examples of bivalent acetylcholinesterase inhibitors (bis(7)-tacrine (both Carlier and Pang) and (*S*,*S*)-(-)-17 (Carlier), and its corresponding monomers (tacrine, (-)-Huperzine A and simplified fragment (±)-**18**)

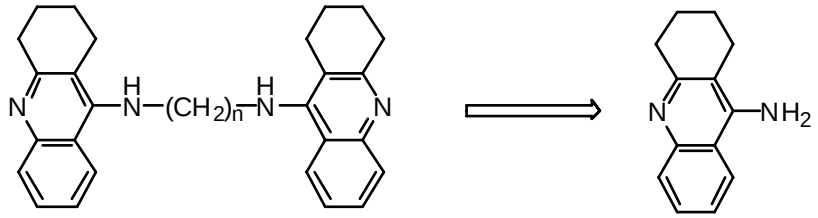

IC_{50} (nM) 1.5 ± 0.3 (n = 7, bis(7)-tacrine) 223 ± 11 (tacrine)

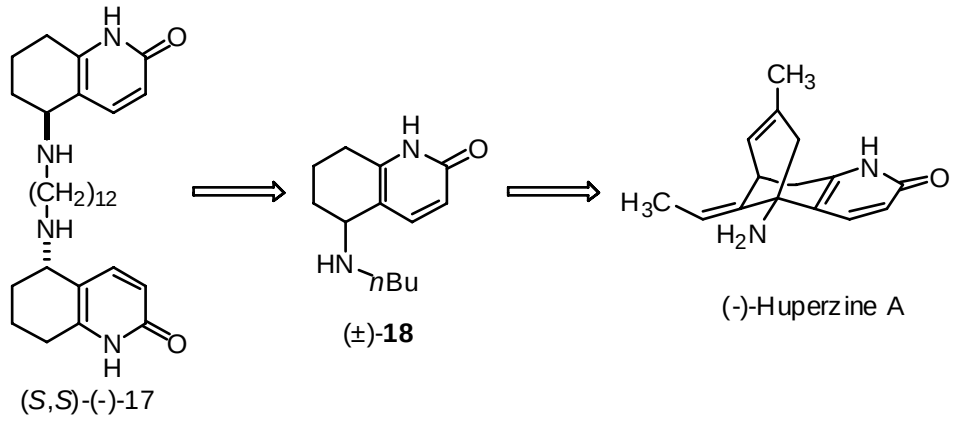

IC_{50} (nM) 52 ~500,000 114

Therefore, we expect that the dimerization of $GABA_A$ agonists may provide similar dramatic performance improvements as in the case of AChE inhibitors, when the appropriate distances are realized. Each dimer will be tested for tether- length dependent $GABA_A$ agonism using the $^{36}Cl^-$ influx assay. Significant tether length-dependent enhancement of EC_{50} values relative to a monomeric control will be considered as an evidence of dual-site binding.

The amide-bond forming protocols were used to prepare the corresponding PEG-linked dimers (Scheme 2.12). PEGs are available from Aldrich and have average molecular weights (M_n) ranging from 200 to 10,000. From the average molecular weights we can calculate the average degree of polymerization N (Table 2.5), which can be used to calculate the root mean square (rms) length of the polymer. According to the polymer theory,[42] the rms length of a flexible polymer is proportional to the square root of the number of monomers (i.e. N): rms length = $N^{1/2}$*L. From the light-scattering experiments of Knoll and Hermans[43] it is possible to extract a value of 5.76 Å for the L value of PEG. Using this figure we can calculate that the rms lengths for PEGs range from 12-87 Å (Table 2.5), which meets our above stated requirement.

Table 2.5 Selected commercially available PEGs and their molecular properties

PEG	a	b	c	d	E	f
PEG (M_n)	200	400	1500	3400	8000	1000
N[a]	4.1	8.7	33.7	45.0	181.4	226.9
rms length (n) (Å)[b]	11.7	17.0	33.4	50.5	77.6	86.8

[a]N = (M_n-18)/44, where 18 and 44 are the molecular masses of water and ethylene oxide, respectively.
[b]rms length = sqrt(N)*5.76

Prior to reaction with Boc protected **5c** precursor, the corresponding PEGs were activated by bis(4-nitrophenylcarbonate) (PNP) in CH_2Cl_2 at room temperature for 3 days in the presence of *N,N*-diisopropylethylamine (Scheme 2.12). The synthesis of activated PEGs in our group was first worked out by our former group member Dr. Polo Lam. The detail analysis of percentage of capping of end hydroxyl groups of PEG can be found in Dr. Lam's thesis. As can be seen below in Table 2.6, if we chose H_a in the aromatic ring

as the internal reference, there is about 15-20% discrepancy between the predicted internal CH_2 integral of PEG monomer units and the actual internal CH_2 integral of PEG monomer units that was determined from ^1H NMR. There are two possible reasons for such discrepancy. Firstly, there may be an error in the reported average molecular weights of PEGs from Aldrich. For example, the molecular weight of PEG 2000 from Aldrich is 136Da higher than that we obtained from MALDI-TOFMS. This demonstrates that the average molecular weights of PEG from Aldrich are estimated values, as stated in the label. Secondly, the desired activated PEG dimers were contaminated with either mono-activated PEGs or non-activated (free) PEGs. As reported by Dr. Lam, the % activation of PEG dimer by PNP is usually less than 100%. He has also proven that neither prolonged reaction time nor use of excess of reagents increase the % activation. If we are taking the second reason into account and neglect the fact that the average molecular weights of PEG from Aldrich are estimated values, the % activation for four of the PNP PEG dimers that we obtained ranges from 80%-86% (Table 2.6). Attempts to synthesize PNP PEG 400 dimer from PEG 400 and PNP proved to be fruitless since at least 5 to 6 side products were observed on TLC. No pure desired PEG 400 dimer can be isolated.

Scheme 2.12 Synthesis of PEG-linked GABA amide dimers

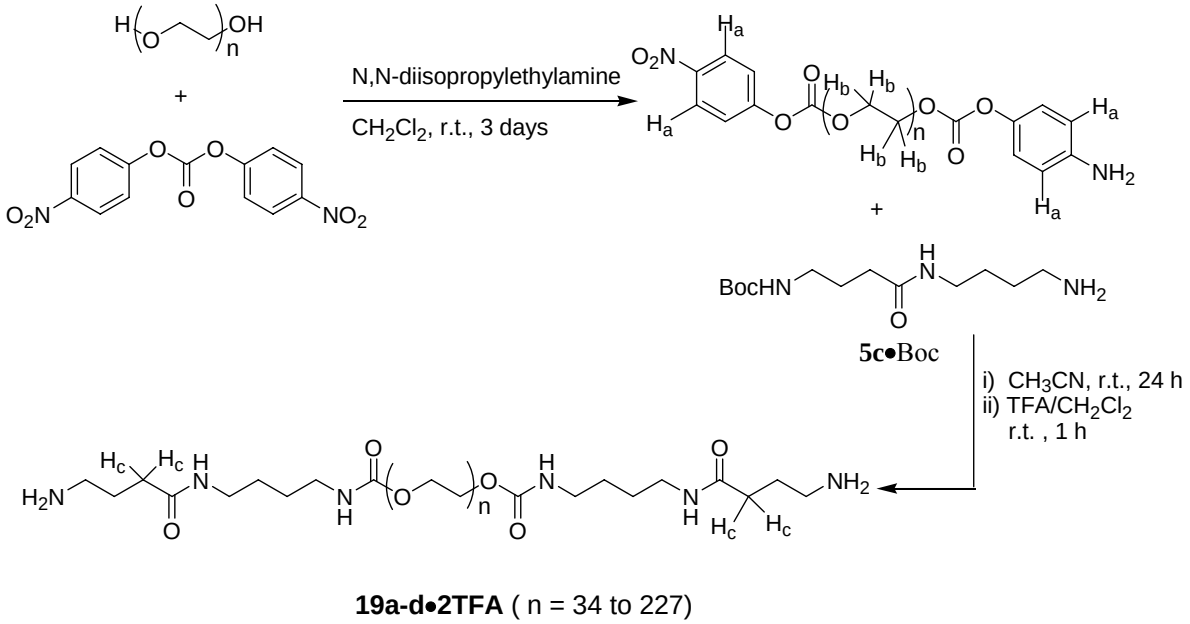

19a-d•2TFA (n = 34 to 227)

Table 2.6 % Activations and yields of PNP activated-PEG dimers

Entry	PEG ca. (M_n)	Predicted monomer units (n)	Predicted H_c:H_b ratio	^{1}H NMR H_c:H_b ratio	% Activation[a]	rms length (Å)	% yield
1	400	9	4:36	N/A	N/A	17	N/A
2	1500	34	4:136	4:170	80	33.4	45
3	3400	77	4:308	4:359	86	50.5	64
4	8000	181	4:724	4:878	82	77.6	87
5	10000	227	4:908	4:1071	85	86.8	88

[a]% activation = (Thereoretical internal PEG mononer CH_2 integral in column 4/Actual PEG mononer CH_2 integral in column 5)*100%

Stirring Boc protected **5c** precursor and corresponding activated PEGs in CH_3CN at room temperature for 24 hours afforded the Boc protected PEG-linked GABA amide dimers in good yields (Scheme 2.12, Table 2.6). TFA deprotection provided the desired

PEG-link GABA amide dimers as ditrifluoacetate salts. Based on the % activation that we calculated for the activated PEG dimers, we also calculated the % incorporation of **5c** into the PEG linkers, using H_c as the internal reference (Scheme 2.12, Table 2.7).

Table 2.7 % Incorporations and yields of PEG-linked GABA amide dimers

PEG-linked dimers	PEG ca. (M_n)	Predicted monomer units (n)	Predicted H_c:H_b ratio	^{1}H NMR H_c:H_b ratio	% Incorporation[a]	rms length (Å)	% yield
17a	1500	34	4:136	4:166	82	33.4	74
17b	3400	77	4:308	4:348	89	50.5	85
17c	8000	181	4:724	4:875	83	77.6	89
17d	10000	227	4:908	4:1118	81	86.8	84

[a]%Incorporation is based on estimated monomer units

The average molecular weights of PEGs that provided by Aldrich were measured according to their viscosity. Since there is discrepancy between predicted internal CH_2 integral of PEG monomer units and the actual internal CH_2 integral of PEG monomer units that was determined from ^{1}H NMR, we characterized all four of these PEG-linked GABA amide dimers (**19a-d**) by MALDI-TOFMS (Table 2.8). For the shorter PEG-linked dimers (**19a** and **b**), the molecular weights that we found from MALDI-TOFMS are close to the estimated values; however, as the molecular weights become bigger, there is much larger discrepancy between the experimental values and the estimated values from Aldrich (**19c** and **d**, Table 2.8). Clearly, the average molecular weights are more difficult to estimate as the molecular weight become bigger and the PEGs become more viscous (**19c** and **d**). We therefore believe that the molecular weights that we obtained from MALDI-TOFMS are more convincing than the ones from Aldrich because the

average molecular weights that measured by Aldrich were based on viscosity. MALDI-TOFMS should be a more accurate measurement.

Table 2.8 MALDI-TOFMS data of PEG-linked GABA amide dimers

PEG-linked dimers	PEG ca. (M_n)	Predicted monomer units (n)	Calc. PEG dimers (M_n)	MALDI-TOF PEG dimers (M_n)	Calc. monomer units (n)
17a	1500	34	1913.2	2089.3	38
17b	3400	77	3806.3	3718.2	75
17c	8000	181	8385.0	9265.5	201
17d	10000	227	10410.2	11863.1	260

2.4.2 Bioassay Results of PEG-linked GABA amide dimers

As in the case of other GABA amides, all four of these PEG dimers were screened for their activity as $GABA_AR$ agonists at 500 μM in the functional assay. Disappointingly, none of these four PEG-linked dimers (**19a-d**) were shown to be active as $GABA_AR$ agonists (Figure 2.18).

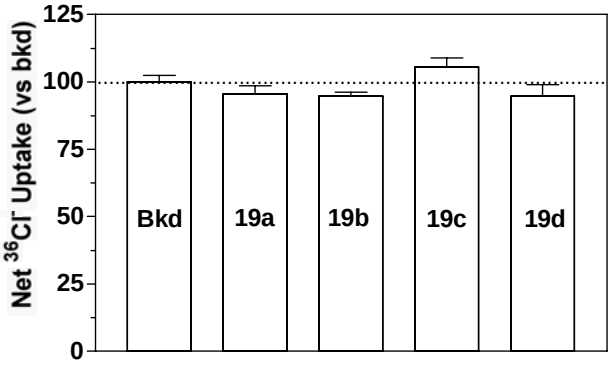

Figure 2.18 Ion flux elicited by **19a-d** (500 μM) in mouse brain synaptoneurosomes; bkd represents background, uptake in the absence of agonist

We postulated two possible reasons for lack of activity for these dimers. Firstly, the GABA amide (**5c**) that we used to couple with PEG-linker is a weak agonist; a 10-fold loss in affinity would give no detectable agonism at 500 μM. It would be reasonable to observe that the activity was lost upon coupling to a long chain linker. Secondly, the $GABA_AR$ binding sites, which we mentioned in chapter 1, are located in a narrow pocket. The **5c** portion of PEG dimers would be able to reach down to the binding pocket if the PEG dimers remain in a straight chain conformation; however, the binding would be hindered if the flexible chains of PEG linkers formed a coil or any possible loop conformations.

The effect of PEG-linked 10000 GABA amide dimer (**19d**) on GABA induced chloride uptake was studied by coincubating GABA (100 μM) with five different concentrations (1 μM to 1 mM) of **19d** (Figure 2.19). Interestingly, the chloride uptake that elicted by GABA was greatly enhanced in the presence of 1 mM **19d**, but not by other concentrations. As we mentioned previously, compound **19d** did not induce any net chloride uptake when it was tested by itself, suggesting that it does not bind to the same binding sites as GABA. Therefore, we proposed following three possible reasons for this unusual result. Firstly, compound **19d** may have blocked chloride pump of the $GABA_AR$, so that less $^{36}Cl^-$ ions would have been pumped out of the cell, resulting in more $^{36}Cl^-$ ions being trapped inside the receptor than otherwise. Secondly, it may have blocked the voltage-gated Cl^- channel, which means that most of the $^{36}Cl^-$ ions that entered the receptor through GABA-gated channel would remain inside. Thirdly, compound **19d** may have also blocked the desensitization state of the $GABA_AR$ so that the receptor would remain opening state longer, resulting in a larger count of $^{36}Cl^-$ ions that it would have been.

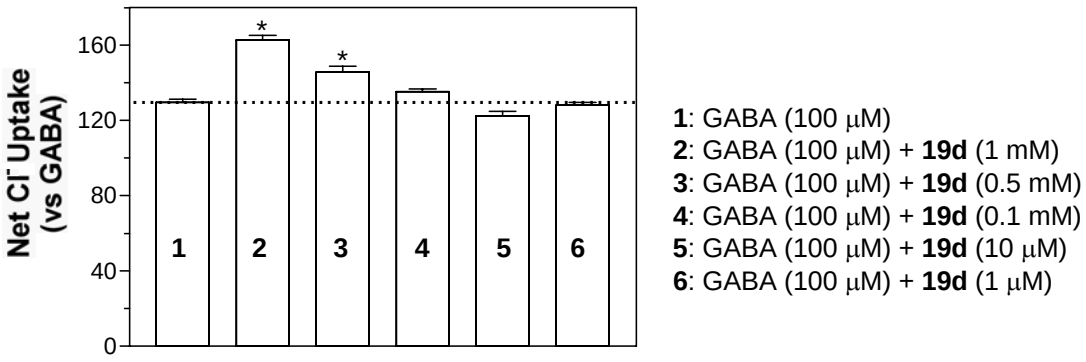

Figure 2.19 Effect of **19d** on chloride uptake elicited by GABA (100 μM) in mouse brain synaptoneurosomes; backgroud uptake was at 100%. Dash line represented chloride uptake induced by GABA (100 μM). An asterisk signifies that uptake is significantly different than background ($p<0.05$, *t*-test)

We have also synthesized two PEG-linked GABA amide heterodimers (**20a-b**, Scheme 2.13) using the same synthetic methods we described above to see whether the simple coupling of a PEG-linker would affect the activity of **5c** or not. Both **20a** and **20b** were tested at 1 mM, and were shown to be inactive. These data are consistent with the results of homodimers, which means the activity of GABA amides was lost upon coupling of **5c** with a long chain PEG-linker.

Scheme 2.13 PEG-linked GABA amide heteromers (**20a-b**)

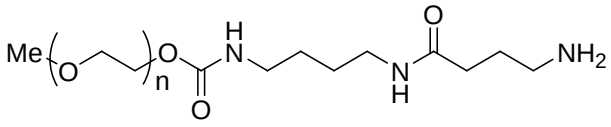

n = 17 **20a**•TFA
n = 45 **20b**•TFA

2.4.3 Synthesis of PEG-linked ZAPA analogs

PEG-linked GABA amide dimers were shown to be inactive as $GABA_AR$ agonists. We therefore focused on our attention on the PEG-linked ZAPA analogs due to the fact that ZAPA is a more potent agonist than GABA. Since ZAPA itself would not directly

react with the activated PEG linkers, compound **15** was chosen to couple to the PEG linkers (Table 2.9). Two syntheses were attempted, as shown below; however, neither of these reactions worked under the condition that was used for the synthesis of PEG-linked GABA amide dimers.

Table 2.9 Attempted synthesis of PEG-linked ZAPA analogs

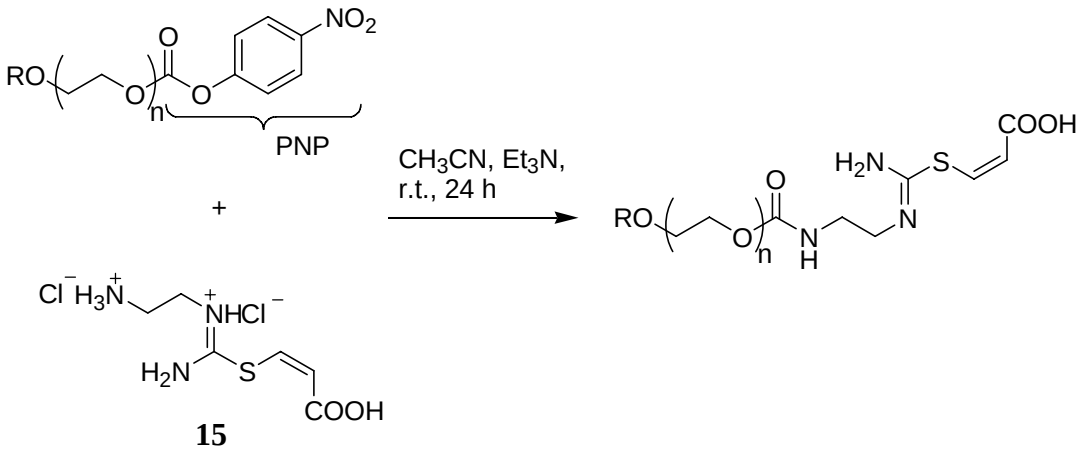

Entry	R	PEG ca. M_n	rms length (Å)	Remarks
1	CH_3	2000	39	No reaction; recovered PEG linker
2	PNP	10000	87	No reaction; recovered PEG linker

As we discussed previously, compound **15** was 40-fold less potent than ZAPA. We were concerned about the bioactivities of these PEG-linked ZAPA analogs would be lost upon coupling with **15**, in addition to the failure in synthesizing these two analogs. We therefore did not pursue further for the study of PEG-linked ZAPA analogs.

2.5 HPLC Analysis of GABA amides

Some of the non-zwitterionic GABA amides that we synthesized were Boc-deprotected in concentrated HCl/CH_3OH, which raised a question of potential

contamination of GABA amides with GABA. Scheme 2.14 showed how the contamination would occur during deprotection of the Boc group, H_2O would act as a nucleophile and react with GABA amides under strong acid conditions.

Scheme 2.14 Proposed mechanism for acid-catalyzed Boc deprotection of GABA amides. Boc protected **5a** was used as an example

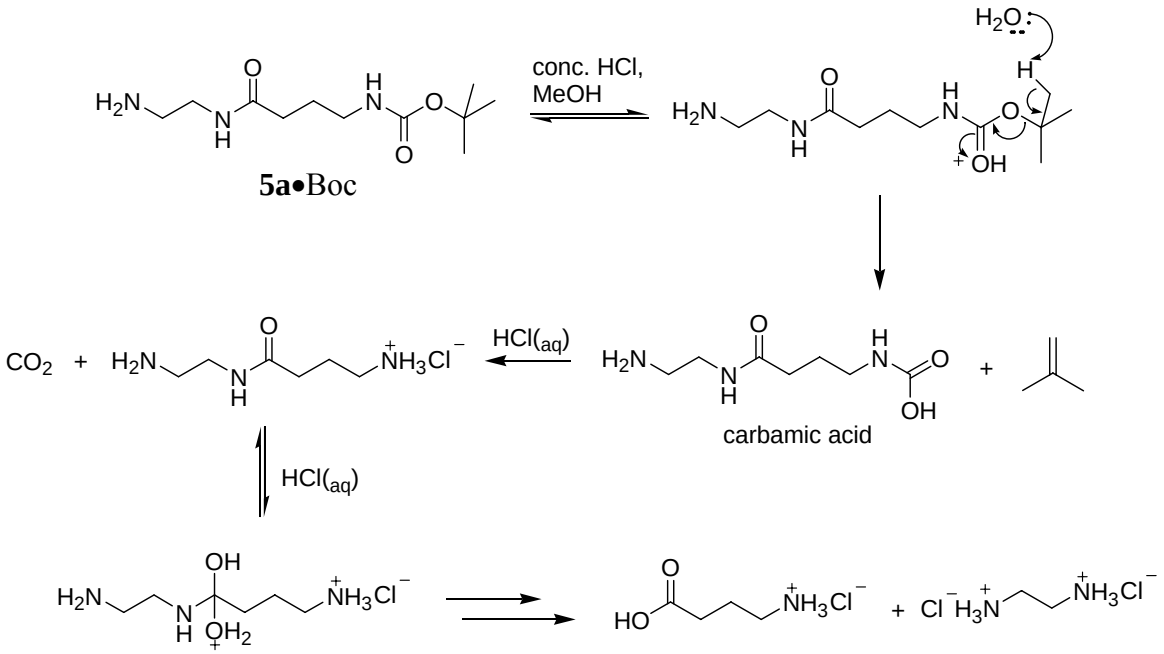

If this decomposition occurred, our GABA amide samples would be contaminated with GABA. Thus the weak agonism displayed by GABA amides would be due to the presence of trace of GABA. To rule out the possibility, we assayed our GABA amides for free GABA using Saller's modified procedure, we analyzed some of the GABA amides by HPLC to ensure that these GABA amides were GABA free (<0.1 wt%). Refluxing GABA or GABA amides with dansyl chloride in $NaHCO_3$ and acetone/CH_2Cl_2 for 0.5 h to 12 h and followed by column chromatography (9:1 CH_2Cl_2-CH_3OH) afforded the desired dansylated products in good yields for GABA or mono-dansylated GABA amides (Scheme 2.15).

Scheme 2.15 Synthetic scheme of selected GABA amides with dansyl chloride

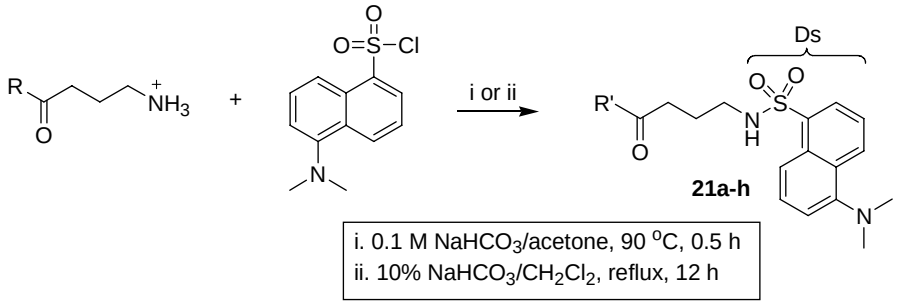

Starting **material**	Compound	**R =**	**R' =**	**Reaction conditions**	**% Yield**
GABA	**21a**	O^-	OH	i	quantitative
1a·HCl	**21b**	NH_2	NH_2	i	quantitative
1b·HCl	**21c**	NH	NH	ii	87
5a·2HCl	**21d**	H_3N^+ NH	Ds N H NH	ii	17
6a·HCl	**21e**	H_3C H N O NH	H_3C H N O NH	ii	47
5c·2HCl	**21f**	H_3N^+ NH	Ds N H NH	ii	24
6c·HCl	**21g**	H_3C H N O NH	H_3C H N O NH	ii	66
2c·2HCl	**21h**	H_3N^+ H N O NH	Ds N H H N O NH	ii	20

The retention times of each purified compound **21a-h** were first determined by HPLC using RP18 column and H_2O/CH_3CN (85:15, v/v) as mobile phase with 0.1% TFA as additive. In order to determine whether each of the GABA amides that we studied was contaminated with GABA or not, the syntheses of compounds **21a-h** were repeated. The crude mixture of each compound was also analyzed by HPLC. By comparing the spectrum of each crude mixture with that of the corresponding pure compound, we discovered that the hydrochloride salts of **1a**, **6a** and **6b** were contaminated with GABA (Table 2.10). The other four compounds were proven to be GABA free (<0.1 wt%) due

to their crystalline nature; recystallization of these four compounds from MeOH would have removed any GABA impurity.

Table 2.10 HPLC* data of selected GABA amides

GABA/GABA amides	Retention time of pure dansylated GABA/GABA amides	Retention time of crude mixtures	Wt% GABA
GABA	7.06	7.15	-
1a•HCl	3.48	3.52	1.4
1b•HCl	18.5	18.68	< 0.1
5a•2HCl	18.23	18.38	0.46
6a•HCl	3.53	3.52	0.89
5c•2HCl	18.99	19.00	< 0.1
6c•HCl	4.95	4.74	< 0.1
2c•2HCl	19.38	18.50	< 0.1

*HPLC conditions:
- Mobile phase: H_2O:CH_3CN (85:15, v/v) with 0.1 % (v/v) TFA; isocratic at first 10 min, gradient from 10 to 30 min. (15% to 100% CH_3CN)
- Flow rate: 1 mL/min
- Injection volume: 5 μL
- UV detection: 254 nm

The purity of each GABA amide was important because it would give a false positive if the agonism of a particular amide was due to the presence of small amount of GABA. The contaminated GABA amide would seem like an agonist, but actully it was not. The hydrochloride salts of **1a**, **5a** and **6a** were shown to be contaminated with GABA and found to be $GABA_AR$ full agonists when they were first tested in the functional assay. Therefore, the agonism of these GABA amides is yet to be proven. We resynthesized these three amides and removed Boc groups by use of TFA/CH_2Cl_2 instead of concentrated HCl/CH_3OH. Only trifluoroacetate salt of **1a** was found to be a partial

agonist and both **5a** and **6a** were inactive at the highest concentration tested (4 mM) when the trifluoroacetate salts of these three GABA amides were analyzed in the same assay.

The controversial bioassay results of these two kind salts of GABA amides raises a question: does trifluoroacetate ion (CF_3COO^-) have any inhibitory effect on the GABA activated chloride uptake? Figure 2.20 shows the effect of sodium trifluoroacetate on the chloride uptake of GABA. Sodium trifluoroacetate (1 mM) is coincubated with synaptoneurosomes for 10 minutes prior to the addition of GABA solution (1 mM). The net chloride uptake that elicted by GABA will decrease if the trifluoroacetate ion is a channel blocker. As can be seen, the chloride uptake that induced by GABA with or without sodium trifluoroacetate remains nearly the same. This experiment demonstrates that trifluoroacetate ion is not a channel blocker and the full agonism of the hydrochloride salts of **1a**, **5a** and **6a** are indeed due to the contamination of small amount of GABA.

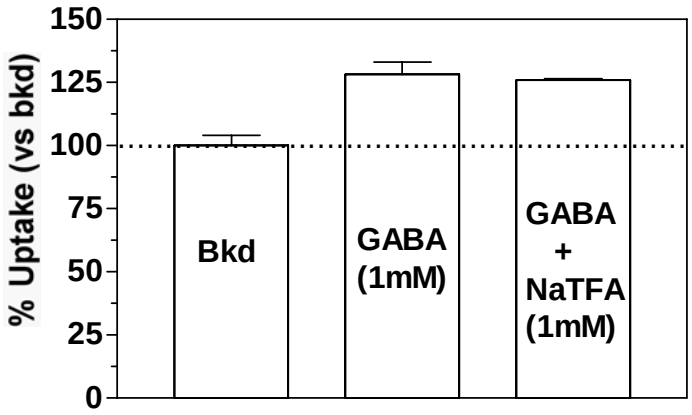

Figure 2.20 Effect of NaTFA (1 mM) on chloride uptake elicited by GABA (1 mM), expressed as % uptake versus background (bkd)

2.6 Conclusions

In chapter 2.1-2.2, we described the syntheses and bioassay results of non-zwitterionic GABA amides. We first demonstrated that appropriately functionalized GABA amides are partial, full and superagonists, despite their non-zwitterionic structures. Note that none of these GABA amides has been tested *in vivo* assay, but the agonism of these GABA amides is comparable to that of THIP, as shown by *in vitro* assay results. The bioassay results of all three series of GABA amides showed that the agonism of these amides are tether-length dependent, with a optimum tether length appearing to be four methylenes. Based on the agonism of both homodimers and heterodimers, we observed that the pendant amide group (**2c** and **6c**) seemed to be superior to the ammonium group (**5c**). We proposed that superior activity of **2c** and **6c** over **5c** the was due to the presence of a proximal subsite to the agonist binding site that can weakly bind the pendant amide group.

In chapter 2.1, we focused on the syntheses and bioassay results of GABA amide homodimers (**2a-i**). Compound **2c** which has a flexible four methylene tether was found to be the most potent dimer among this series of compounds. Compound **2c** was a 'superagonist', and both co-application with GABA and [^{3}H]musicimol binding experiments demonstrated that **2c** binds to the same site as GABA. Replacing the flexible four methylenes tether of **2c** by eight more rigid tethers (**4a-h**) revealed a significant loss of activity compared with the original compound **2c**. Six derivatives of **2c** were found to be competitive antagonists. [^{3}H]musicimol binding experiments further confirmed the competitive antagonism of one of these antagonists (**4b**). Structural modifications of **2c** demonstrated the importance of flexible tether length for the agonism of these GABA amide homodimers.

In chapter 2.2, the syntheses and bioassay results of two series of simple GABA amide heterodimers were described. Compound 6, which has a pendant amide group was found to be the best heterodimer among these two series of compounds. Optimization of pendant amide group by other nine groups (**7a-i**) revealed a significant loss of activity compared with the original compound **6c**. Structural modifications of **6c** demonstrated that the amide group is important in the investigated bioactivity. It also showed that the proximal binding site for the pendant amide is small. The superior activity of **6c** over **7c** (note they differ only in that **6c** has an additional amine group) must be due to another complementary binding interaction of the amino group in **6c**.

In chapter 2.3, we described the syntheses and first assays of four ZAPA derivatives in the Cl^- uptake functional assay. The agonism of these four ZAPA derivatives was shown to be related to the size of the alkyl groups. The agonism of these derivatives increased as the alkyl group became longer and the potency was greatly improved as the alkyl group changed from hydrophilic to hydrophobic groups.

The syntheses and bioassay data of PEG-linked GABA amide homodimers were described in chapter 2.4. PEG-linked dimers were designed to span the distances between two low-affinity binding sites. However, little information is known about the binding sites on the $GABA_AR$ and lack of crystal structure have made this approach fruitless. GABA amide **5c** lost activity upon coupling to PEG linkers. PEG-linked GABA amide heterodimers were also shown to be inactive. Attempted to synthesize PEG-linked ZAPA derivatives did not yield any desired products.

Finally, in chapter 2.5, the purity of some GABA amides were analyzed by HPLC based on modification of Saller's procedure (assay of the dansyl sulfonamide derivatives). Three of the small GABA amides (**1a**, **5a** and **6a**) that we studied were found to be contaminated with GABA impurity (>0.1 wt%). The contaminated GABA

amides gave false positive assay results, which demonstrated the importance of the purity of GABA amides in bioassay experiments.

References and notes for chapter 2

1 Jones, M. V.; Shar, Y.; Dzubay, J. A.; Westbrook, G. L. Defining affinity with the $GABA_A$ receptor. *J. Neurosci.* **1998**, *18*, 8590-8604.

2 Jones proposed that β-alanine, muscimol, and GABA bound to the $GABA_AR$ in their fully extended conformations; the quoted 4.7-6.0 Å range spans the intercharge distances in these molecules.

3 Breckenridge, R. J.; Nicholson, S. H.; Nichol, A. J.; Suckling, C. J.; Leigh, B.; Iversen, L. Inhibition of [^{3}H] GABA Binding to Postsynaptic Recetors in Human Cerebellar Synaptic Membranes by Carboxyl and Amino Derivatives of GABA. *J Neurochem.* **1981**,*37*, 837-844.

4 Varga, V.; Kontro, P.; Oja, S. S. Modulation of GABAergic Neurotransmission in the Brain by Dipetides. *Neurochem. Res.* **1988,** *13,* 1027-1034.

5 Varga *et al.* showed that preincubation (5 min) of GABA-His and GABA-Gly with mouse brain synaptosomal preparations enhanced 0.1 mM GABA-induced chloride flux. However, in the absence of GABA these compounds did not induce chloride flux.

6 Silman, I.; Karlin, A. Acetylcholine receptor covalent attachment of depolarizing groups at the active site. *Science (Washington, D. C.)* **1969,** *164,* 1420-1421.

7 Li, L.; Zhong, W.; Zacharias, N.; Gibbs, C.; Lester, H. A.; Dougherty, D. A. The tethered agonist approach to mapping ion channel proteins-toward a structural model for the agonist binding site of the nicotinic acetylcholine receptor. *Chem. Biol.* **2001,** *8,* 47-58.

8 Carlier, P. R.; Chow, E. S.-H.; Barlow, R. L.; Bloomquist, J. R. Discovery of Non-Zwitterionic $GABA_A$ Receptor Full Agonists and a Superagonist. *Bioorg. Med. Chem. Lett.* **2002,** *12,* 1985-1988.

9 Flynn, D. L.; Zelle, R. E. Grieco, P. A. A Mild Two-Step Method for the Hydrolysis /Methanolysis of Secondary Amides and Lactams. *J. Org. Chem.* **1983,** *48,* 2424-2427.

10 Bloomquist, J. R.; Soderlund, D. M. Neurotoxic Insecticides Inhibit GABA-Dependent Chloride Uptake by Mouse Brain Vesicles. *Biochem. Biophys. Res. Commun.* **1985,** *133,* 37-43.

11 Saller, C. F.; Czupryna, M. J. γ-Aminobutyric acid, glutamate, glycine and taurine analysis using revesed-phased high-performance liquid chromatography and ultraviolet detection of dansyl chloride derivatives. *J. Chromatogr.* **1989,** *487,* 167-172.

12 Luu, M. D.; Morrow, A. L.; Paul, S. M.; Schwartz, R. D. Characterization of $GABA_A$ Receptor-mediated 36Chloride Uptake in Rat Brain Synaptosomes. *Life Sci.* **1987,** *41, 1277-1287.*

13 Schuda, P. F.; Greenlee, W. J.; Chakravarty, P. K. A Short and Efficient Synthesis of (3*S*,4*S*)-4-[(*tert*-Butyloxycarbonyl)amino]-5-cyclohexyl-3-hydroxypentanoic Acid Ethyl Ester. *J. Org. Chem.* **1988,** *53*, 873-875.

14 Kawahara, S.-I.; Uchimaru, T. One-Pot Preparation of *o*-Xylylene Diamine and its Related Amines. *Zeit. fur Nat. B: Chem. Sci*. **2000,** *55*, 985-987.

15 Compounds **3a-h** were screened at 1 mM; they were pre-incubated with mouse brain synaptoneurosomes (200 μL) for 10 minutes at room temperature. These compounds were then co-incubated with GABA (0.1 mM in $^{36}Cl^-$ flux buffer) for 15 seconds at 30°C.

16 DeLorey, T. M.; Brown, G. B. γ-Aminobutyric $acid_A$ Receptor Pharmacology in Rat Cerebral Cortical Synaptoneurosomes. *J. Neurochem.* **1992,** *58*, 2162-2169.

17 Edgar, P. P.; Schwartz, R. D. Functionally Relevant γ–Aminobutyric $Acid_A$ Receptors: Equivalence between Receptor Affinity (K_d) and Potency (EC_{50})? *Mol. Pharmacol.* **1992,** *41*, 1124-1129.

18 Johston, G. A. R.; Allan, R. D.; Kennedy, S. M. E.; Twitchin B. In *GABA- Neuro-Transmitters;* Krogsgaard-Larsen, P.; Scheel-Kruger, J.; Kofod, H.; Eds.; Munkgaard: Copenhagen, **1979**, 149-164.

19 Krogsgaard-Larsen, P.; Frolud, B.; Jorgensen, F.S.; Shousaboe, A. $GABA_A$ Receptor Agonists, Partial Agonists, and Antagonists. Design and Therapeutic Propects. *J. Med. Chem.* **1994**, *37* (16), 2489-2505.

20 Larsen, S. D.; Connell, M. A.; Cudahy, M. M.; Evans, B. R.; May, P. D.; Meglasson, M. D.; O'Sullivan, T. J.; Schostarez, H. J.; Sih, J. C.; Stevens, F. C.; Tanis, S. P.; Tegley, C. M.; Tucker, J. A.; Vaillancourt, V. A.; Vidmar, T. J.; Watt, W.; Yu, J. H. Synthesis and biological activity of analogues of the antidiabetic/antiobesity agent 3-guanidinopropionic acid: discovery of a novel aminoguanidinoacetic acid antidiabetic agent. *J. Med. Chem.* **2001,** *44,* 1217-1230.

21 Allan, R. D.; Dickenson, H. W.; Hiern, B. P.; Johnson, G. A. R.; Kazlauskas, R. Isothiouronium compounds as γ–aminobutyric acid agonists. *Br. J. Pharmacol.* **1986,** *88,* 379-387.

22 Allan, R. D.; Dickenson, H. W.; Johnston, G. A. R.; Kazlauskas, R.; Mewett, K. N. Structural Analogues of ZAPA as $GABA_A$ Agonists. *Neurochem. Int.* **1997,** *30*, 583-591.

23 Takagi, S.; Tanaka, H.; Yano, M.; Machida, K. Studies on the Syntheses of Polymethylene-bisthioureas and their Derivatives. I. *Chem. Phar. Bull***, 1959,** *7*, 206-208.

24 Poss, M. A.; Iwanowicz, E.; Reld, J. A.; Lin. J.; Gu Z. A Mild and Efficient Method for the Preparation of Guanidines. *Tetrahedron Lett.* **1992,** *33,* 5933-5936.

25 Rasmussen, C. R.; Villani, F. J.; Weaner, L. E.; Reynolds, B. E.; Hood, A. R.; Hecker, L. R.; Nortey, S. O.; Hanslin, N. A.; Costanzo, M .J.; Powell, E. T.; Molinari, A. J. Improved Procedures for the preparation of Cycloalkyl-, aryalkyl- and Arylthioureas. *Synthesis,* **1988,** 456-459.

26 Tobe, Y.; Sasaki, S.-I.; Mizuno, M.; Hirose, K.; Naemura, K. Novel Self-Assembly of m-Xylylene Type Dithioureas by Head -to-Tail Hydrogen Bonding. *J. Org. Chem.* **1998,** *63,* 7481-7489.

27 Buschauer, A. Synthesis and in vitro pharmacology of arpromidine and related phenyl(pyridylalkyl)guanidines, a potential new class of positive inotropic drugs. *J. Med. Chem.* **1989,** *32,* 1963-1970.

28 Perkins, J. J.; ZarTman, A .E.; Meissner, R. S. Synthesis of 2-(Alkylamino)benzimidazoles. *Tetrahedron lett.* **1999,** *40*, 1103-1106.

29 Nannini, G.; Perrone, E.; Severino, D.; Bedeschi, A.; Biasoli, G. Synthesis and Structure-Activity Relationships of New 7-Vinylenethioacetamido and Thioacrylamindo Cephalosporins. *J. Antibiot.* **1981,** *34*, 412-426.

30 Kash, T. L.; Trudell, J. R.; Harrison, N. L. Structural elements involved in activation of the γ-aminobutryic acid type A ($GABA_A$) receptor. *Biochem. Soc. Trans.* **2004,** *32,* 540-546.

31 Baumann, S. W.; Baur, R.; Sigel, E. Individual properties of the two functional agonist sites in $GABA_A$ receptors. *J. Neurosci.* **2003,** *23,* 11778.

32 Nayeem, N.; Green, T. P.; Martin, I. L.; Barnard, E. A. Quaternary Structure of the Native $GABA_A$ Receptor Determined by Electron Microscopic Image Analysis. *J. Neurochem.* **1994**, *62*, 815-818.

33 Miyazawa, A.; Fuiyoshi, Y.; Stowell, M.; Unwin , N. Nicotinic Acetylcholine Receptor at 4.6 Å Resolution: Transverse Tunnels in the Channel Wall. *J. Mol. Biol.* **1999,** *288,* 765-786.

34 Unwin, N. Acetylcholine receptor channel imaged in the open state. *Nature,* **1995,** *373,* 37-43.

35 Arias, H. R. Topology of ligand binding sites on the nicotinic acetylcholine receptor. *Brain, Res. Rev.* **1997,** *25,* 133-191.

36 Brejc, K.; van Dijk, W. J.; Klaassen, R. V.; Schuurmans, M.; van der Oost, J.; Smit, A. B.; Sixma, T. K. Crystal structure of an ACh-binding protein reveals the ligand-binding domain of nicotinic receptors. *Nature,* **2001,** *411,* 269-276.

37 Smith, G. B.; Olsen, R. W. Functional domains of $GABA_A$ receptors. *Trends Pharmacol. Sci.* **1995,** *16,* 162-168.

38 Kramer, R. H.; Karpen, J. W. Spanning binding sites on allosteric proteins with polymer-linked dimers. *Nature* **1998**, 710-713.

39 Fan, E.; Zhang, Z.; Minke, W. E.; Hou, Z.; Verlinde, L. C.; Hol, W. G. J. High affinity Pentavalent Ligands of Escherichia coli Heat-Labile Enterotoxin by Modulator Structure-Based Design. *J. Am. Chem. Soc.* **2000,** *122,* 2663-2664.

40 Carlier, P. R.; Han, Y. F.; Chow, E. S.-H.; C. Li, P.-L; Wang, H.; Lieu, T. X.; Wong,H. S.; Pang, Y.-P. Evaluation of Short-tether Bis-THA AChE Inhibitors. A Further Test of the Dual Binding Site Hypothesis. *Bioorg. Med. Chem.* **1999**, *7*, 351-357.

41 Carlier, P. R.; Du, D.-M.; Han, Y.-F.; Liu, J.; Perola, E.; Williams, I. D.; Pang Y.-P. Dimerization of an Inactive Fragment of Huperzine A Produces a Drug with twice Potency of the Natural Product. *Angew. Chem. Int. Ed. in English* **2000**, *39,* 1775-1777.

42 Hiemenz, P. C. *Polymer Chemistry:* The Basic Concepts; Marcel Dekker: New York, **1984**, 48.

43 Knoll, D.; Hermans, J. J. Polymer-Protein Interactions. *J. Biol Chem.* **1983,** *258.* 5710-5715.

Chapter 3 Experimental Section of GABA Project

3.1 Chemistry

3.1.1 General Methods

GABA was obtained from Aldrich. *N*-Boc-GABA (**3**) was prepared according to the literature method.[1] 2-Pyrrolidinone was purchased from Acros. *N*-Boc-2-pyrrolidinone was prepared according to the published method.[2] ^{1}H and ^{13}C NMR spectra were recorded on a Bruker R-300 300 MHz, Bruker JOEL 500 MHz or INOVA 400 MHz spectrometer. All chemical shifts are expressed in ppm and the coupling constants in Hertz. Stardards for chemical shifts are as follows:

Nuclei	Standard	Chemical Shifts (ppm)
^{1}H	TMS	0
	$CDCl_3$	7.26
	CD_3OD	3.3
	DMSO-d_6	2.5
	D_2O	4.8
^{13}C	$CDCl_3$	77
	CD_3OD	49.5
	DMSO-d_6	39.5

Chemical ionization (CI) mass spectra were acquired using CH_4 as the reagent gas. Positive ion high resolution FAB+ mass spectra were collected on a JEOL HX110 dual

focusing mass spectrometer using a direct inlet with 3-nitrobenzyl alcohol as the sample matrix. Elemental analysis was performed by Atlantic Microlab, Inc.

Analytical thin-layer chromatography (TLC) was performed with aluminum sheets coated with RDH silica gel 60 F254. Flash column chromatography was performed using VWR silica gel 60 (60-240 mesh). High-performance liquid chromatography (HPLC) analysis was performed on a Xterrra^{TM} RP_{18} column (5.6 x 150 mm, 5 μM), detection at 254 nM, flow rate 1.0 mL/min with isocratic at first 10 minutes and gradient in the next 20 minutes. Elution program: H_2O:CH_3CN (85/15, v/v) at 0-10 minutes with 0.1 % TFA as additive; 15-100% CH_3CN at 10-30 minutes with 0.1 % TFA as additive.

3.1.2 Procedures

Synthesis of 4-amino-butyramide trifluoroacetic acid salt (gabamide, 1a)

N-Boc-2-pyrrolidinone (330.1 mg, 1.78 mmol) and concentrated NH_3 (29.3 wt %, 10 mL) were combined and heated to reflux for 2 hours. After cooling to room termperature. the mixture was diluted with CH_2Cl_2 (50 mL), which was then extracted with H_2O (40 mL). The CH_2Cl_2 layer was collected and the aqueous layer was extracted with CH_2Cl_2 (3 x 50 mL). The combined CH_2Cl_2 layers were dried over Na_2SO_4, filtered and evaporated under reduced pressure to afford the corresponding Boc-protected **1a** as white solid. The TFA salt was prepared by dissolving the white solid in CH_3OH (1mL), followed by addition of trifluoroacetic acid (2 mL). The resulting solution was stirred at room temperature for 1 hour, and concentrated in vacuum to yield the title compound as a brown oily liquid (317.9 mg, 88%). ^{1}H NMR (CD_3OD): δ 1.91 (5-let, J = 7.5 Hz, 2H),

2.35 (t, J = 7.2 Hz, 2 H), 2.96 (t, J = 7.6 Hz, 2 H); ^{13}C NMR (CD_3OD): δ 24.75, 33.58, 40.88, 177.79; MS (FAB+): calcd for $C_4H_{11}N_2O$ $[M+1]^+$, 103.0866, found 103.1

Synthesis of *N*-4-aminobutyl butyramide hydrochloride salt (1b)

N-Boc-2-pyrrolidinone (524 mg, 2.83 mmol) and n-butylamine (1.1 mL, 8.49 mmol) were combined in dioxane (10 mL) and heated to reflux for overnight. After cooling to room termperature, the mixture was diluted with CH_2Cl_2 (25 mL), which was then extracted with H_2O (2 x 25 mL). The CH_2Cl_2 layer was collected, dried over $MgSO_4$, filtered and evaporated under reduced pressure to give a crude brown residue. Purified by flash column chromatography (10% MeOH-CH_2Cl_2 with 7 mL of concentrated NH_3 per liter) on silica gel afforded corresponding Boc-*N* protected **1b** as pale yellow solid. The HCl salt was prepared by redissolving the white solid in 5 mL of CH_3OH, followed by addition of HCl (37 % in H_2O, 1 mL). The resulting solution was stirred at room temperature for 2 h, and concentrated in vacuum to yield the title compound as yellow solid (294 mg, 53 %). ^{1}H NMR (CD_3OD): δ 0.93 (t, J = 7.4 Hz, 3H), 1.32-1.39 (m, 2 H), 1.44-1.50 (m, 2 H), 1.91 (5-let, J = 7.3 Hz, 2H), 2.34 (t, J = 7.2 Hz, 2H), 2.96 (t, J = 7.6 Hz, 2H), 3.17 (t, J = 7.0 Hz, 2H); ^{13}C NMR (CD_3OD): δ 14.57, 21.58, 25.05, 32.97, 34.28, 40.70, 40.93, 174.88; MS (FAB+): calcd for $C_8H_{19}N_2O$ $[M+1]^+$ 159.1497, found 159.1493 (-2.7 ppm, -0.4 mmu).

Synthesis of *N*-(4'-aminobutanoyl)aniline trifluoroacetate (1c•TFA)

To a solution of Boc-GABA (624 mg, 3.07 mmol), EDCI (631 mg, 3.29 mmol) and DMAP (295 mg, 2.41 mmol) in CH_2Cl_2 (10 mL) was added aniline (100 μL, 1.10

mmol). The yellow mixture was then stirred at room temperature for 12 hours. The mixture was partitioned between CH_2Cl_2 (1 x 50 mL) and H_2O (40 mL). The CH_2Cl_2 layers was collected, dried over Na_2SO_4, filtered and evaporated under reduced pressure. Purified by flash column chromatography (5% MeOH-CH_2Cl_2 with 7 mL of concentrated NH_3 per liter) on silica gel afforded corresponding Boc-*N* protected **1c** as a yellow solid. The TFA salt was prepared by dissolving the yellow solid in CH_2Cl_2 (5mL), followed by addition of trifluoroacetic acid (2 mL). The resulting solution was stirred at room temperature for 1 hour, and concentrated in vacuo to yield the title compound **1c** as a pale yellow solid (256.5 mg, 95 %). ^{1}H NMR (CD_3OD): δ 2.00 (5-let, *J* = 7.1 Hz, 2H), 2.53 (t, *J* = 7.0 Hz, 2H), 3.01 (t, *J* = 7.6 Hz, 2H), 7.08 (t, *J* = 7.4 Hz, 1H), 7.29 (t, *J* = 7.8 Hz, 2H), 7.53 (apparent d, *J* = 7.6 Hz, 2H); ^{13}C NMR (CD_3OD): δ 24.75, 34.91, 40.87, 121.75, 125.77, 130.30, 140.19, 173.30; MS (FAB+): 179.1184, found 179.1191 (+3.7 ppm, +0.7 mmu).

General procedures for the preparation of GABA amide homodimers (2a-i)

N-Boc-2-pyrrolidinone (3.90 mmol, 2.5 equiv) and 1,*n*-diaminoalkane (*n* = 2-12, 1.56 mmol, 1.0 equiv) were combined in 10 mL of dioxane, and refluxed overnight. After cooling to room temperature, the volatiles were removed and ether was added to the residue, which was then stirred for another hour. *N*-Boc-GABA amide dimer derivatives were collected as white precipitates and washed with ether, followed by H_2O. Either HCl or trifluoroacetic acid deprotection provided the desired compounds (**2a-i**) in good yields.

***N,N'*-bis(4-amino-1-butanoyl)-1,2-ethanediamine dihydrochloride** (**2a**) The general procedures for the synthesis of homodimers were followed: *N*-Boc-2-pyrrolidinone **2** (1.79 mg, 9.67 mmol) and 1,2-diaminoethane (232 mg, 3.87 mmol) were combined in dioxane (20 mL), and treated as above. The title compound **2a** was obtained as a straw-colored solid (836 mg, 71%). ^{1}H NMR (CD_3OD): δ 1.93 (5-let, J = 7.3 Hz, 4H), 2.39 (t, J = 7.1 Hz, 4 H), 2.97 (t, J = 7.4 Hz, 4 H), 3.28 (s, 4 H); ^{13}C NMR (CD_3OD): δ 24.88, 34.27, 40.51, 40.91, 175.37; MS (CI^+): calcd 231, found 231 $[M+1]^+$. Anal. ($C_{10}H_{26}N_4O_2$•2.1HCl) C, H, N.

***N,N'*-bis(4-amino-1- butanoyl)-1,4-butanediamine dihydrochloride** (**2c**) The general procedures for the synthesis of homodimers were followed: *N*-Boc-2-pyrrolidinone **2** (721 mg, 3.90 mmol) and 1,4-diaminobutane (138 mg, 1.56 mmol) were combined in dioxane (10 mL), and treated as above. The title compound **2c** was obtained as a pale yellow solid (403 mg, 78%). ^{1}H NMR (CD_3OD): δ 1.53-1.56 (m, 4H), 1.95 (5-let, J = 7.3 Hz, 4 H), 2.40 (t, J = 7.2 Hz, 4 H), 2.95 (t, J = 7.4 Hz, 4 H); 3.21-3.23 (m, 4 H); ^{13}C NMR (CD_3OD): δ 25.09, 28.01, 34.10, 40.79, 40.84, 175.34; MS (CI^+): calcd 259, found 259 $[M+1]^+$. Anal. ($C_{12}H_{26}N_4O_2$•2.2HCl•0.8H_2O) C, H, N.

***N,N'*-bis(4-amino-1- butanoyl)-1,6-hexanediamine dihydrochloride** (**2e**) The general procedures for the synthesis of homodimers were followed: *N*-Boc-2-pyrrolidinone **2** (670 mg, 3.62 mmol) and 1,6-diaminohexane (168 mg, 1.45 mmol) were combined in dioxane (10 mL), and treated as above. The title compound **2e**was obtained as a pale yellow solid (403 mg, 77%). ^{1}H NMR (CD_3OD): δ 1.35-1.41 (m, 4H), 1.50-1.54 (m,

4H), 1.94 (5-let, J = 7.3 Hz, 4H), 2.39 (t, J = 7.2 Hz, 4 H), 2.97 (t, J = 7.4 Hz, 4 H), 3.18 (t, J = 6.9 Hz, 4 H); ^{13}C NMR (CD_3OD): δ 25.11, 28.00, 30.55, 34.10, 40.84, 41.06, 175.22; MS (CI+): calcd 287, found 287 $[M+1]^+$. Anal. ($C_{14}H_{30}N_4O_2 \bullet 2.0HCl \bullet 0.2H_2O$) C, H, N.

***N,N'*-bis(4-amino-1- butanoyl)-1,8-octanediamine dihydrochloride** (**2f**) The general procedures for the synthesis of homodimers were followed: *N*-Boc-2-pyrrolidinone **2** (526 mg, 2.84 mmol) and 1,8-diaminooctane (178 mg, 1.23 mmol) were combined in dioxane (10 mL), and treated as above. The title compound **2f** was obtained as a pale yellow solid (290 mg, 59%). ^{1}H NMR (CD_3OD): δ 1.33 (s, br, 8H), 1.50-1.52 (m, 4H), 1.95 (5-let, J = 7.4 Hz, 4H), 2.42 (t, J = 7.3 Hz, 4 H), 2.98 (t, J = 7.4 Hz, 4 H), 3.20 (t, J = 7.0 Hz, 4 H); ^{13}C NMR (CD_3OD): δ 25.14, 28.34, 30.54, 30.68, 33.92, 40.77, 41.41, 175.46; MS (CI^+): calcd 315, found 315 $[M+1]^+$.

***N,N'*-bis(4-amino-1- butanoyl)-1,9-nonanediamine dihydrochloride** (**2g**) The general procedures for the synthesis of homodimers were followed: *N*-Boc-2-pyrrolidinone **2** (529 mg, 2.86 mmol) and 1,9-diaminononame (181 mg, 1.14 mmol) were combined in dioxane (10 mL), and treated as above. The title compound **2g** was obtained as a pale yellow solid (195 mg, 43%). ^{1}H NMR (CD_3OD): δ 1.31 (s, br, 10H), 1.50 (s, br, 4H), 1.91 (5-let, J = 7.2 Hz, 4H), 2.34 (t, J = 7.1 Hz, 4 H), 2.96 (t, J = 7.4 Hz, 4 H), 3.15 (t, J = 7.0 Hz, 4 H); ^{13}C NMR (CD_3OD): δ 25.06, 28.49, 30.84, 30.86, 31.08, 34.29, 40.95, 40.98, 174.86; MS (CI^+): calcd 329, found 329 $[M+1]^+$.

***N,N'*-bis(4-amino-1- butanoyl)-1,10-decanediamine dihydrochloride** (**2h**) The general procedures for the synthesis of homodimers were followed: *N*-Boc-2-pyrrolidinone **2** (1.22 g, 6.61 mmol) and 1,10-diaminodecane (569 mg, 3.30 mmol) were combined in dioxane (10 mL), and treated as above. The title compound **2h** was obtained as a pale yellow solid (443 mg, 32%). ^{1}H NMR (CD_3OD): δ 1.31 (s, br, 12H), 1.47-1.51 (m, 4H), 1.91 (5-let, J = 7.3 Hz, 4H), 2.34 (t, J = 7.1 Hz, 4 H), 2.96 (t, J = 7.5 Hz, 4 H), 3.15 (t, J = 7.1 Hz, 4 H); ^{13}C NMR (CD_3OD): δ 25.08, 28.53, 30.89, 30.91, 31.14, 34.30, 40.96, 41.01, 174.86; MS (CI^+): calcd 343, found 343 $[M+1]^+$.

***N,N'*-bis(4-amino-1- butanoyl)-1,12-dodecanediamine dihydrochloride** (**2i**) The general procedures for the synthesis of homodimers were followed: *N*-Boc-2-pyrrolidinone **2** (532 mg, 2.87 mmol) and 1,12-diaminododecane (250 mg, 1.25 mmol) were combined in dioxane (10 mL), and treated as above. The title compound **2i** was obtained as a pale yellow solid (266 mg, 48%). ^{1}H NMR (CD_3OD): δ 1.29 (s, br, 16H), 1.46-1.81 (s, br, 4H), 1.93 (5-let, J = 7.2 Hz, 4H), 2.34 (t, J = 7.1 Hz, 4 H), 2.96 (t, J = 7.4 Hz, 4 H), 3.15 (t, J = 7.1 Hz, 4 H); ^{13}C NMR (CD_3OD): δ 25.05, 28.53, 30.87, 30.92, 31.18, 31.19, 34.28, 40.93, 41.01, 174.86; MS (CI^+): calcd 371, found 371 $[M+1]^+$.

General procedures for the preparation of GABA amide dimer derivatives (4a-h)

Diamines or diamine dihydrochloride salts (2.42 mmol, 1.0 equiv), Boc-GABA (**3**)[1] (6.04 mmol, 2.5 equiv), EDCI (6.04 mmol, 2.5 equiv), DMAP (6.04 mmol, 2.5

equiv) and Et_3N (7.26 mmol, 3 equiv it was needed only when dihydrochlorides were used) were combined in CH_2Cl_2 (or pyridine in case of hydrochloride salts were used) (10 mL), and stirred at room temperature for 12 hours. The mixture was then partitioned between CH_2Cl_2 (30 mL) and $KHSO_4$ (1N, 2 x 20 mL). The CH_2Cl_2 layer was collected, dried over Na_2SO_4, filtered and evaporated *in vacuo* to dryness. Either recrystallization or purification by column chromatography on silica gel yielded the corresponding *N*-Boc GABA derivatives. Trifluoroacetic acid deprotection provided the desired compounds (**4a-h**) in modest to good yields.

***N,N'*-bis(4-amino-1-butanoyl)-*trans*-1,4-cyclohexanediamine bis(trifluoroacetic acid) salts** (**4a**) The general procedures for the synthesis of **4a-h** were followed: *trans*-1,4-cyclohexanediamine (276 mg, 2.42 mmol), Boc-GABA (**3**)[1] (1.23 g, 6.04 mmol), EDCI (1.16 g, 6.04 mmol), DMAP (738 mg, 6.04 mmol) were combined in CH_2Cl_2 (10 mL) and treated as above. The corresponding N-Boc GABA derivative was recrystallized from EtOH/H_2O (1:2). The title compound **4a** was obtained as a brown solid (195 mg, 76%). ^{1}H NMR (CD_3OD): δ 1.29-1.34 (m, 4H), 1.86-1.93 (m, 8H), 2.28-2.32 (m, 4H), 2.94 (t, J = 7.6 Hz, 4H), 2.99 (t, J = 7.6 Hz, 4H), 3.60-3.63 (m, 2H); ^{13}C NMR (CD_3OD): δ 24.99, 32.68 (two peaks overlapped), 34.29, 40.90, 174.19; HRMS (FAB+): calcd for $C_{14}H_{31}N_4O_2$ $[M+1]^+$ 285.2285, found 285.2293.

***N,N'*-bis(4-amino-1- butanoyl)-3-aminobenzylamine bis(trifluoroacetic acid) salts** (**4b**) The general procedures for the synthesis of **4a-h** were followed: 3-aminobenzylamine (287 mg, 0.94 mmol), Boc-GABA (**3**)[1] (559 mg, 2.63 mmol), EDCI

(540 mg, 2.82 mmol), DMAP (253 mg, 2.07 mmol) were combined in CH_2Cl_2 (10 mL) and treated as above. The corresponding *N*-Boc-GABA derivative was purified by flash column chromatography on silica gel (15:85 MeOH-CH_2Cl_2 with 7 mL of concentrated NH_3 per liter). The title compound **4b** was obtained as a yellow oil (437 mg, 89%). ^{1}H NMR (CD_3OD): δ 1.92-2.05 (m, 4H), 2.41 (t, *J* = 7.0 Hz, 2H), 2.54 (t, *J* = 7.2 Hz, 2H), 3.00 (5-let *J* = 7.7 Hz, 4H), 4.35 (s, 2H), 7.03 (d, *J* = 7.6 Hz, 1H), 7.27 (t, *J* = 8.0 Hz, 1H), 7.40 (apparent d, *J* = 8.1 Hz, 1H), 7.56 (s, br, 1H); ^{13}C NMR (CD_3OD): δ 24.78, 24.90, 34.21, 34.93, 40.87, 40.92, 44.59, 120.50, 120.79, 124.80, 130.53, 140.48, 141.24, 173.33, 174.89; HRMS (FAB+): calcd for $C_{15}H_{25}N_4O_2$ $[M+1]^+$ 293.1972, found 293.1989 (+4.0 ppm, +1.2 mmu).

***N,N'*-bis(4-amino-1- butanoyl)-4-aminobenzylamine bis(trifluoroacetic acid) salts (4c)** The general procedures for the synthesis of **4a-h** were followed: 4-aminobenzylamine (60 μL, 0.53 mmol), Boc-GABA (**3**)[1] (448 g, 2.21 mmol), EDCI (423 mg, 2.21 mmol), DMAP (270 mg, 2.21 mmol) were combined in CH_2Cl_2 (10 mL) and treated as above. The corresponding *N*-Boc-GABA derivative was purified by flash column chromatography on silica gel (15:85 MeOH-CH_2Cl_2 with 7 mL of concentrated NH_3 per liter). The title compound **4c** was obtained as yellow oil (251 mg, 97%). ^{1}H NMR (CD_3OD): δ 1.93 (5-let, *J* = 7.5 Hz, 2H), 1.99 (5-let, *J* = 7.5 Hz, 2H), 2.38 (t, *J* = 7.0 Hz, 2H), 2.53 (t, *J* = 7.0 Hz, 2H), 4.32 (s, 2H), 7.23 (d, *J* = 8.4 Hz, 2H), 7.23 (apparent d, *J* = 8.4 Hz, 2H); ^{13}C NMR (CD_3OD): δ 24.74, 24.96, 34.21, 34.90, 40.94, 44.27, 96.33, 121.84, 129.65, 136.28, 139.38, 173.28, 174.80; HRMS (FAB+): calcd for $C_{15}H_{25}N_4O_2$ $[M+1]^+$ 293.1972, found 293.1975 (-0.8 ppm, -0.2 mmu).

***N,N'*-bis(4-amino-1- butanoyl)-*m*-xylylenediamine bis(trifluoroacetic acid) salts** (**4d**)

The general procedures for the synthesis of **4a-h** were followed: m-xylylendiamine (51.8 mg, 0.38 mmol), Boc-GABA (**3**)[1] (238 g, 1.17 mmol), EDCI (224 mg, 1.17 mmol), DMAP (143 mg, 1.17 mmol) were combined in CH_2Cl_2 (10 mL) and treated as above. The corresponding *N*-Boc-GABA derivative was purified by flash column chromatography on silica gel (10:90 MeOH-CH_2Cl_2 with 7 mL of concentrated NH_3 per liter). The title compound **4d** was obtained as yellow oil (165 mg, 87%). ^{1}H NMR (CD_3OD): δ 1.94 (5-let, J = 7.3 Hz, 4H), 2.39 (t, J = 7.2 Hz, 4H), 2.96 (t, J = 7.6 Hz, 4H), 4.35 (s, 4H), 7.17-7.20 (m, 3H), 7.26-7.30 (m, 1H); ^{13}C NMR (CD_3OD): δ 25.01, 34.21, 40.91, 44.58, 127.95, 128.38, 130.33, 140.82, 174.85; HRMS (FAB+): calcd for $C_{16}H_{27}N_4O_2$ $[M+1]^+$ 307.2129, found 307.2117 (-5.5 ppm, -1.7 mmu).

***N,N'*-bis(4-amino-1- butanoyl)-*o*-xylylenediamine bis(trifluoroacetic acid) salts** (**4e**)

o-Xylylenediamine was prepared from α, α'-dibromo-*o*-xylene according to the literature method in 81% yield.[3] The general procedures for the synthesis of **4a-h** were followed: *o*-xylylenediamine (58 mg, 0.44 mmol), Boc-GABA (**3**)[1] (265 g, 1.31 mmol), EDCI (251 mg, 1.31 mmol), DMAP (160 mg, 1.31 mmol) were combined in CH_2Cl_2 (10 mL) and treated as above. The corresponding *N*-Boc GABA derivative was purified by flash column chromatography on silica gel (10:90 MeOH-CH_2Cl_2 with 7 mL of concentrated NH_3 per liter). The title compound **4e** was obtained as yellow oil (193 mg, 88%). ^{1}H NMR (CD_3OD): δ 1.94 (5-let, J = 7.2 Hz, 4H), 2.39 (t, J = 7.0 Hz, 4H), 2.97 (t, J = 7.6 Hz, 4H), 4.43 (s, 4H), 7.24-7.30 (m, 4H); ^{13}C NMR (CD_3OD): δ 24.97, 34.13, 40.89,

42.12, 129.37, 130.33, 137.82, 174.77; HRMS (FAB+): calcd for $C_{16}H_{27}N_4O_2$ $[M+1]^+$ 307.2129, found 307.2133 (-0.4 ppm, -0.1 mmu).

***N,N'*-bis(4-amino-1-butanoyl)-*trans*-1,4-diaminobut-2-ene bis(trifluoroacetic acid) salts** (**4f**) *trans*-1,4-Diaminobut-2-ene dihydrochloride was prepared from *trans*-1,4-dibromo-2-butene according to the literature method in 99% yield.[3] The general procedures for the synthesis of **4a-h** were followed: *trans*-1,4-diaminobut-2-ene dihydrochloride (147 mg, 0.92 mmol), Boc-GABA (**3**)[1] (469 g, 2.31 mmol), EDCI (443 mg, 2.31 mmol), DMAP (282 mg, 2.31 mmol), Et_3N (520 μL, 3.68 mmol) and were combined in pyridine (10 mL) and treated as above. The corresponding *N*-Boc-GABA derivative was recrystallized from Hexane/EtOAc/Dioxane (4:4:2). The title compound **4f** was obtained as a brown oil (132 mg, 31%). ^{1}H NMR (CD_3OD): δ 1.91 (5-let, J = 7.3 Hz, 4H), 2.34 (t, J = 7.2 Hz, 4H), 2.95 (t, J = 7.6 Hz, 4H), 3.76-3.77 (m, 4H), 5.61-5.62 (m, 2H); ^{13}C NMR (CD_3OD): δ 24.94, 34.14, 40.89, 42.18, 129.58, 174.72; HRMS (FAB+): calcd for for $C_{12}H_{25}N_4O_2$ 257.1972 $[M+1]^+$, found 257.1989 (+4.5 ppm, +1.2 mmu).

***N,N'*-bis(4-amino-1- butanoyl)-*cis*-1,4-diaminobut-2-ene bis(trifluoroacetic acid) salts** (**4g**) *cis*-1,4-Diaminobut-2-ene dihydrochloride was prepared from *cis*-1,4-dichloro-2-butene according to the literature method in 94%.[3] *cis*-1,4-diaminobut-2-ene dihydrochloride (189 mg, 1.19 mmol), Boc-GABA (**3**)[1] (603 g, 2.97 mmol), EDCI (569 mg, 2.97 mmol), DMAP (363 mg, 2.97 mmol), Et_3N (498 μL, 3.57 mmol) and were combined in pyridine (10 mL) and treated as above. The corresponding *N*-Boc-GABA

derivative was recrystallized from Hexane/EtOAc/Dioxane (4:4:2). The title compound **4g** was obtained as brown oil (213 mg, 39%). ^{1}H NMR (CD_3OD): δ 1.91 (5-let, *J* = 7.3 Hz, 4H), 2.34 (t, *J* = 7.0 Hz, 4H), 2.96 (t, *J* = 7.4 Hz, 4H), 2.92-2.98 (m, 4H) 3.88 (apparent d, *J* = 5.2 Hz, 4H), 5.52 (t, *J* = 4.4 Hz, 2 H); ^{13}C NMR (CD_3OD): δ 24.94, 34.15, 37.85, 40.87, 129.85, 174.75; HRMS (FAB+): calcd for $C_{12}H_{25}N_4O_2$ $[M+1]^+$ 257.1972, found 257.1991 (+5.2 ppm, +1.3 mmu).

***N,N'*-bis(4-amino-1-butanoyl)-1,4-diaminobut-2-yne bis(trifluoroacetic acid) salts** (**4h**) 1,4-Diaminobut-2-yne dihydrochloride was prepared from 1,4-dichloro-2-butyne according to the literature method in 71%.[3] 1,4-diaminobut-2-yne dihydrochloride (144 mg, 0.92 mmol), Boc-GABA (**3**)[1] (465 g, 2.29 mmol), EDCI (439 mg, 2.29 mmol), DMAP (280 mg, 2.29 mmol), Et_3N (520 μL, 3.68 mmol) and were combined in pyridine (10 mL) and treated as above. The corresponding *N*-Boc-GABA derivative was recrystallized from Hexane/EtOAc/Dioxane (4:4:2). The title compound was obtained as a brown oil (291 mg, 70%). ^{1}H NMR (CD_3OD): δ 1.87 (5-let, *J* = 7.3 Hz, 4H), 2.30 (t, *J* = 7.0 Hz, 4H), 2.91 (t, *J* = 7.6 Hz, 4H), 3.91 (s, 4H); ^{13}C NMR (CD_3OD): δ 24.79, 30.21, 33.90, 40.84, 79.83, 174.56; HRMS (FAB+): calcd for $C_{12}H_{23}N_4O_2$ $[M+1]^+$ 255.1816, found 255.1819 (-0.8 ppm, -0.2mmu).

General procedures for the preparation of GABA amide heterodimers with pendant ammonium group (5a-e)

N-Boc-2-pyrrolidone (3.95 mmol, 1 equiv) and 1,*n*-diaminoalkane (*n* = 3-6, 11.86 mmol, 3 equiv) were combined in dioxane (5 mL) and refluxed overnight. After cooling

to room temperature, the mixture was evaporated in vacuum to dryness. The corresponding *N*-Boc-GABA amide derivatives were purified by flash column chromatography (2:8 MeOH-CH_2Cl_2 with 7 mL of concentrated NH_3 per liter) on silica gel. Either HCl or trifluoroacetic acid deprotection provided the desired compounds (**5a-e**) in good yields.

***N*-(4'-aminobutanoyl)-1,2-diaminoethane bis(trifluoroacetic acid) salts** (**5a**) The general procedures for the synthesis of heterodimers **5a-e** were followed: *N*-Boc-2-pyrrolidinone **2** (753 mg, 4.07 mmol) and 1,2-diaminoethane (816 μL, 12.20 mmol) were combined in dioxane (10 mL), and treated as above. The title compound **5a** was obtained as brown oil (709 mg, 80%). ^{1}H NMR (CD_3OD): δ 1.94 (5-let, J = 7.1 Hz, 2H), 2.42 (t, J = 7.0 Hz, 2H), 3.00 (t, J = 6.9 Hz, 2H), 3.07 (t, J = 6.2 Hz, 2H), 3.46 (t, J = 5.7 Hz, 2H); ^{13}C NMR (CD_3OD): δ 22.75, 32.20, 36.88, 39.10, 39.51, 174.45; MS (DICI+): calcd for $C_6H_{16}N_3O$ $[M+1]^+$ 146, found 146.

***N*-(4'-aminobutanoyl)-1,3-diaminopropane bis(trifluoroacetic acid) salts** (**5b**) The general procedures for the synthesis of heterodimers **5a-e** were followed: *N*-Boc-2-pyrrolidinone **2** (663 mg, 3.58 mmol) and 1,3-diaminopropane (1.51 mL, 17.9 mmol) were combined in dioxane (20 mL), and treated as above. The title compound **5b** was obtained as brown oil (729 mg, 51%). ^{1}H NMR (CD_3OD): δ 1.92 (5-let, J = 7.3 Hz, 2H), 1.84 (5-let, J = 7.1 Hz, 2H), 2.36 (t, J = 7.2 Hz, 2H), 2.92-2.98 (m, 4H) 3.28 (t, J = 6.6 Hz, 2H); ^{13}C NMR (CD_3OD): δ 24.88, 29.21, 33.99, 37.53, 38.74, 40.86, 175.76; HRMS (FAB+): calcd for $C_7H_{18}N_3O$ $[M+1]^+$ 160.1450, found 160.1450 (+0.1ppm, 0.0 mmu).

***N*-(4'-aminobutanoyl)-1,4-diaminobutane bis(trifluoroacetic acid) salts** (**5c**) The general procedures for the synthesis of heterodimers **5a-e** were followed: *N*-Boc-2-pyrrolidinone **2** (731 mg, 3.95 mmol) and 1,4-diaminobutane (1.20 mL, 11.86 mmol) were combined in dioxane (10 mL), and treated as above. The title compound **5c** was obtained as brown oil (733 mg, 75%). ^{1}H NMR (CD_3OD): δ 1.57-1.61 (m, 2H), 1.65-1.70 (m, 2H), 1.92 (5-let, J = 7.3 Hz, 2H), 2.36 (t, J = 7.2 Hz, 2H), 2.93-2.98 (m, 4H) 3.22 (t, J = 6.9 Hz, 2H); ^{13}C NMR (CD_3OD): δ 23.21, 24.56, 25.98, 32.49, 38.31, 39.11, 173.34; HRMS (FAB+): calcd for $C_8H_{20}N_3O$ $[M+1]^+$ 174.1606, found 174.1612 (+3.2 ppm, +0.6 mmu).

***N*-(4'-aminobutanoyl)-1,5-diaminopentane bis(trifluoroacetic acid) salts** (**5d**) The general procedures for the synthesis of heterodimers **5a-e** were followed: *N*-Boc-2-pyrrolidinone **2** (659 mg, 3.56 mmol) and 1,5-diaminopentane (1.25 mL, 10.68 mmol) were combined in dioxane (20 mL), and treated as above. The title compound **5d** was obtained as brown oil (1.13 g, 74%). ^{1}H NMR (CD_3OD): δ 1.36-1.43 (m, 2H), 1.54 (5-let, J = 7.4 Hz, 2H), 1.66 (5-let, J = 7.7 Hz, 2H), 1.91 (5-let, J = 7.2 Hz, 2H), 2.33 (t, J = 7.2 Hz, 2H), 2.89-2.97 (m, 4H) 3.18 (t, J = 7.2 Hz, 2H); ^{13}C NMR (CD_3OD): δ 25.01, 25.23, 28.67, 30.34, 34.20, 40.57, 40.89, 41.07, 174.98; HRMS (FAB+): calcd for $C_9H_{22}N_3O_2$ $[M+1]^+$ 188.1763, found 188.1757 (-3.1ppm, -0.6 mmu)

***N*-(4'-aminobutanoyl)-1,6-diaminohexane bis(trifluoroacetic acid) salts** (**5e**) The general procedures for the synthesis of heterodimers **5a-e** were followed: *N*-Boc-2-pyrrolidinone **2** (520 mg, 2.81 mmol) and 1,6-diaminohexane (1.63 g, 14.10 mmol) were

combined in dioxane (10 mL), and treated as above. The title compound **5e** was obtained as brown oil (1.15 g, 92%). ^{1}H NMR (CD_3OD): δ 1.34-1.45 (m, 4H), 1.52 (5-let, *J* = 7.0 Hz, 2H), 1.65 (5-let, *J* = 7.5 Hz, 2H), 1.90 (5-let, *J* = 7.4 Hz, 2H), 2.33 (t, *J* = 7.2 Hz, 2H), 2.89-2.97 (m, 4H) 3.18 (t, *J* = 7.0 Hz, 2H); ^{13}C NMR (CD_3OD): δ 25.02, 27.53, 27.89, 28.95, 30.63, 34.22, 40.75, 40.91, 41.13, 174.91; HRMS (FAB+): calcd for $C_{10}H_{24}N_3O_2$ $[M+1]^+$ 202.1914, found 202.1929 (+4.8 ppm, +1.0 mmu)

General procedures for the preparation of GABA amide heterodimers with pendant acetamide group (6a-e)

To a solution of **5c** (197.3 mg, 0.73 mmol) in CH_2Cl_2 (5 mL) was added acetic anhydride (103 μL, 1.09 mmol) and 0.5 M NaOH (2.9 mL, 2.0 mmol). The reaction mixture was stirred at room temperature for overnight. The mixture was then partitioned between CH_2Cl_2 (20 mL) and H_2O (2 x 20 mL). The CH_2Cl_2 layer was collected, dried over Na_2SO_4, filtered and evaporated *in vacuo* to afford pure *N*-Boc-GABA amide derivative of **6c** as a pale yellow solid; and no further purification step was required. Either HCl or trifluoroacetic acid deprotection provided the desired compounds (**6a-e**) in good yields.

***N*-acetyl-*N'*-(4'-aminobutanoyl)-1,2-diaminoethane trifluoroacetic acid salt** (**6a**) The general procedures for the synthesis of **6c** were followed: **5a** (187.3 mg, 0.76 mmol) and acetic anhydride (108 μL, 1.15 mmol) and 0.5 M NaOH (3.04 mL, 1.52 mmol) were combined in CH_2Cl_2 (5 mL) and treated as above. The title compound **6a** was obtained

as a brown oil (110 mg, 48%). ^{1}H NMR (CD_3OD): δ 1.91 (5-let, *J* = 7.0 Hz, 2H), 1.94 (s, 3H), 2.34 (t, *J* = 7.0 Hz, 2H), 2.96 (t, *J* = 7.4 Hz, 2H), 3.27 (s, br, 2H); MS (DICI-): calcd for $C_8H_{16}N_3O_2$ [M-1] 186, found 186.

***N*-acetyl-*N'*-(4'-aminobutanoyl)-1,3-diaminopropane trifluoroacetic acid salt** (**6b**) The general procedures for the synthesis of **6c** were followed: **5b** (119 mg, 0.46 mmol) and acetic anhydride (65 μL, 0.69 mmol) and 0.5 M NaOH (1.84 mL, 0.92 mmol) were combined in CH_2Cl_2 (10 mL) and treated as above. The title compound **6b** was obtained as a brown oil (123 mg, 85%). ^{1}H NMR (CD_3OD): δ 1.67 (5-let, *J* = 6.8 Hz, 2H), 1.91 (5-let, *J* = 7.2 Hz, 2H), 1.93 (s, 3H), 2.34 (t, *J* = 7.0 Hz, 2H), 2.96 (t, *J* = 7.26Hz, 2H), 3.19 (q, *J* = 7.2 Hz, 4H); ^{13}C NMR (CD_3OD): δ 23.06, 24.96, 30.58, 34.25, 38.25, 38.28, 40.90, 173.90, 175.03; HRMS (FAB+): calcd for $C_9H_{20}N_3O_2$ $[M+1]^+$ 202.1550, found 202.1559 (+1.7 ppm, +0.3 mmu).

***N*-acetyl-*N'*-(4'-aminobutanoyl)-1,4-diaminobutane hydrochloride** (**6c**) The title compound **6c** was obtained as a yellow solid (112 mg, 61%). ^{1}H NMR (CD_3OD): δ 1.50-1.53 (m, 4H), 1.92 (5-let, *J* = 7.3 Hz, 2H), 1.95 (s, 3H), 2.34 (t, *J* = 7.2 Hz, 2H), 2.96 (t, *J* = 7.6 Hz, 2H), 3.17-3.19 (m, 4H); ^{13}C NMR (CD_3OD): δ 22.91, 25.02, 34.30, 40.54, 40.73, 40.97, 173.97, 174.95; HRMS (FAB+): calcd for $C_{10}H_{22}N_3O_2$ $[M+1]^+$ 216.1712, found 216.1716 (+2.3 ppm, +0.5 mmu)

***N*-acetyl-*N'*-(4'-aminobutanoyl)-1,5-diaminopetane trifluoroacetic acid salt** (**6d**) The general procedures for the synthesis of **6c** were followed: **5d** (108 mg, 0.37 mmol) and

acetic anhydride (53 μL, 0.56 mmol) and 0.5 M NaOH (1.5 mL, 0.74 mmol) were combined in CH_2Cl_2 (10 mL) and treated as above. The title compound **6d** was obtained as a brown oil (121 mg, 95%). ^{1}H NMR (CD_3OD): δ 1.31-1.37 (m, 2H), 1.47-1.55 (m, 4H), 1.90 (5-let, *J* = 7.3 Hz, 2H), 1.92 (s, 3H), 2.33 (t, *J* = 7.2 Hz, 2H), 2.95 (t, *J* = 7.4 Hz, 2H), 3.12-3.18 (m, 4H); ^{13}C NMR (CD_3OD): δ 23.03, 25.00, 25.73, 30.47, 30.53, 34.26, 40.82, 40.95, 173.75, 174.89; HRMS (FAB+): calcd for $C_{11}H_{24}N_3O_2$ $[M+1]^+$ 230.1863, found 230.1877 (+3.7 ppm, +0.8 mmu).

***N*-acetyl-*N*'-(4'-aminobutanoyl)-1,6-diaminohexane trifluoroacetic acid salt** (**6e**) The general procedures for the synthesis of **6c** were followed: **5e** (157 mg, 0.52 mmol) and acetic anhydride (75 μL, 0.78 mmol) and 0.5 M NaOH (2.0 mL, 1.04 mmol) were combined in CH_2Cl_2 (12 mL) and treated as above. The title compound **6e** was obtained as a brown oil (155 mg, 83%). ^{1}H NMR (CD_3OD): δ 1.32-1.37 (m, 4H), 1.47-1.51 (m, 4H), 1.90 (5-let, *J* = 7.3 Hz, 2H), 1.91 (s, 3H), 2.32 (t, *J* = 7.0 Hz, 2H), 2.95 (t, *J* = 7.6 Hz, 2H), 3.12-3.18 (m, 4H); ^{13}C NMR (CD_3OD): δ 23.03, 25.03, 28.02, 30.71, 30.73, 34.26, 40.81, 40.84, 40.93, 173.70, 174.86; HRMS: calcd for $C_{12}H_{26}N_3O_2$ $[M+1]^+$ 244.2025, found 244.2017 (-3.3 ppm, -0.8 mmu).

General procedures for the preparation of GABA amide derivatives (7a-b)

To a solution of **5c** (0.73 mmol) in CH_2Cl_2 (5 mL) was added a pendant group synthon as described below (1.10 mmol) and 0.5 M NaOH or Et_3N or pyridine. The reaction mixture was stirred at room temperature for 12h. The mixture was then

partitioned between CH_2Cl_2 (20 mL) and H_2O (2 x 20 mL). The CH_2Cl_2 layer was collected, dried over Na_2SO_4, filtered and evaporated *in vacuo* to dryness. The corresponding *N*-Boc GABA derivatives were purified by flash column chromatography (2:8 MeOH-CH_2Cl_2 with 7 mL of concentrated NH_3 per liter). Trifluoroacetic acid deprotection provided the desired compounds (**7a-b**) in good yields.

***N*-cyclopropyl-N'-(4'-aminobutanoyl)-1,4-diaminobutane trifluoroacetic acid salt** (**7a**) The general procedures for the preparation of **7a-b** were followed: **5c** (105.3 mg, 0.39 mmol), cyclopropanecarbonyl chloride (45 mg, 0.59 mmol) and 0.5 M NaOH (1.6 mL, 0.78 mmol) were combined as above. The title compound **7a** was obtained as a yellow solid (111 mg, 80%). ^{1}H NMR (CD_3OD): δ 0.70-0.75 (m, 2H), 0.80-0.83 (m, 2H), 1.50-1.55 (m, 4H), 1.90 (5-let, *J* = 7.3 Hz, 2H), 2.33 (t, *J* = 7.0 Hz, 2H), 2.95 (t, *J* = 7.6 Hz, 2H), 3.16-3.19 (m, 4H); ^{13}C NMR (CD_3OD): δ 7.10, 14.82, 24.49, 27.68, 27.95, 33.74, 40.08, 40.17, 40.41, 174.42, 176.46. HRMS (FAB+): calcd $C_{12}H_{24}N_3O_2$ $[M+1]^+$ 242.1863, found 242.1869.

***N*-chloroacetyl-N'-(4'-aminobutanoyl)-1,4-diaminobutane trifluoroacetic acid salt** (**7b**) The general procedures for the preparation of **7a-b** were followed: **5c** (106.6 mg, 0.39 mmol), chloroacetic anhydride (100.8 mg, 0.59 mmol) and 0.5 M NaOH (1.6 mL, 0.78 mmol) were combined as above. The title compound **7b** was obtained as a brown oil (104 mg, 73%). ^{1}H NMR (CD_3OD): δ 1.50-1.55 (m, 4H), 1.90 (5-let, *J* = 7.3 Hz, 2H), 2.33 (t, *J* = 7.0 Hz, 2H), 2.95 (t, *J* = 7.4 Hz, 2H), 3.18-3.24 (m, 4H), 4.02 (s, 2H); ^{13}C

NMR (CD_3OD): δ 25.00, 28.08, 28.11, 34.24, 40.50, 40.89, 43.69, 96.32, 169.85, 174.93; HRMS: calcd $C_{10}H_{21}N_3O_2Cl$, $[M+1]^+$ 250.1317, found 250.1322.

Synthesis of *N*-benzoylamino-*N*-pentylthiourea (8)[4]

To a solution of NH_4NCS (3.76 g, 49.4 mmol)) in dry acetone (37 mL) was added benzyol chloride (5.8 mL, 49.4 mmol) dropwise and heated to reflux for 15 min. The reaction mixture was allowed to cool to room temperature, followed by addition of n-amylamine (7.0 mL) in acetone (10 mL). The reaction mixture was then stirred at room temperature for additional 1 h. White precipitate was filtered off, and the filtrate was concentrated under vacuum to afford the desired product **8** as yellow solid (7.90 g, 67%). The desired product was pure by TLC and NMR. No further purification step was required. ^{1}H NMR ($CDCl_3$): δ 0.92 (t, *J* = 7.0 Hz, 3H), 1.32-1.43 (m, 4H), 1.71 (5-let, *J* = 7.6 Hz, 2H), 3.68 (q, *J* = 7.1 Hz, 2H), 7.48-7.53 (m, 2H), 7.56-7.62 (m, 1H), 7.79-7.84 (m, 1H), 9.07, (s, 1H), 10.73 (s, 1H); ^{13}C NMR ($CDCl_3$): δ 13.85, 22.24, 27.83, 29.01, 45.87, 127.30, 127.37, 128.52, 129.02, 131.81, 131.93, 133.41, 166.85, 179.62; HRMS: calcd $C_{10}H_{21}N_3O_2Cl$, $[M+1]^+$ 251.1218, found 251.1213 9 (-2.0 ppm, -0.5 mmu).

General procedures for the preparation of n-alkylthioureas (9, 10, 13 and 14)

To a stirring solution of 1,1'-thiocarbonyldiimidazole (4.83 mmol, 2.0 equiv) and imidazole (7.23 mmol, 3.0 equiv) in CH_3CN (15 mL) at 0 °C, was added *n*-alkylamine (2.41 mmol, 1.0 equiv) in CH_3CN (2 mL) dropwise. The yellow mixture was then stirred

at room temperature for 18 h. The reaction mixture was then cooled to 0 °C, NH_4OH (29.2 wt% in H_2O, 1.5 mL) was added. The ice-bath was removed, and the reaction mixture was stirred at room temperature for 1 h. Solvent was removed under reduced pressure to afford brown liquid residue, which was then purified by column chromatography on silica gel (1:9 CH_2Cl_2-CH_3OH).

***n*-Butylthiourea** (**9**) The general procedures for the preparation of *n*-alkylthioureas were followed: 1,1'-thiocarbonyldiimidazole (1.18 g, 6.62 mmol), imidazole (676 mg, 9.92 mmol), and *n*-butylamine (327 μL, 3.31 mmol) were combined in CH_3CN (15 mL) and treated as above. The title compound **9** was obtained as a yellow solid (325 mg, 74%). ^{1}H NMR ($CDCl_3$): δ 0.9 (t, *J* = 7.4 Hz, 3H), 1.22-1.28 (m, 4H), 1.42-1.43 (m, 2H), 3.31 (s, br, 2H), 6.84 (s, br, 2H), 7.61 (s, br, 1H); ^{13}C NMR ($CDCl_3$): δ 13.61, 19.97, 30.27, 31.09, 43.88, 45.15, 180.53, 182.91; HRMS (FAB+): calcd for $C_5H_{13}N_2S$ $[M+1]^+$ 133.0799, found 133.0798 (-1.1 ppm, -0.1 mmu).

***N*-Pentylthiourea** (**10**) The general procedures for the preparation of *n*-alkylthioureas were followed: 1,1'-thiocarbonyldiimidazole (860 mg, 4.83 mmol), imidazole (492 mg, 7.23 mmol), and *n*-pentylamine (280 μL, 2.41 mmol) were combined in CH_3CN (10 mL) and treated as above. The title compound **10** was obtained as a yellow solid (314 mg, 89%). The title compound was obtained as yellow solid in 89% yield as described above. ^{1}H NMR (DMSO): δ 0.85 (t, *J* = 7.1 Hz, 3H), 1.33-1.38 (m, 2H), 1.56 (s, br, 2H), 3.13 (s, br, 1H), 3.49 (s, br, 1H), 6.40 (s, br, 2H), 7.17 (s, br, 1H); ^{13}C NMR ($CDCl_3$): δ 13.90,

21.85, 27.93, 28.53, 42.84, 43.85, 45.15, 180.21, 183.06; HRMS (FAB+): calcd for $C_6H_{15}N_2S$ $[M+1]^+$ 147.0956, found 147.0953 (-2.0 ppm, -0.3 mmu).

***N*-(2-diaminoethyl)thiourea** (**13**) The general procedures for the preparation of *n*-alkylthioureas were followed: 1,1'-thiocarbonyldiimidazole (884 mg, 4.96 mmol), imidazole (507 mg, 7.44 mmol), and *N*-tert-butoxylcarbonyl-1,2-diaminoethane (397 mg, 2.48 mmol) were combined in CH_3CN (9 mL) and treated as above. The title compound **13** was obtained as a yellow solid (191 mg, 35%). ^{1}H NMR (CD_3CN): δ 1.41 (s, 9H), 3.00-3.01 (m, 2H), 3.38 (s, br, 2H), 6.82 (s, br, 1H), 7.00 (s, br, 1H), 7.52 (s, br, 1H); FTIR (neat film): 1511, 1683, 2979, 3184, 3295, 3350, 3374, 3403 cm^{-1}. ^{13}C NMR (DMSO): 28.30, 43.56, 77.72, 155.70, 183.37.

***N*-ethylenethiourea** (**14**) The title compound **14** was obtained as ayellow solid (303 mg, 60%) as described above. Compound **14** is a side product in the synthesis of **13**. ^{1}H NMR ($CDCl_3$): δ 1.54 (s, 9H), 3.57 (t, J = 8.7 Hz, 2H), 3.57 (apparent t, J = 8.8 Hz, 2H), 7.04 (s, 1H); FTIR (neat film): 1504, 1700, 1732, 2974, 3293, 3243 cm^{-1}. MS ($DIEI^+$): calcd for $C_8H_{14}N_2O_2S$ $[M]^+$ 202.0776, found 202.

General procedures for the preparation of N-alkyl ZAPA (11, 12, 15 and 16)

To a solution of *n*-alkylthiourea (0.92 mmol, 1.0 equiv) in glacial acetic acid (3 mL) and 2 N HCl (10 mL) at room temperature was added propiolic acid (1.02 mmol, 1.1

equiv) in H_2O (2 mL) dropwise. The reaction mixture was then stirred at room temperature for 12 h. Solvent was removed under reduced pressure to provide gummy residue, which would not recrystallize from any attempted solvent.

***N*-butyl -3-[(aminoiminomethyl)thio]prop-2-enoic acid (11)** The general procedures for the synthesis of *N*-alkyl ZAPA were followed: *n*-butylthiourea (218 mg, 0.92 mmol), glacial acetic acid (3 mL), 2 N HCl (10 mL) and propiolic acid (115 μL, 1.02 mmol) were combined and treated as above. The title compound **11** was obtained as yellow gum of Z/E isomers (Z/E ratio: 9:1) in quantitative yield (395 mg, 100 %). ^{1}H NMR (CD_3OD): δ 0.87 (t, *J* = 7.4 Hz, 3H), 1.3 (6-let, *J* = 7.5 Hz, 2H), 1.53 (5-let, *J* = 7.3 Hz, 2H), 3.33-3.39 (m, 2H), 6.23 (d, *J* = 9.6 Hz, 1H), 6.31 (d, *J* = 15.2 Hz, 0.12H), 7.65 (d, *J* = 9.6 Hz, 1H), 7.75 (d, *J* = 15.6 Hz, 0.11H), 9.68 (s, 1H), 9.93 (s, 1H), 10.33 (s, 1H); ^{13}C NMR (CD_3OD): δ 13.46, 19.30, 29.25, 43.92, 117.57, 138.36, 163.80, 167.20; HRMS (FAB+): calcd for $C_8H_{15}N_2O_2S$ $[M+1]^+$ 203.0854, found 203.0865 (+5.3 ppm, +1.1 mmu).

***N*-pentyl -3-[(aminoiminomethyl)thio]prop-2-enoic acid (12)** The general procedures for the synthesis of *N*-alkyl ZAPA were followed: *n*-pentylthiourea (137 mg, 0.94 mmol), glacial acetic acid (3 mL), 2 N HCl (10 mL) and propiolic acid (64 μL, 1.03 mmol) were combined and treated as above. The title compound **12** was obtained as yellow gum of Z/E isomers (Z/E ratio: 2:1) in quantitative yield (239 mg, 100 %). ^{1}H NMR (CD_3OD): δ 0.96-0.99 (m, 3H), 1.39-1.43 (m, 4H), 1.71-1.74 (m, 2H), 3.40-3.45 (m, 2H), 6.28 (d, *J* = 9.2 Hz, 0.65H), 6.35 (d, *J* = 15.6 Hz, 0.31H), 7.52 (d, *J* = 9.2 Hz,

0.65H), 7.79 (d, *J* = 15.2 Hz, 0.31H); HRMS (FAB+): calcd for $C_9H_{17}N_2O_2S$ $[M+1]^+$ 217.1011, found 217.1027 (+7.5 ppm, +1.6 mmu).

***(Z)-N*-aminoethyl-3-[(aminoiminomethyl)thio]prop-2-enoic acid (15)** The general procedures for the synthesis of *N*-alkyl ZAPA were followed: *N*-(2-diaminoethyl)thiourea (228 mg, 1.04 mmol), glacial acetic acid (2 mL), 2 N HCl (5 mL) and propiolic acid (78 μL, 1.25 mmol) were combined and treated as above. The title compound **15** was obtained as an off-white solid after recrystallizing from iPr/CH_2OH (8:2) (154 mg, 57 %). ^{1}H NMR (DMSO): δ 3.06-3.08(m, 2H), 3.71-3.72 (m, 2H), 6.22 (d, *J* = 10 Hz, 1H), 7.77 (d, *J* = 10 Hz, 1H), 8.42 (s, 2H), 9.95 (s, 1H), 10.2 (s, 1H), 10.48 (s, 1H); ^{13}C NMR (DMSO): δ 36.92, 41.81, 117.50, 138.69, 165.22, 167.26; HRMS (FAB+): calcd for $C_6H_{12}N_3O_2S$ $[M+1]^+$ 190.0650, found 190.0643 (-3.8 ppm, -0.7 mmu).

***(Z)-N*-ethylene-3-[(aminoiminomethyl)thio]prop-2-enoic acid (16)** The general procedures for the synthesis of *N*-alkyl ZAPA were followed: *N*-ethylenethiourea (1.56 g, 7.12 mmol), glacial acetic acid (5 mL), 2 N HCl (15 mL) and propiolic acid (530 μL, 5.84 mmol) were combined and treated as above. The title compound **16** was obtained as an off-white solid after recrystallizing from iPr/CH_2OH (8:2) (1.07 g, 72 %). ^{1}H NMR (DMSO): δ 3.91 (s, 4H), 6.34 (d, *J* = 9 Hz, 1H), 7.76 (d, *J* = 9 Hz, 1H), 10.83 (s, 2H); ^{13}C NMR (DMSO): δ 45.28, 119.42, 135.39, 166.86, 167.26; HRMS (FAB+): calcd for $C_6H_{11}N_2O_2S$ $[M+1]^+$ 173.0379, found 173.0362.

General procedures for the synthesis of PEG-linked GABA amide homodimers (19a-d)

PNP (*p*-nitrophenyl carbonate) activated PEG 10000[9] (56 μmol, 1.0 equiv) and **5c•**Boc (168 μmol, 3.0 equiv) were combined in CH_3CN (500μL) and stirred at room temperature for 24 h. The reaction mixture was then diluted to 50 mL CH_2Cl_2, washed with 0.1 N HCl (1 x 40 mL) and 10% $NaHCO_3$ (2 x 40 mL). The organic layer was collected and dried over Na_2SO_4, filtered and concentrated under reduced pressure to provide yellow oily residue. Column chromatography on silica gel, eluting with 95:5 CH_2Cl_2-CH_3OH was used to remove the side product *p*-nitrophenol and with 80:20 CH_2Cl_2-CH_3OH was used to yield the corresponding *N*-Boc PEG 10000 GABA amide. Trifluoroacetic acid deprotection provided the desired compounds (**19a-d**) in good yields.

PEG 1500 bis[4-(4-aminobutanoyl)butyl] carbamate•2TFA (**19a**) PNP activated PEG 1500 (205 mg, 112 μmol) and **5c•**Boc (91 mg, 336 μmol) were combined in CH_3CN (620 μL) as described above. The title compound **19a** was otained as off-white solid (197 mg, 74%). ^{1}H NMR (CD_3OD): δ 1.92 (5-let, *J* = 7.7 Hz, 4H), 2.33 (t, *J* = 7.5 Hz, 4H), 2.99 (t, *J* = 7.6 Hz, 4H), 3.11-3.12 (m, 4H), 3.18-3.19 (m, 4H), 3.63-3.78 (m, 166H), 4.15 (apparent t, *J* = 5.1 Hz, 4H).

PEG 3400 bis[4-(4-aminobutanoyl)butyl] carbamate•2TFA (**19b**) PNP activated PEG 3400 (430 mg, 115 μmol) and **5c•**Boc (93 mg, 346 μmol) were combined in CH_3CN (640 μL) as described above. The title compound **19b** was otained as off-white solid (384 mg,

85%). The title compound was otained as off-white solid in 85% yield as described above. ^{1}H NMR (CD_3OD): δ 1.92 (5-let, *J* = 7.7 Hz, 4H), 2.33 (t, *J* = 7.0 Hz, 4H), 3.00 (t, *J* = 7.1 Hz, 4H), 3.11-3.12 (m, 4H), 3.19-3.20 (m, 4H), 3.61-3.70 (m, 348H), 4.14-4.16 (m, 4H).

PEG 8000 bis[4-(4-aminobutanoyl)butyl] carbamate•2TFA (**19c**) PNP activated PEG 8000 (408 mg, 49 μmol) and **5c**•Boc (40 mg, 147 μmol) were combined in CH_3CN (500 μL) as described above. The title compound **19c** was otained as off-white solid (376 mg, 89%). ^{1}H NMR (CD_3OD): δ 1.93 (5-let, *J* = 7.5 Hz, 4H), 2.33 (t, *J* = 6.9 Hz, 4H), 3.01 (t, *J* = 7.8 Hz, 4H), 3.11-3.12 (m, 4H), 3.20-3.21 (m, 4H), 3.50-3.78 (m, 875H), 4.14-4.16 (m, 4H).

PEG 10000 bis[4-(4-aminobutanoyl)butyl] carbamate•2TFA (**19d**) PNP activated PEG 10000 (579 mg, 56 μmol) and **5c**•Boc (45 mg, 168 μmol) were combined in CH_3CN (500 μL) as described above. The title compound **19d** was otained as off-white solid (529 mg, 89%). ^{1}H NMR (CD_3OD): δ 1.93 (5-let, *J* = 7.8 Hz, 4H), 2.33 (t, *J* = 7.0 Hz, 4H), 3.01 (t, *J* = 7.9 Hz, 4H), 3.11-3.12 (m, 4H), 3.20-3.21 (m, 4H), 3.51-3.3.78 (m, 1118H), 4.14-4.15 (m, 4H).

General procedures for the preparation of dansyl GABA and its derivatives (21a-h)[5]

_N,N'_-bis[4'-(5''-Dimethylnaphthyl-1''-sulfonyl)amido butanoyl]-1,4-diaminobutane (21h)

To a solution of **2c•**2HCl (65.3 mg, 0.20 mmol) in 10% $NaHCO_3$ (2 mL) was added dansyl chloride (53.1 mg, 0.20 mmol) in 2 mL CH_2Cl_2. The two phase reaction mixture was heated to reflux for 12 h. After cooling to room temperature, the reaction mixture was partitioned between CH_2Cl_2 (2 x 25 mL) and H_2O (1 x 25 mL). The combined organic layer were dried over $MgSO_4$, filtered and concentrated under reduced pressure to provide a viscous yellow residue. Column chromatography on silica gel, eluting with 90:10 CH_2Cl_2-CH_3OH afforded the title compound **21h** as a green solid (27.3 mg, 20%). ^{1}H NMR ($CDCl_3$): δ 1.56 (s, br, 2H), 1.76-1.78 (m, 4H), 1.98 (s, 3H), 2.25 (t, *J* = 6.7 Hz, 4H), 2.86(s, 12H), 2.91 (apparent q, *J* = 5.8 Hz, 4H), 3.24-3.25 (m, 4H), 6.15 (t, *J* = 5.7 Hz, 2H), 6.47 (t, *J* = 5.6 Hz, 2H), 7.15 (d, *J* = 7.6 Hz, 2H), 7.50 (q, *J* = 7.9 Hz, 4H), 8.20 (dd, *J* = 7.4 Hz, 2H), 8.31 (d, *J* = 8.7 Hz, 2H), 8.51 (d, *J* = 8.5 Hz, 1H); HRMS (FAB+): calcd for $C_{36}H_{49}N_6O_6S_2$ $[M+1]^+$ 725.315, found 725.455; HPLC: 18.38 min.

4'-(5''-Dimethylnaphthyl-1''-sulfonyl)amido butanoyl alcohol (21a) The general procedures for the synthesis of **21h** were followed: GABA (27.1 mg, 0.26 mmol in 1 mL 0.1 $NaHCO_3$) and dansyl chloride (7.0 mg, 0.026 mmol) were combined acetone (2 mL) and treated as above. The title compound **21a** was obtained as a green solid (8.7 mg,

100%). ^{1}H NMR ($CDCl_3$): δ 1.73 (5-let, *J* = 6.8 Hz, 2H), 2.31 (apparent t, *J* = 6.8 Hz, 2H), 2.88 (s, 6H), 2.94-2.95 (m, 2H), 4.97 (s, br, 1H), 7.17 (d, *J* = 7.4 Hz, 1H), 7.50 (apparent d, *J* = 7.9 Hz, 1H), 7.55 (apparent, J = 8.3 Hz, 1H), 8.22 (dd, *J* = 7.3, 1.2 Hz, 1H), 8.25 (d, *J* = 8.5 Hz, 1H), 8.5(d, *J* = 8.5 Hz, 1H); HPLC: 7.06 min.

4'-(5''-Dimethylnaphthyl-1''-sulfonyl)amido butanoyl amine (21b) The general procedures for the synthesis of **21h** were followed: **1a•**HCl (12.9 mg, 0.09 mmol in 1 mL 0.1 $NaHCO_3$) and dansyl chloride (2.5 mg, 0.009 mmol) were combined acetone (2 mL) and treated as above. The title compound **21b** was obtained as a green solid (3.2 mg, 100 %). ^{1}H NMR ($CDCl_3$): δ 1.76 (5-let, *J* = 6.4 Hz, 2H), 2.34 (t, *J* = 6.9 Hz, 2H), 2.88 (s, 6H), 2.94 (q, *J* = 6.3 Hz, 2H), 5.36-5.38 (m, 2H), 5.54 (s, br, 1H), 7.18 (d, *J* = 7.4 Hz, 1H), 7.52 (apparent d, *J* = 8.5 Hz, 1H), 7.57 (apparent, J = 8.3 Hz, 1H), 8.21 (d, *J* = 8.5 Hz, 1H), 8.27 (d, *J* = 8.7 Hz, 1H), 8.53 (d, *J* = 8.5 Hz, 1H); HRMS (FAB+): calcd for $C_{16}H_{21}N_2O_3S$ $[M+1]^+$ 336.1376, found 336.1380 (+1.2 ppm); HPLC: 3.48 min.

***N*-butyl-4'-(5''-Dimethylnaphthyl-1''-sulfonyl)amido butanoyl amine (21c)** The general procedures for the synthesis of **21h** were followed: **1b•**HCl (45.2 mg, 0.23 mmol in 2 mL 10% $NaHCO_3$) and dansyl chloride (75.1 mg, 0.28 mmol) were combined CH_2Cl_2 (2 mL) and treated as above. The title compound **21c** was obtained as a brown solid (82.0 mg, 87%). ^{1}H NMR ($CDCl_3$): δ 0.90 (t, *J* = 7.4 Hz, 3H), 1.31 (6-let, *J* = 7.7 Hz, 2H), 1.43 (5-let, *J* = 7.3 Hz, 2H), 1.75 (5-let, *J* = 6.5 Hz, 2H), 2.16 (t, *J* = 6.8 Hz, 2H), 2.88 (s, 6H), 2.91 (q, *J* = 6.2 Hz, 2H), 3.17 (q, *J* = 7.1 Hz, 2H), 5.38 (t, *J* = 6.2 Hz,

2H), 5.52 (s, br, 1H), 7.17 (d, *J* = 7.1 Hz, 1H), 7.51 (apparent d, *J* = 8.7 Hz, 1H), 7.56 (apparent, J = 8.5 Hz, 1H), 8.21 (d, *J* = 8.5 Hz, 1H), 8.28 (d, *J* = 8.7 Hz, 1H), 8.52 (d, *J* = 8.5 Hz, 1H); HRMS (FAB+): calcd for $C_{20}H_{29}N_3O_3S$ $[M+1]^+$ 392.2008, found 392.2011 (+0.8 ppm/+0.3 mmu); HPLC: 18.50 min.

***N,N'*-bis[4'-(5''-Dimethylnaphthyl-1''-sulfonyl)amido] butanoyl-1,2-diaminoethane (21d)** The general procedures for the synthesis of **21h** were followed: **5a•**2HCl (30.8 mg, 0.14 mmol in 2 mL 10% $NaHCO_3$) and dansyl chloride (25.3 mg, 0.09 mmol) were combined CH_2Cl_2 (2 mL) and treated as above. The title compound **21d** was obtained as a green solid (9.6 mg, 17%). ^{1}H NMR ($CDCl_3$): δ 1.74 (5-let, *J* = 6.2 Hz, 2H), 2.18 (t, *J* = 6.9 Hz, 2H), 2.84-2.91 (m, 16H), 3.06 (apparent q, *J* = 5.4 Hz, 2H), 3.28 (apparent q, *J* = 5.4 Hz, 2H), 5.63 (t, *J* = 6.1 Hz, 1H), 6.06 (t, *J* = 6.1 Hz, 1H), 6.31 (t, *J* = 5.9 Hz, 1H), 7.13 (d, *J* = 7.5 Hz, 1H), 7.16 (d, *J* = 7.4 Hz, 1H), 7.47-7.57 (m, 4H), 8.17 (d, *J* = 8.5 Hz, 1H), 8.21 (d, *J* = 8.7 Hz, 1H), 8.32 (dd, *J* = 8.7, 2.6 Hz, 1H), 8.52 (d, *J* = 8.5 Hz, 1H); HRMS (FAB+): calcd for $C_{30}H_{37}N_5O_5S_2$ $[M+1]^+$ 612.2314, found 612.2304 (-1.6 ppm); HPLC: 18.29 min.

***N*-acetyl-*N'*-[4'-(5''-Dimethylnaphthyl-1''-sulfonyl)amidobutanoyl]-1,2-diaminoethane (21e)** The general procedures for the synthesis of **21h** were followed: **6a•**HCl (15.5 mg, 0.07 mmol in 2 mL 10% $NaHCO_3$) and dansyl chloride (12.4 mg, 0.05 mmol) were combined CH_2Cl_2 (2 mL) and treated as above. The title compound **21e** was obtained as a brown solid (9.1 mg, 47%). ^{1}H NMR ($CDCl_3$): δ 1.79 (5-let, *J* = 6.4 Hz,

2H), 1.97 (s, 3H), 2.27 (t, *J* = 6.5 Hz, 2H), 2.88 (s, 6H), 2.91 (q, *J* = 6.1 Hz, 2H), 3.36-3.39 (m, 4H), 5.71 (t, *J* = 6.2 Hz, 1H), 6.44-6.45 (m, 1H), 6.55 (s, br, 1H), 7.17 (d, *J* = 7.6 Hz, 1H), 7.52-7.55 (m, 2H), 8.18 (d, *J* = 8.4 Hz, 1H), 8.26 (d, *J* = 8.5 Hz, 1H), 8.53 (d, *J* = 8.5 Hz, 1H); HRMS (FAB+): calcd for $C_{20}H_{28}N_4O_4S$ $[M+1]^+$ 421.1910, found 421.1915 (+1.1 ppm); HPLC: 4.88 min.

***N,N'*-bis[4'-(5''-Dimethylnaphthyl-1''-sulfonyl)amido] butanoyl-1,4-diaminobutane (21f)** The general procedures for the synthesis of **21h** were followed: **5c•**2HCl (23.4 mg, 0.10 mmol in 2 mL 10% $NaHCO_3$) and dansyl chloride (14.9 mg, 0.06 mmol) were combined CH_2Cl_2 (2 mL) and treated as above. The title compound **21f** was obtained as a green solid (8.4 mg, 24%). ^{1}H NMR ($CDCl_3$): δ 1.44-1.45 (m, 4H), 1.74 (5-let, *J* = 6.4 Hz, 2H), 2.18 (t, *J* = 6.8 Hz, 2H), 2.87-2.91 (m, 16H), 3.11 (apparent q, *J* = 6.1 Hz, 2H), 5.24 (t, *J* = 6.2 Hz, 1H), 5.44 (t, *J* = 6.1 Hz, 1H), 5.70 (t, *J* = 5.5 Hz, 1H), 7.16 (apparent t, *J* = 8.5 Hz, 2H), 7.48-7.53 (m, 4H), 8.20 (d, *J* = 8.5 Hz, 1H), 8.23 (d, *J* = 8.7 Hz, 1H), 8.9 (t, *J* = 9.1 Hz, 2H), 8.52 (d, *J* = 8.5 Hz, 2H); HRMS (FAB+): calcd for $C_{32}H_{42}N_5O_5S_2$ $[M+1]^+$ 640.2622, found 640.25; HPLC: 18.99 min.

***N*-acetyl-*N'*-[4'-(5''-Dimethylnaphthyl-1''-sulfonyl)amidobutanoyl]-1,4-diaminobutane (21g)** The general procedures for the synthesis of **21h** were followed: **6c•**HCl (20 mg, 0.08 mmol in 2 mL 10% $NaHCO_3$) and dansyl chloride (14.3 mg, 0.05 mmol) were combined CH_2Cl_2 (2 mL) and treated as above. The title compound **21g** was obtained as a green solid (15.6 mg, 66%). ^{1}H NMR ($CDCl_3$): δ 1.54-1.57 (m, 4H), 1.77

(5-let, J = 6.2 Hz, 2H), 1.98 (s, 3H), 2.23 (t, J = 6.2 Hz, 2H), 2.89-2.95 (m, 8H), 3.26-3.27 (m, 4H), 5.78 (s, br, 1H), 6.17 (s, br, 2H), 7.22 (d, J = 7.4 Hz, 1H), 7.53 (apparent t, J = 7.8 Hz, 2H), 7.56 (apparent t, J = 8.3 Hz, 2H), 8.20 (dd, J = 7.3, 0.9 Hz, 1H), 8.32 (d, J = 8.7 Hz, 1H), 8.56 (d, J = 8.5 Hz, 1H); HRMS (FAB+): calcd for $C_{22}H_{32}N_4O_4S$ $[M+1]^+$ 449.2223, found 449.2212 (-1.2 ppm/-0.5 mmu); HPLC: 4.95 min.

3.2 Biological Assays

Agonism tests:[6]

The procedures for GABA-gated chloride flux into brain vesicles are similar to those of Bloomquist and Soderlund.[26] The brains of two male ICR mice (Harlan Sprague Dawley, Dublin, VA) are removed following sacrifice by cervical dislocation. The brains are minced in cold buffer containing 118 mM NaCl, 5 mM KCl, 1.2 mM $MgSO_4$, 2.5 mM $CaCl_2$, and 54 mM glucose, and 20 mM HEPES, pH = 7.4 (low-Cl buffer). The tissue is homogenized gently by hand in 2.5 ml of cold buffer using 5 strokes of a Dounce glass-glass homogenizer. The membranes are then diluted with 12 ml of additional cold low-Cl buffer and filtered through 3 layers of 100 mesh nylon to remove any unhomogenized tissue. The filtrate is then centrifuged for 15 min at 1000 g to pellet synaptoneurosomes. Finally, the supernatant is decanted and the pellet gently resuspended in 3 mL low-Cl buffer containing 1 mg/mL BSA. The influx of $^{36}Cl^-$ (> 3 mCi/g Cl, Amersham Corporation) is measured by vacuum filtration assay from established methods.[26] Membranes are aliquotted into triplicate tubes, flux is initiated by the addition of agonist solution in high-Cl buffer (145 mM NaCl, 27 mM glucose)

containing 0.5 μCi/ml $^{36}Cl^-$ and agonist. After a 15 second incubation at 30 °C, uptake is stopped by addition of 4 ml of ice cold high-Cl buffer w/o BSA and vacuum filtered through Whatman GF/C glass fiber filters. The filter is then washed twice with 4 ml cold buffer, and the radiation on the filter quantified by liquid scintillation counting.

Antagonism tests

Synaptoneurosomes are prepared as above. Membranes are aliquotted into triplicate tubes, with compounds **4a-h** added to the membranes in deionized water and preincubated for 10 min at 25 °C. Flux is initiated by the addition of GABA solution containing antagonist in high-Cl buffer (145 mM NaCl, 27 mM glucose) containing 0.5 μCi/ml $^{36}Cl^-$. After a 15 second incubation at 30 °C, chloride uptakes are determined as above.

Filtration binding assay:[7]

Synaptoneurosomes were prepared as in the chloride flux assay. A stock solution of [^{3}H]muscimol (70 nM) was prepared in HEPES buffer (same buffer that was used in the chloride flux assay) immediately before assay. Stock solutions of unlabeled ligands (0.5 M, GABA, **2c** or **4b**) were similarly prepared in HEPES buffer. Each assay tube was charged with [^{3}H]muscimol solution (50 μL) and unlabeled ligand (50 μL, GABA, **2c** or **4b**). Binding reactions were initiated by addition of 100 μL of synaptoneurosome suspension for a total assay volume of 200 μL. Each triplicate set of sample was incubated at 20 °C for 20 minutes. The binding reaction was terminated by diluting with 4 mL of ice-cold buffer. The tissue was immediately collected on Whatman GF/C filters

by vacuum fitration and washed once within 10 seconds with another 4 mL cold buffer. Radioactivity was determined by scintillation counting.

Centrifugation binding assay:[8]

Synaptoneurosomes were prepared as in the chloride flux assay. A stock solution of [^{3}H]muscimol (70 nM) was prepared in HEPES buffer (same buffer that was used in the chloride flux assay) immediately before assay. Stock solutions of unlabeled ligands (0.5 M, GABA, **2c** or **4b**) were similarly prepared in HEPES buffer. Each assay tube was charged with [^{3}H]muscimol solution (50 μL) and unlabeled ligand (50 μL, GABA, **2c** or **4b**). Binding reactions were initiated by addition of 100 μL of synaptoneurosome suspension for a total assay volume of 200 μL. Each triplicate set of sample was incubated at 30 °C for 30 minutes. The binding reaction was terminated by centrifugation (13,000 x g, 0-4 °C, 10 min), and the supernatant was removed. Pellets were washed superficially, without disturbance, twice with 500 μL of cold buffer. The washed pellet was mixed with 100 μL buffer and placed in a scintillation vial. The centrifugation tube was subsequently rinsed with buffer twice (100 μL), and the washings were also transferred to the scintillation vial. Radioactivity was determined by scintillation counting.

Bradford Protein Assay-Dynex Plate Reader Assay

Stock solution of dye: the stock solution of dye is made of Coomassie Brilliant Blue G250 (1g/500 mL EtOH). The dye working solution contains 50 mL of stock

solution of dye, 100 mL of H_4PO_3 and 850 mL of D.I. H_2O. The dye working solution must be filtered until it reaches an amber color and may need to be re-filtered weekly.

General Procedures: four standards and a control in 12 x 75 mm borosilicate test tubes were prepared using the following table:

Standard (STD)	BSA[a] (μL)	Dye (μL)	Serial Dilution from previous Standard	Conc. (μg/μL)
1	90	2910	N/A	0.030
2	-	1500	1500 μL from STD 1	0.015
3	-	1500	1500 μL from STD 2	0.008
4	-	1500	1500 μL from STD 3	0.004
CTL[b]	20	2980	N/A	0.013

[a]BSA (bovine serum albumin)= 1 mg/mL H_2O
[b]CTL: Control

The analysis of each protein sample was performed in two different volumes (2 and 4 μL) and the protein sample was aliquotted into a set of triplicate wells in a 96-well plate reader, followed by addition of 348 μL and 346 μL of dye working solution respectively (a total of 350 μL solution in each well). 350 μL of each standard, control and blank (containing dye working solution only) were placed into the plate in triplicate accordingly. The plate was then incubated at room temperature for 15 minutes and placed in Dynex plate reader for protein analysis. The sample's protein concentration in μg/μL was calculated based on the concentrations that produced by curve fitting output by taking the dilutions into consideration. Thus, the calculation of the final concentration of protein sample is shown below:

Final concentration of each protein sample = (C1 x 175 + C2 x 87.5)/2 where C1 is the concentration output (from curve fitting) of 2 μL protein sample and C2 is the concentration output (from curve fitting) of 4 μL protein sample.

References for chapter 3

1 Schuda, P. F.; Greenlee, W. J.; Chakravarty, P. K. A Short and Efficient Synthesis of (3*S*,4*S*)-4-[(*tert*-Butyloxycarbonyl)amino]-5-cyclohexyl-3-hydroxypentanoic Acid Ethyl Ester. *J. Org. Chem.* **1988,** *53*, 873-875.

2 Flynn, D. L.; Zelle, R. E.; Grieco, P. A. A Mild Two-Step Method for the Hydrolysis /Methanolysis of Secondary Amides and Lactams. *J. Org. Chem.* **1983,** *48,* 2424-2427.

3 Kawahara, S.-I.; Uchimaru, T. One-Pot Preparation of *o*-Xylylene Diamine and its Related Amines. *Zeit. fur Nat. B: Chem. Sci*. **2000,** *55*, 985-987.

4 Takagi, S.; Tanaka, H.; Yano, M.; Machida, K. Studies on the Syntheses of Polymethylene-bisthioureas and their Derivatives. I. *Chem. Phar. Bull***, 1959,** *7,* 206-208.

5 Saller, C. F.; Czupryna, M. J. γ-Aminobutyric acid, glutamate, glycine and taurine analysis using revesed-phased high-performance liquid chromatography and ultraviolet detection of dansyl chloride derivatives. *J. Chromatogr.* **1989,** *487,* 167-172.

6 Bloomquist, J. R.; Soderlund, D. M. Neurotoxic Insecticides Inhibit GABA-Dependent Chloride Uptake by Mouse Brain Vesicles. *Biochem. Biophys. Res. Commun.* **1985,** *133,* 37-43.

7 DeLorey, T. M.; Brown, G. B. γ-Aminobutyric $acid_A$ Receptor Pharmacology in Rat Cerebral Cortical Synaptoneurosomes. *J. Neurochem.* **1992,** *58*, 2162-2169.

8 Edgar, P. P.; Schwartz, R. D. Functionally Relevant γ–Aminobutyric $Acid_A$ Receptors: Equivalence between Receptor Affinity (K_d) and Potency (EC_{50})? *Mol. Pharmacol.* **1992,** *41*, 1124-1129.

9 The details of synthesis of PNP activated PEG: Lam, P. C.-H. PhD dissertation: Experimental and Computational Studies in Bioorganic and Synthetic Organic Chemistry. **2004**, 129-130.

Chaper 4 Introduction and Background of 1,4-benzodiazopines

4.1 Importance of 1,4-benzodiazopine scaffolds in medical chemistry

Drug candidates containing the 1,4-benzodiazepine pharmacophore have demonstrated activity in diverse therapeutic areas.[1,2] The best known subtype is the 1,4-benzodiazepin-2-one (**I**) class (Scheme 4.1), which were first known as $GABA_A$ receptor agonistic modulators.[3] 1,4-benzodiazepin-2-ones such as diazepam (**1**) and flurazepam (**2**) have a sedative, anxiolytic, muscle relaxant, hypnotic and anticonvulsant action.[4] (*S*)-Trp derived 1,4-benzodiazepin-2-ones and structural analogues have shown activities as the CCK-A/CCK-B antagonists, (**3-5**)[5-7] which are potential drugs for treating digestive disorders. Benzodiazepine peptidomimetics have demonstrated promising anti-cancer activity in inhibiting and Ras farnesylation e.g. (**6**).[8] Moreover, 1,4-benzodiazepin-2-ones derived from tyrosine have also demonstrated anti-cancer activity in inhibiting the Src Protein Tyrosine Kinase (**7**).[9] The phenylalanine-derived 1,4-benzodiazepin-2-ones have shown activities as the human bradykinin B_2 receptors antagonists (**8-9**),[10] which could be useful in treating pain/inflammation. In addition, 1,4-benzodiazepin-2-one. Bzd-423 (**10**) and its derivatives have been reported recently as promising anti-cancer candidates, which have both cytotoxic and anti-Proliferative properties against Malignant B-cells.[11-13] Bzd-423 also shows good activity as an immunomodulatory agent, which could be useful in treating defective Fas signaling.[12] Finally, 1,4-benzodiazepin-2-ones have shown promise as antiarrhythmic drugs (**11**)[14] and HIV-1 Tat antagonists (**12**).[15]

Scheme 4.1 Bioactive 1,4-benzodiazepin-2-ones **1-12**

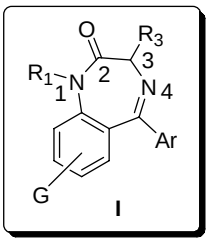

I

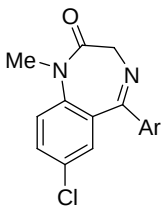

1

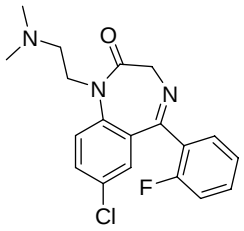

2

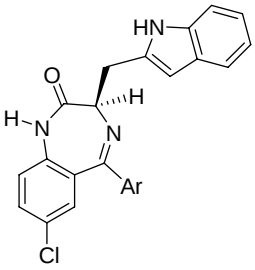

3

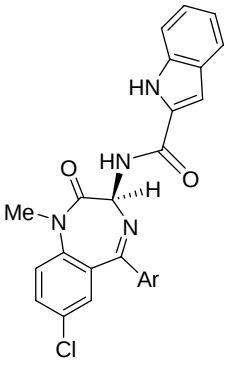

4

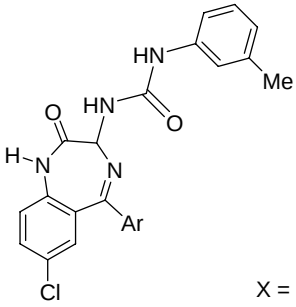

5

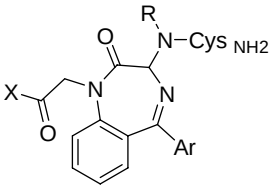

6

X = Met $_{COOH}$, Leu $_{COOH}$ or Ser $_{COOH}$
R = H or CH_3

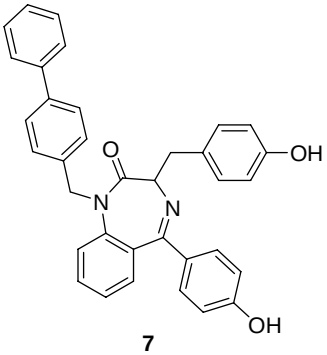

7

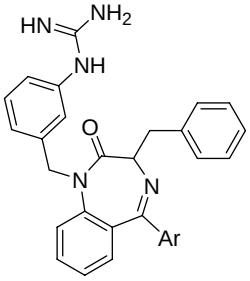

8

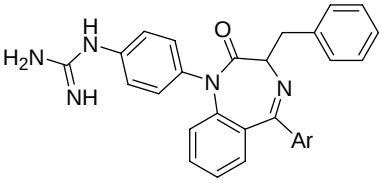

9

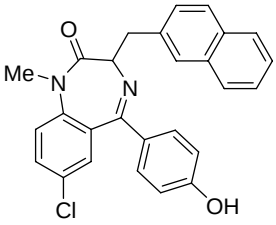

10 (Bzd-423)

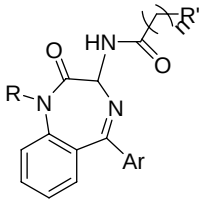

11

R = Alkyl groups
R' = Alkyl or aryl groups
n =0-2

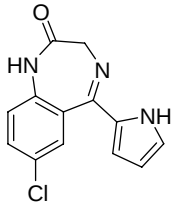

12

The tetrahydro-1,4-benzodiazepin-3-one scaffold (**II**, Scheme 4.2) has been found to be useful for the preparation of fibrinogen receptor antagonists (**13,** SB 214857 and **14**),[16-18] angiostensin II analogs (**15**),[19] and protein kinase C activators (**16**).[20] Compounds **13** and **14** have been shown to be selective, potent and orally active GPIIb/IIIa Integrin antagonists, which could be useful in treating thrombogenic disorders.[16,17] Compound **15** shows high affinity binding at the angiotensin II AT_2 receptor, which has attracted much attention as a new potential therapeutic target due to its possible role in mediating anti-Proliferation, cellular differentiation, apoptosis, and vasodilation. The tetrahydro-1,4-benzodiazepin-2-ones (**III**, so-called TIBO derivatives, Scheme 4.2) on the other hand have been shown to possess anti-HIV-1 activity.[21] TIBO are a class of 4,5,6,7-tetrahydro-5-methylimidazo-[4,5,1-*jk*]benzodiazepin-e-(1*H*)-one compounds; examples of TIBO derivatives including **R86183**, **R82913** and **R84923** are shown in Scheme 4.2.

Scheme 4.2 Medicinally important tetrahydro-1,4-benzodiazepin-2 & 3-ones

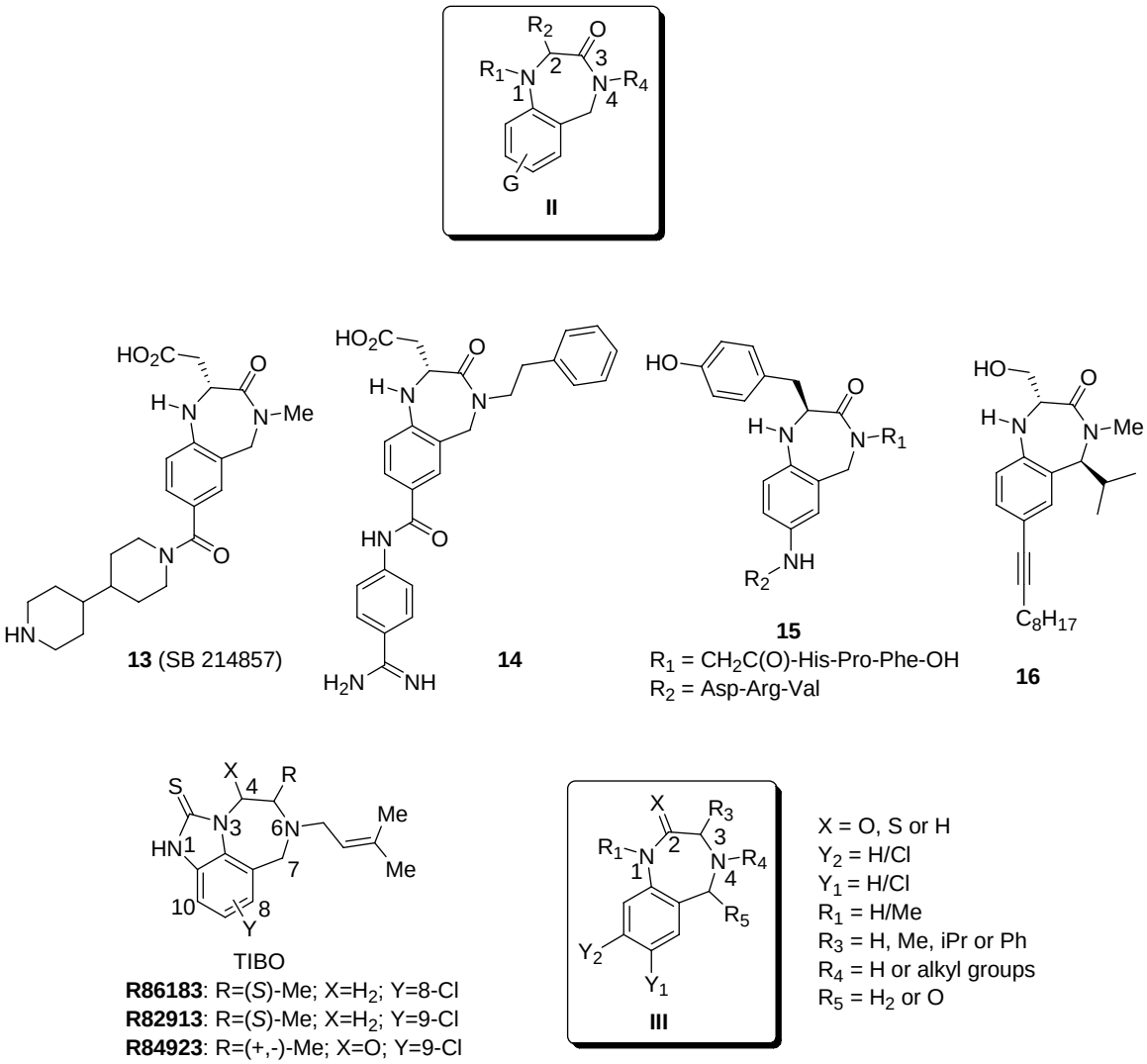

4.2 Importance of exploring enantiopure quaternary 1,4-benzodiazepines

The three subtypes of 1,4-benzodiazepines (**I-III**) that we mentioned in previous section are all prepared from α-amino acids derivatives. There are only a few cases that 3,3-disubstitution was reported (subtypes **I**),[22] and prior to our group's communication,[23] the published examples of enantiopure 3,3-disubstitution 1,4-benzodiazepines have

merely relied upon lipase-catalyzed kinetic resolution.[24,25] One possibility for the development of quaternary 1,4-benzodiazepines is to extend the existing synthetic methods for **I**-**III** to the use of enantiomerically pure quaternary amino acids. However, despite the fact that several asymmetric methods have been developed for the synthesis of quaternary amino acids,[26,27] few enantiomerically pure quaternary amino acids are available commercially. Moreover, the amide (**I** and **III**) and amination (**II**) bond-forming reactions during the ring closure that led to these heterocycles may be problematic with the quaternary amino acids. A direct synthesis of quaternary 1,4-benzodiazepines from commercially available 'tertiary' amino acids might then be the key to therapeutically discovery quaternary 1,4-benzodiazepines as promising agents.

Our research group has developed such a procedure for the preparation of quaternary 1,4-benzodiazepin-2-ones. The route to quaternary 1,4-benzodiazepin-2-ones depends on enantioselective functionalization of the already-formed heterocycles, which were prepared using normal, enantiomerically pure α-amino acids. This method relies on the "memory of chirality (MOC)" imparted by the conformation of the benzodiazepine ring. The concept of MOC was introduced by Fuji and Kawabata as a useful strategy for asymmetric synthesis.[28] As defined by Carlier, MOC is "often used to describe formal substitution reactions at the sole sp^3 center of an enantiopure starting material, which proceed by trigonalization of that center, and yet retain high enantiomeric purity in the product." Such process can occur when the static, central chirality of the reactants is preserved in the form of dynamic conformational chiral reactive intermediate.[29] One of the best examples of this phenomenon is demonstrated by Fuji and Kawabata (Scheme 4.3).[30]

Scheme 4.3 The MOC alkylation protocol of Fuji & Kawabata

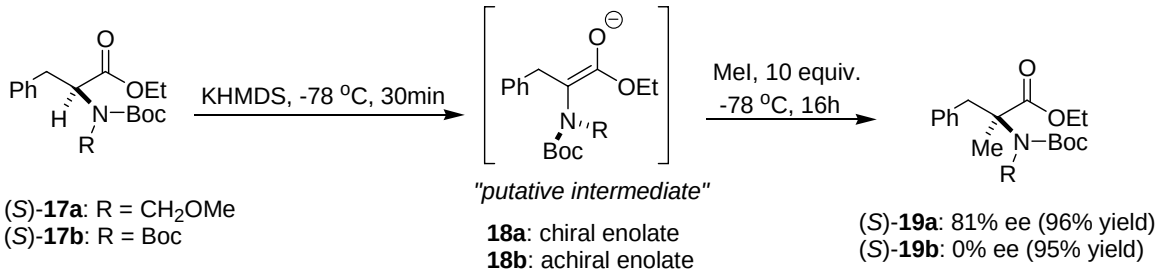

(*S*)-**17a**: R = CH_2OMe
(*S*)-**17b**: R = Boc

"putative intermediate"

18a: chiral enolate
18b: achiral enolate

(*S*)-**19a**: 81% ee (96% yield)
(*S*)-**19b**: 0% ee (95% yield)

Enantiomerically pure phenylalanine ester (*S*)-**17a** and **b** are both deprotonated by KHMDS, and subsequently methylated with MeI. Compound (*S*)-**17a** undergoes α-methylation to give (*S*)-**19a** in 81% ee, symmetrically protected (*S*)-**17b** gives product **19b** in 0% ee. How can these divergent results be explanted? Furthermore, how did the enantioselective transformation of (*S*)-**17a** succeed? The authors have proposed that deprotonation of (*S*)-**17a** generated a chiral non-racemic enolate intermediate **18a** with a dynamically chiral C(2)-N axis, and that subsequent reaction is stereospecific, giving (*S*)-**19a**. On the other hand, deprotonation of symmetrically protected (*S*)-**17b** would give an achiral enolate **18b**, which then undergoes methylation to give racemic **19b**.

Prior to our work, the MOC protocols[30-33] developed by Fuji & Kawabata were the most general and successful examples of MOC.[34-40] MOC has also been reported in many other reactions, including acyliminium ion chemistry,[41,42] radical and diradical chemistry,[43-45] and other chemistry involving trigonal intermediates.[46]

4.3 Overview of Pioneering Work in Carlier's Research Group

As mentioned earlier, our group has also developed an asymmetric alkylation that depends upon MOC. The success of this method depends upon the nature of the benzodiazepine ring. Despite the absence of a chiral center, glycine-derived 1,4-benzodiazepin-2-ones such as diazepam (**1**) are chiral, due to the boat-shaped conformation of the diazepine ring (Scheme 4.4).[47,48] Based on the sign of the τ2345 torsional angle, the helical descriptors (*M*)- and (*P*)- have been used to describe the sense of chirality of the ring. A negative dihedral angle is denoted (*M*)-, meaning "minus"' a positive dihedral angle is denoted (*P*)-. The same sense of chirality is noted using the more easily perceived τ2176 torsional angle in this thesis.

Scheme 4.4 Dynamic chirality of **1**, **20a**[47,49]

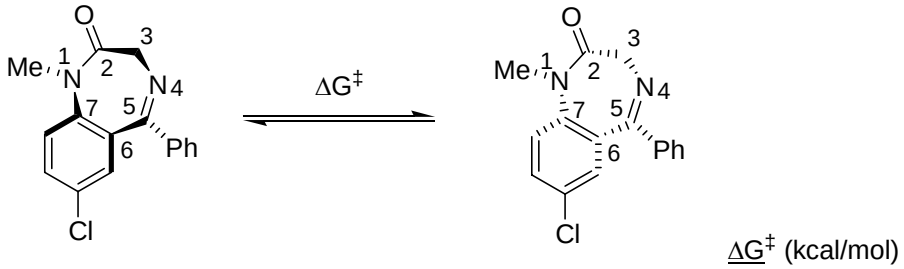

		ΔG‡ (kcal/mol)
(*M*)-**20a**: R = H	(*P*)-**20a**: R = H	12.3
(*M*)-**1**: R = Me	(*P*)-**1**: R = Me	17.6
(*M*)-**20b**: R = *i*-Pr*	(*P*)-**20b**: R = *i*-Pr*	21.1

*$\Delta G^{\ddagger}$ was measured by Dr. Polo Lam.

When the N1 substituent is small (e.g. R = H or Me), rapid racemization (via ring inversion) prevents the resolution of these compounds at room temperature.[47,49] In such

cases, the addition of a single substitutent at C3 (e.g. **21a**, Scheme 4.5) exclusively shifts the conformation of equilibrium to the pseudo-equatorial methyl confomer.

Scheme 4.5 Stereochemical cooperativity in **21a**

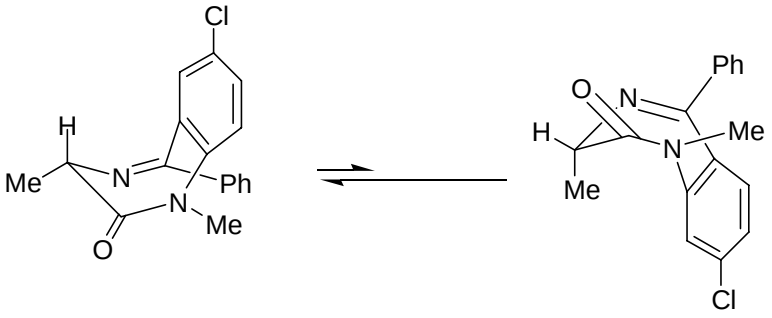

pseudoequatorial methyl in (*M*)-conformer of (3*S*)-**21a**

pseudoaxial methyl in (*P*)-conformer of (3*S*)-**21a**

Therefore, (3*S*)-stereochemistry will induce the diazepine ring to adopt the (*M*)-conformation.[50,51] The stereochemical cooperativity demonstrated by compounds like **21a** provides the basis for enantioselective α-alkylation conditions that developed by our former postdoctoral associate Dr. Hongwu Zhao (Scheme 4.6).

Scheme 4.6 Schematic of a successful MOC deprotonation/alkyaltion sequence of a (*S*)-alanine-derived 1,4-benzodiazepin-2-one

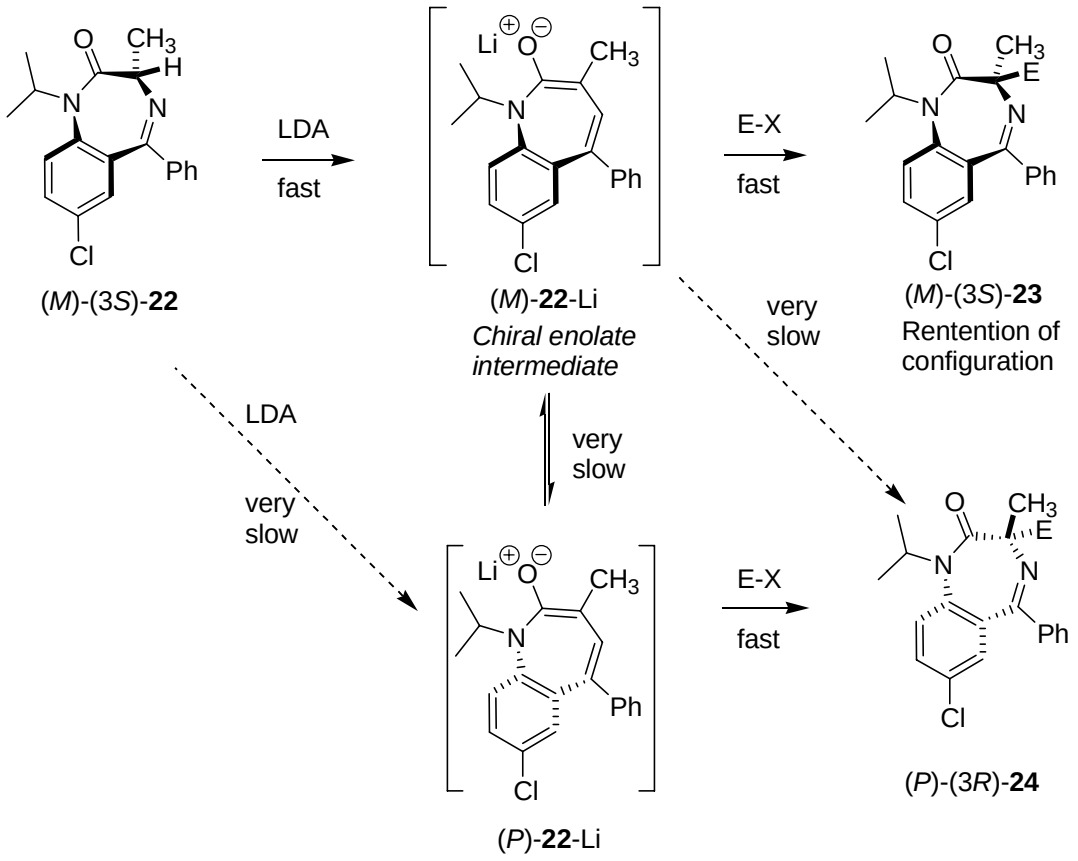

The success of our MOC strategy (Scheme 4.6) depends on at least two requirements, as shown in Scheme 6. Firstly, deprotonation of the stereogenic center by LDA in the reactant (*M*)-(3*S*)-**22** must generate a chiral non-racemic enolate intermediate, (*M*)-**22**-Li. Secondly, this chiral enolate intermediate must react with electrophile (E-X) in high stereospecificity to produce product (*M*)-(3*S*)-**23**. Failure to meet these two requirements will result in a racemic mixture.

Clearly, these two requirements must have been met in the highly enantioselective deprotonation/alkylation of (*S*)-alanine -derived 1,4-benzodiazepines-2-ones (Scheme

4.7), as first developed by Dr. Zhao. Note that the treatment of enolate of *N*1-Me 1,4-benzodiazepin-2-one (*3S*)-**21a** gave racemic products. In contrast, application of this protocol to the enolate of *N*1-*i*-Pr analog (*3S*)-**21b** gave the desired product in high enantiomeric excess (97% ee) with retention of configuration.

Scheme 4.7 MOC enantioselective alkylation of (*S*)-alanine derived 1,4-benzodiazepin-2-ones

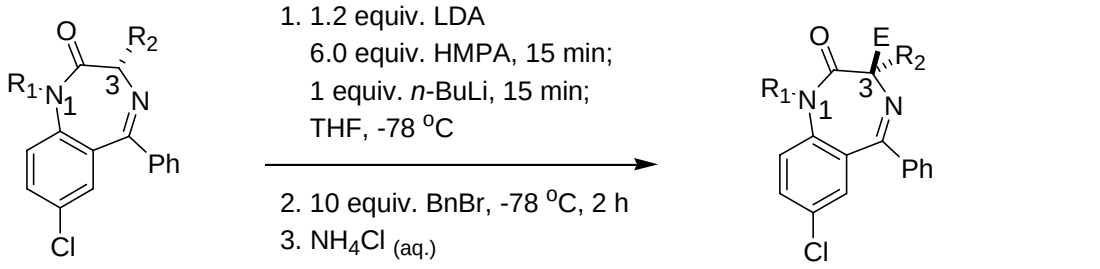

	R_1	R_2
(*3S*)-**21a**:	Me	Me
(*3S*)-**21b**:	*i*-Pr	Me

	R_1	R_2	% Yield	% ee
25a:	Me	Me	75	0
(*3R*)-**25b**:	*i*-Pr	Me	74	97

We attribute the racemic outcome of (*3S*)-**21a** and the enantioselective outcome of (*3S*)-**21b** to differences in the size of the *N*1-substitutent. We have shown that the inversion barrier of the enolate is a function of the size of the *N*1substitutent. Thus we propose that the inversion barrier of the enolate of *N*1-Me benzodiazepine is not sufficient to maintain enantiopurity of the enolate ring at -78 ºC under this deprotonation/alkylation protocol. On the other hand, when a bulkier *i*-Pr group is used in place of Me at *N*1 position, the reaction turns out to be highly enantioselective. Clearly, the enolate of *N*1-*i*-Pr benzodiazepine has a higher inversion barrier (cf Scheme 4.4), which helps preserving the chirality of the starting material (*3S*)-**21b** under the same

reaction conditions and thus yield the desired product in high enantiomeric excess with retention of configuration.

Density functional theory (DFT) calculations of the inversion barriers of 1,4-benzodiazepin-2-one enolates indicate that the equilibrium geometries of **21a** and **21b** are chiral. The free energies of activation for ring inversion of **21a** (*N*1-Me) and **21b** (*N*1-*i*-Pr) at 195 K are 12.4 and 17.5 kcal/mol, which correspond to racemization half-life values of 0.11 min and 970 h, respectively. Dr. Polo Lam has performed enolate trapping experiments that confirm this proposal.[52]

The optimized conditions involve use of LDA and *n*-BuLi as bases and HMPA as additive and the reactions were conducted at -78 ºC. Dr. Zhao has discovered that HMPA was essential for this type of reaction; only traces of the desired products were yielded in the absence of HMPA. Use of DMPU in place of HMPA also proved to be fruitless. He has also found that use of LiHMDS in place of LDA gave none of the desired products.

Using this basic MOC strategy, we will attempt to prepare three other classes of 1,4-benzodiazepine from enantiomerically pure α-amino acids. These include (*S*)-alanine-derived tetrahydro-1,4-benzodiazepin-3-ones, (*S*)-phenylalanine-derived tetrahydro-1,4-benzodiazepin-2-ones, and (*S*)-serine-derived 1,4-benzodiazepin-2-ones.

Reference for chapter 4

1 Ellman, J. A. Design, Sythesis, and Evaluation of Small-Molecule Libraries. *Acc. Chem. Res.* **1996,** *29,* 132-143.

2 Boojamra, C. G.; Burow, K. M.; Thomson, L. A.; Ellman, J. A. Solid-Phase Sythesis of 21,4-Benzodiazepin-2,5-diones. Library Preparation and Demonstration of Synthesis Generally. *J. Org. Chem.* **1997,** *62,* 1240.

3 Sakmann, B.; Hamill, O. P.; Bormann, J. Patch-clamp measurements of elementary chloride currents activated by the putative inhibitory transmitters GABA and glycine in mammalian spinal neurons. *J. Neural Transmission.* **1983**, *18*, 83-95.

4 Lancel, M.; Steiger, A. Sleep and its modulation by drugs that affect GABAA receptor function. *Angew. Chem. Int. Ed.* **1999**, *111*, 2852-2864.

5 Evans, B. E.; Rittle, K. E.; Bock, M. G.; DiPardo, R. M.; Freidinger, R. M.; Whitter, W. L.; Could, N. P.; Lundell, G. F.; Homnick, C. F.; Veber, D. F.; Anderson, P. S.; Chang, R. S. L.; Lotti, V. J.; Cerino, D. J.; Chen, T. B.; King, P. J.; Kunkel, K. A.; Springer, J. P.; Hirschfield, J. Design of Nonpeptidal Ligands for a Peptide Receptor: Cholecystokinin Antagonists. *J. Med. Chem.* **1987,** *30,* 1229-1239.

6 Bock, M. G.; DiPardo, R. M.; Rittle, K. E.; Veber, D. F.; Anderson, P. S.; Freidinger, R. M. Benzodiazpine Gastrin and Brain Cholecystkinin Receptor Ligands: L-365,260. *J. Med. Chem***. 1989,** *32,* 13-16.

7 Showell, G. A.; Bourrain, S.; Neduvelil, J. G.; Flethcher, S. R.; Baker, R.; Watt, A. P.; Fletcher, A. E.; Freedman, S. B.; Kemp, J. A.; Marshall, G. R.; Patel, S.; Smith, A. J.; Matassa, V. G. High-affinity and Potent, Water-Soluble 5-Amino-1,4-Benzodiazepine CCKB/Gastrin Receptor Antagonists Containing a Cationic Solubilizing Group. *J. Med. Chem.* **1994,** *37,* 719-721.

8 James, G. L.; Goldstein, J. L.; Brown, M. S.; Rawson, T. E.; Somers, T. C.; McDowell, R. S.; Crowley, C. W.; Lucas, B. K.; Levinson, A. D.; Masters, J. C. Benzodiazepine Peptidomimetics: Potent Inhibitors of Ras Farneslylation in Animal Cells. *Science (Washington, D. C.)* **1993,** *260,* 1937-1942.

9 Ramads, L.; Bunnin, B. A.; Plunkett, M, J.; Sun, G. Ellman, J. Gallick, G.; Budde, R. J. A. Benzodiazepine Compounds as Inhibitors of the Src protein Tyrosine Kinase: Screening of a Combinatory Library of 1,4-Benzodiazepines. *Arch. Biochem. Biophys***. 1999,** *368,* 394-400.

10 Dziadulewicz, E. K.; Brown, M. C.; Dunstan, A. R.; Lee, W.; Said, N. B.; Garratt, P. J. The design of non-peptide human bradykinin B2 receptor antagonists employing the benzodiazepine peptidomimetic scaffold. *Bioorg. Med. Chem. Lett***. 1999,** *9,* 463-468.

11 Boitano, A.; Ellman, J. A.; Glick, G. D.; Opipari, Jr., A. W. The Proapoptotic Benzodiazepine Bz-423 Affects the Growth and Survival of Malignant B Cells. *Cancer Res***. 2003,** *63,* 6870-6876.

12 Bednarski, J. J.; Warner, R. E.; Rao, T.; Leonetti, F.; Yung, R.; Opipari, Jr., A. W., Glick, G. D. Attenuation of autoimmune disease in Fas-deficient mice by treatment with a cytotoxic benzodiazepine. *Arthritic & Rheumatism***, 2003,** *48,* 757-766.

13 Boitano, A.; Emal, C. D.; Leonetti, F,; Blatt, N. B.; Dineen, T. A;. Ellman, J. A.; Roush, W. R.; Opipari, A. W. Structure activity studies of a novel cytotoxic benzodiazepine. *Bioorg. Med. Chem. Lett.* **2003,** *63,* 3327-3330.

14 Selnick, H. G.; Liverton, N. J.; Baldwin, J. J.; Butcher, J. W.; Claremon, D .A.; Elliott, J. M.; Freidlinger, R. M.; King, S. A.; Libby, B. E.; Mclntyre, C. J.; Pribush, D. A.; Remy, D. C.; Smith, G. R.; Tebben, A. J.; Juriewicz, N. K.; Lynch, J. J.; Salata, J. J.; Snguinetti, M. C.; Siegl, P. K. S.; Slaughter, D. E.; Vyas, K. Class III Antiarrhythmic Activity in Vivo by Selective Blockade of the Slowly Activating Current Delayed Rectifier Potassium Current Iks by (*R*)-(2,4-Trifluoromethyl)-*N*-[2-oxo-5-phenyl-1-(2,2,2-trifluoroethyl)-2,3-dihydro-1*H*-benzo[e][1,4]diazepine-3-yl-acetaminde. *J. Med. Chem.* **1997,** *40,* 3865-3868.

15 Hsu, M.-C.; Schutt, A. D.; Holly, M.; Slice, L. W.; Sherman, M. I.; Richman, D. D.; Potash, M .J.; Volsky, D. J. Inhibition of HIV Replication in Acute and Chronic Invections in Vitro by a Tat Antagonist. *Science (Washington, D. C.)* **1991,** *254,* 1799-1802.

16 Miller, W. H.; Ku, T. W.; Ali, F. E.; Bondinell, W. E.; Calvo, R. R.; Davis, L. D.; Erhard, K. F.; Hall, L. B.; Huffman, W. F.; Keenan, R. M.; Kwon, C.; Newlander, K. A.; Ross, S. T.; Samanen, J. M.; Takata, D. T.; Yuan, C.-K. Enantiospecific Synthesis of SB 214857, a Potent, Orally Active Nonspecific Fibrinogen Receptor Antagonist. *Tetrahedron Lett.* **1995**, *36*, 9433-9436.

17 Samanen, J. M.; Ali, F. E.; Barton, L. S.; Bondinell, W. E.; Burgess, J. L.; Callahan, J. F.; Calvo, R. R.; Chen, W.; Chen, L.; Erhard, K.; Feuerstein, G.; Heys, R.; Hwang, S.-M.; Jakas, D. R.; Keenan, R. M.; Ku, T. W.; Kwon, C.; Newlander, K. A.; Nichols, A.; Parker, M.; Peishoff, C. E.; Rhodes, G.; Ross. S.; Shu, A.; Simpson, R.; Takata, D.; Yellin, T. O.; Uzsinskas, I.; Venslavsky, J. W.; Yuan, C.-K,; Huffman, W. F. Potent, Selective Orally Active 3-Oxo-1,4-benzodiazepine GPIIb/IIIa Integrin Antagonists. *J. Med. Chem***. 1996,** *39*, 4867-4870.

18 Keenan, R. M.; Callahan, J. F.; Samanen, J. M.; Bondinell, W. E.; Calvo, R. R.; DeBrosse, C.; Eggleston, D. S.; Haltiwanger, R. C.; Hwang, S.-M.; Jakas, D. R.; Ku, T. W.; Miller, W. H.; Newlander, K. A.; Nichols, A.; Parker, M. F.; Southhall, L. S.; Uzinskas, I.; Vasko-Moser, J. A.; Venslavsky, J. W.; Wong, A. S.; Huffman, W. F. Conformational Preferences in a Benzodiazepine Series of Potent Nonpeptide Fibrinogen Receptor Antagonists. *J. Med. Chem.* **1999**, *42*, 545-559.

19 Rosenström, U.; Sköld, C.; Lindeberg, G.; Botros, M.; Nyberg, F.; Karlén, A.; Halberg, A Selective AT2 Receptor Ligand with a γ-Turn-Like Mimetic Replacing the Amino Acid Residues 4-5 of Angiotensin II. *J. Med. Chem.* **2004,** *47,* 859.

20 Ma, D.; Wang, G.; Wang, S.; Kozikowski, A. P.; Lewin, N. E.; Blumberg, P. M. Synthesis and Protein Kinase Binding Activity of Benzolactam-V7. *Bioorg. Med. Chem. Lett.* **1999,** *9,* 1371-1374.

21 Breslin, H. J.; Kukla, M. J.; Kromis, T.; Cullis, H.; Knaep, F. D.; Pauwels, R.; Andries, K.; Clercq, E. D.; Janssen, M. A. C.; Janssen, P. A. J. Synthesis and Anti-HIV Activity of 1,3,4,5-Tetrahydro-2*H*-1,4—benzodiazepine-2-one (TBO) Derivatives. Truncated 4,5,6,7-Tetrahydro-5-methylimidazolo[4,5,1-*jk*][1,4]benzodiazepin-2-(1*H*)-ones (TIBO) Analogues. *Bioorg. Med. Chem.* **1999,** *7,* 2427-2436.

22 Simonyi, M.; Kaksay, G.; Kovacs, I.; Tegyey, Z.; Parkanyi, L.; Kalman, A.; Otvos, L. Conformational Recognition by Central Benzodiazepine Receptors. *Bioorg. Chem.* **1990,** *18,* 1-12.

23 Carlier, P. R.; Zhao, H.-W.; DeGuzman, J.; Lam, P. C.-H. Enantioselective Sythesis of "Quaternary" 1,4-Benzodiazepin-2-one Scaffolds via Memory of Chirality. *J. Am. Chem. Soc.* **2003,** *125,* 11482-11483.

24 Avdagić, A.; Lesac, A.; Šunjić, V. First Example of the Solvent Effect on Absolute Conformation of Chiral 3,3-Diustituted 1,4-benzodiazepin-2-ones. *Tetrahedron* **1999,** *55,* 1407.

25 Avdagić, A.; Lesac, A.; Majer, Z.; Hollòsi, M.; Šunjić, V. Lipase-Catalyzed Acetylation of 3-Substituted 2,3-Dihydro-1*H*-1,4-benzodiazepin-2-ones: Effect of Temperature and Conformation on Enantioselectivity and Configuration. *Helv. Chim, Acta* **1998,** *81,* 1567-1582.

26 Seebach, D. Self-Regeneration of Stereocenters (SRS)-Applications, Limitations, and Abandonment of a Synthetic Principle. *Angew. Chem. Int. Ed.* **1996,** *35,* 2708-2748.

27 Cativiela, C.; Díaz-de-Vallagas, M. D. Stereoselective synthesis of quaternary α-amino acids. *Tetrahedron: Asymmetry* **1998,** *40,* 3517-3599.

28 Fuji, K.; Kawabata, T. Memory of Chirality-A New Principle in Enolate Chemistry. *Chem Eur. J.* **1998,** *4,* 373-376.

29 Lam, P. C.-H.; Carlier, P. R. Experimental and Computational Studies of Ring Inversion of 1,4-Benzodiazepin-2-ones: Implications for Memory of Chirality Transformation. *J. Org. Chem.* **2005***, 70,* 1530-1538.

30 Kawabata, T.; Suzuki, H.; Nagae, Y.; Fuji, K. Chiral Nonracemic Enolate with Dynamic Axial Chirality: Direct Asymmetric α-Amino Acid Derivatives. *Angew. Chem. Int. Ed.* **2000,** *39,* 2155-2157.

31 Kawabata, T.; Wirth, T.; Yahiro, K.; Suzuki, H.; Fuji. K. Direct Asymmetric α-Alkylation of Phenylalanine Derivatives Using No External Chiral Sources. *J. Am. Chem. Soc.* **1994,** *116,* 10809-10810.

32 Kawabata, T.; Chen, J.; Suzuki, H.; Nagae, Y.; Kinoshita, T.; Chnacharunee, S.; Fuju, K. Memory of Chirality in Diastereoselective α-Alkylation of Isoleucine and *allo*-Isoleucine Derivatives.*Org. Lett.* **2000,** *2,* 3883-3885.

33 Kawabata, T.; Kawakami, S.-P.; Fuji, K. Enantioselective α-Allylation of a phenylalanine derivative under the control of aggregation of a chiral nonracemic enolate. *Tetrahedron Lett.* **2002,** *43,* 1465-1467.

34 Seebach, D.; Wasmuth, D. Alkylation of Amino Acids without Loss of Optical Activity: α- and β-Alkylation of an Aspartic Acid Derivative. *Angew. Chem Int. Ed.* **1981,** *20,* 971.

.

35 Beagley, B.; Betts, M. J.; Pritchard, R. G. Schofield, A.; Stoodley, R. J.; Vohra,, S. A Cyclisation Reaction of Methyl (4*R*)-3-(2-Diazo-3-oxoabutanoyl)thiazolidine-4-carboxylate which proceeds with Retention of Configuration, probably via a Planar Ester Enolate Intermediate possessing Axial Chirality. *Chem. Commun.* **1991,** 924-925.

36 Kawabata, T.; Yahiro, K. Fuji, K. Memory of Chirality: Enantioselective Alkylation Reactions at an Asymmetric Carbon Adjacent to a Carbonyl Group. *J. Am. Chem. Soc.* **1991,** *113,* 9694-9696.

37 Gees, T.; Schweizer, W. B.; Seebach, D. An Unusual Rearrangement of a Lithiated N-Acyl-tetrahydroisoquinoline to an Amino-indan Skeleton and Structural Comparison of 3-Amino-2-methyllindane- and -tetrahydronaphthalene-2-carboxylic Acids as Possible Building Block for Peptide-Turn Mimics. *Helv. Chim. Acta* **1993,** *76,* 2640-2653.

38 Beagley, B.; Betts, M. J.; Pritchard, R. G. Schofield, A.; Stoodley, R. J.; Vohra,, S. 'Hidden' Axial Chirality as a Stereodirecting Element in Reactions Involving Enol(ate) Intermediate. Part1 1. Cyclisation Reactions of Methyl (4*R*)-3-(2-Diazo-3-oxoabutanoyl)thiazolidine-4-carboxylate and Related Compounds. *J. Chem. Soc. Perkin Trans. I* **1993,** 1761-1770.

39 Gerona-Navarro, G.; Bonache, M. A.; Herranz, R.; García-López, M. T.; Gonzalez-Muñiz, R. Entry to New Conformationally Constrained Amino Acids. First Synthesis of 3-Unsubstituted -4-Alkyl-4-carboxy-2-azedidinone Derivatives via an Intramolecular Nα-Cα-Cyclisation Strategy. *J. Org. Chem.* **2001,** *66,* 3538.

40 Brewster, A. G.; Jayatissa, J.; Mitchell, M. B.; Schofield, A.; Stoodley, R. J. Memory of chirality effects in aldol cyclisations of 1-(3-oxobutyryl) derivatives of -L-4-oxaproline and L-proline isopropyl esters. *Tetrhedron Lett.* **2002,** *43,* 3919-3922.

41 Matsumura, Y.; Shirakawa, Y.; Satoh, Y.; Umino, M.; Tanaka, T.; Maki, T.; Onomura, O. First Example of Memory of Chirality in Carbenium Ion Chemistry. *Org. Lett.* **2000,** *2,* 1689-1691.

42 Wanyoike, G. N.; Onomura, O.; Maki, T.; Matsumura, Y. Highly Enhanced Enantioselectivtiy in the Memory of Chirality via Acyliminium Ions. *Org. Lett***. 2002,** *4,* 1875-1877.

43 Buckmelter, A. J.; Kim, A. I.; Rychnovsky, S. D. Conformational Memory in Enantioselective Radical Reduction and a New Radical Clock Reaction. *J. Am. Chem. Soc.* **2000,** *122,* 9386-9390.

44 Giese, B.; Wettstein, P.; Stähelin, C.; Barbosa, F.; Neuberger, M.; Zehnder, M.; Wessig, P. Memory of Chirality in Photochemistry. *Angew. Chem. Int. Ed***. 1999,** *38,* 2586-2587.

45 Griesbeck, A. G.; Kramer, W.; Lex, J. Diastereo- and Enantioselective Synthesis of Pyrrolo[1,4]benzodiazepines through Decarboxylate Photocyclization. *Angew. Chem. Int. Ed***. 2001,** *40,* 577-579.

46 Schmalz, H.-G.; Koning, C. B. d.; Bernicke, D.; Siegel, S.; Pflethschinger, A. Memory of Chirality in Electron Transfer Mediated Benzylic Umolung Reactions of Arene-Cr(CO_3) complexes. *Angew. Chem. Int. Ed***. 1999,** *38,* 1620-1623.

47 Linscheid, P.; Lehn, J.-M. Étude cinétiques et conformationnelles par résonance magnétique nucléaire. VII. Inversion de cycle dans des benzo-diazépinones. *Bull. Chim. Soc. Fr.* **1967,** 992-997.

48 Konowal, A.; Snatzke, G.; Alebic-kolbah, T.; Kajfez, F.; Rendic, S.; Sunjic, V. General Approach to Chiroptical Characterization of Binding to Prochiral and Chiral 1,4-Benzodiazepin-2-ones to Human Serum Albumin. *Biochem. Pharmacol.* **1979,** *28,* 3109-3113.

49 Gilman, N. W.; Rosen, P.; Earley, J. V.; Cook, C.; Todaro, L. J. Atropisomers of 1,4-Benzodiazepines. Synthesis and Resolution of a Diazepam-Related 1,4-Benzodiazepine. *J. Am. Chem. Soc.* **1990,** *112,* 3969-3978.

50 Sunjic, V.; Lisini, A.; Sega. A.; Kovac, T.; Kajfez, F.; Ruscic, B. Conformation of 7-Chloro-5-phenyl-d5-3(*S*)-mehtyl-dihydro-1,4-Benzodiazepin-2-one in Solution. *J. Heterocylic Chem.* **1979,** *16,* 757-761.

51 Paizs, B. Simonyi, M. Ring Inversion Barrier of Diazepam and Derivatives: An *ab Initio* Study. *Chirality* **1999,** *11,* 651.

52 Lam, P. C.-H. PhD dissertation: Experimental and Computational Studies in Bioorganic and Synthetic Organic Chemistry. **2004**, 212-216.

Chapter 5 Syntheses of 1,4-Benzodiazepine Analogs

5.1 Investigation of Enantioselective Synthesis of Quaternary (*S*)-alanine Derived Tetrahydro-1,4-benzodiazepin-3-ones

As we mentioned in chapter 4, some members of the tetrahydro-1,4-benzodiazepin-3-ones subtype have been found to be important therapeutic agents (**13-16**, chapter 4). Note that all of these compounds (**13-16**) were prepared from proteinogenic amino acid derivatives. The lack of 2,2-substituted analogs has motivated us to extend our MOC strategy to the enantioselective synthesis of quaternary (*S*)-alanine derived tetrahydro-1,4-benzodiazepin-3-ones.

5.1.1 Synthesis of (*S*)-alanine Derived Tetrahydro-1,4-benzodiazepin-3-ones

We have recently published the improved synthesis of (*S*)-alanine derived tetrahydro-1,4-benzodiazepin-3-ones.[1] The synthesis began with commercially available 2-fluoro-5-nitrotoluene **1** (Scheme 5.1) by adopting the basic strategy of Miller *et al.*:[2] treatment with NBS in CCl_4 afforded **2** as off-white, needle-like crystals in 66% yield. Compound **2** was previously prepared by Sveinbjornsson *et al.*[3] from *o*-fluorobenzyl bromide and fuming nitric acid (>90%) in 81% yield; However, our attempts to repeat this synthesis using regular nitric acid (70%) with concentrated sulfuric acid as catalyst, gave a low yield (20%). Subsequent reaction of **2** with excess allyamine in THF gave **3** in 87%. The reaction of **2** with methylamine was however less selective, giving a mixture of the desired product **4** and the undesired nucleophilic aromatic substitution product **5**, which were difficult to separate. Coupling of **3** with either (*S*)-Boc-Ala-OH,

(*S*)-Boc-*N*-Me-Ala-OH, or (*S*)-*N*-*i*-Pr-Ala-OH (DCC, HOBT in CH_2Cl_2) afforded (*S*)-**6** (86%), (*S*)-**7** (86%), and (*S*)-**8** (68%) respectively. Apparently, the *i*-Pr group was large enough to prevent self-condensation of the unprotected *N*-*i*-Pr-Ala-OH under these conditions.

Scheme 5.1 Synthesis of tetrahydro-1,4-benzodiazepin-3-ones

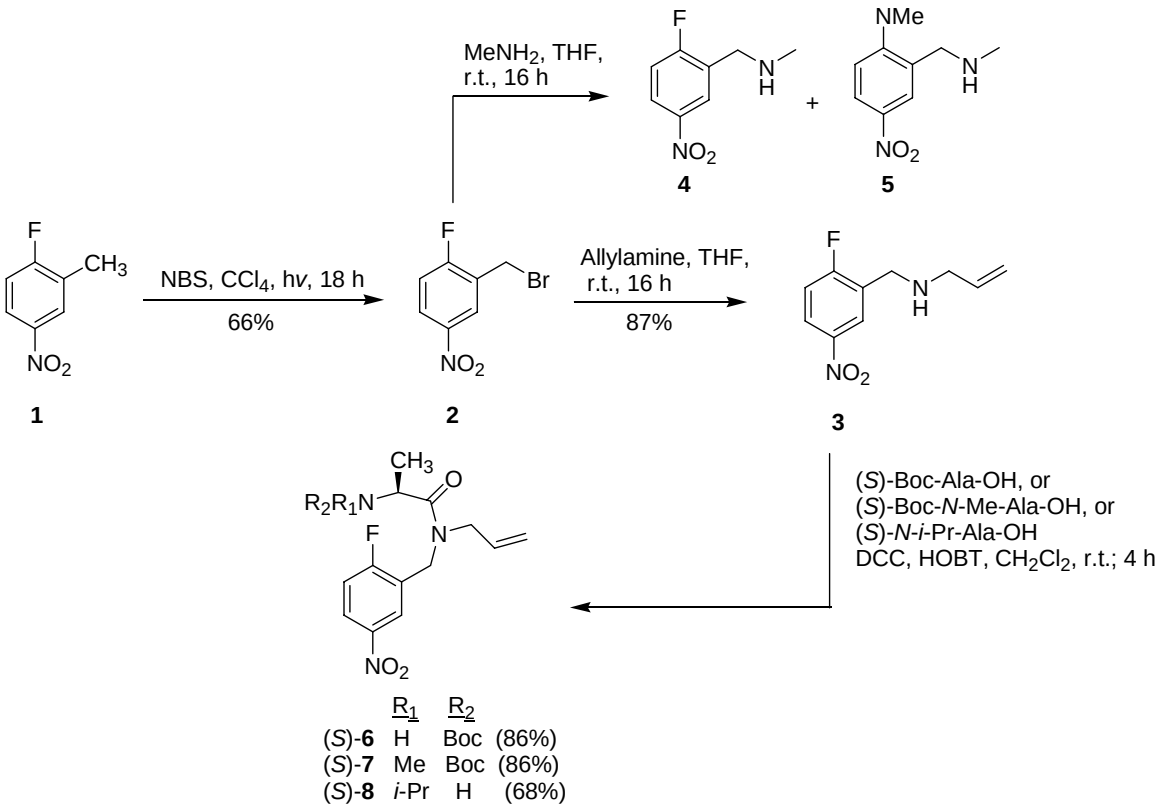

The key step in most syntheses of tetrahydro-1,4-benzodiazepin-3-ones is closure of the heterocyclic ring by intramolecular nucleophilic aromatic substitution. To accelerate substitution, a carboxyl ester[2,4] or a nitro group[5,6] is usually placed *para* to the leaving group. However, prior to our work, these reactions either afford the desired product in low yield (18%) or require long reaction times. Furthermore, previous syntheses of tetrahydro-1,4-benzodiazepin-3-ones from intermediates like **6** required the

removal of the *N*1-protecting group (Boc and Fmoc) in a separate step prior to cyclization under basic conditions.[5,6] To attempt a stream-lined synthesis, we carried out the ring closure of the hetercyclic ring (*S*)-**9** at the temperature (DMSO, 125°C) that Miller *et al.*[2] suggested, but we did not carry out the Boc-deprotection prior to the ring closure. The desired product was obtained in low yield (26%, Table 5.1). We therefore explored different reaction conditions in order to improve the yield for the ring closure of (*S*)-**6**. Results are shown in Table 5.1. The yield for the ring closure of (*S*)-**6** in dioxane was reasonable. But it required both a separate deprotection step and long reaction time.

Table 5.1 Ring closure reaction conditions

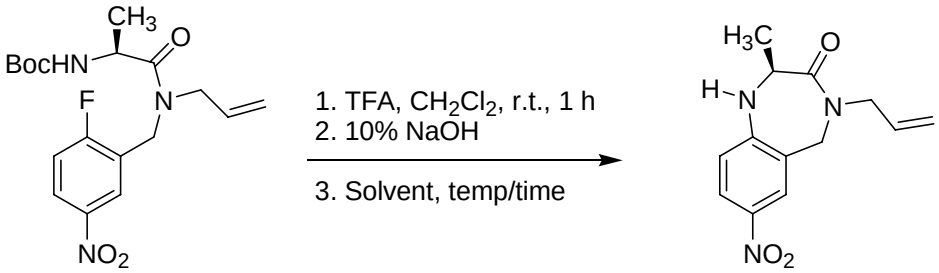

(*S*)-**6** (*S*)-**9**

Entry	Solvent	Temp./Time	% Yield	Remarks
1	DMSO	125°C/44 h	26%	No separate Boc-deprotection steps were carried out before ring closure
2	THF	Reflux/23 h	56%	-
3	Dioxane	Reflux/8-19 h	26-69%	-

Based on the result in Entry 1 of Table 5.1, we discovered that simple heating of (*S*)-**6** and (*S*)-**7** to 200 °C in DMSO without base for 30 min to 3 h caused the thermolysis of the Boc group and cyclization, yielding (*S*)-**9** (67%) and (*S*)-**10** (92%) (Scheme 5.2).

Therefore, cyclization of (*S*)-**9** and (*S*)-**10** can be carried out directly without a separate deprotection step. Cyclization of *N*-*i*-Pr analog (*S*)-**8** proceeded in 61 % yield, despite the steric hindrance provided by the secondary alkyl group. All three of the tetrahydro-1,4-benzodiazepin-3-ones **9**-**11** were analysed by chiral stationary phase HPLC; the results indicated that no racemization had occurred during the high temperature cyclization to **9**-**11**. The cyclizations of (*S*)-**7** and (*S*)-**8** are especially noteworthy as they demonstrate for the first time that 2º amines are competent nucleophiles for the ring closure.

Scheme 5.2 Ring closure of heterocyclic ring (*S*)-9 to 11 at 200 ºC

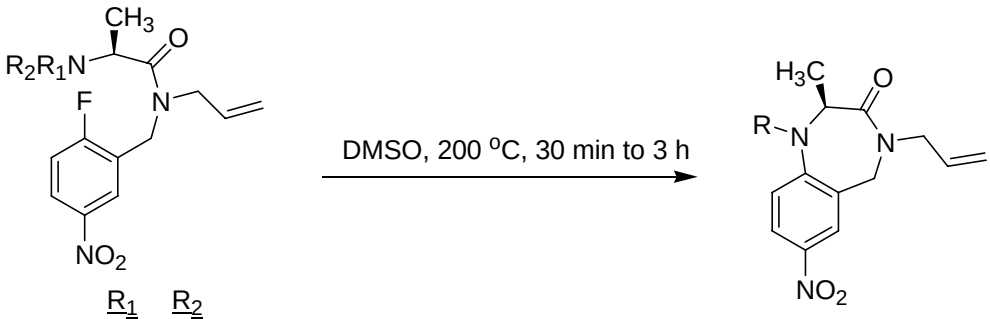

	R_1	R_2	
(*S*)-**6**	H	Boc	(86%)
(*S*)-**7**	Me	Boc	(86%)
(*S*)-**8**	*i*-Pr	H	(68%)

(*S*)-**9** R = H (67%)
(S)-**10** R = Me (92%)
(S)-**11** R = *i*-Pr (61%)

(*S*)-Boc-*N*-methyl-Ala-OH is commercially available. However, it can be economically prepared from (*S*)-Boc-Ala-OH and MeI in THF by use of NaH as base in 92% yield .[7] (*S*)-*N*-*i*-Pr-Ala-OH is on the other hand not commercially, but it can be synthesized from (*S*)-Ala-OH and acetone in CH_3OH by use of $NaBH_3CN$ as the reducing agent in good yield (65%) according to the modified literature method.[8]

Based on Miller *et al.*'s method,[2] we have also employed two other starting materials that have a carboxyl group as electron-withdrawing group *para* to the leaving group in the synthesis of tetrahydro-1,4-benzodiazepin-3-ones (Scheme 5.3).

Scheme 5.3 Synthetic scheme of carboxyl ester-accelerated substitution

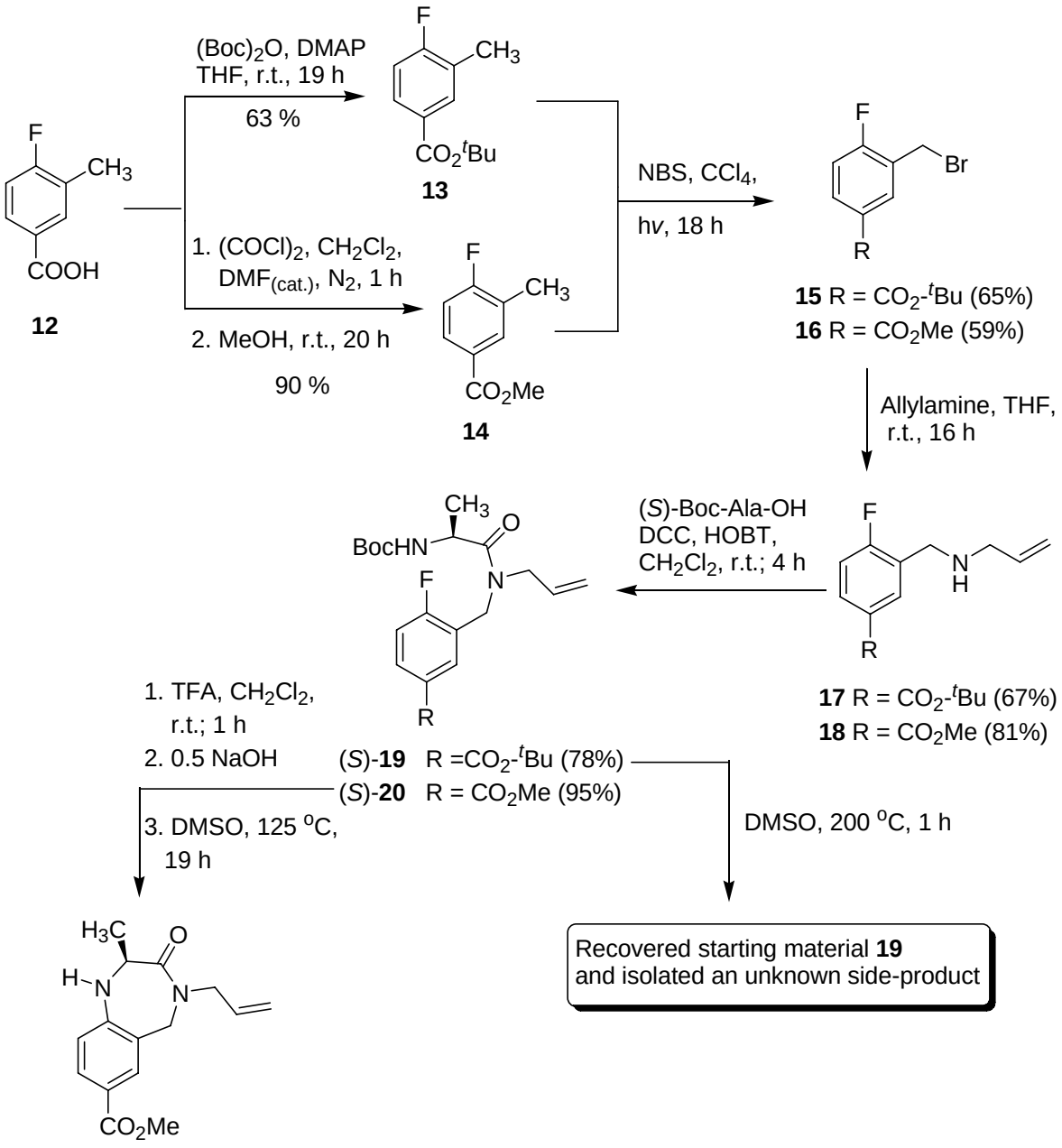

Reaction of 4-fluoro-3-methyl-benzoic acid with $(Boc)_2O$[9] and oxalyl chloride/MeOH[10] afforded **13** (63%) and **14** (90%) accordingly; subsequent treatment with NBS in CCl_4 afforded **15** and **16** in 65% and 59% yield correspondingly. Reactions of **15** and **16** with allyamine and subsequent couplings with (*S*)-Boc-Ala-OH provided (*S*)-**19** and (*S*)-**20** in good yields respectively. Attempts to ring close (*S*)-**19** in DMSO at 200 °C were not successful; a majority of the starting material (*S*)-**19** was recovered, which demonstrated that the successful cyclization of (*S*)-**6** to **8** involved nucleophilic substitution of the fluoride group by the corresponding amide, followed by loss of the Boc group. Small amounts of an unidentified side product from attempted cyclization of (*S*)-**19** were also obtained. Therefore, due to the unsuccessful ring closure of (*S*)-**19** at 200 °C, we carried out the Boc deprotection step prior to performing the ring closure at 125 °C in DMSO. The desired compound (*S*)-**21** was however obtained in low yield (21%), which indicates that stronger electron-withdrawing effect of NO_2 group facilitates the ring closure of (*S*)-**9** to **11**. Finally, attempts to methylate the *N*1of (*S*)-**21** by use of NaH and MeOTf yielded none of the desired product.

5.1.2 Synthesis of Quaternary (*S*)-alanine Derived Tetrahydro-1,4-benzodiazepin-3-ones Via "Memory of Chirality" (MOC)

We then attempted extension of our previously described[11] synthesis of quaternary tetrahydro-1,4-benzodiazepine-3-one (*S*)-**10**. Surprisingly, (*S*)-**10** appears unreactive toward alkylation under many different reaction conditions (Table 5.2). Apparently, the electron-withdrawing NO_2 group *para* to the *N*1-Me either prevents the enolate formation or reduces the reactivity of the enolate towards the electrophile. We

believe that the NO_2 group somehow prevented the enolate formation, because only the starting material seen by TLC during attempted reaction.

Table 5.2 Attempted alkylations of (*S*)-**10**

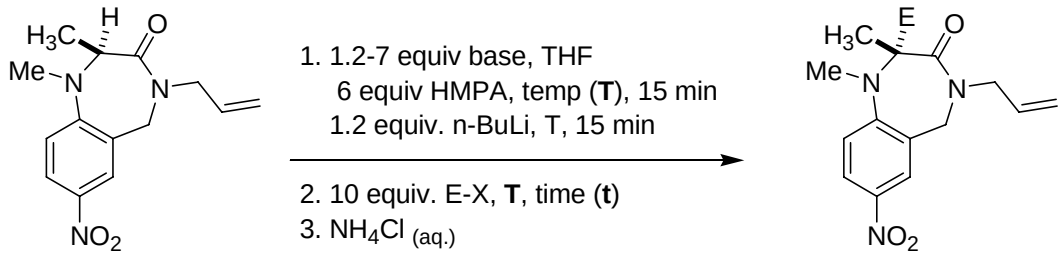

(*S*)-**10**

No desired product formed

Entry	Base	T	E-X	t	Remarks
1	1.2 equiv LDA	-100 °C	BnBr	2 h	Recovery of (*S*)-**10**
2	1.2 equiv LDA	-100 °C	BnBr	8 h	Recovery of (*S*)-**10**
3	1.2 equiv LDA	-78 °C to 0 °C to r.t.	D_2O/ d-TFA	3 to 18 h	Recovery of (*S*)-**10**
4	1.2 equiv LDA	-78 °C to 0 °C to r.t.	MeI	3 to 18 h	Recovery of (*S*)-**10**
5	1.2 equiv KHMDS (witout *n*-BuLi)	0 °C	D_2O/ d-TFA	3 h	Recovery of (*S*)-**10**
6	1.2 equiv KHMDS (witout *n*-BuLi)	0 °C	MeI	3 h	Recovery of (*S*)-**10**
7	7.0 equiv LDA	-78 °C	MeOTf	3 h	Recovery of (*S*)-**10**
8	1.3 equiv *t*-BuLi (without *n*-BuLi	-78 °C	BnBr	2 h	Recovery of (*S*)-**10**
9	2 equiv NaH (without *n*-BuLi and HMPA)	r.t.	MeOTf	2 h	Recovery of (*S*)-**10**; MeOTf caused the polymerization of THF at room temp.

There are four possible pathways for the prevention of enolate formation for (*S*)-**10** (Schemes 5.4 and 5.5). As shown in Scheme 5.4, two possible mechanisms via single electron reduction[12] deactivation towards deprotonation are proposed. In pathway **I**, LDA reduces the carbonyl group of (*S*)-**10** via a free radical mechanism to give a radical-anion intermediate **22**. In pathway **II**, the aromatic ring of (*S*)-**10** reacts with LDA via one-electon transfer to form the radical-anion intermediate **23**. Both intermediates (**22** and **23**) are unreactive towards additional base, thus both **22** and **23** are converted back to the starting material upon treatment with saturated NH_4Cl (Scheme 5.4), which accounts for the recovery of starting material after the reactions (cf Table 5.2).

Scheme 5.4 Proposed pathways **I** and **II** for the deactivation of enolization for (*S*)-**10** via single electron reduction

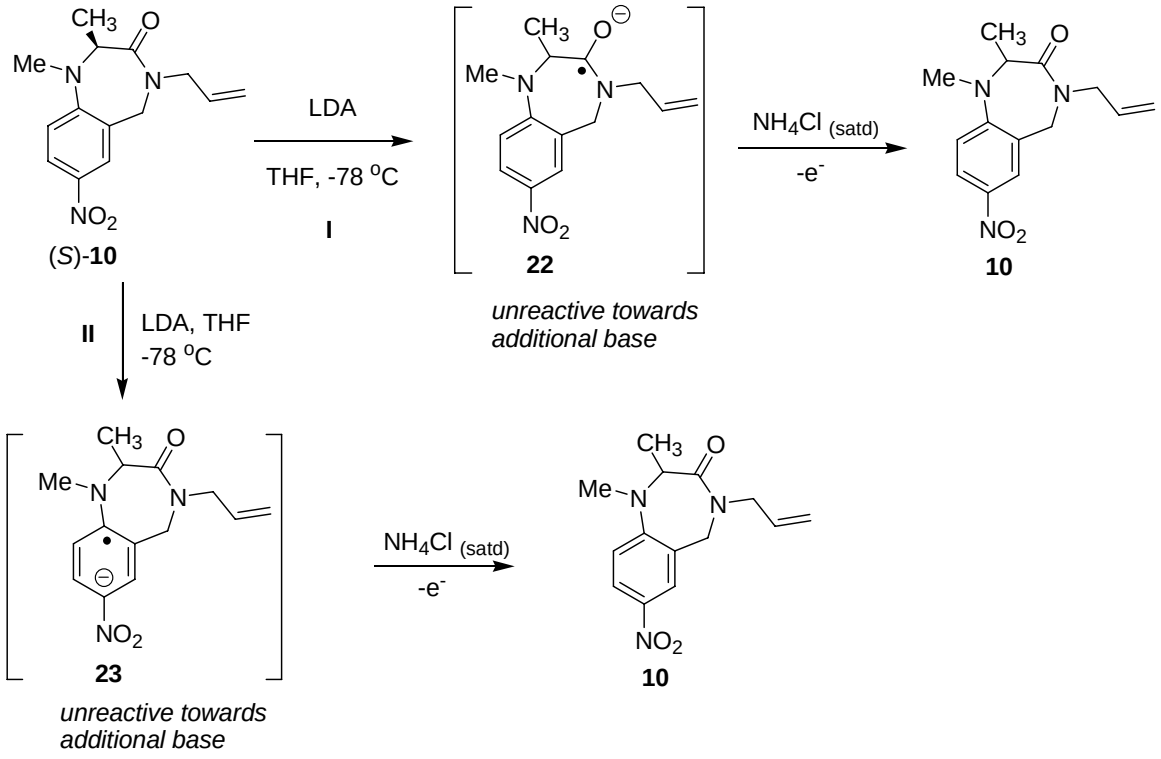

In Scheme 5.5, mechanisms (pathways **III** and **IV**) involving addition reactions that deactivate deprotonation of (*S*)-**10** are proposed. In pathway **III**, LDA reacts with (*S*)-**10** via a 1,2-addition mechanism to afford intermediate **24**. In pathway **IV**, the aromatic ring of (*S*)-**10** undergoes a nucleophilic substitution upon treatment with LDA to, give **25**. Both intermediates (**24** and **25**) are also unreactive towards additional base, thus both **24** and **25** are likewise converted back to the starting material upon treatment with saturated NH_4Cl (Scheme 5.5), which could also account for the recovery of starting material after the reactions (cf Table 5.2).

Scheme 5.5 A proposed mechanism involving addition reactions that deactivate deprotonation of (*S*)-**10**

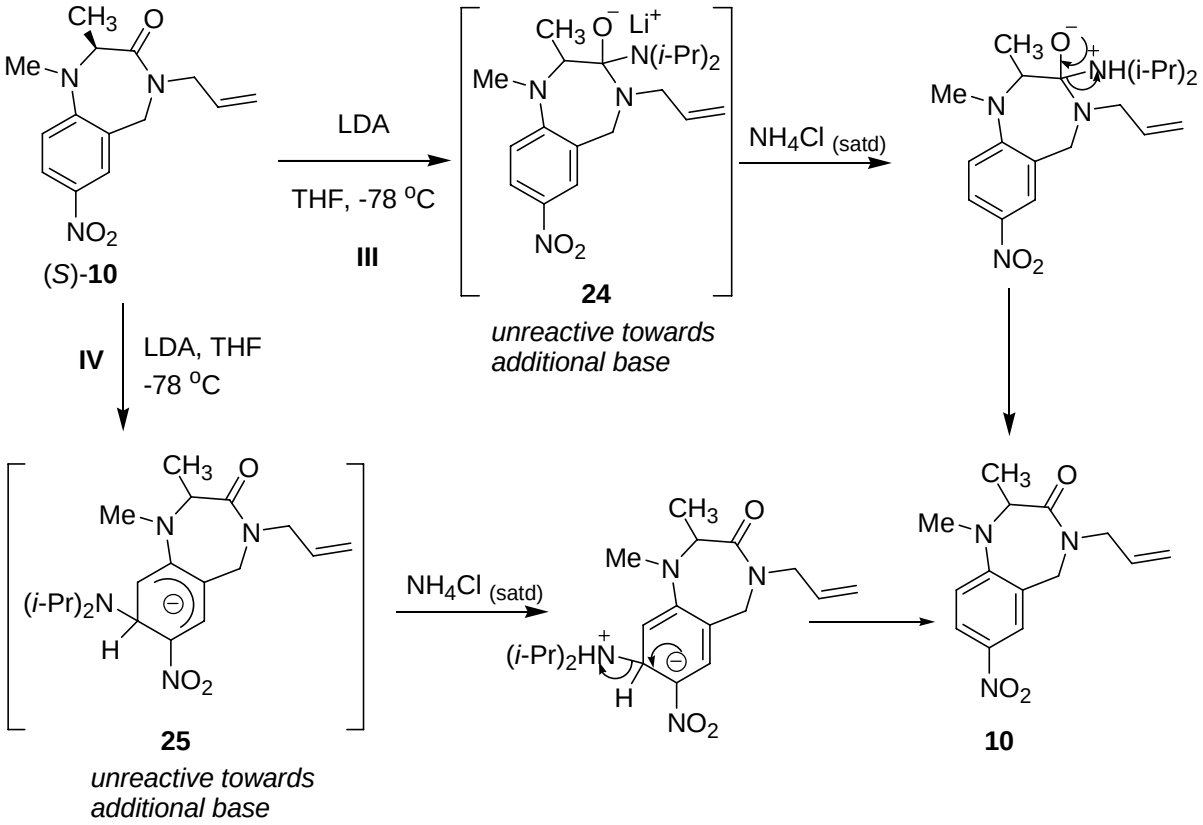

Based on *electron spin resonance* (ESR) spectroscopy studies, Russell *et al.* reported that one electron transfer occurred (pathways **I** and **II**) from organometallic reagent such as *n*-BuLi to an aromatic nitro or unsaturated compound in basic solution. On the other hand, the LiHMDS-mediated 1,2-addition mechanism of pyrrolidine to 2-methylcyclohexanone has been proposed by Collum *et al.*[13] previously. Based on in situ IR spectroscopy studies, Collum and coworkers have found that the reaction of 2-methylcyclohexanone with LiHDMS in pyrrolidine gave exclusive 1,2-addition of pyrrolidine **26** (Scheme 5.6).

Scheme 5.6 1,2-Addition of pyrrolidine to 2-methylcyclohexanone proposed by Collum *et al.*

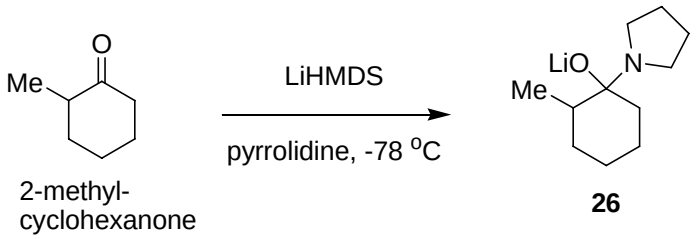

Thus pathways **I** to **III** may be responsible for unsuccessful deprotonation/alkylation of (*S*)-**10**. Pathway **IV** is feasible based on the well known ability of the NO_2 group to activate substitution at the *ortho* & *para* position. However, without a leaving group on **25**, substitution cannot occur; intermediate **25** would revert to starting material upon aqueous workup. One factor arguing against this mechanism is that compound **10** is a *para*-nitro aniline derivative, which is much less nucleophilic towards substitution than nitro benezene, as shown below. Thus, pathway **IV** may be less likely than pathways **I**-**III**.

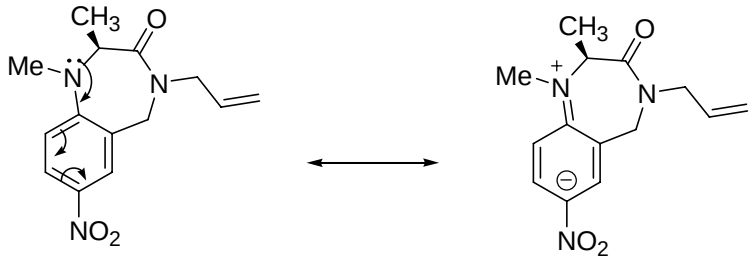

Thinking that the NO_2 group may have been responsible for our failure to achieve the deprotonation/alkylation, we therefore reduced it and functionalized it as the phthalimido or *N*,*N*-dimethyl group derivative.

Nitro compounds (*S*)-**10** and (*S*)-**11** were first reduced to primary aromatic amines (*S*)-**27** and (*S*)-**28** accordingly by refluxing in CH_3OH for 3 h in the presence of Fe powder and aq. NH_4Cl (Scheme 5.7).[14]

Scheme 5.7 Conversion of nitro compounds **10** and **11** to other 1,4-benzodiazepin-3-ones

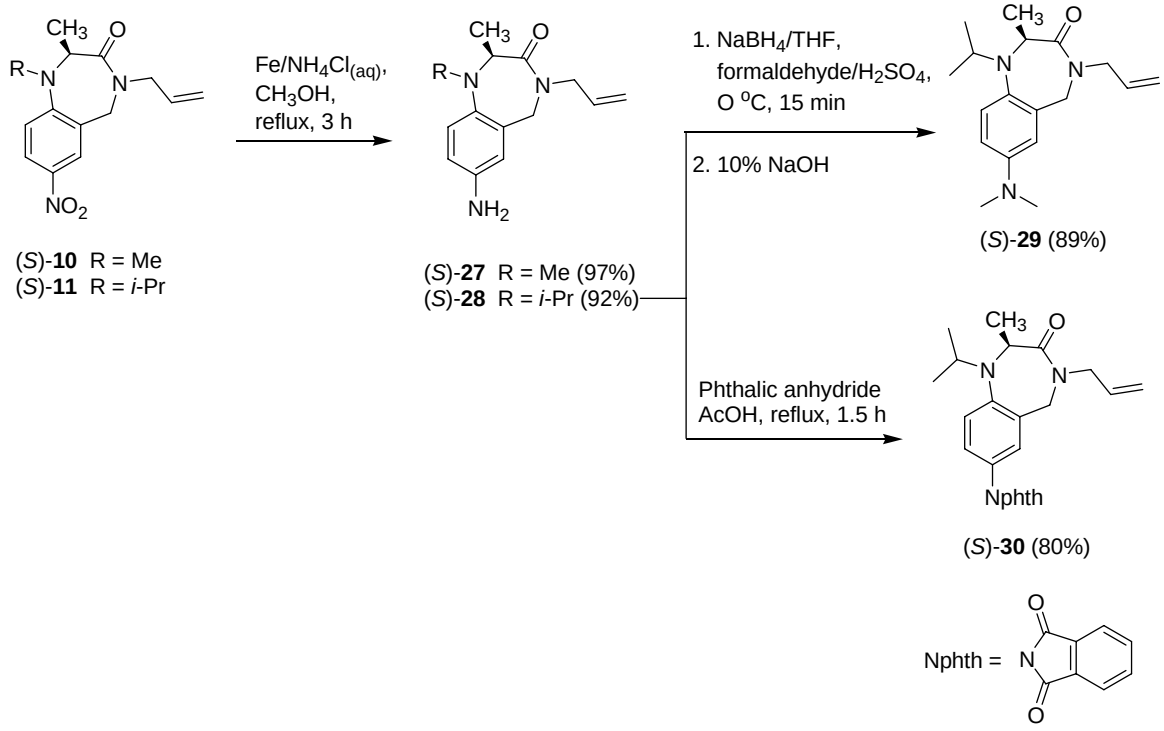

The primary amine of (*S*)-**28** was converted to corresponding *N*,*N*-dimethylamine (*S*)-**29** in 89% in the presence of $NaBH_4$ and formaldehyde in THF.[15] Refluxing (*S*)-**28** with phthalic anhydride in acetic acid for 1.5 h[16] afforded (*S*)-**30** in 80% yield. HPLC analysis of both (*S*)-**29** and (*S*)-**30** indicated 99% and 98% ee, respectively.

We carried out the alkylations with both (*S*)-**29** and (*S*)-**30** based on the MOC strategy. The details of the results are summarized in Table 5.3. As can be seen, attempts to carry out alkylation at C2 with these two compounds were also fruitless. However, these two compounds behaved differently than (*S*)-**10** under deprotonation/alkylation conditions. Whereas (*S*)-**10** seemed to be stable at the reaction conditions that we attempted, (*S*)-**29** and (*S*)-**30** either decomposed or gave undesired products in most of the reactions attempted. O-alkylation of (*S*)-**29** was observed when benzyl bromide was used as electrophile; the O-alkylation was evidenced by one new product spot (starting material was consumed) observed on TLC immediately followed the reaction. However, this new product **31** rapidly decomposed upon aqueous workup, which suggested that this new product is likely a O-alkylation product (Scheme 5.7). Although no pure O-alkylation product could be characterized by either ^{1}H or ^{13}C NMR characterization. Both GC-MS[17] and HRFAB MS indicated the presence of a compound with the correct mass.

Table 5.3 Attempted C-alkylations of (*S*)-**29** and (*S*)-**30**

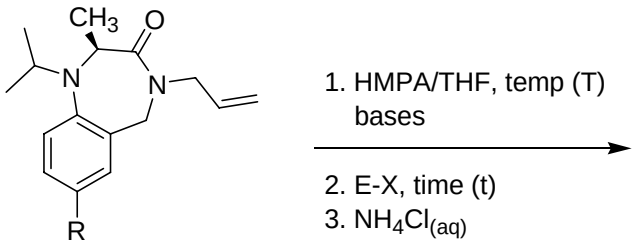

(*S*)-**29** R = NMe_2
(*S*)-**30** R = Nphth

Starting material	Bases	E-X	T	t	Remarks
(*S*)-**29**	1.2 equiv. LDA, 15 min /*n*-BuLi, 15 min	BnBr	-78 °C	1 h	O-alkylation product **31** based on TLC; result confirmed by GC/HRFABMS
(*S*)-**29**	1.2 equiv. LDA, 15 min /*n*-BuLi, 15 min	MeI	-78 °C	1 h	Decomposition product observed on TLC
(*S*)-**29**	1.2 equiv. LDA, 15 min /*n*-BuLi, 15 min	EtI	-78 °C	1 h	Decomposition products observed on TLC
(*S*)-**29**	1.2 equiv. LDA, 15 min /*n*-BuLi, 15 min	D_2O/ d-TFA	-78 °C	1 h	No reaction based on TLC
(*S*)-**30**	6.0 equiv. LDA, 15 min /*n*-BuLi, 15 min	BnBr	-78 °C/ 0 °C to r.t.	3 h/ 18h	A mixture of **30** and side products observed in ^{1}H NMR
(*S*)-**30**	20 equiv. NaH	BnBr	r.t.	3 h	A mixture of **30** and side products observed in ^{1}H NMR
(*S*)-**30**	4.5 equiv. NaH	D_2O/ d-TFA	r.t.	3 h	A mixture of **30** and side products observed in ^{1}H NMR
(*S*)-**30**	KO-^{t}Bu/n-BuLi, 30 min	BnBr	-78 °C	3 h	Decomposition products observed on TLC

A proposed mechanism for the formation of O-alkylation product **31** and subsequent decomposition of **31** upon aqueous workup is shown in Scheme 5.8. As seen in Scheme 5.8, the enolate intermediate generated from deprotonation of **29** by bases reacted with BnBr to give the O-alkylation product **31**. Compound **31** was then hydrolyzed by aq. NH_4Cl to afford recovered starting material **29.**

Scheme 5.8 A proposed mechanism for the formation and decomposition of O-alkylation product **31**

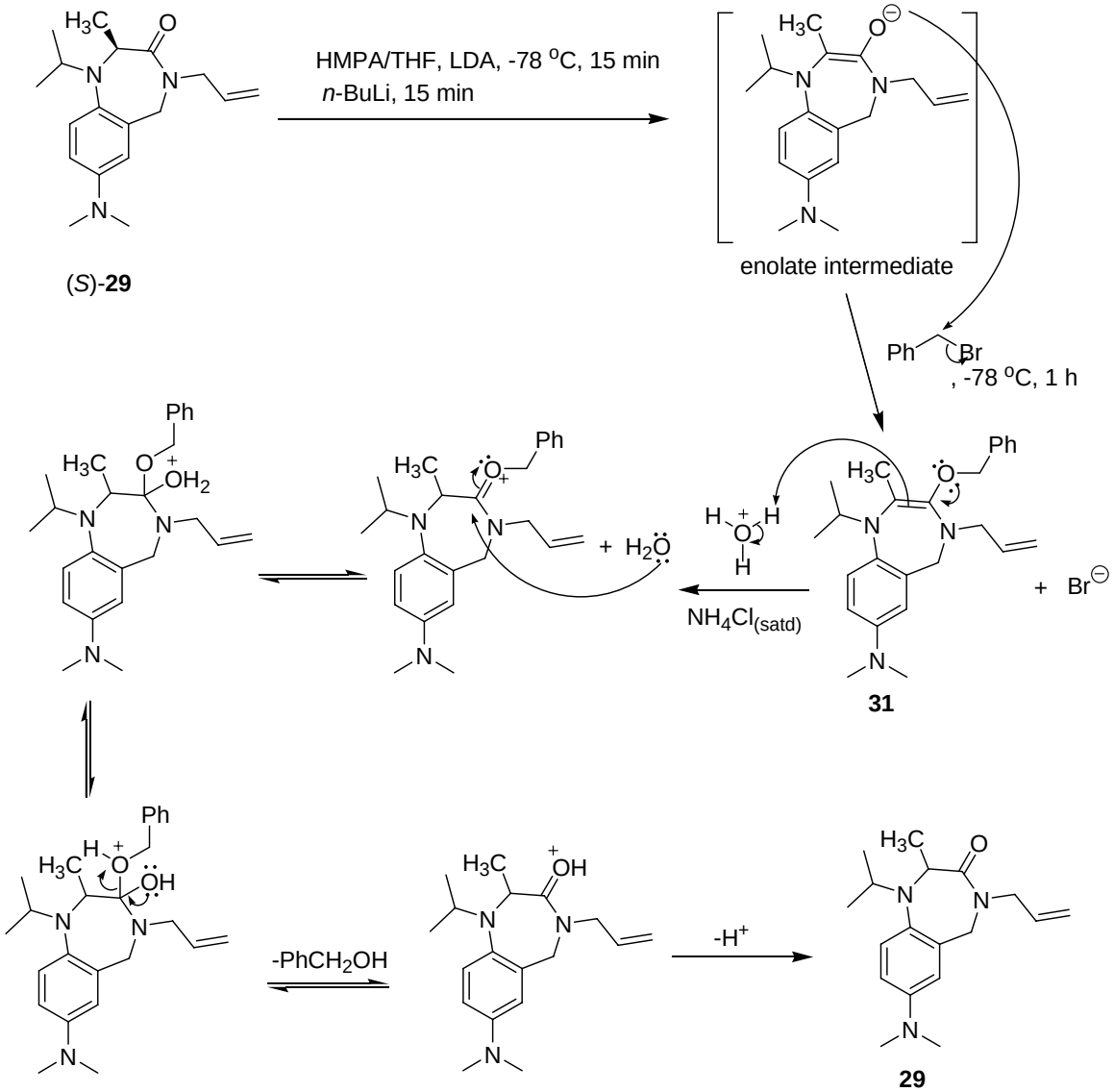

Clearly, the substitutents *para* to the *N*1 position greatly affected the reactivity of these three tetrahydro-1,4-benzodiazepin-3-ones. We thus eliminated the NO_2 substituent by reduction and deamination (Scheme 5.9).

Scheme 5.9 Deamination of (*S*)-**27** and (*S*)-**28**

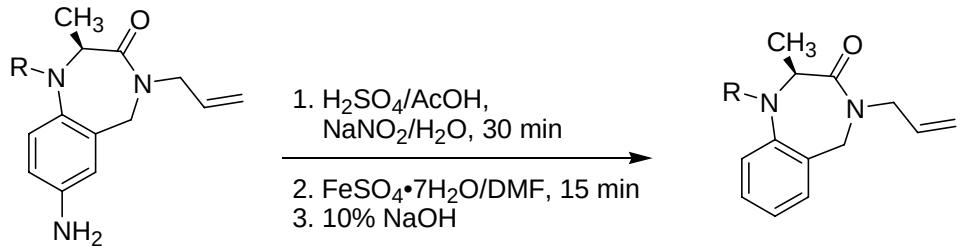

(*S*)-**27** R = Me
(*S*)-**28** R = *i*-Pr

(*S*)-**32** R = Me (57%)
(*S*)-**33** R = *i*-Pr (44%)

Amines (*S*)-**27** and (*S*)-**28** from reduction of nitro compounds were deaminated by use of $NaNO_2$ and $FeSO_4$ in DMF[18] to afford (*S*)-**32** and (*S*)-**33** in moderate yields, respectively. HPLC analysis of both compounds indicated 99% ee.

Based on catalyst studies, Wassmundt and coworker proposed that the reductive deaminations occurred via a free-radical mechanism. As shown in Scheme 5.10, compound (*S*)-**27** or (*S*)-**28** was first diazotized by aqueous $NaNO_2$ to give the corresponding diazonium cation in the presence of AcOH and H_2SO_4 at room temperature, followed by reduction of this diazonium cation to the diazenyl radical by Fe^{2+}. The diazenyl radical then underwent cleavage to form the aryl radical and N_2. Abstraction of a hydrogen by the aryl radical from DMF generated the desired product (*S*)-**32** and **33** and the corresponding radical derived from the solvent.

Scheme 5.10 A proposed mechanism for reductive deamination of (*S*)-**32** and **33**

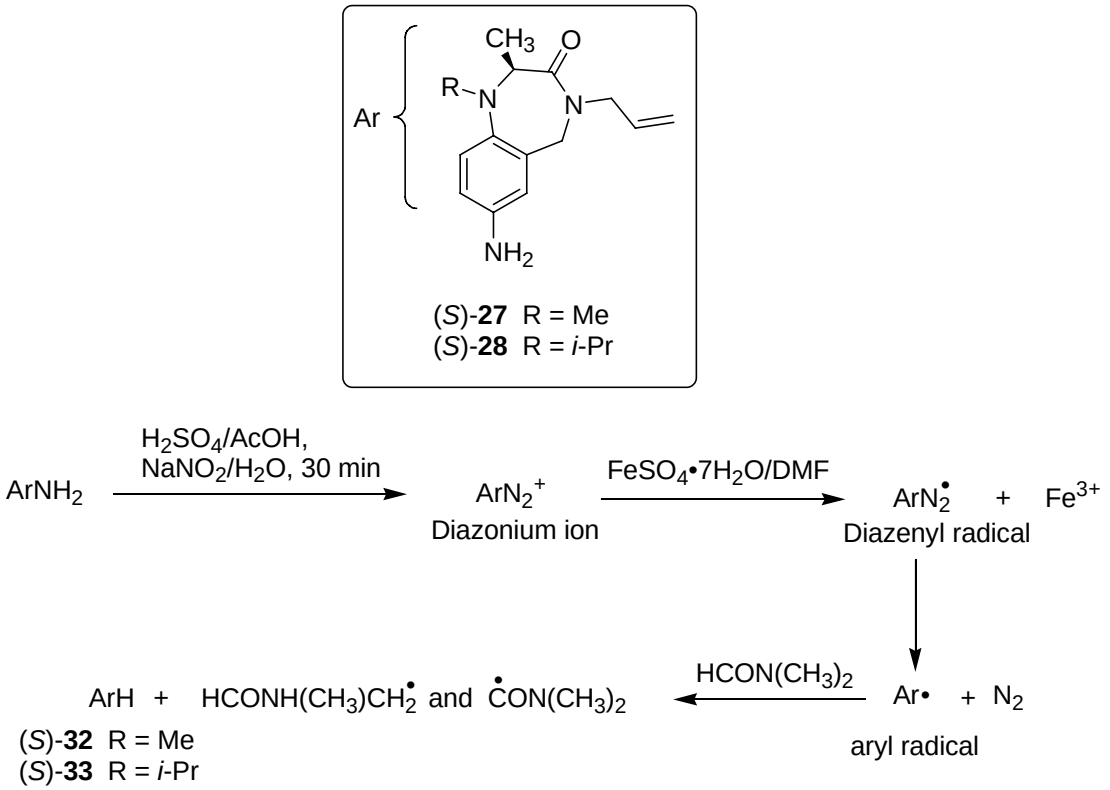

Alkylation reactions were carried out with (*S*)-**32** by use of our standard deprotonation/alkylation protocol for 1,4-benzodiazepin-2-ones (Table 5.4). As can be seen, 2,2-substituted *N*1-Me-1,4-benzodiazepin-3-ones were obtained in moderate yields when the smaller electrophiles were used (Entries 2-4). All of these 2,2-substituted *N*1-Me-1,4-benzodiazepin-3-ones were obtained as racemic products. Though unfortunate, this outcome was not surprising, since the small *N*1-methyl group of (*S*)-**32** might be expected to impart a low inversion barrier.

Table 5.4 Attempted alkylations of (*S*)-**32** and (*S*)-**33**

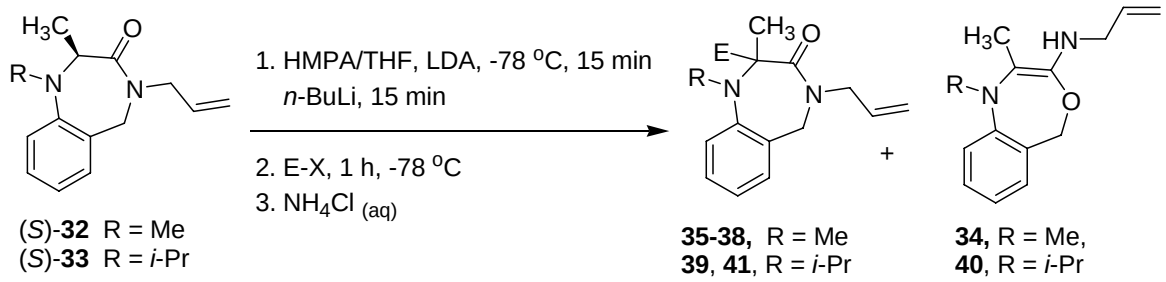

(*S*)-**32** R = Me
(*S*)-**33** R = *i*-Pr

35-38, R = Me
39, **41**, R = *i*-Pr

34, R = Me,
40, R = *i*-Pr

Entry	Starting material	E-X	% Yield	Remarks	% ee[a]
1	(*S*)-**32**	BnBr	61%	Obtained proposed rearrangement product (**34**) instead of the desired product, based on ^{1}H and ^{13}C NMR	-
2	(*S*)-**32**	D_2O/d-TFA	45%	80 % deuterium incorporation based on ^{1}H NMR; product (**35**) confirmed by both ^{1}H NMR and HRMS	0
3	(*S*)-**32**	MeI	56%	Product (**36**) confirmed by both ^{1}H NMR and HRMS	-
4	(*S*)-**32**	EtI	50%	Product (**37**) confirmed by both ^{1}H NMR and HRMS	0
5	(*S*)-**32**	$BrCH_2CO_2Et$	19%	Product (**38**) confirmed by both ^{1}H NMR and HRMS	0
6	(*S*)-**32**	*n*-PrI	8%	Obtained rearrangement product (**34**) instead of the desired product based on ^{1}H NMR and HRMS	-
7	(*S*)-**33**	D_2O/d-TFA	6%	85 % deuterium incorporation (**39**) based on ^{1}H NMR	-
8	(*S*)-**33**	EtI	25%	Obtained similar rearrangement product (**40**) as **34**	-
9	(*S*)-**33**	$BrCH_2CO_2Et$	-	No pure product (**41**) was isolated	-

[a]%ee was measured by chiral stationary HPLC.

On the other hand, when a larger electrophile like BnBr or *n*-PrI (Table 5.4, Entry 1 & 6) was used, no desired product was obtained. Instead, these reactions yielded an isomer of the starting material (*S*)-**32**, as confirmed by both GC-MS and HRMS. In any event, the isolation of desired alkylation products **35**-**38**, and the rearrangement product **34** indicates that enolate formation from **32** is not problematic. Attempted deprotonation of *N*1-*i*-Pr analogs (S)-**33** was less successful. No alkylation products were obtained with EtI or $BrCH_2CO_2Et$ (Table 5.4, Entry 8 & 9). Instead the analogous *N*-iPr rearrangement product **40** was however obtained. These results indicate that the reactivity of the enolate is so low that the rearrangement reaction outcompetes alkylation.

To determine what role, if any, the allyl group played in this rearrangement. We hydrogenated the allyl group to *n*-propyl group by 10% Pd/C in CH_3OH to afford *N*4-*n*-propyl benzodiazepine-3-one (*S*)-**42** in quantitative yield.[19] Results of alkylation of (*S*)-**42** are summarized in Table 5.5.

Table 5.5 Attempted alkylations (*S*)-**42**

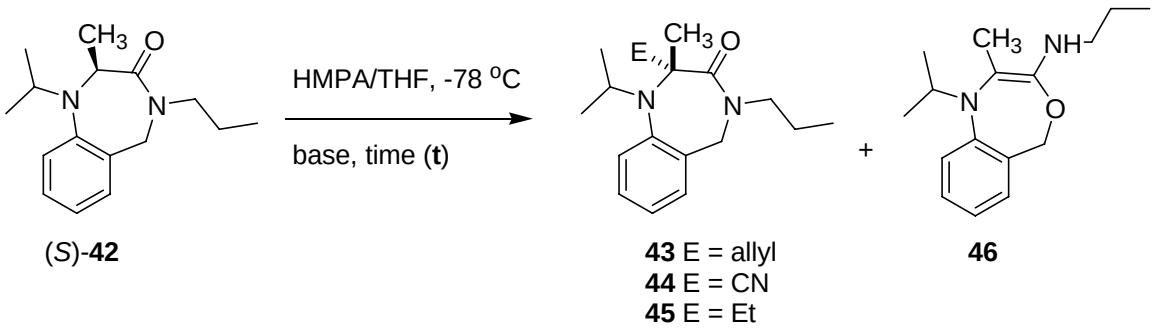

(*S*)-**42**

43 E = allyl
44 E = CN
45 E = Et

46

Entry	Base	E-X	t	Method	Results
1	KHMDS	Allyl bromide	5 h @ -78 °C, 18 h @ r.t.	In situ	Recovered 77% of **42**; obtained no desired product **43**
2	LDA/*n*-BuLi (30 min)	*p*-TsCN (no HMPA)	0.5 h	Inverse[a]	Obtained desired product **44** (55 %)
3	LDA/*n*-BuLi (30 min)	EtI	4 h	Direct	Obtained 11% of **46** & recovered 58% of **42**; no desired product **45**

[a]Addition of enolate solution to the electrophile in THF.

A majority of the starting material was recovered when KHMDS was used as base and allyl bromide was used as electrophile. Apparently, either KHMDS was not strong enough to deprotonate (*S*)-**42** or the allyl bromide was not reactive enough for the alkylaton. The desired product **44** was obtained in 55% yield when LDA and *n*-BuLi were used as bases and *p*-tosyl cyanide (*p*-TsCN) was used as electrophile (Entry 2). Note that Dr. Zhao has successfully obtained the 3,3-substituted 1,4-benzodiazepin-2-ones in high yields using *p*-TsCN as electrophile (unpublished results). The identity of **44** was confirmed by both ^{1}H NMR and HRMS. However, compound **44** was unstable

and decomposition was observed at room temperature. Finally, attempted reaction of the enolate derived from (*S*)-**42** with ethyl iodide gave an apparent rearrangement product **46**. The ^{1}H NMR spectrum of **46** is highly similar to that of **40**, except the allyl and *n*-propyl regions (Table 5.6). The ^{1}H NMR data of both compounds **40** and **46** are summarized in Table 5.6. HRMS confirmed that **46** is a constitutional isomer of **42**.

Table 5.6 Summary of ^{1}H NMR data of both compounds **40** and **46**

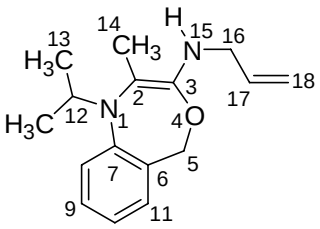

40

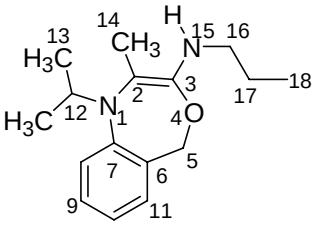

46

Position	40 (δ_H, multiplicity, coupling constant, # of protons)	46 (δ_H, multiplicity, coupling constant, # of protons)
5	4.50, s, 2 H	4.51, s, 2 H
8	6.61, apparent d, 8.0 Hz, 1 H	6.61, apparent d, 8.0 Hz, 1 H
9	7.19-7.23, m, 1 H	7.18-7.23, m, 1 H
10	6.55-6.59, m, 1H	6.56-6.60, m, 1H
11	7.00, dd, 7.4, 1.4 Hz, 1 H	7.02, dd, 7.2, 1.4 Hz, 1 H
12	3.65, 7-let, 6.0 Hz, 1 H	3.65, s, br, 1 H
13	1.21, d, 6.4 Hz, 6 H	1.21, d, 6.4 Hz, 6 H
14	2.41, s, 3 H	2.43, s, 3 H
15	4.90, s, br, 1 H (NH)	4.83, s, br, 1 H (NH)
16	3.76, apparent d, 6.0 Hz, 2 H	3.06-3.08, m, 2 H
17	5.68-5.77, m, 1 H	1.53-1.63, m, 2 H
18	5.18-5.30, m, 2 H	0.83, t, 7.2 Hz, 3 H

A possible rearrangement mechanism for the formation of compounds **40** and **46** is proposed in Scheme 5.11; and a previously proposed mechanism for a related reaction is shown in Scheme 5.12.

Scheme 5.11 Proposed rearrangement mechanism for compounds **40** and **46**

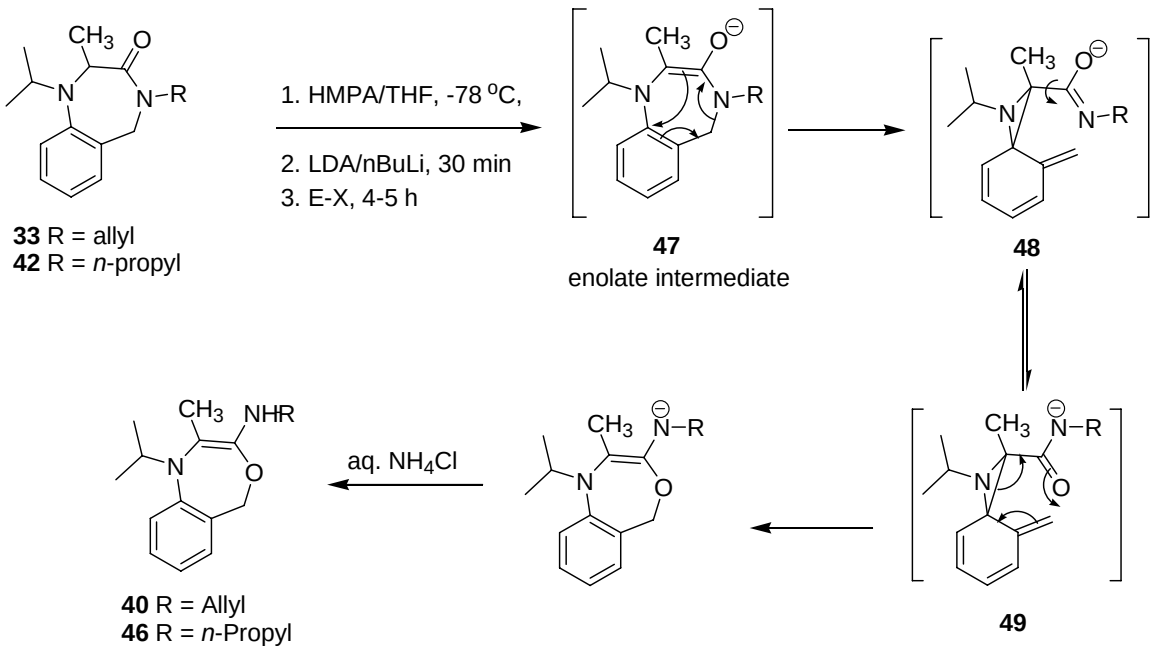

Following the formation of enolate **47**, a 3,3-sigmatropic rearrangement occurs to open the benzodiazepine ring and form a spirocyclic intermediate **48**. Single bond rotation and a second pericyclic reaction would lead to formation of an oxazepine heterocycle. Treatment with aq. NH_4Cl affords the final rearrangement products.

A similar rearrangement of 1,4-benzodiazepin-2-one enolate has been proposed by Fryer *et al.* (Scheme 5.12).[20] They have found that diazepam **50** and its derivatives underwent ring contraction rearrangement upon treatment with NaH at 0-75 °C, to give isoindole derivatives. As seen in Scheme 5.12, their proposed rearrangement mechanism involves the removal of one of the C3 protons by NaH, is followed by a ring contraction to give two possible tricyclic intermediates. Further ring contraction of either intermediates give the salt of isoindole carbanion **51**; treatment with H_2O yielded

isoindolenine **52**. Though Fryer *et al.* did not draw a discrete enolate intermediate, the basic mechanism remains unchanged.

Scheme 5.12 Two ring contraction rearrangement mechanisms of diazepam proposed by Fryer *et al* [20]

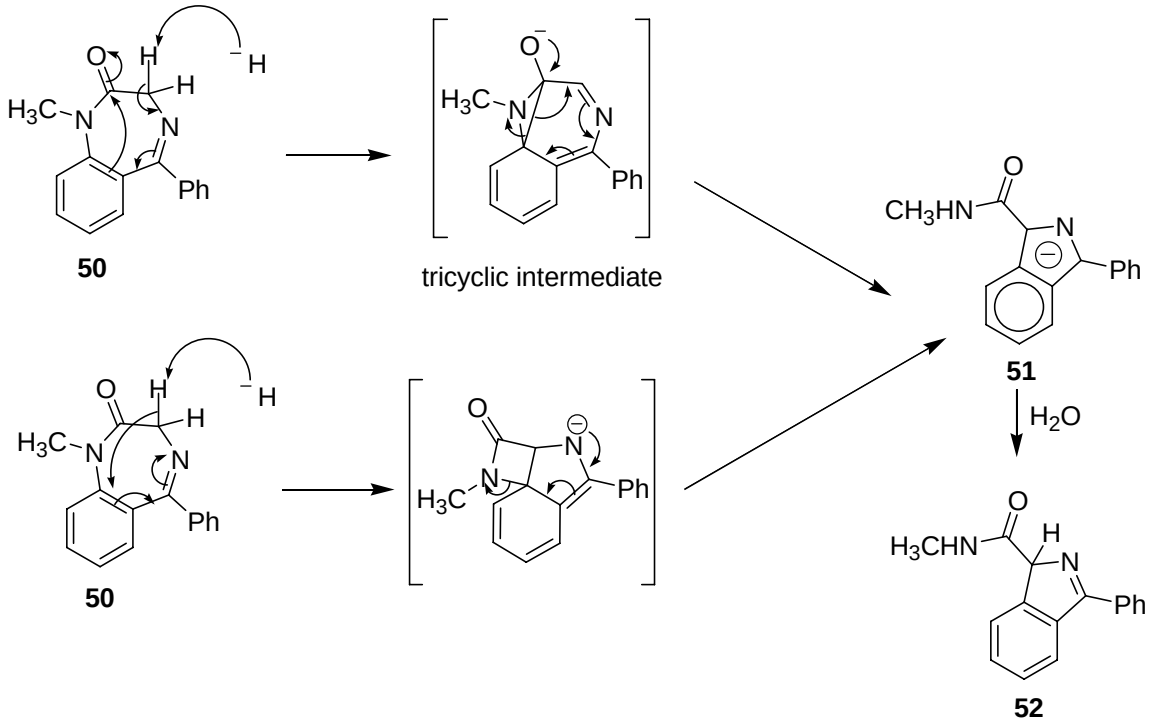

The proposed mechanism in Scheme 5.11 like that in Scheme 5.12 involves the disruption of aromaticity in the enolate intermediate **47** to form a strained 3-membered ring intermediate **48**. Such process would be expected to have a high activation barrier. In order to assess the feasibility of our proposed mechanism (Scheme 5.11), we conducted equilibrium geometry optimization calculations of both enolate **47** and spirocylic intermediate **48** at B3LYP/6-31G(d) level. The energy difference between these two intermediates (**47** and **48**) would give us an idea about the activation barrier of this reaction. According to the energy that we obtained at B3LYP/6-31G(d), the enolate intermediate **47** is lower in energy than the intermediate **48** by 27.0 kcal/mol, which

means that the activation barrier for this reaction would be higher than 27.0 kcal/mol. Therefore, the proposed mechanism in Scheme 5.11 is not likely to be rapid at -78 °C. Note that the rearrangement reported by Fryer *et al.* occurs at 0-75 °C (cf Scheme 5.12).

We therefore propose the following free radical mechanism (Scheme 5.13) to account for the formation of the rearrangement products **40** and **46**. As seen in Scheme 5.13, single electron reduction of either **33** or **42** by LDA gives a radical-anion intermediate **53**; fragmentation of the 7-membered ring forms a benzylic radical-anion intermediate **54**. Single bond rotation of **54** and cyclization lead to third radical-anion intermediate **55**. Finally, oxidation of **55** upon treatment of aq. NH_4Cl affords the rearrangement products. This proposed free radical mechanism is more feasible than that proposed in Scheme 5.11 due to two reasons; firstly, this mechanism does not involve the disruption of aromaticity of the aromatic ring nor involve the formation of a strained 3-membered ring. Secondly, the benzylic radical intermediate **54** can be stabilized by the aromatic ring by delocation.

Scheme 5.13 Proposed reduction/oxidation free radical mechanism for the formation of rearrangement products **40** and **46**

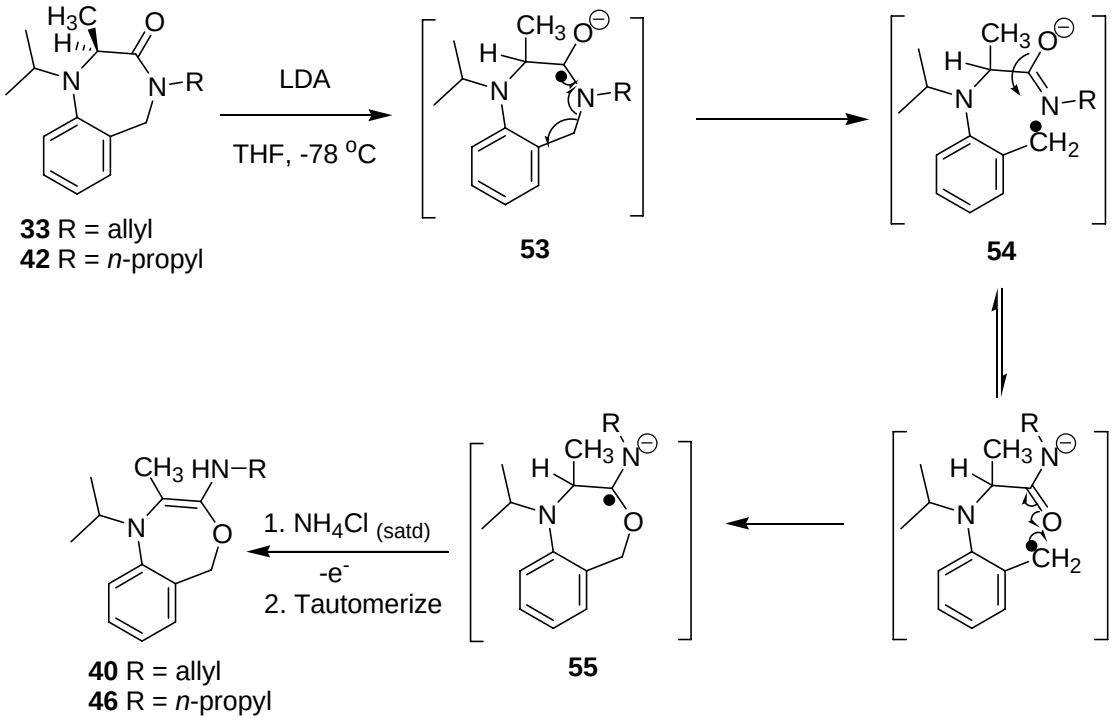

Despite the unsuccessful alkylations of tetrahydro-1,4-benzodiazepin-3-ones, we developed an efficient synthesis of tetrahydro-1,4-benzodiazepin-3-ones derived from (*S*)-alanine and introduced diversity at N1. In order to introduce the diversity at N4, we need to remove the N4-allyl group. However, removal of the N4-allyl group from the tetrahydro-1,4-benzodiazepin-3-ones proved more difficult than anticipated. As shown in Table 5.7, we carried out deallylations at different reaction conditions; disappointing results were obtained from most of the reactions. Traditional $Pd(PPh_3)_4$ catalyzed deallylation methods, either with *N*,*N*'-dimethylbarbturic acid (NDMBA),[21] or with Et_3N/HCO_2H system recommended for imides,[22] were fruitless. Catalysis by

$RhCl(PPh)_3$[23] also proved ineffectual, and $RuCl_2(PPh)_3$[24] catalyzed deallylation proceeded only in low to moderate yields.

Table 5.7 Attempted deallylation of tetrahydro-1,4-benzodiazepin-3-ones

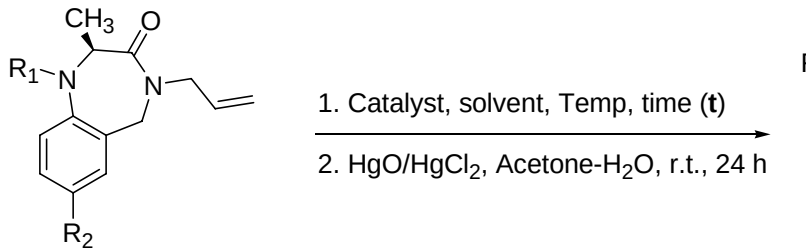

	R_1	R_2
(*S*)-**10**	Me	NO_2
(*S*)-**11**	*i*-Pr	NO_2
(*S*)-**29**	*i*-Pr	NMe_2
(*S*)-**30**	*i*-Pr	Nphth
(*S*)-**33**	*i*-Pr	H

	R_1	R_2
(*S*)-**56**	Me	NO_2
(*S*)-**57**	*i*-Pr	NO_2
(*S*)-**58**	*i*-Pr	NMe_2
(*S*)-**59**	*i*-Pr	Nphth
(*S*)-**60**	*i*-Pr	H

Entry	Catalyst	Solvent/t	Temp.	R_1	R_2	Results
1	$RhCl(PPh)_3$ (no 2nd step)	CH_3CN-H_2O/ 24 h	Reflux	*i*-Pr	NMe_2	No reaction
2	$RuCl_2(PPh)_3$ (with DIPEA)	Toluene/24 h	Reflux	*i*-Pr	H	51-54 % of desired product (*S*)-**60**
3	$RuCl_2(PPh)_3$ (with DIPEA)	Toluene/24 h	Reflux	*i*-Pr	NMe_2	37 % of desired product (*S*)-**58**
4	$RuCl_2(PPh)_3$ (with DIPEA)	Toluene/24 h	Reflux	*i*-Pr	Nphth	No reaction
5	$RhCl(PPh)_3$ (with DABCO)	EtOH-H_2O/ 24 h	Reflux	iPr	NMe_2	8 % of desired product (*S*)-**58**
6	$RuCl_2(PPh)_3$ (with DIPEA)	Toluene/24 h	Reflux	Me	NO_2	14 % of desired product (*S*)-**56**; contaminated with $P(=O)Ph_3$
7	$RuCl_2(PPh)_3$ (with DIPEA)	Toluene/24 h	Reflux	*i*-Pr	NO_2	Trace of desired product ((*S*)-**57**) seen on TLC
8	$RhCl(PPh)_3$ (with DABCO)	Toluene/ 24 h	Reflux	Me	NO_2	No reaction
9	$Pd(PPh_3)_4$ (with NDMBA)	CH_2Cl_2/3 h	35 ºC	*i*-Pr	H	No reaction
10	$Pd(PPh_3)_4$ (with Et_3N/HCO_2H)	Dioxane/24 h	Reflux	Me	NO_2	No reaction

Rh (I) or Ru (II) catalyzed deallylations involve isomerization of allylamine to enamine **61** (Scheme 5.14), followed by acidic hydrolysis the amine. The isomerization of **33** to **61** should not be problematic. However, for deprotection of N4-allyl of tetrahydro-1,4-benzodiazepin-3-ones, the enamine intermediate **61** is actually an enamide and is thus rather non basic. The unfavorable formation of acyliminium ion **62** is thus likely the rate-determining step for Rh (I) or Ru (II) catalyzed deallylations of **33**, which may accounts for the low yielding in these reactions (cf Table 5.7, Entries 1-8).

Scheme 5.14 A proposed mechanism for an example of Rh (I) or Ru (II) catalyzed deallylations of tetrahydro-1,4-benzodiazepin-3-one (*S*)-**33**

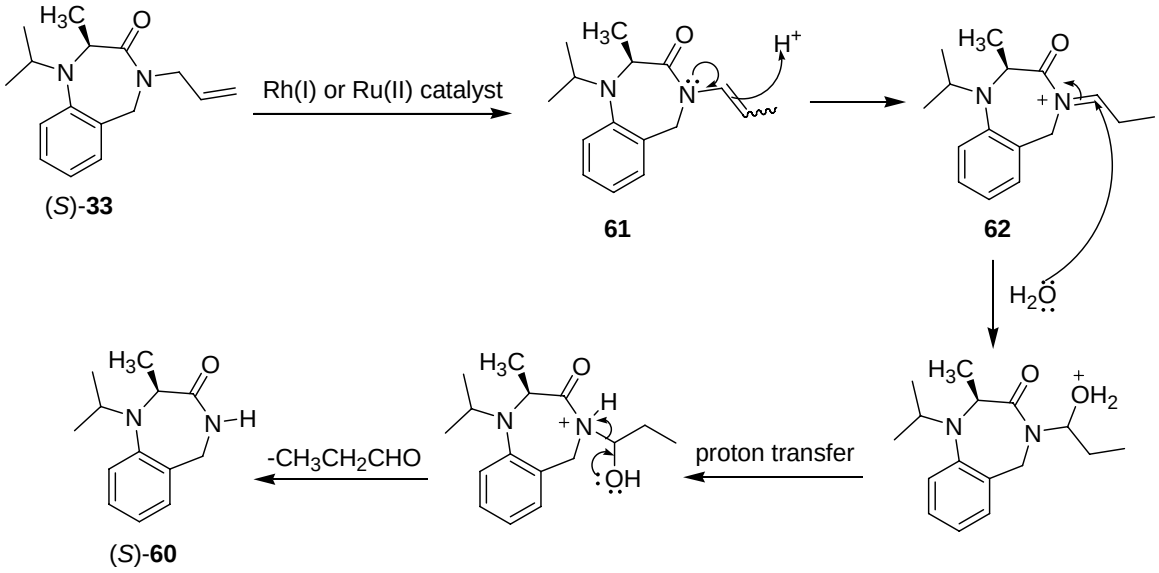

In order to understand why the deallylations of tetrahydro-1,4-benzodiazepin-3-ones by $Pd(PPh_3)_4$ in the presence of NMDBA were unsuccessful, we present in Scheme 5.15 a general catalytic cycle involved in the deallylation of allylamines by $Pd(PPh_3)_4$ /NMDBA as proposed by Guibé *et al*.

Scheme 5.15 Palladium(0)-catalyzed deallylation of allylamines

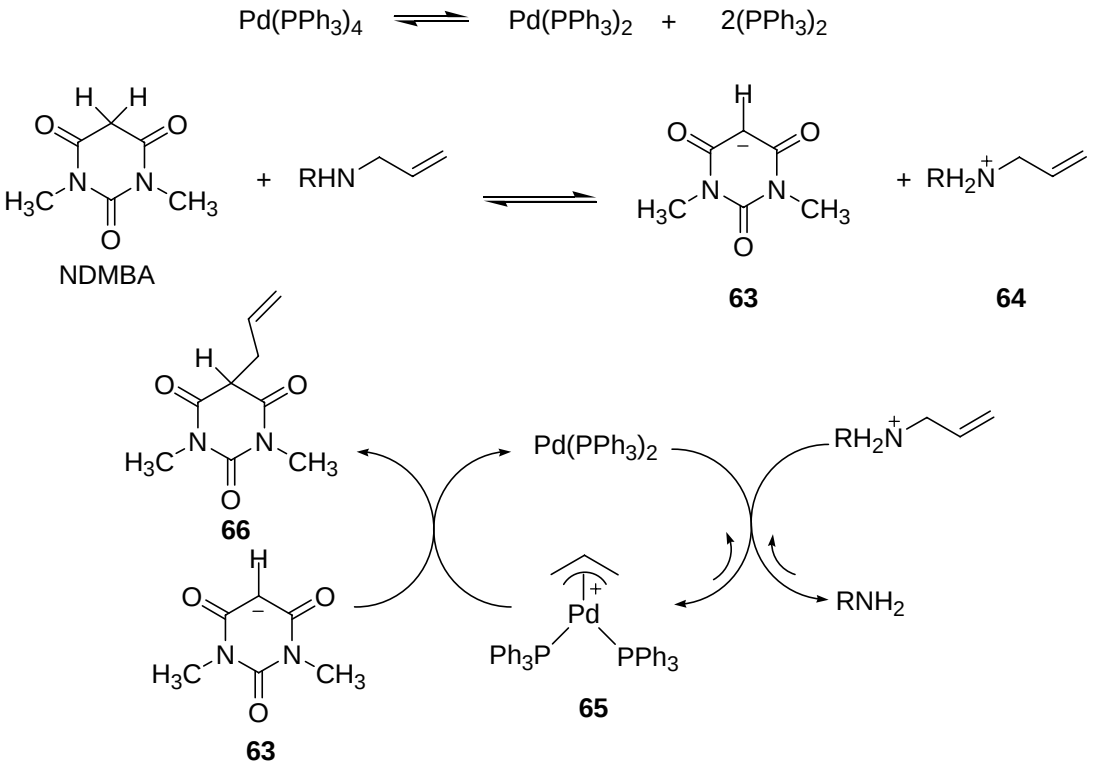

Allylamine is represented by a general formula: RHN R = any alkyl group

As seen in Scheme 5.15, allylamine is first protonated by NMDBA to form an allylammonium species **64**. The formation of allylammonium species **64** is necessary for transfer of the allyl group to the palladium (0) catalyst $Pd(PPh_3)_2$. The allylammonium species **64** then reacts with $Pd(PPh_3)_2$ to give a π-allyl palladium (II) complex **65** and the deallylated amine RNH_2. Complex **65** is then trapped by allyl group scavenger **63** irreversibly to give the corresponding C-alkylated derivative **66** and the regenerated palladium (0) catalyst $Pd(PPh_3)_2$.

Tetrahydro-1,4-benzodiazepin-3-ones are much less basic than an aliphatic amine. Thus the failed deallylation of the compounds shown in Table 5.7 (Entry 9 and 10) by

$Pd(PPh_3)_4$ /NMDBA is perhaps due to the difficulty in formation of allylammonium species, as shown below.

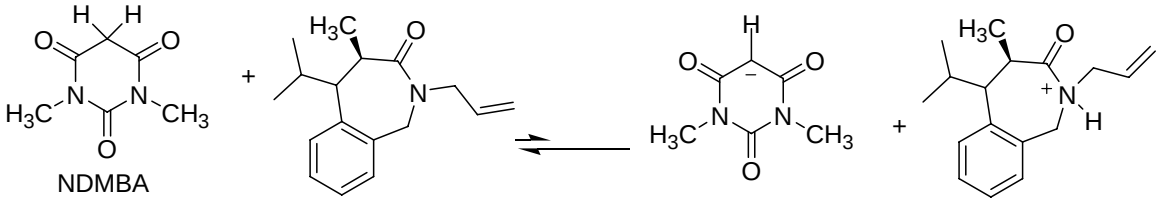

Finally, we attempted deallylation under Bundle's oxidative deallyation protocol.[25] Heating (*S*)-**10** and (*S*)-**29** in dioxane-H_2O with 8-10% potassium osmate in the presence of *N*-methyl morpholine *N*-oxide (NMO) and sodium periodate afforded (*S*)-**56** and (*S*)-**58** in 75% and 64% respectively (Scheme 5.16). Chiral stationary HPLC indicated that no racemization had occurred during the deallylation. Prolonged heating of (*S*)-**29** (18 h) caused the complete decomposition of the desired product. We have also carried out the oxidative deallylations with (*S*)-**10**, (*S*)-**29** and (*S*)-**30** by use of only 2-4% potassium osmate. Although the reduced catalyst loading was successful for (*S*)-**29,** incomplete deallylation was observed for both (*S*)-**10** and (*S*)-**30**.

Scheme 5.16 Bundle's oxidative deallyation protocol of (*S*)-**10** and (*S*)-**29**

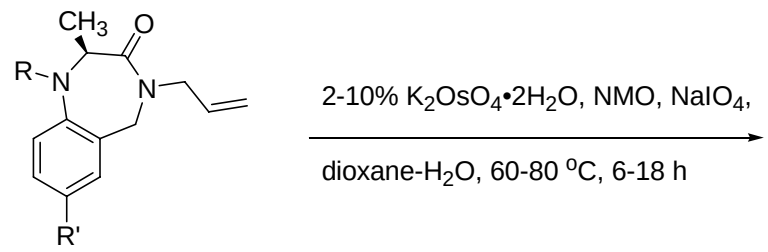

	R	R'
(*S*)-**10**	Me	NO_2
(*S*)-**29**	*i*-Pr	NMe_2

	R	R'	% Yield
(*S*)-**56**	Me	NO_2	75%
(*S*)-**58**	*i*-Pr	NMe_2	64%

Bundle's mechanism for the oxidative deallylation is despicted for tetrahydro-1,4-benzodiazepin-3-ones in Scheme 5.17.

Scheme 5.17 A proposed mechanism of deallylation of (*S*)-**10**

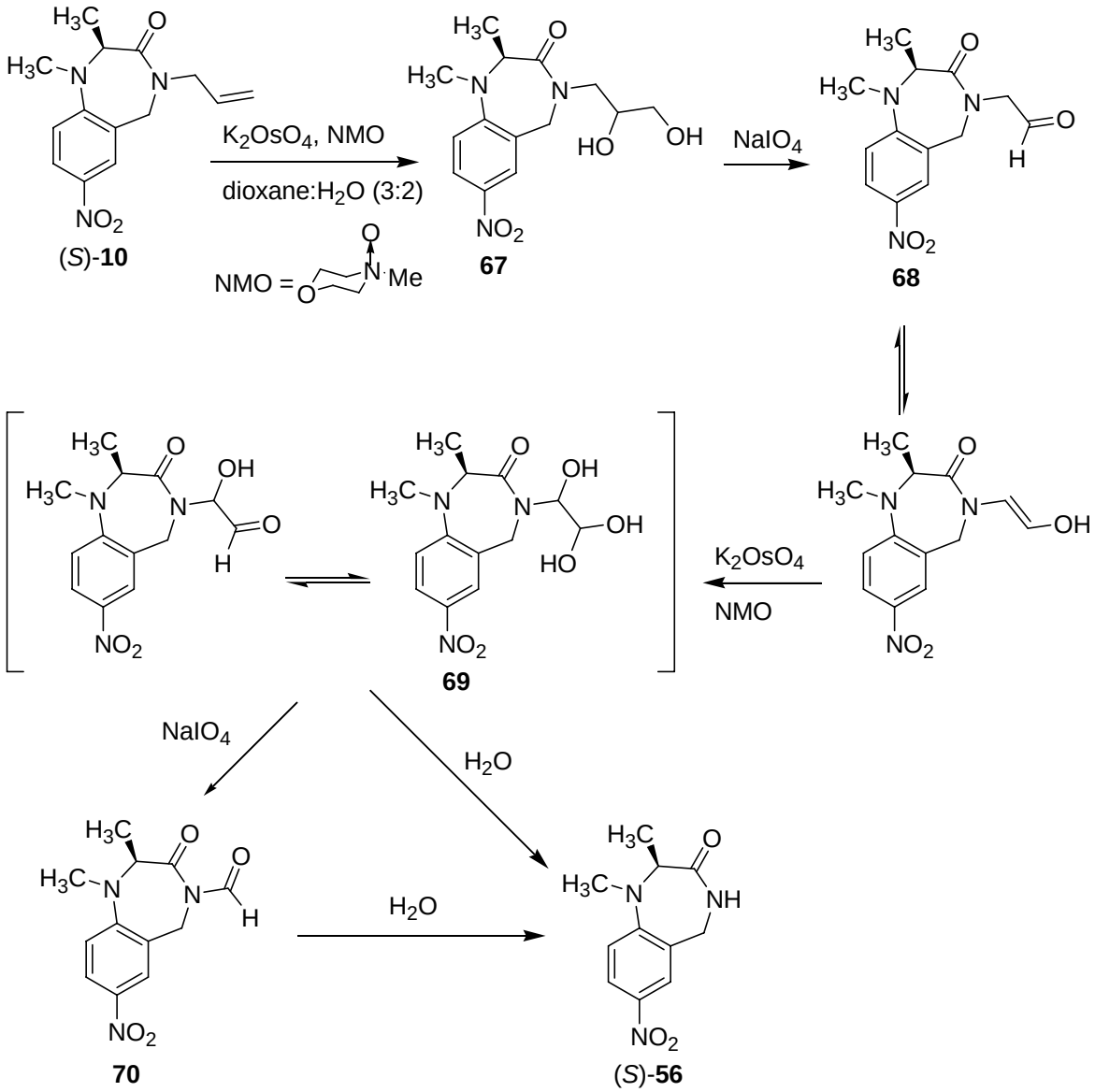

The proposed mechanism first involves the osmium tetroxide (OsO_4)-catalyzed dihydroxylation of the allyl double bond in (*S*)-**10**. The resulting glycerol derivative **67** is then oxidized by $NaIO_4$ to give the α-amino-aldehyde **68**, followed by further oxidation of the enol tautomeric form of **68** by OsO_4 to afford aldehyde hydrate hemiaminal **69**. The final deallylated product (*S*)-**56** may be obtained either by direct hydrolysis of the

hemiaminal **69** or hydrolysis of the formimide **70** that formed from further oxidation by $NaIO_4$.

5.1.3 Computational Studies of Tetrahydro-1,4-benzodiazepin-3-ones

Compound (*S*)-**56** and its racemic mixture were analyzed by chiral stationary HPLC. Unexpectedly, a pair of peaks were observed for (*S*)-**56**, and two pairs were observed for (*S/R*)-**56**, as shown in Figure 5.1.

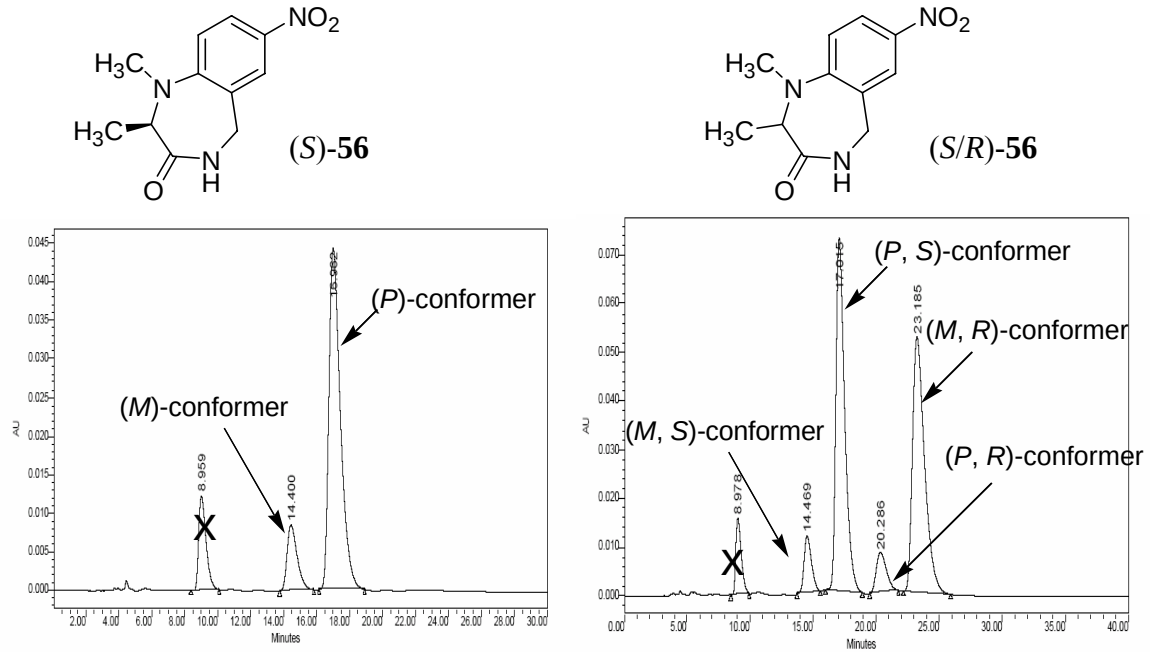

Figure 5.1 HPLC chromatograms of (*S*)-**56** (left) and its racemic mixture (*S*/*R*)-**56** (right); X denotes an unknown impurity

Our initial analysis is that unlike alanine-derived 1,4-benzodiazepin-2-ones, alanine-derived 1,4-benzodiazepin-3-ones existed as mixtures of the pseudoequatorial and pseudoaxial confomers. ^{1}H NMR spectroscopy of **44** supported this proposal (Table 5.8).

Table 5.8 Calculated ratios of (*P*)- and (*M*)-conformers (cf Figure 5.1) and C2-CH_3 proton signals of (*S*/*R*)-**56**.

	(*M*,*S*)-conformer	**(*P*,*S*)-conformer**	**(*M*,*S*)/(*P*,*S*) ratio**	**(*M*,*R*)-conformer**	**(*P*,*R*)-conformer**	**(*M*,*R*)/(*P*,*R*) ratio**
% Area	5.70	41.69	7.4	5.56	41.37	7.3
R_T[a](min)	14.47	17.02	-	20.29	23.19	-
Proton integrals[b]	0.45	2.73	6.1	-	-	-

[a]R_T = Retention time
[b]C2-CH_3 integrals (dd) are chosen for calculation.

If interconversion of these conformers was slow (i.e. on the HPLC time scale), then the pairs of peaks might arise from the pseudoequatorial and pseudoaxial confomers. In order to test this explanation, we performed geometry optimization calculations[26] of (*S*)-**56** (B3LYP/6-31G(d)). As we mentioned previously, 1,4-benzodiazepines are classified using (*M*)- and (*P*) descriptors. (*S*)-alanine-derived 1,4-benzodiazepin-2-ones ((*S*)-**71**, see Table 5.9) prefer to adopt an (*M*)-conformation due to the pseudoequatorial preference for the methyl. As shown for **56**, the equatorial preference of the methyl induces (*S*)-alanine-derived tetrahydro-1,4-benzodiazepin-3-ones to adopt the (*P*)-conformation (Figure 5.2).

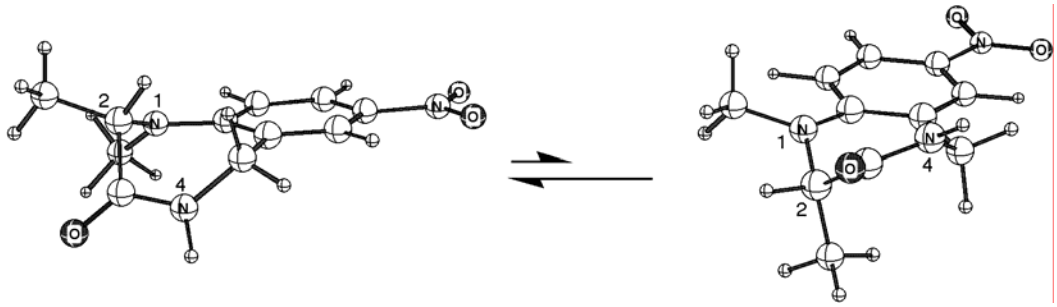

(*P*)-(*S*)-**56**
pseudoequatorial-Me
0 kcal/mol

(*M*)-(*S*)-**56**
pseudoaxial-Me
+2.0 kcal/mol

Figure 5.2 B3LYP/6-31G(d) electronic energy difference between the (*M*)- and (*P*)- conformers of (*S*)-**56**; the sign of the dihedral angle C6-C7-N1-C2 defines the helical chirality descriptor (*M* (minus) or *P* (plus))

As can be seen in Figure 5.2, two equilibrium geometries were found for the (*S*)-enantiomer of **56**. The (*P*)-conformer of **56**, which features an equatorial C2-Me, is lower in energy than the (*M*)-conformer by 2.0 kcal/mol. Thus the equatorial preference for tetrahydro-1,4-benzodiazepin-3-ones is calculated to be considerably less than that of tetrahydro-1,4-benzodiazepin-2-ones[27] (Table 5.9). The calculated electronic energy difference of (*S*)-**56** and sum of internal angles of both (*S*)-**56** and (*S*)-**71** are summarized in Table 5.9. The sum of the internal angles of the (*P*)- and (*M*)-conformers of (*S*)-**56** are 829° and 844° respectively. These angles are between the value of 809° calculated for a puckered ring from simple VSEPR considerations[28] and the value of 900° calculated for a flat heptagon.[29] The calculated sum of internal angles for (*S*)-**71** is 833°, which corresponds to a calculated value of 829° based on the simple VSEPR considerations. Since the calculated sum of internal angles for (*S*)-**71** is close to the estimate based on VSEPR considerations, while the sum of internal angles for (*P*)-*S*-**56** and (*M*)-*S*-**56** are 20° and 35° different than the VSEPR estimate, then N1-Me (*S*)-alanine-derived

tetrahydro-1,4-benzodiazepin-3-ones appear to be flatter than N1-Me (*S*)-alanine-derived 1,4-benzodiazepin-2-ones. This greater flatness may account for the smaller pseudoequatorial preference for the methyl seen in the tetrahydro-1,4-benzodiazepin-3-ones, because a flatter structure may make interconversion between the two conformations easier.

To test our argument, we also performed equilibrium geometry calculations for glycine-derived tetrahydro-1,4-benzodiazepine-3-one **72** by use of the same basis set. The (*P*)- and (*M*)-conformers of **72** are enantiomers and therefore equal in energy. In the equilibrium geometries, the sum of the internal angles of both (*P*) and (*M*)-conformers is 833° (Table 5.9), which is close to the sum of internal angles of (*P*)- and (*M*)-conformers of (*S*)-**56**. So, since the sum of internal angles for (*P*)- and (*M*)-conformers of (*S*)-**56** are close to the sum of internal angles for (*M*)- or (*P*)-**72**, for which there is no conformational preference, then these calculations support the idea that there is little preference between (*P*)- and (*M*)-conformers of (*S*)-**56** as well. The observed pseudoequatorial:pseudoaxial ratios (cf Table 5.8) of 6:1 (^{1}H NMR) and 7:1 (HPLC) for (*S*)-**56** correspond to an energy difference of 1.1 kcal/mol at 298 K, which is very close to the calculated electronic energy difference of 2.0 kcal/mol.

Table 5.9 Summary of sum of internal angles and energy differences (B3LYP/6-31G(d))

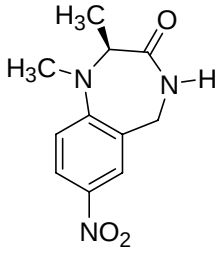

(2*S*)-**56**

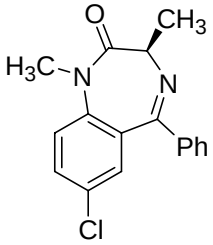

(3*S*)-**71**

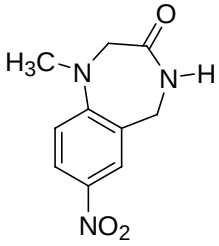

72

Compound	C3 methyl	ΔE[a] (kcal/mol)	Sum of internal angle (°) based on computational studies	Sum of internal angle (°) based on simple VSEPR considerations
(*P*)-(*S*)-**56**	eq	0	829	809
(*M*)-(*S*)-**56**	ax	2.0	844	809
(*M*)-(*S*)-**71**[b]	eq	0	833	829
(*P*)-(*S*)-**71**[b]	ax	4.7	848	829
(*P*)-**72**	na	0	833	809
(*M*)-**72**	na	0	833	809

[a]Difference in electronic energies between axial and equatorial conformers
[b]ΔE and sum of internal angles of compound **71** were calculated by Dr. Polo Lam.

5.2 Investigation of Enantioselective Synthesis of Quaternary (*S*)-phenylalanine Derived Tetrahydro-1,4-benzodiazepin-2-ones

5.2.1 Synthesis of (*S*)-phenylalanine Derived Tetrahydro-1,4-benzodiazepin-2-ones

As mentioned previously, various tetrahydro-1,4-benzodiazepin-2-ones have been found to possess important biological activity.[30] As in the case of tetrahydro-1,4-

benzodiazepin-3-ones, 3,3-substituted derivatives are unexplored territory. We are therefore also interested in extending our MOC protocol to this subtype.

The synthesis of certain tetrahydro-1,4-benzodiazepin-2-ones has been previously reported either by solid phase synthesis[31] or via phenyliodine (III)bis(trifluoroacetate)-mediated intramolecular cyclization.[32] We carried out the synthesis of (*S*)-phenylalanine-derived tetrahydro-1,4-benzodiazepin-2-ones based on modified literature method (Scheme 5.18). The synthesis started with commercially available 2-nitrobenzylbromide (**73**): treatment with (*S*)-phenylalanine methyl ester hydrochloride in the presence of DIEA in DMF afforded (*S*)-**74** in 95% yield. Heating of (*S*)-**74** with either excess CH_3I or allyl bromide in DMF at the boiling point of the alkylating agent in the presence of DIEA provided (*S*)-**75** and (*S*)-**76** respectively in good yields. However, attempts to carry out reductive ring closure of (*S*)-**75** by use of $SnCl_2 \bullet 2H_2O/NH_4OAc$ were completely unsuccessful. (*S*)-**75** decomposed to (*S*)-*N*-methyl phenylalanine methyl ester (**77**) and 2-amino benzylethylether (**78**) via elimination/addition (Scheme 5.18).

Scheme 5.18 Synthesis of (*S*)-**75**, (*S*)-**76** and proposed mechanism for the decomposition of (*S*)-**75**

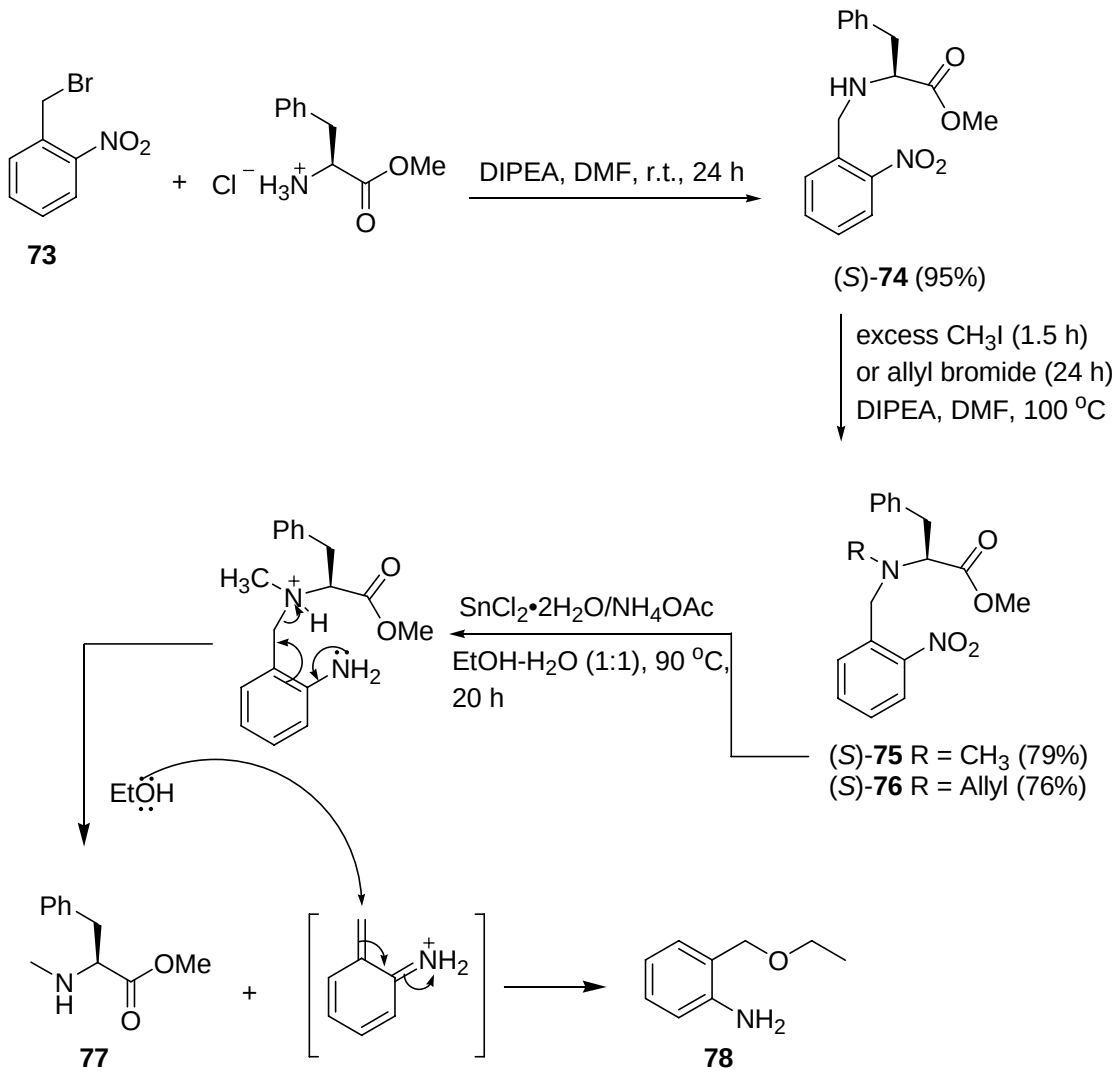

We then explored other methods for the ring closure of the heterocyclic ring. As shown in Scheme 5.19, the nitro groups was reduced to corresponding amines (*S*)-**79** and (*S*)-**80** in good yields by use of Fe powder and $NH_4Cl_{(aq.)}$, and the methyl ester of (*S*)-**80** was hydrolyzed to corresponding sodium carboxylate (*S*)-**81** in the presence of 2 N NaOH in CH_3CN in quantitative yield.[33] Subsequent intramolecular amide coupling of

(*S*)-**81** in the presence of DCC/HOBT in CH_2Cl_2 at room temperature for 18 hours afforded the desired product (*S*)-**82** in 77% yield.

Scheme 5.19 Ring closure of heterocyclic ring

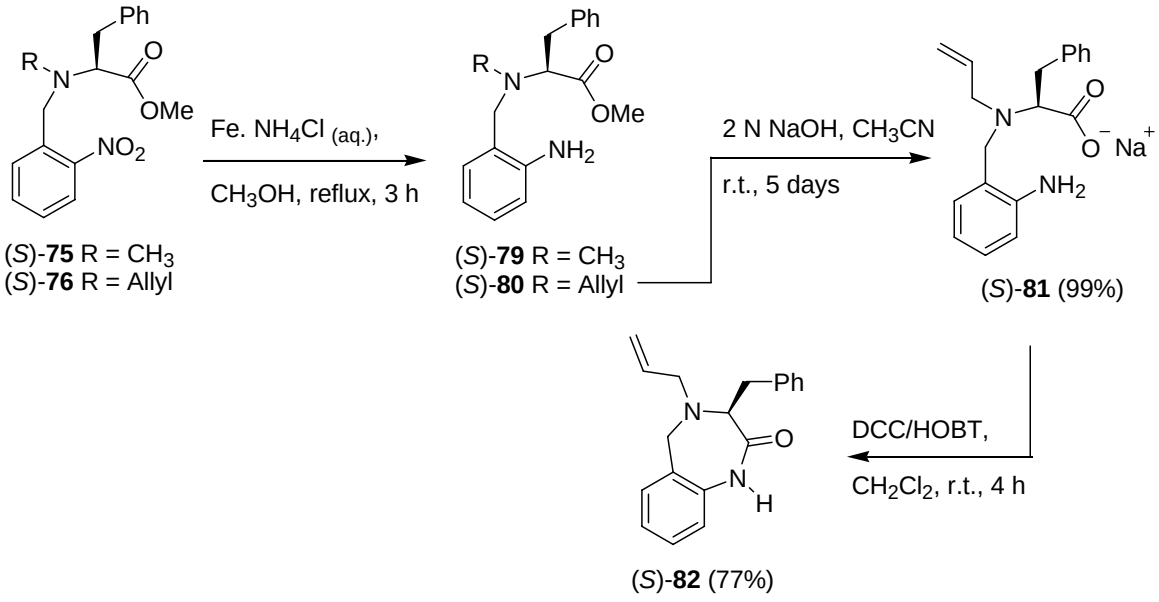

5.2.2 Attempted Synthesis of Quaternary Tetrahydro-1,4-benzodiazepin-2-ones Via MOC

Before we attempting deprotonation/alkylation, it is necessary to replace the acidic H on N1 of (*S*)-**82**. Thus, we carried out the alkylation at *N*1 with dianisylmethyl bromide (DAM-Br) at 0 ºC (Table 5.10). The desired product (*S*)-**83** was obtained in 72% yield. DAM-Br was synthesized from 4,4'-dimethoxybenzhydrol and acetyl bromide in benzene at 75 ºC for 1.5 h according to a modified literature method.[34] As we mentioned previously, the ring inversion barrier is expected to increase with increasing size of the alkyl group at N1-position. Based on Dr. Zhao's research on 1,4-

benzodiazepin-2-ones, the DAM group should be larger enough to prevent the enolate from racemizing at -78 ºC.

Table 5.10 Attempted alkylations of (*S*)-**83**

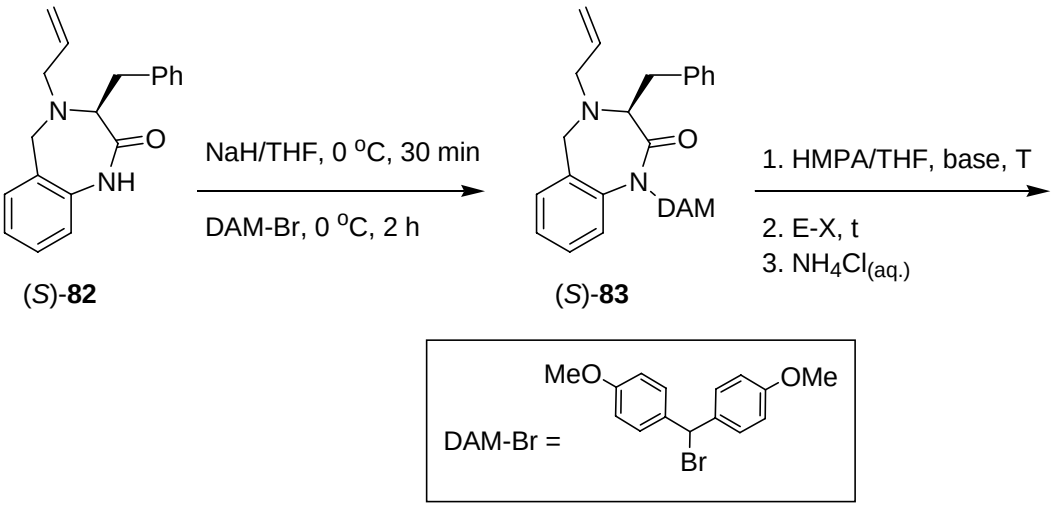

Entry	Base	T	E-X	T	Results
1	LDA/*n*-BuLi (30min)	-78 ºC	D_2O	1 h	A mixture of **82** and **83** based on ^{1}H NMR
2	LDA/*n*-BuLi (30min)	-78 ºC	CH_3I	1 h	Recovered 47% of **83**; obtained two by products: 26% of **82** and 20% of **84** based on ^{1}H NMR and HRMS
3	KHMDS (30min)	-78 ºC	CH_3I	2-5 h	No reaction

As shown in Table 5.10, we attempted trapping the enolate with D_2O using the deprotonation/alkylation protocol published for 1,4-benzodiazepin-2-ones. Surprisingly, none of the desired product was detected. Alkylation with CH_3I in the presence of LDA/*n*-BuLi was also unsuccessful; in addition to recovered starting

material (47%), N1-deprotected by product **82** (26%) and the DAM-OH oxidation product **84** (20%) were obtained. Both by products were (**82** and **84**) confirmed by ^{1}H NMR and HRMS. Apparently, LDA/*n*-BuLi was not suitable for the deprotonation of N-DAM benzodiazepines; such decomposition in 1,4-benzodiazepin-2-ones has also been noted by Dr. Hongwu Zhao. We thus used weaker base KHMDS (Entry 3, Table 5.10) for the deprotonation of (*S*)-**83**. However, none of the desired product was obtained. We then abandoned deprotonation/alklylation of (*S*)-**83**.

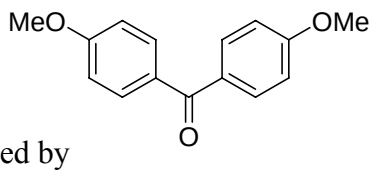

84

5.2.3 Computational Studies of (*S*)-phenylalanine-derived Tetrahydro-1,4-benzodiazepin-2-ones

In order to understand why the (*S*)-phenylalanine-derived tetrahydro-1,4-benzodiazepin-2-one (*S*)-**83** was unreactive towards the deprotonation/alkylation protocol, we performed equilibrium geometry calculations of this compound (B3LYP/6-31G(d)). Note that phenylmethylene group was replaced by a methyl group to speed up the calculation.

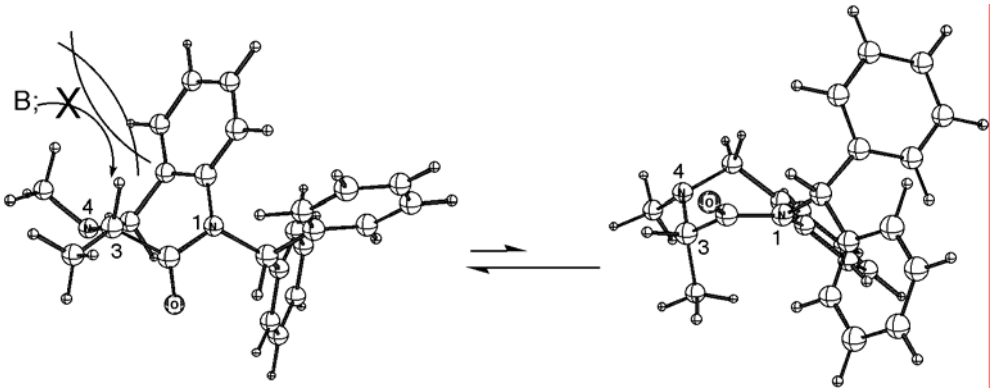

(*M*)-(3*S*)-**83**
pseudoequatorial-Me
0 kcal/mol
∠H3-C3-C2-O: +139.0°
Sum of internal angles: 812°

(*P*)-(3*S*)-**83**
pseuoaxial-Me
+5.0 kcal/mol
∠H3-C3-C2-O: -2.5°
Sum of internal angles: 819°

Figure 5.3 B3LYP/6-31G(d) electronic energy difference between the (*P*)- and (*M*)- conformers of (*S*)-**83**; the sign of the dihedral angle C6-C7-N1-C2 defines the helical chirality descriptor (*M* (minus) or *P* (plus)); B denotes a base such as KHMDS or LDA

As shown in Figure 5.4, the pseudoequatorial (*M*)-conformer is 5.0 kcal/mol lower in energy than the pseudoaxial (*P*)-conformer. This energy difference corresponds to an approximate equilibrium ratio of 4670:1 at room temperature, which suggests that (*S*)-**83** will exclusively exist as the (*M*)-conformer at this temperature. The dihedral angle H3-C3-C2-O of the pseudoequatorial-Me is 139.0° (Figure 5.4, Table 5.11), but dihedral angle of the less favorable pseudoaxial-Me (*P*)-conformer is nearly eclipsed (-2.5°). These dihedral angles suggest that the lowest energy (*M*)-conformer is more suitable for deprotonation than the (*P*)-conformer.[35] We propose that the deprotonation is sterically difficult due to two contributing factors. Firstly, as seen in Figure 5.4, the sum of internal angles in the (*M*)- conformer is 812° (Table 5.11), close to the value of 809° that is calculated from simple VSEPR considerations for a puckered ring. The H3-C8 and H3-

C11 distances are 3.37 Å and 3.65 Å (Table 5.11) respectively. These relatively short distances of suggest that the benzo ring might block the approach of bulky base to H3. Secondly, N4-CH_3 is pointing up and the distance of H3 to N4-CH_3 is only 2.60 Å (Table 5.11), which also suggest that approach of bulky base to H3 may be sterically hindered by N4-CH_3 group. The steric hindrance from both benzo ring and N4-CH_3 group may account for the failure of deprotonation/alkylations of (*S*)-**83**. On the other hand, the distances from H2 to C8/C11 and H2 to N1-CH_3 (Table 5.11) of the (*P*)-conformer of the (*S*)-alanine-derived tetrahydro-1,4-benzodiazepin-3-one such as (*S*)-**32** are longer than those of (*S*)-**83**. In these cases, H2 is free from steric hindrance from both the benzo ring and N1-CH_3 group, as both the benzo ring and the N1-CH_3 group are not crowding around H2. That is, H2 is more easily accessed by LDA due to its flatter ring geometry, which alleviates the steric hindrance. The flatter ring geometry of (*S*)-**32** is also reflected in the sum of internal angles (Table 5.11). Furthermore, the dihedral angle H2-C2-C3-O of pseudoequatorial-Me is 138° (Table 5.11), suggesting that the (*P*)-conformer of (*S*)-**32** is suitable for deprotonation, which is consistent with the successful alkylations of (*S*)-**32** (cf Table 5.4).

Table 5.11 Selected structural parameters for (*S*)-alanine-derived tetrahydro-1,4-benzodiazepin-2 & 3-ones equilibrium geometries

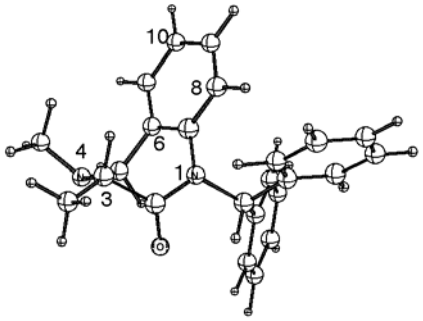

(3*S*)-**83**

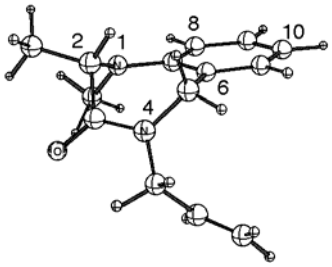

(2*S*)-**32**

Compound	Dihedral angles	Sum of internal angles	H3/H2-C8 distance	H3/H2-C11 distance	H2/H3-N-CH_3 distance
(3*S*)-**83**	139° (H3-C3-C2-O)	812° (809°)[a]	3.37 Å (H3-C8)	3.65 Å (H3-C11)	2.60 Å (N4-CH_3)
(2*S*)-**32**	138° (H2-C2-C3-O)	829° (809°)[a]	3.77 Å (H2-C8)	3.98 Å (H2-C11)	3.37 Å (N1-CH_3)

[a]Sum of internal angles in parenthesis is calculated from the simple VSEPR considerations

5.3 Investigation of Enantioselective Synthesis of Quaternary (*S*)-serine -derived 1,4-benzodiazepin-2-ones through Michael Addition

1,4-Benzodiazepin-2-ones comprise the most well known class of the 1,4-benzodiazepine scaffold in medicinal chemistry. Members of this class have shown activities in diverse therapeutic areas.[36,37] We have previously discussed the synthesis of 1,4-benzodiazepin-2-ones via MOC alkylations of conformationally chiral enolates. We would like to develop a complementary approach to quaternary 1,4-benzodiazepin-2-ones that relies upon conjugate addition to an enantiopure conformationally chiral Michael acceptor (*M*)-**85** (Scheme 5.20).

Scheme 5.20 Design of 3,3-disubstituted 1,4-benzodiazepin-2-ones through conjugate addition

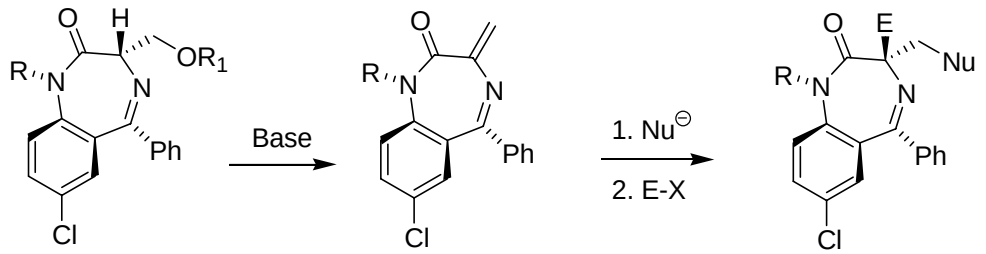

(*M*)-(*S*)-**85**
R = *i*-Pr or DAM
R_1 = Bn, TBDMS or Ts

(*M*)-**86**

(*M*)-(*S*)-**87**

The synthesis of (*R*)-O-benzyl protected serine derived 1,4-benzodiazepin-2-one ((3*R*)-**90**) was reported by Evans, *et. al* (Scheme 5.21),[38] and this compound was shown to be weak CCK antagonist.

Scheme 5.21 Synthesis of (3*R*)-**90** by Evan *et al.*

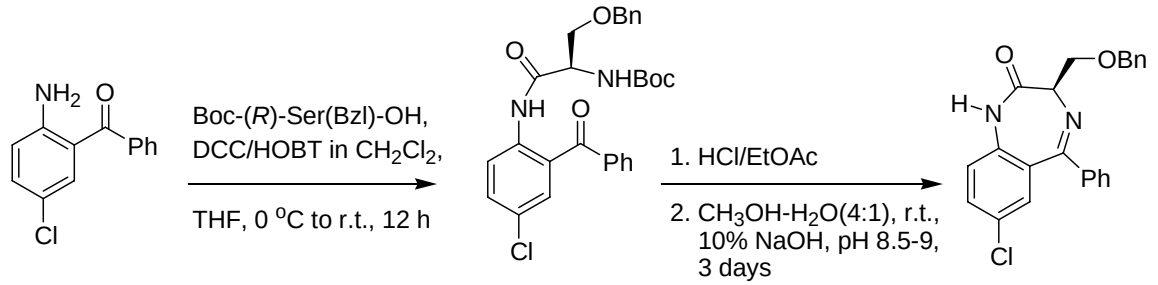

88

(*R*)-**89**

(3*R*)-**90** (78%)

Coupling of Boc-(*R*)-ser(Bzl)-OH with 5-chloro-2-aminobenzophenone (**88**) in the presence of DCC/HOBT afforded the coupling product (*R*)-**89**, which was subsequently subjected to ring closure to provide (*R*)-serine derived 1,4-benzodiazepin-2-one ((*R*)-**90**) in 78% yield. Quaternary serine-derived1,4-benzodiazepin-2-ones have been prepared in enantioenriched-form by lipase-catalyzed kinetic resolution. (Scheme 5.22).[39,40] First, a racemic mixture of serine-derived 3,3-disubstituted 1,4-benzodiazepin-2-one **94** was

prepared from deprotonation/methylation of corresponding acetate derivative **91** and subsequent reduction of **93**. Lipase (*Novozym 435*)-catalyzed acetylation and kinetic resolution afforded the corresponding diastereomers ((*M*,3*S*)-**95** and (*M*,3*R*)-**96** respectively).

Scheme 5.22 Synthetic scheme of 3,3-disubstituted 1,4-benzodiazepin-2-ones

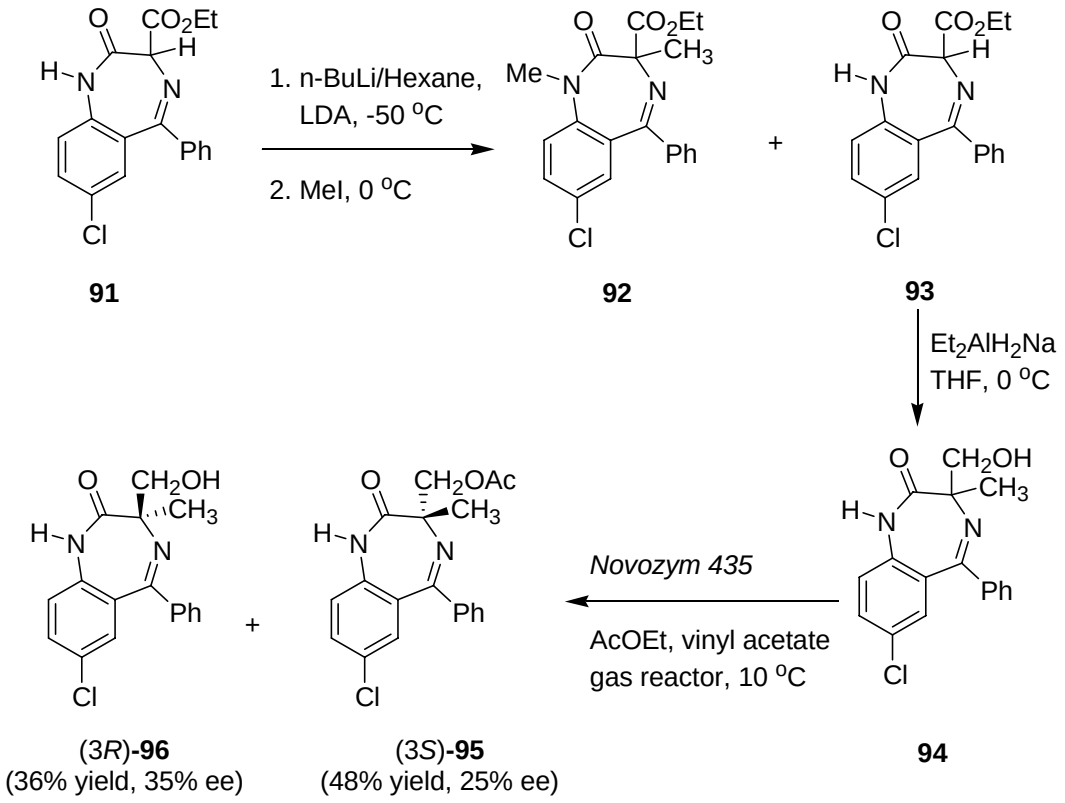

Clearly, (*S*)-serine derived 3,3-disubstituted 1,4-benzodiazepin-2-ones are unexplored territory; we are therefore also motivated to attempt deprotonation/alkylation of (*S*)-serine-derived 1,4-benzodiazepin-2-ones under conditions that do not undergo β-elimination (Scheme 5.23).

Scheme 5.23 Design of proposed MOC route to quaternary serine-derived 1,4-benzodiazepin-2-ones.

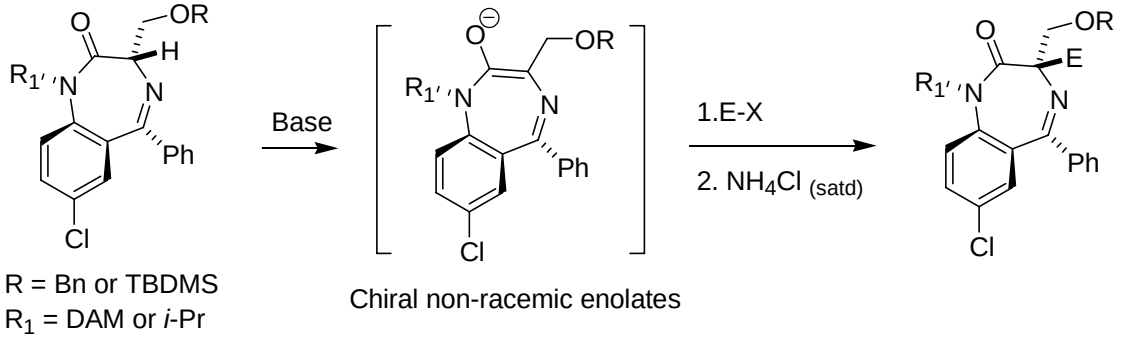

R = Bn or TBDMS
R_1 = DAM or *i*-Pr

Chiral non-racemic enolates

5.3.1 Sythesis of (*S*)-serine -derived 1,4-benzodiazepin-2-ones

The synthesis started with commercially available 2-amino-5-chlorobenzophenone (**88**): coupling with O-Bn or TBDMS[41] protected Boc-(*S*)-serine in the presence of DCC in CH_2Cl_2 afforded (*S*)-**89** and (*S*)-**90** respectively (Scheme 5.24). Subsequent Boc-deprotection by TFA in neat CH_2Cl_2 and ring closure of the heterocyclic ring at pH 7 in the presence of $NH_4Cl/NaHCO_3$ (1:1) was unsuccessful, as no desired product collected after stirring the reaction mixture at room temperature for 18-66 h. Evan *et al.* reported that ring closure of (*R*)-**88** at pH 8.5-90 with addition of 10% NaOH to yield (*R*)-O-benzyl-protected serine-derived 1,4-benzodiazepin-2-one ((3*R*)-**90**) did not cause racemization (>99% ee); so, Boc-deprotection of (*S*)-**89** and (*S*)-**97** by TFA followed by cyclization in CH_3OH-H_2O (2:1) at pH 8.5-9.0 with addition of 10% NaOH provided (3*S*)-**90** and (3*S*)-**98** in 76% and 50 % yield accordingly. HPLC analysis of (3*S*)-**90** and (3*S*)-**98** indicated 68% and 86% ee, respectively. Apparently, though basic conditions were required for the cyclization reaction, basic conditions may have also

contributed to the partial racemization of our compounds ((3*S*)-**90** and (3*S*)-**98**). Thus we postponed the development of a non-racemizing cyclization of **90** until the subsequent synthetic steps were proven successful.

Scheme 5.24 Synthetic scheme of (*S*)-serine-derived 1,4-benzodiazepin-2-ones

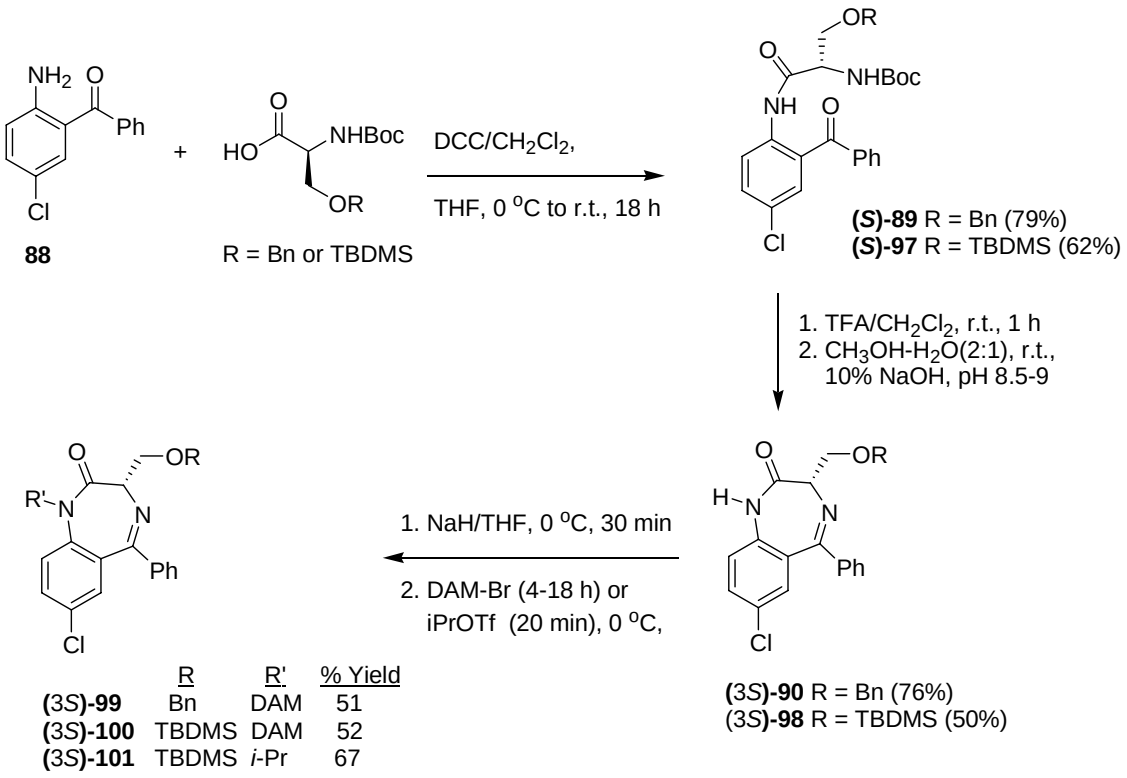

Treatment of (3*S*)-**90** and (3*S*)-**98** with DAM-Br for 4-18 h by use of NaH afforded the corresponding *N*1-DAM (3*S*)-**99** and (3*S*)-**100** in moderate yields. Treatment of (3*S*)-**98** with *i*-PrOTf[42] at 0 °C also afforded *N*1-*i*-Pr (3*S*)-**101** in good yield after 20 min.

Ring closure of (*S*)-**97** at pH 8.5-9 only provided the desired product in 50% yield. We explored other reaction conditions for the ring closure step of this compound and found that % yield of (3*S*)-**98** was improved to 60% by heating (*S*)-**97** in CH_3OH-H_2O (2:1) at pH 7 for 22 h at 40 ºC. Interestingly, HPLC analysis of the subsequent

product (3*S*)-**98** indicated >99% ee. The HPLC result suggested the importance of pH during ring closure, but it is not clear why a similar result was not obtained with benzyl protected analog **90**. A side product (3*S*)-**102** was observed due to the deprotection of TBDMS group at higher temperature (Scheme 5.25). Treatment of (*S*)-**102** with TBDMSCl in DMF in the presence of imidazole recovered (*S*)-**98** in 79% yield.

Scheme 5.25 Ring closure of (*S*)-**98** at 40 ºC.

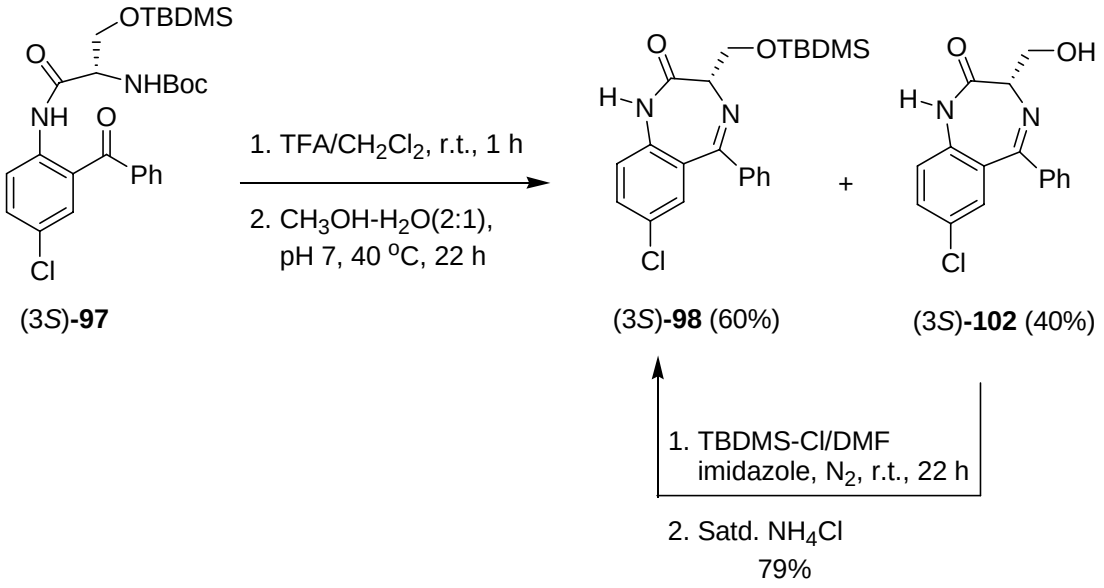

5.3.2 Attempted Synthesis of 3,3-Substituted (*S*)-serine -derived 1,4-benzodiazepin-2-ones

From our first attempted deprotonation of (3*S*)-**101**, we were surprised to see that (3*S*)-**101** underwent elimination to give **103** (Scheme 5.26) in 55% yield when KHMDS was used as base at -78 ºC. No such elimination was however observed in the deprotonation of either (3*S*)-**99** or (3*S*)-**100**, which contains *N*1-DAM group instead of

*N*1-i-Pr group. In fact, no elimination was obtained in the case of (3*S*)-**100** until the TBDMS group was converted to tosylate (Ts) group (Scheme 5.26).

Scheme 5.26 Elimination reaction of (3*S*)-**101** and (3*S*)-**102**.

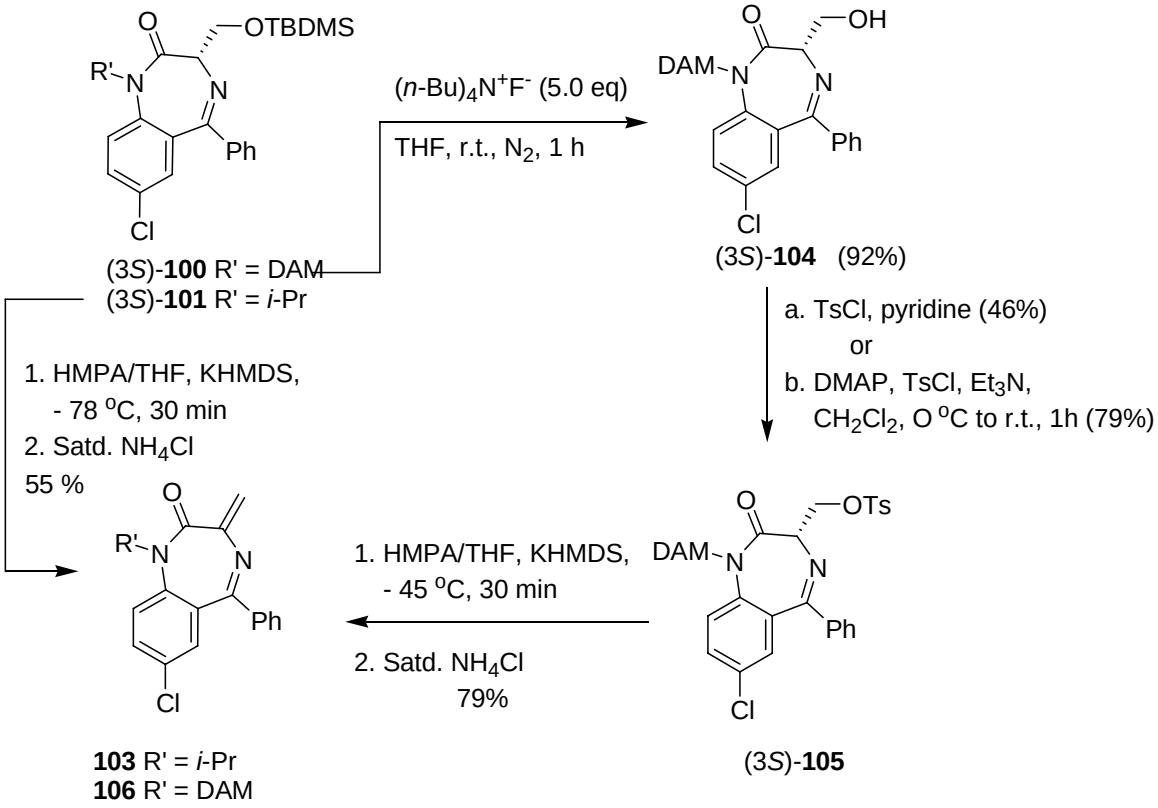

In the case of (3*S*)-**100**, the TBDMS group was converted to hydroxy group by tetrabutylammonium fluoride in THF[43] to afford (3*S*)-**104** in 92% yield. Subsequent treatment of (3*S*)-**104** with TsCl in the presence of DMAP and Et_3N in CH_2Cl_2[44] provided (3*S*)-**105** in good yield. Finally, compound (3*S*)-**105** underwent elimination in the presence of KHMDS at -45 ºC to provide α,β-unsaturated amide **106** in 79% yield. No elimination of **105** was detected at -78 ºC. In any event, as hoped, we were able to effect low temperature formation of the α-methylene benzodiazepine. Thus, it may be

possible to generate **103** and **106** in enantiopure form as intermediates for conjugate addition/alkylation (cf Scheme 5.20).

Before discussing our attempts at conjugate addition of **103** and **106**, it is worthy noting that the failure of **99** and **100** to undergo elimination with KHMDS at the temperature as high as -45 °C, which means that these substrates might be useful for deprotonation/alkylation (cf Scheme 5.23). Thus, we attempted several deprotonation/alkylation experiments at both -78 °C and -45 °C. Results are summarized in Table 5.12. To our surprise, these 1,4-benzodiazepin-2-ones were also unreactive towards the deprotonation/alkylation protocol. Most of the starting material was recovered at low reaction temperatures (-78 ºC); decomposition was observed when the temperature was raised to -45 ºC and the reaction time was extended.

Table 5.12 Attempted alkylations of (3*S*)-**99** and **100**

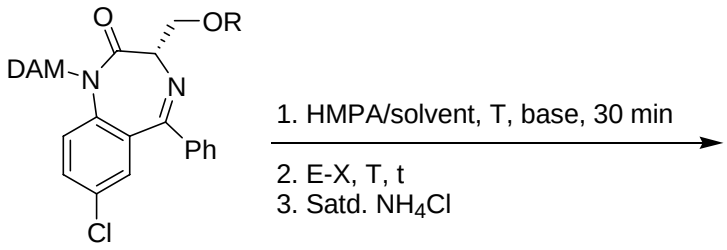

(3*S*)-**99** R = Bn
(3*S*)-**100** R = TBDMS

Entry	R	R'	Base/Solvent	T	E-X	t	Results
1	Bn	DAM	KHMDS/THF	-78 ºC	MeI	4 h	Recovered 50% **99**
2	TBDMS	DAM	KHMDS/THF	-78 ºC	MeI	21 h	Recovered 70% **100**
3	Bn	DAM	KHMDS/Et_2O	-45 ºC	MeI	10 min.	Observed mainly **99** on TLC
4	Bn	DAM	KHMDS/Et_2O	-45 ºC	BnBr	1.5 h	A mixture of **99** and decomposition products on TLC
5	TBDMS	DAM	KHMDS/THF	-45 ºC	MeI	10 min.	Recovered 70% **100**

5.3.3 Investigation of Enantioselective Synthesis of 1,4-benzodiazepin-2-ones Via Michael addition

The successful use of organometallic (organolithium[45-48] or organocuprates[49-51]) reagents in enantio- or diasteroselective conjugate additions to acyclic α,β-unsaturated amide/ketone/ester systems has been studied extensively in the literature. However, to date, there are only a few published examples of conjugate additions of organometallic

reagents to cyclic carbonyl compounds where α,β unsaturation is exocyclic.[52-54] These reactions involve 1,4-additions of either organolithium or organocuprate reagents to 2-methylenecycloalkanones, as shown in Scheme 5.27.

Scheme 5.27 Examples of 1,4-conjugate addition to 2-methylenecycloalkanones

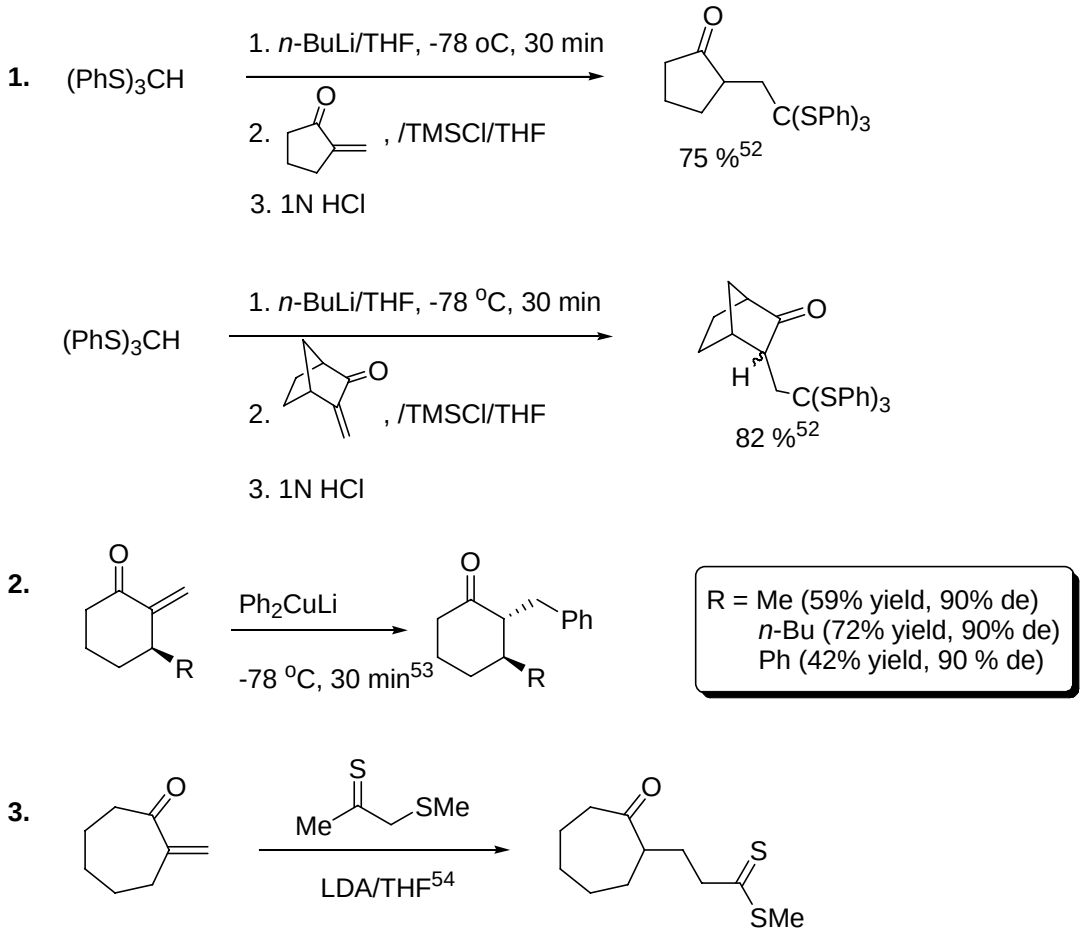

Since both compounds **103** and **106** are structurally similar to these 2-methylenecycloalkanones, we envisioned that conjugate additions of organometallic reagents to **103** and **106** would be possible. However, to date all our attempts have been unsuccessful.

Our first attempts to effect conjugate addition employed *n*-BuLi in the reaction with **106** to generate a lithium enolate at -78 °C, followed by trapping of this enolate CH_3I (Reaction 1, Scheme 5.28). To our surprise, mainly starting material **106** was observed on TLC after 2.5 h. Attempts to carry out the 1,4-conjugate additions to this α,β-unsaturated amide system in other reaction conditions[49-51] were also unsuccessful, as shown in Scheme 5.28.

Scheme 5.28 Attempted conjugate additions to compound **106**

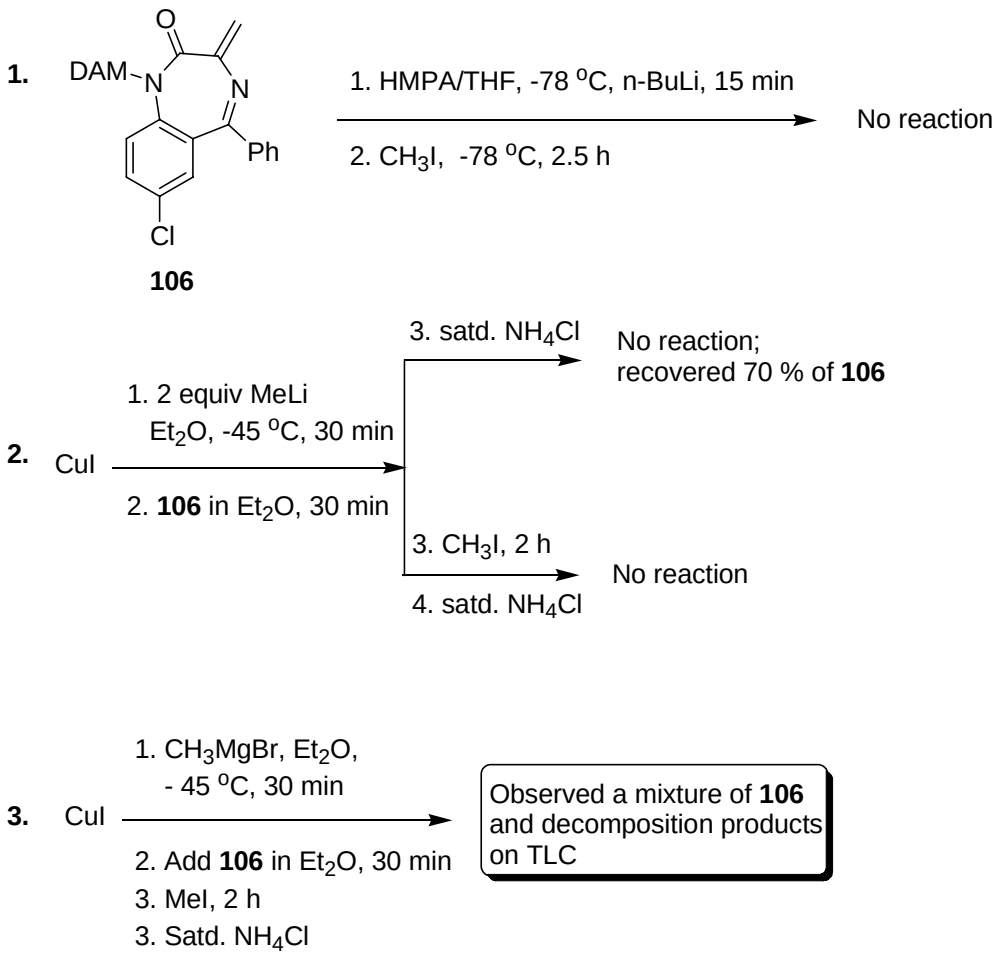

In the case of N-*i*-Pr analog **103**, we attempted alkylations under two different reaction conditions, as shown in Table 5.13. In Entry 1, organolithium/cuprate reagent was used as the nucleophile, but disappointingly, starting material **103** was recovered after the aqueous workup. At last, we attempted the conjugate reduction-alkylation of **103** (Entry 2 and 3) by use of hydrido(triphenylphosphine) copper (I) hexamer, which is also known as Stryker's reagent.[55] The common application of Stryker's reagent has been in the conjugate reduction of α,β-unsaturated carbonyl compounds.[55-57] The successful use of Stryker's reagent in tandem 1,4-reduction/alkylation reactions of α,β-unsaturated ketones has also been reported by Lipshutz *et al.*[58] Other applications of Stryker's reagent includes tandem conjugate reduction-aldol cyclization.[59,60] Despite the successful use of Stryker's reagent in other reactions, no desired product was however obtained in our case (Table 5.13, Entries 2 and 3).

Table 5.13 Attempted conjugate additions to **103**

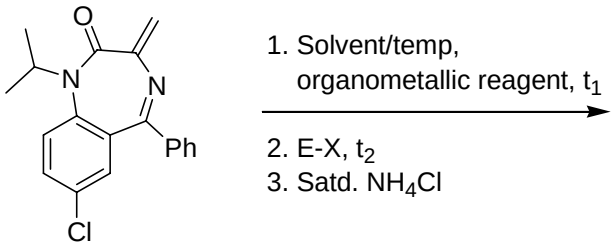

103

Entry	Solvent/temp	t_1	Organometallic reagent	E-X/t_2	Results
1	Et_2O/-78 °C	5 h	CuI/LiMe	CH_3I/1 h	Recovered **103**
2	Toluene/-45 °C	1 h	$[(Ph_3P)CuH]_6$	-	Recovered 69 % of **103**
3	Toluene/reflux	1.5 h	$[(Ph_3P)CuH]_6$	-	Recovered **103**

5.3.4 Computational Studies of 2-Methylenecycloalkanones and Heterocyclic 2-methylenecycloalkanones

In the hope of understanding the lack of reaction of **103** and **106** towards nucleophiles, we studied the structures of many α-methylene cyclic carbonyl compounds. In particular, we were interested to learn whether the reactivity towards conjugate addition could be correlated with the dihedral angle made by the C=O and C=C. Since the conjugate addition of organometallic reagents to α,β-unsaturated carbonyl system would generate an enolate as the intermediate, which means the good conjugation of the double bond with the carbonyl group should be required. We thus calculated dihedral angles (C_β=C_α-C=O) of the selected molecules at B3LYP/6-31G(d). Larger dihedral angles would suggest the poor or no overlap of the double bond with the carbonyl group during the enolate formation.Results are shown in Figure 5.5.

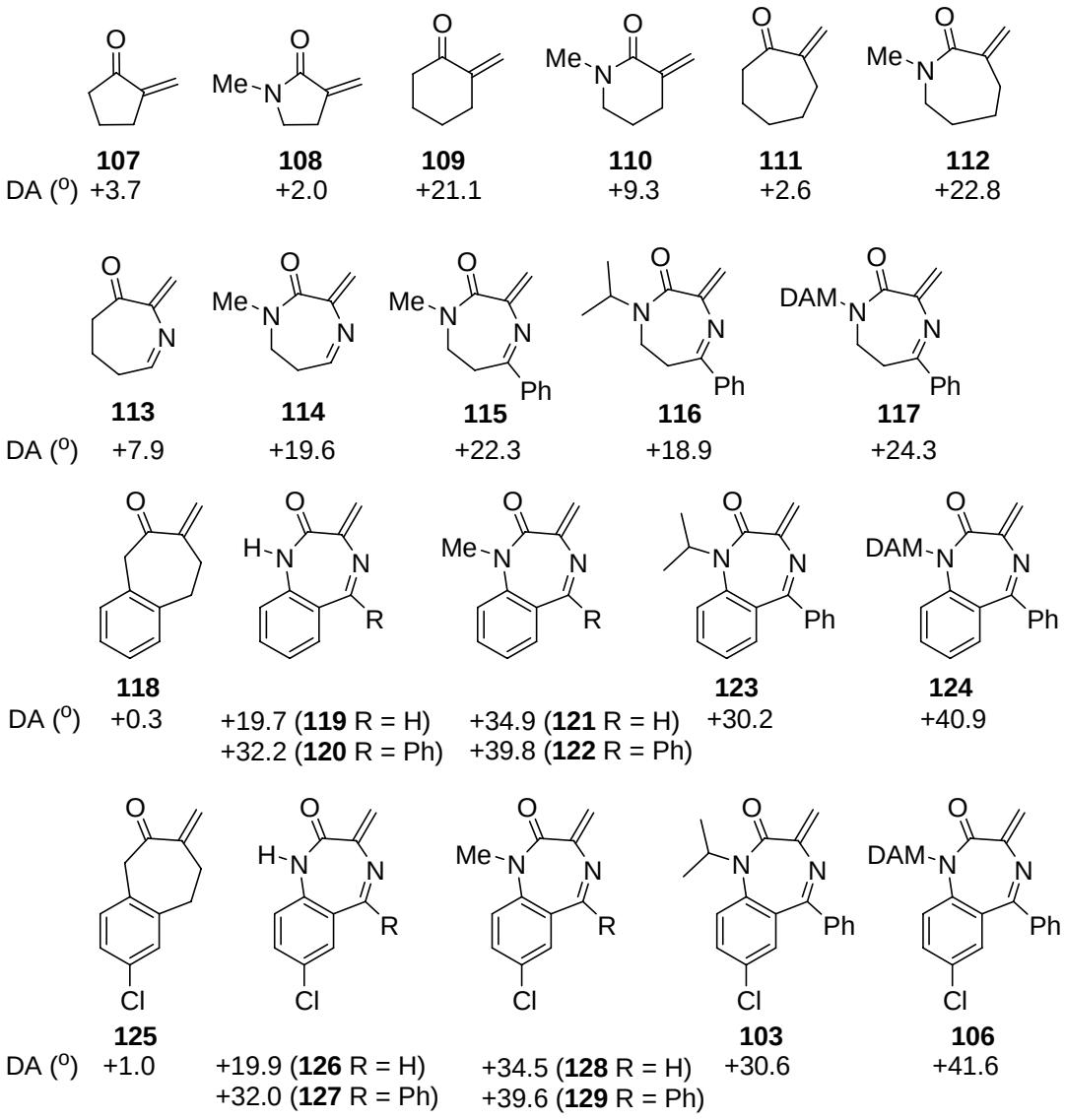

Figure 5.4 Calculated dihedral angles (C_β=C_α-C=O) of α,β-unsaturated carbonyl system of selected molecules at B3LYP/6-31G(d)

As seen in Figure 5.5, the dihedral angle is small for 5-membered ring compounds (**107** and **108**). The dihedral angle of **109** is larger possibly due to a preference for more stable chair conformation. The dihedral angles of 7-membered ring systems vary considerably, depending on the number of ring N and upon the hybridization of the ring atoms. For reference, we show the dihedral angles (Figure 5.6) for substrates that successfully underwent conjugate addition (cf Scheme 5.27). Apparently, there is a good

conjugation of the double bond with the carbonyl group during enolate formation of these compounds.

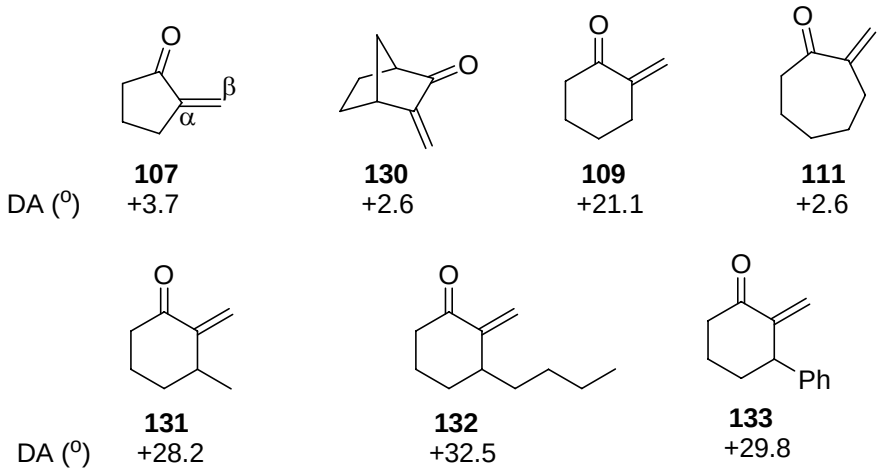

	107	**130**	**109**	**111**
DA (°)	+3.7	+2.6	+21.1	+2.6

	131	**132**	**133**
DA (°)	+28.2	+32.5	+29.8

Figure 5.5 Calculated dihedral angles(C_β=C_α-C=O) of α,β-unsaturated carbonyl system of substrates that underwent successful conjugate addition at B3LYP/6-31G(d)

From this analysis, it is not clear why **103** and **106** proved unreactive to conjugate addition, since the dihedral angles in **103** and **106** (+30.6° and +41.6°, respectively) are not greatly removed from that of **132** (32.5°). As an alternative approach to understanding conjugate addition reactivity, we calculated the shape of the LUMO of the compounds that are shown in Figures 5.5 and 5.6. In this way we would get an idea where these molecules would accept a nucleophile. Selected LUMOs are shown in Figure 5.7. Clearly, in the cases of α,β-unsaturated ketone systems such 2-methylenecyclohexanones (**109**, **131-133**) and 2-methylenecycloheptanone (**111**), the LUMO is shown to have a large orbital coefficient at the β-carbon (Figure 5.7). This result is consistent with the successful conjugate addition of organocuprate reagent to compounds **111** and **131-133**. Compound **112** is the N-Me amide analog of **111** and it should also be an effective Michael acceptor, as judged the large LUMO orbital

coefficient at the β-carbon (Figure 5.7). However, in the case of **113**, the LUMO also includes imine C=N. When both amide and imine are present on the ring, as in the case of **116**, LUMO is delocalized over the imine C=N and the 5-phenyl ring (Figure 5.7). In the case of **103**, which is the Michael acceptor we synthesized, the LUMO is very delocalized over the imine and both benzene rings (Figure 5.7), but not over the carbonyl group. As we mentioned previously, good conjugation of the double bond with the carbonyl group should be required for the conjugate addition in order to form an enolate intermediate. The highly delocalized LUMO of **103** over the imine and both benzene rings instead of the carbonyl group might suggest that the enolate formation might not be feasible for this reaction. Therefore, we suggest that this highly delocalized LUMO fails to direct nucleophiles to the β-carbon, which accounts for the low reactivity of the α-methylene benzodiazepines towards nucleophiles. One final caveat is that both the dihedral angle and the LUMO structure approaches are ground state argument. A more convincing explanation of the failed Miacheal addition reactions would require analysis of possible reaction transition structures.

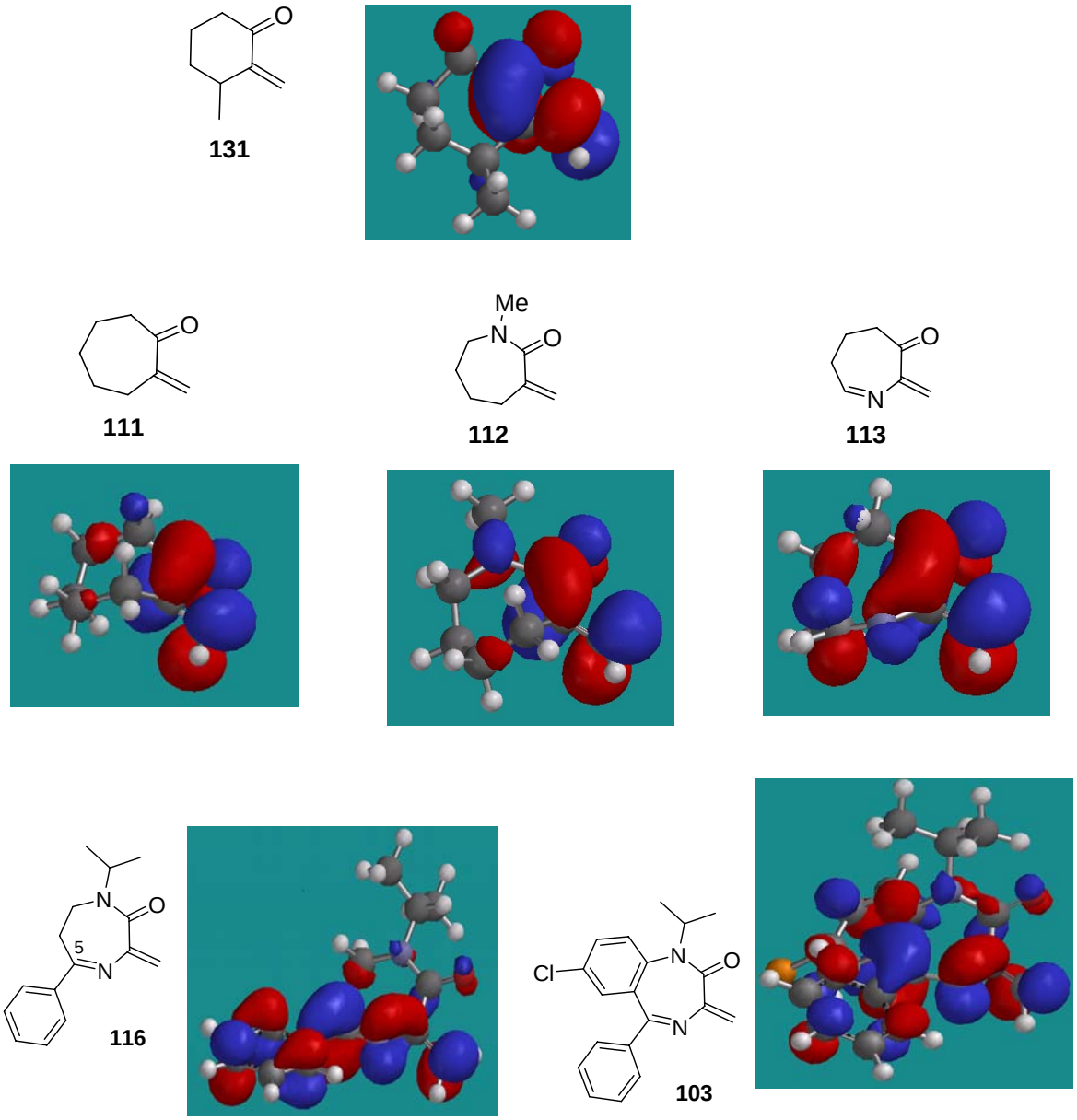

Figure 5.6 LUMOs of selected compounds arranged to the right of or below the bold-line structural drawings. LUMOs were calculatid at B3LYP/6-31-G(d)

5.4 Conclusions

In chapter 5, we improved the synthesis of three different subtypes of 1,4-benzodiazepines, including (*S*)-alanine derived tetrahydro-1,4-benzodiazepin-3-ones, (*S*)-phenylalanine derived tetrahydro-1,4-benzodiazepin-2-ones and (*S*)-serine derived 1,4-benzodiazepin-2-ones. Since the members of these subtypes possess important biological activities, the synthetic methods described here may be useful for the corresponding examples derived for other amino acids.

Our goal was to synthesize three different subtypes of quaternary 1,4-benzodiazepines by use of the MOC strategy. Disappointingly, most of the deprotonation/alkylations failed, due to various reasons. In the case (*S*)-alanine derived tetrahydro-1,4-benzodiazepin-3-ones, 2,2-disubstituted analogs were obtained when smaller electrophiles such as D_2O, MeI or EtI were used in the alkylation of the *N*1-CH_3 benzodiazepine. O-alkylation or rearrangement reaction was seen when larger electrophiles such as BnBr or *n*-PrI were used in the reaction. The same rearrangement reaction was seen in the case of *N*1-*i*-Pr tetrahydro-1,4-benzodiazepine-3-one. The failure of these reactions was probably due to the steric hindrance of enolate alkylation.

The reason for our failure to achieve deprotonation/alkylation of tetrahydro-1,4-benzodiazepin-2-ones are much less clear. Computational studies suggest that steric hindrance by both benzo ring and N4-allyl group might retard deprotonation at C3 by bulky bases like KHMDS or LDA.

Finally, (*S*)-serine derived 1,4-benzodiazepin-2-ones and their elimination products were prepared. These proved unreactive towards deprotonation/alkylations and conjugate additions respectively. The low reactivity of the α-methylene benzodiazepines

towards nucleophiles was attributed to highly delocalized LUMOs. In the ground state, the LUMOs of these compounds were delocalized over the imine and both benzene rings, but not the carbonyl group. These LUMOs would then fail to direct nucleophiles to the β-carbons due to the lack of overlap between the carbonyl carbon and the α methylene carbon in the LUMOs.

References for chapter 5

1 Clement, E. C.; Carlier, P. R. A Simple route to tetrahydro-1,4-benzodiazepin-3-ones bearing diverse N1, N4, and C10 functionalization. *Tetrahedron Lett.* **2005,** *46,* 3633-3635.

2 Miller, W. H.; Ku, T. W.; Ali, F. E.; Bondinell, W. E.; Calvo, R. R.; Davis, L. D.; Erhard, K. F.; Hall, L. B.; Huffman, W. F.; Keenan, R. M.; Kwon, C.; Newlander, K. A.; Ross, S. T.; Samanen, J. M.; Takata, D. T.; Yuan, C.-K. Enantiospecific Synthesis of SB 214857, a Potent, Orally Active Nonspecific Fibrinogen Receptor Antagonist. *Tetrahedron Lett.* **1995**, *36*, 9433.

3 Sveinbjornsson, A.; Vander Werf C. A. Synthesis of 2-Diethylaminoethyl-4-(7-chloro-4-quinolyl)-aminofluorobenzene Dihydrobromide. *J. Am. Chem. Soc.* **1951,** *73,* 1378.

4 Samanen, J. M.; Ali, F. E.; Barton, L. S.; Bondinell, W. E.; Burgess, J. L.; Callahan, J. F.; Calvo, R. R.; Chen, W.; Chen, L.; Erhard, K.; Feuerstein, G.; Heys, R.; Hwang, S.-M.; Jakas, D. R.; Keenan, R. M.; Ku, T. W.; Kwon, C.; Newlander, K. A.; Nichols, A.; Parker, M.; Peishoff, C. E.; Rhodes, G.; Ross. S.; Shu, A.; Simpson, R.; Takata, D.; Yellin, T. O.; Uzsinskas, I.; Venslavsky, J. W.; Yuan, C.-K,; Huffman, W. F. Potent, Selective Orally Active 3-Oxo-1,4-benzodiazepine GPIIb/IIIa Integrin Antagonists. *J. Med. Chem*. **1996**, *39*, 4867-4870.

5 Keenan, R. M.; Callahan, J. F.; Samanen, J. M.; Bondinell, W. E.; Calvo, R. R.; DeBrosse, C.; Eggleston, D. S.; Haltiwanger, R. C.; Hwang, S.-M.; Jakas, D. R.; Ku, T. W.; Miller, W. H.; Newlander, K. A.; Nichols, A.; Parker, M. F.; Southhall, L. S.; Uzinskas, I.; Vasko-Moser, J. A.; Venslavsky, J. W.; Wong, A. S.; Huffman, W. F. Conformational Preferences in a Benzodiazepine Series of Potent Nonpeptide Fibrinogen Receptor Antagonists. *J. Med. Chem.* **1999,** *42,* 545-559.

6 Rosenström, U.; Sköld, C.; Lindeberg, G.; Botros, M.; Nyberg, F.; Karlén, A.; Halberg, A Selective AT2 Receptor Ligand with a γ-Turn-Like Mimetic Replacing the Amino Acid Residues 4-5 of Angiotensin II. *J. Med. Chem.* **2004,** *47,* 859.

7 Schutkowski, M.; Mrestani-Klaus, C.; Neubert, K. Synthesis of dipeptide 4-nitroanilides containing non-proteinogenic amino acids. *Int. J. Pept. Protein Res.* **1995,** *45,* 257-265.

8 Ohfune, Y.; Kurokawa, N.; Higuchi, N.; Saito. M.; Hashimoto, M.; Tanaka, T. An efficient one-step reductive *N*-monoalkylation of α-amino acids. *Chem. Lett.* **1984,** 441-444.

9 Takeda, K.; Akiyama, A.; Nakamura, H.; Takizama, S. -I.; Mizuno, Y.; Takayanagi, H.; Harigaya, Y. Dicarbonates: Convenient 4-Dimethylaminopyridine Catalyzed Esterification Reagents. *Synthesis,* **1994,** 1063.

10 Petersen, L.; Jensen, K. J. A New, Efficient Glycosylation Method for Oligosaccharide Synthesis under Neutral Conditions: Preparation and Use of New DISAL Donors. *J. Org. Chem.* **2001,** *66,* 6268-6275.

11 Carlier, P. R.; Zhao, H.-W.; DeGuzman, J.; Lam, P. C.-H. Enantioselective Sythesis of "Quaternary" 1,4-Benzodiazepin-2-one Scaffolds via Memory of Chirality. *J. Am. Chem. Soc***. 2003,** *125,* 11482-11483.

12 Russell, G.; Janzen, E. G.; Strom, E. T. Electron-Transfer Process. I. The Scope of the Reaction between Carbanions or Nitrations and Unsaturated Electron Acceptors. *J. Am. Chem. Soc.* **1964**, *86,* 1807-1814.

13 Zhao, P.; Condo, A.; Keresztes, I.; Collum, D. B. Reactions of Ketones with Lithium Hexamethyldisilazide: Competitive Enolizations and 1,2-Additions. *J. Am. Chem. Soc.* **2004,** *126,* 3113-3118.

14 Wissner, A.; Overbeek, E.; Reich, M. F.; Floyd, M. B.; Johnson, B. D.; Mamuya, N.; Rosfjord, E. C.; Discafani, C.; Shi, X.-Q.; Rabindran, S. K.; Gruber, B. C.; Ye, F.; Hallett, W. A.; Nilakantan, R.; Shen, R.; Wang, Y.-F.; Greenberger, L. M.; Tsou, H.-R. Synthesis and Structure-Activity Relationship of 6,7-Disubstituted 4-Anilinoquinoline-3carbonitriles. The design of an Orally Active, Irreversible Inhibitor of the Tyrosine Kinase Activity of the Epidermal Growth Factor Receptor (EGFR) and the Human Epidermal Growth Factor Receptor-2 (HER-2) *J. Med. Chem*. **2003**, *46*, 49-63.

15 Giumanini, A. G.; Chiavari, G.; Gusiani, M. M.; Rossi, P. *N*-Permethylation of Primary and Secondary Aromatic Amines. *Synthesis*, **1980**, 743-746.

16 Perry, C. J.; Parveen, Z. The cyclisation of substituted phthalanilic acids in acetic acid solution. A kinetic study of substituted N-phenylphthalimide formation. *J. Chem. Soc., Perkin Trans*. **2001**, *2*, 512-521.

17 GC-MS was performed by Dr. Emre Isin from Castagnoli' group.

18 Wassmundt, F. M.; Kiesman, W. F. Efficient Catalytic of Hydrodediazoniations in Dimethylformamide. *J. Org. Chem.* **1995,** *60,* 1713-1719.

19 Lubell, W.; Rapoport, H. Surrogates for Chiral Aminomalondialdehyde. Synthesis of *N*-(9-Phenylfluoren-9-yl) and *N*-(9-Phenylfluoren-9-yl)vinylglycianl. *J. Org. Chem.* **1989,** *54,* 3824-3831.

20 Fryer, R. I.; Earley, J. V.; Sternbach, L. H.Quinazolines and 1,4-Benzodiazepines. XLIV.1a The Formation of Isoindoles by the Ring Contraction of 1-Alkyl-1,4-benzodiazepines 1b. *J. Org. Chem.* **1969,** *34,* 649-654.

21 Garro-Helion, F.; Merzouk, A.; Guibe, F. Mild and Selective Palladium (0)-Catalyzed Deallylation of Allylic Amine. Allylamine and Diallylamines as Very Convenient Ammonia Equivalents for the Synthesis of Primary Amines. *J. Org. Chem.* **1993,** *58,* 6109-6113.

22 Koch, T.; Hesse, M. Synthesis of Macrocyclic *N*-Unsubstituted Imides. *Synthesis,* **1992,** 931.

23 Doi, H.; Sakai,T.; Yamada, K.-i.; Tomioka, K. *N*-Allyl- *N*-*tert*-butyldimethylsilylamine for chiral ligand-controlled asymmetric conjugate addition to *tert*-butyl alkenoates. *Chem. Commun*. **2004,** 1850.

24 Hu, Y.-J.; Dominique, R.; Das, S. K.; Roy, R. A facile new procedure for the deprotection of allyl ethers under mild conditions. *Can. J. Chem.* **2000,** *78,* 838.

25 Kitov, P. I.; Bundle, D. R. Mild Oxidative One-Pot Allyl Group Cleavage. *Org. Lett.* **2001,** *3,* 2835-2838.

26 Geometry optimization calculations were conducted using PC Spartan 3.0.

27 Lam, P. C.-H.; Carlier, P. R. Experimental and Computational Studies of Ring Inversion of 1,4-Benzodiazepin-2-ones: Implications for Memory of Chirality Transformation. *J. Org. Chem.* **2005***, 70,* 1530-1538.

28 The sum of internal angles in the benzodiazepine ring was calculated based on the standard bond angles for sp2 (120°) and sp3 (109.5°).

29 The sum of internal angles of a polygon is (180n-360°), where n is the number sides of the polygon.

30 Breslin, H. J.; Kukla, M. J.; Kromis, T.; Cullis, H.; Knaep, F. D.; Pauwels, R.; Andries, K.; Clercq, E. D.; Janssen, M. A. C.; Janssen, P. A. J. Synthesis and Anti-HIV Activity of 1,3,4,5-Tetrahydro-2*H*-1,4—benzodiazepine-2-one (TBO) Derivatives. Truncated 4,5,6,7-Tetrahydro-5-methylimidazolo[4,5,1-*jk*][1,4]benzodiazepin-2-(1*H*)-ones (TIBO) Analogues. *Bioorg. Med. Chem.* **1999,** *7,* 2427-2436.

31 Wu. Z.; Ercole, F.; FitzGerald, M.; Perera, S.; Riley, P.; Campbell, R.; Pham, Y.; Rea, P.; Sandanayake, S.; Mathieu, M. N.; Bray, A. M.; Ede, N. J. Synthesis of Tetrahydro-1,4-benzodiazepin-2-ones on Hydrophilic Polyamide SynPhase Lanterns *J. Com. Chem.* **2003***, 5,* 166-171.

32 Herrero, M. T.; Tellitu, I.; Dominguez, E.; Moreno, I.; SanMartin, R. A novel and efficient iodine (III)-mediated access to 1,4-benzodiazepin-2ones *Tetrahedron Lett.* **2002***, 43,* 8273.

33 Cheguillaume, A.; Salaün, A.; Sinbandhit, S.; Potel, M.; Gall, P.; Gaudy-Floćh, M.; Le Grel, P. Solution synthesis and characterization of aza-beta(3)-peptides (N(alpha)-substituted hydrazino acetic acid oligomers). *J. Org. Chem.* **2001,** *66,* 4923-4929.

34 Sekine, M.; Iwase, R.; Masuda, N.; Tsujiaki, H. Synthesis of Oligogibonucleotides by Use of 4,4',4''-Tris(acyloxy)trityl Groups for Protection of the 6-Amino Group of Adenosine. *Bull. Chem. Soc. Jpn,* **1988,** *61,* 1669-1677.

35 Behnam, S. M.; Behnam, S. E.; Ando, K.; Green, N. S.; Houk, K. N. Stereoelectronic, Torsional, and Steric Effect on Rates of Enolation of Ketones. *J. Org. Chem.* **2000,** *65,* 8970-8978.

36 Ellman, J. A. Design, Synthesis, and Evaluation of Small-Molecule Libraries. *Acc. Chem. Res.* **1996,** *29,* 132-143.

37 Boojamra, C. G.; Burow, K. M.; Thomson, L. A.; Ellman, J. A. Solid-Phase Synthesis of 1,4-benzodiazepine-2,5-diones. Library Preparation and Demonstration of Synthesis Generally. *J. Org. Chem.* **1997,** *62,* 1240-1256.

38 Evans, B. E.; Rittle, K. E.; Bock, M. G.; DiPardo, R. M.; Freidinger, R. M.; Whitter, W. L.; Could, N. P.; Lundell, G. F.; Homnick, C. F.; Veber, D. F.; Anderson, P. S.; Chang, R. S. L.; Lotti, V. J.; Cerino, D. J.; Chen, T. B.; King, P. J.; Kunkel, K. A.; Springer, J. P.; Hirschfield, J. Design of Nonpeptidal Ligands for a Peptide Receptor: Cholecystokinin Antagonists. *J. Med. Chem.* **1987,** *30,* 1229-1239.

39 Avdagić, A.; Lesac, A.; Majer, Z.; Hollòsi, M.; Šunjić, V. Lipase-Catalyzed Acetylation of 3-Substituted 2,3-Dihydro-1*H*-1,4-benzodiazepin-2-ones: Effect of Temperature and Conformation on Enantioselectivity and Configuration. *Helv. Chim, Acta* **1998,** *81,* 1567-1582.

40 Avdagić, A.; Šunjić, V. Biocatalytic Deracemization of 1,4-Benzodiazepines in the synthesis of Enantiomerically Pure Serine. *Helv. Chim, Acta* **1998,** *81,* 85-93.

41 Boc-O-TBDMS-(*S*)-serine was synthesized from Boc-(*S*)-serine based on the literature method (92% yield, lit. 85%). Yoo, D.-W.; Oh, J. S.; Lee, D. –W.; Kim, Y.-G. Efficient Synthesis of a Configurationally Stable L-Serinal Derivatives. *J. Org. Chem***. 2003,** *68,* 2979-2982.

42 Isopropyl triflate was prepared from isopropyl alcohol and triflate anhydride in pyridine/CH_2Cl_2 at 0 ºC immediately prior to the alkylation. The synthesis of *i*PrOTf was developed by Dr. Hongwu Zhao.

43 Scheidt, K. A.; Chen, H.; Fellows, B. C.; Chemler, S. R.; Coffey, D. S.; Roush, W. R. Tris(dimethylamino)sulfonium Difluorotrimethylsilicate (TAS-F), a Mild Reagent fro the Removal of Silicon Protecting Groups. *J. Org. Chem.* **1998,** *63,* 6436.

44 Langenhan, J. M.; Gellman, S. H. Preparation of Protected syn-α,β-Dialkyl-β-Amino Acids That Contain Polar Side Chain Functionality. *J. Org. Chem.* **2003***, 68,* 6440-6443.

45 Etxebarria, J.; Vicario, J. L.; Badia, D.; Carrillo, L. Asymmetric Synthesis of β-Amino Esters by Aza-Michael Reactions of α,β-Unsaturated Amides Using (*S*,*S*)-(+)-Pseudoephedrine as Chiral Auxiliary. *J. Org. Chem.* **2004,** *69,* 2588-2590.

46 Kanernasa, S.; Nomura, M.; Yoshinaga, S.; Yamamoto, H. High Enantiocontrol of Michael Additions by Use of 2,2-Dimethyloxazolidine Chiral Auxiliaries. Exclusively *ul*, *lk*-1,4-Inductive Michael Additions of the Lithium (*Z*)-Enolates of (*S*)-4-Benzyl-2,2,5,5-tetramethyl-3-propanoyl oxazolidine to α,β-Unsaturated Ester. *Tetrahedron* **1995,** *51,* 10463-10476.

47 Oare, D. A.; Henderson, M. A.; Sanner, M. A.; Heathcock, C. H. Stereochemistry of the Michael Additions of N,N-Disubstituted Amide and Thioamide Enolates to α,β-Unsaturated Ketones. *J. Org. Chem.* **1990,** *55,* 132-157.

48 Evans, D. A.; Ennis, M. D.; Le. T. *J. Am .Chem. Soc.* **1984,** *106,* 1154.

49 Dambacher, J.; Anness, R.; Pollock, P.; Bergdahl, M. Highly diastereoselective conjugate additions of monoorganocopper reagents to a chiral imides. *Tetrahedron* **2004,** *60,* 2097-2110.

50 Arai, Y.; Ueda, K.; Xie, J.; Masaki, Y. 1,6-Asymmetric Induction During the Conjugate Addition of Arylcopper Reagents to a Chiral Sulfinyl-Substituted Pyrrolyl-α,β-Unsaturated Amides. *Chem. Pharm. Bull.* **2001,** *49,* 1609-1614.

51 Kanemasa, S.; Suenaga, H.; Onimura, K. Effective Enantiocontrol in Conjugate Additions of Organocuprates. Highly Selective 1,5-Chiral Induction in the Conjugate Additions of Cuprates to -α,β-Unsaturated Amide Derivatives of 2,2-Dimethyloxazolidine Chiral Auxilliaries. *J. Org. Chem.* **1994,** *59,* 6949-6954.

52 Liu, H.; Cohen, T. Yield and Selectivity Enhancement by Trimethylsilyl Chloride in the Conjugate Addition of Stabilized Organolithiums. *Tetrahedron Lett.* **1995,** *36,* 8925-8928.

53 Tamura, R.; Watabe, K.-I.; Katayama, H.; Suzuki, H.; Yamamoto, Y. Asymmetric Synthesis of 3-Substituted 2-*exo*-Methylenecyclohexanones via 1,5-Diastereoselection by Using a Chiral Amine. *J. Org. Chem.* **1990,** *55,* 408-410.

54 Berrada, S.; Metzner, P.; Rakotonirina, R. 1,4-Addition of lithium thioenolates of dithio esters to ethylenic ketones. *Bull de la Soc Chim de Fr.* **1985,** *5,* 881-890.

55 Mahoney, W. S.; Brestensky, D. M.; Stryker, J. M. S. Selective hydride-mediated conjugate reduction of α,β-unsaturated carbonyl compounds using $[(Ph_3P)CuH]_6$. *J. Am.Chem. Soc.* **1988,** *110,* 291-293.

56 Brestensky, D. M.; Stryker, J. M. S. Regioselective conjugate reduction and reductive silylation of α,β-unsaturated aldehydes using copper(I) hydride complex $[(Ph_3P)CuH]_6$. *Tetrahedron Lett.* **1989,** 5677-5780.

57 Koenig, T. M.; Daeuble, J. F.; Brestensky, D. M.; Stryker, J. M. S. Conjugate reduction of polyfunctional α,β-unsaturated carbonyl compounds using $[(Ph_3P)CuH]_6$. Compatibility with halogen, sulfonate, and γ-oxygen and sulfur substituents. *Tetrahedron Lett.* **1990,** *31,* 3237-3240.

58 Lipshutz, B. H.; Chrisman, W.; Noson, K.; Papa, P.; Sclafani, J. A.; Vivian, R. W., Keith, J. M. Copper hydride-catalyzed tandem 1,4-reduction/alkylation reactions. *Tetrahedron* **2000,** *56,* 2779-2788.

59 Chiu, P.; Szeto, C.-P.; Geng, Z.; Cheng, K.-F.Tandem Conjugate Reduction-Aldol Cyclization Using Stryker's Reagent. *Organic Lett.* **2001,** *3,*1901-1903.

60 Chiu, P.; Szeto, C.-P.; Geng, Z.; Cheng, K.-F. Application of the tandem Stryker reduction-aldol cyclization strategy to the asymmetric synthesis of lucinone. *Tetrahedron Lett.* **2001,** *42,* 4091-4093.

Chapter 6 Experimental Section of 1,4-Benzodiazepine Analogs

6.1 General Methods

^{1}H and ^{13}C NMR spectra were recorded on a INOVA 400 MHz spectrometer. All chemical shifts are expressed in ppm and the coupling constants in Hertz. Stardards for chemical shifts are as follows:

Nuclei	Standard	Chemical Shifts (ppm)
^{1}H	TMS	0
	$CDCl_3$	7.26
	CD_3OD	3.3
	DMSO-d_6	2.5
	D_2O	4.8
^{13}C	$CDCl_3$	77
	CD_3OD	49.5
	DMSO-d_6	39.5

Positive ion high resolution FAB+ mass spectra were collected on a JEOL HX110 dual focusing mass spectrometer using a direct inlet with 3-nitrobenzyl alcohol as the sample matrix.

Analytical thin-layer chromatography (TLC) was performed with aluminum sheets coated with RDH silica gel 60 F254. Flash column chromatography was performed using VWR silica gel 60 (60-240 mesh). High-performance liquid chromatography (HPLC) analysis was performed on a CHIRALPAK AD column (4.6 x

250 mm), detection at 254 nM, flow rate 1.0 mL/min unless specified with isocratic solvent system; elution program: *i*-PrOH:Hexane (Table 6.1).

Table 6.1 HPLC data of chiral (*S*)-Alanine-derived tetrahydro-1,4-benzodiazepin-3-ones

Compounds	R_T[a] of (*S*)-enantiomer	Racemic mixture		Elution *i*PrOH:Hexane	Flow rate (min/mL)
		R_T[a] of (*S*)-enantiomer	R_T[a] of (*R*)-enantiomer		
9	15.52 min	12.08 min	15.63 min	20:80	1.0
10	13.02 min	13.10 min	15.06 min	15:85	1.0
11	26.16 min	26.01 min	29.61 min	1:99	2.0
29	9.56 min	9.53 min	11.06 min	5:95	1.0
30	13.31 min	13.36 min	16.62 min	20:80	1.0
32	12.16 min	12.16 min	13.29 min	3:97	1.0
33	11.24 min	11.14 min	12.92 min	2:98	1.0
56[b]	16.96 min	17.02 min	23.19 min	20:80	1.0

[a]R_T = Retention time
[b]Compound **56** exists as a mixture of pseudoequatorial (*P*)- and pseudoaxial (*M*)- conformers on the HPLC time scale and (*P*, *S*) is the major conformer.

6.2 Procedures

6.2.1 (*S*)-Alanine-derived tetrahydro-1,4-benzodiazepin-3-one project

Both 2-fluoro-5-nitrotoluene and Boc-(*S*)-Ala-OH were purchased from ACROS, and used without purification. Boc-(*S*)-*N*- Me-Ala-OH was prepared from Boc-(*S*)-Ala-OH and MeI according to the literature method.[1] (*S*)-*N*-*i*-Pr-Ala-OH was synthesized from Boc-(*S*)-Ala-OH and acetone based on modified literature method.[2]

Synthesis of 2-Fluoro-5-nitrobenzyl bromide (2)

2-Fluoro-5-nitrotoluene (**1**) (2.74 g, 17.7 mmol) and NBS (3.14 g, 17.7 mmol) were combined in CCl_4 (35 mL). The yellow suspension was irradiated under a Hg lamp for 19 hours. The white solid was filtered and washed with CCl_4 (10 mL). The volatiles were removed under reduced pressure to afford yellow liquid residue, which was then mixed with EtOH/i-PrOH (20 mL, 95/5). The clear yellow solution was placed in the freezer for overnight. Off-white, long needle-like crystals were obtained as desired product (2.75 g, 66% yield) by filtration. ^{1}H NMR ($CDCl_3$): δ 4. 53 (s, 1H), 7.25 (t, J = 8.8 Hz, 1H), 8.21-8.25 (m, 1H), 8.36 (dd, J = 2.4, 8.4 Hz, 1H); ^{13}C NMR ($CDCl_3$): δ 23.55, 23.58, 116.79, 117.03, 126.07, 126.18, 127.06, 127.12, 162.65, 165.25; HRMS (FAB^-): calcd for $C_7H_5BrFNO_2$ $[M]^-$ 232.9488, found 232.9560.

Synthesis of *N*-Allyl-2-fluoro-5-nitrobenzylamine (3)

To a stirring solution of allylamine (682 μL, 8.98 mmol) in THF (6 mL) at 0°C was added **2** (1.05 g, 4.49 mmol) in THF (10 mL) dropwise. The ice-bath was removed, and the reaction mixture was stirred at room temperature for 3 hours. The reaction mixture was then partitioned between CH_2Cl_2 (2 x 40 mL) and 10% NaOH (40 mL). The combined organic layers were dried over Na_2SO_4, filtered and evaporated to dryness. The crude greenish yellow residue was purified by flash column chromatography on silica gel, eluting with CH_2Cl_2-CH_3OH (98/2) to afford the desired product as yellowish green oil (822.3 mg, 87%). ^{1}H NMR ($CDCl_3$): δ 3.36 (ddd, J = 1.2, 3.2, 6 Hz, 2 H), 3.97 (s, 2H), 5.19-5.31 (m, 2H), 5.93-6.03 (m, 1H), 7.24, (t, J = 9 Hz, 1H), 8.20-8.24 (m, 1H), 8.42 (dd, J = 3.0, 6.2 Hz, 1H); ^{13}C NMR ($CDCl_3$): δ 46.66, 45.68, 51.69, 116.04, 116.28,

116.61, 124.44, 124.55, 126.02, 129.29, 129.47, 136.11, 144.32, 163.18, 165.73; HRMS (FAB): calcd for $C_{10}H_{12}FN_2O_2$ $[M+1]^+$ 211.0877, found 211.0896 (+6.2 ppm/+1.3 mmu).

General procedures for the coupling reactions: (S)-6 to (S)-8[3]

To a stirring solution of **3** (1.0 equiv), DCC (1.2 equiv) and HOBT (1.2 equiv) in CH_2Cl_2 (0.1 M) at 0°C was added (*S*)-alanine (1.2 equiv). The ice-bath was removed and the greenish yellow suspension was stirred at room temperature for 12 hours. The white precipitate was filtered off and washed with cold CH_2Cl_2 (10 mL). The filtrate was evaporated under reduced pressure to provide greenish yellow oil residue, which was purified by flash column chromatography (EtOAc-CH_2Cl_2 2/8) on silica gel.

Synthesis of (*S*)-N_α-Boc, *N*-allyl-*N*-(2-fluoro-5-nitrobenzyl)alaninamide (*S*-6)

Compound **3** (182 mg, 0.87 mmol) and Boc-(*S*)-Ala-OH (80.4 mg, 0.43 mmol) were combined as describe above. The title compound was obtained as green oil (141.3 mg, 86%). ^{1}H NMR ($CDCl_3$): δ 1.36 (d, *J* = 6.4 Hz, 3 H), 1.40 (s, 1 H), 1.44 (s, 8 H), 2.78 (s, 3 H), 3.90-4.00 (m, 1 H), 4.09-4.18 (m, 1 H), 4.63-4.71 (m, 3 H), 5.09-5.33 (m, 3 H), 5.78-5.87 (m, 1 H), 7.19 (t, *J* = 9.2 Hz, 1 H), 8.11-8.21 (m, 2 H); ^{13}C NMR ($CDCl_3$): δ 14.14, 19.22, 28.20, 28.26, 42.53, 42.57, 43.94, 46.18, 48.28, 50.30, 79.80, 116.18, 116.43, 118.23, 124.31, 124.88, 124.98, 125.55, 125.62, 126.12, 126.29, 131.78, 132.09, 144.52, 155.13, 162.89, 165.46, 174.09.

Synthesis of (*S*)-N_α-Boc-N_α-methyl- *N*-allyl-*N*-(2-fluoro-5-nitrobenzyl)alaninamide (*S*-7)

Compound **3** (518 mg, 2.47 mmol) and Boc-(*S*)-*N*-Me-Ala-OH (652 mg, 3.21 mmol) were combined as describe above. The title compound was obtained as green oil (732 mg, 75%). ^{1}H NMR ($CDCl_3$): δ 1.26 (s, 2 H), 1.29 (d, *J* = 7.6 Hz, 3 H), 1.45 (s, 7 H), 2.78 (s, 3 H), 3.77-4.21 (m, 2 H), 4.42-4.49 (m, 1 H), 4.67-4.92 (m, 2 H), 5.15-5.27 (m, 2 H), 5.70-5.79 (m, 1 H), 7.17 (t, *J* = 9.0 Hz, 1 H), 7.99-8.16 (m, 2 H); ^{13}C NMR ($CDCl_3$): δ 14.70, 28.04, 28.29, 28.94, 29.18, 42.47, 43.59, 48.17, 49.83, 49.95, 50.20, 51.8, 80.23, 80.34, 116.15, 116.40, 116.52, 116.75, 117.55, 118.11, 123.99, 124.69, 124.80, 124.91, 125.13, 125.20, 126.06, 126.53, 131.97, 132.26, 132.72, 144.42, 155.41, 162.88, 165.44, 172.37; HRMS (FAB): calcd for $C_{19}H_{27}FN_3O_5$ M+1]$^+$ 396.1935, found 396.1945 (+2.6 ppm/+1.0 mmu). $[\alpha]^{22}_D$ (*S*-**7**) = - 99.9° (*c* 0.020, $CHCl_3$).

Synthesis of (*S*)-N_α-isopropyl-*N*-allyl-*N*-(2-fluoro-5-nitrobenzyl)alaninamide (*S*-8)

Compound **3** (531 mg, 2.53 mmol) and (*S*)-*N*-*i*-Pr-Ala-OH (398 mg, 3.04 mmol) were combined as describe above. The title compound was obtained as yellow oil (556 mg, 68%). ^{1}H NMR ($CDCl_3$): δ 0.99 (d, *J* = 6.4 Hz, 3H), 1.05 (d, *J* = 6.4 Hz, 3 H), 1.27 (d, *J* = 6.8 Hz, 3 H), 2.67 (7-let, *J* = 7.2 Hz, 1H), 3.69 (q, *J* = 7.2 Hz, 1 H), 3.94 (dd, *J* = 5.2, 17.6 Hz, 1 H), 4.04 (dd, *J* = 5.2, 17.4 Hz, 1 H), 4.54 (d, *J* = 15.6 Hz, 1 H), 4.81 (d, *J* = 16 Hz, 1 H), 5.08-5.26 (m, 2 H), 5.75-5.85 (m, 2 H), 7.18 (t, *J* = 8.8 Hz, 1 H), 8.11-8.16 (m, 2 H); ^{13}C NMR ($CDCl_3$): δ 19.72, 19.93, 21.85, 22.07, 23.61, 23.78, 33.90, 42.81, 42.85, 43.39, 46.49, 48.54, 49.90, 50.54, 50.89, 116.22, 116.46, 116.64, 116.88, 117.71, 118.19, 123.93, 124.74, 124.85, 125.26, 125.33, 126.40, 126.56, 132.16, 132.29,144.43,

162.88, 165.44, 176.95; HRMS (FAB): calcd for $C_{16}H_{23}FN_3O_5$ $[M+1]^+$ 324.1723, found 324.1703 (-6.3 ppm/-2.1 mmu). $[\alpha]^{22}_D$ (*S*-**8**) = - 53.4° (*c* 0.016, $CHCl_3$).

General procedures for the ring closure reactions

0.1-0.2 M of (*S*)-**6**, (*S*)-**7**, or (*S*)-**8** in DMSO was heated to 200°C for 30 minutes to 3 hours. After cooling to room temperature, the reaction mixture was partitioned between Et_2O (2 x 30 mL) and H_2O (30 mL). The ether layers were dried over Na_2SO_4, filtered, and evaporated to dryness to provide brown oily residue, which was then purified by flash column chromatography (CH_2Cl_2-EtOAc-Hexane: 7/2/1) on silica gel to afford the desired product.

Synthesis of (*S*)-*N*^{4}-allyl-2-methyl-10-nitro-tetrahydro-1,4-benzodiapin-3-one (*S*-9)

(*S*)-**6** (71.5 mg, 0.19 mmol) was dissolved in DMSO (1.9 mL) and heated to 200°C for 30 minutes. The title compound was obtained as yellow solid (32.5 mg, 67%) after the workup as described above. ^{1}H NMR (DMSO): δ 1.24 (d, *J* = 6.4 Hz, 3 H), 3.92-4.10 (m, 3 H), 5.04-5.14 (m, 2 H), 5.12 (d, *J* = 17.2 Hz, 1 H), 5.37 (d, *J* = 16.4 Hz, 1 H), 5.63-5.73 (m, 1 H), 6.65 (d, *J* = 9.2 Hz, 1 H), 7.20 (apparent d, *J* = 2.8 Hz, 1 NH), 7.85 (dd, *J* = 2.6, 9.0 Hz, 1 H), 7.92 (d, *J* = 2.8 Hz, 1 H); ^{13}C NMR (DMSO): δ 16.10, 48.51, 48.72, 49.22, 66.38, 114.77, 116.84, 118.48, 125.06, 126.30, 133.56, 135.40, 153.12, 169.44. HRMS (FAB): calcd for $C_{13}H_{16}N_3O_3$ $[M+1]^+$ 262.1192, found 262.1176 (-5.9ppm/-1.6mmu); HPLC (2:8 *i*-PrOH:Hexane, CHIRALPAK AD, 4.6 x 250 mm: 1.0

mL/min; UV detection at 254 nM): 15.52 min., 100 % ee; $[\alpha]^{22}_{D}$ (*S*-**9**) = - 528.8° (*c* 0.013, DMSO).

Synthesis of (*S*)-*N*^{4}-allyl-*N*^{1}-methyl-2-methyl-10-nitro-tetrahydro-1,4-benzodiapin-3-one (*S*-10)

(*S*)-**7** (1.28 mg, 3.23 mmol) was dissolved in DMSO (32 mL) and heated to 200°C for 3 hours. The title compound was obtained as yellow solid (814 mg, 92%) after the workup as described above. ^{1}H NMR ($CDCl_3$): δ 1.52 (d, *J* = 6.4 Hz, 3 H), 3.01 (s, 3 H), 3.04-4.19 (m, 2 H), 4.18 (d, *J* = 16.4 Hz, 1 H), 4.59 (q, *J* = 6.9 Hz, 1 H), 4.87 (d, *J* = 16.4 Hz, 1 H), 5.17-5.22 (m, 2 H), 5.67-5.76 (m, 1 H), 6.82 (d, *J* = 10 Hz, 1 H), 7.91 (d, *J* = 2.8 Hz, 1 NH), 8.06 (dd, *J* = 2.8, 9.2 Hz, 1 H); ^{13}C NMR ($CDCl_3$): δ 15.36, 36.80, 49.52, 50.85, 57.83, 117.02, 118.26, 123.23, 124.89, 125.44, 132.80, 138.54, 155.19, 169.60. HRMS (FAB): calcd for $C_{14}H_{18}N_3O_3$ $[M+1]^+$ 276.1348, found 276.1351 (+1.0 ppm/+0.3 mmu). HPLC (15:85 *i*-PrOH:Hexane, 4.6 x 250 mm: 1.0 mL/min; UV detection at 254 nM: 13.02 min., 100 % ee; $[\alpha]^{22}_{D}$ (*S*-**10**) = - 890.6° (*c* 0.014, $CHCl_3$).

Synthesis of (*S*)-*N*^{4}-allyl-*N*^{1}-isopropyl-2-methyl-10-nitro-tetrahydro-1,4-benzodiapin-3-one (*S*-11)

(*S*)-**8** (733 mg, 2.27 mmol) was dissolved in DMSO (15 mL) and heated to 200°C for 3 hours. The title compound was obtained as yellow solid (417 mg, 61%) after the workup as described above. ^{1}H NMR ($CDCl_3$): δ 1.19 (d, *J* = 6.8 Hz, 3 H), 1.37 (d, *J* = 6.8 Hz, 3 H), 1.41 (d, *J* = 7.2 Hz, 3 H), 3.69 (7-let, *J* = 6.8 Hz, 1 H), 4.00-4.06 (m, 2 H), 4.14-4.20 (m, 1 H), 4.42 (q, *J* = 7.2 Hz, 1 H), 4.43 (d, *J* = 15.6 Hz, 1 H), 4.54 (d, *J* = 16.4

Hz, 1 H), 5.18-5.23 (m, 2 H), 5.69-5.79 (m, 1 H), 6.99 (d, *J* = 9.2 Hz, 1 H), 7.94 (d, *J* = 2.8 Hz, 1 NH), 8.06 (dd, *J* = 2.6, 9.0 Hz, 1 H); ^{13}C NMR ($CDCl_3$): δ 17.29, 21.39, 22.30, 50.39, 51.06, 51.49, 56.33, 118.20, 119.55, 124.26, 125.08, 125.53, 132.69, 139.57, 153.48, 171.63. HRMS (FAB): calcd for $C_{16}H_{22}N_3O_3$ $[M+1]^+$ 304.1661, found 304.1659 (-0.7 ppm/-0.2 mmu). HPLC (1:99 *i*-PrOH:Hexane, CHIRALPAK AD, 4.6 x 250 mm: 2.0 mL/min; UV detection at 254 nM): 26.16 min., 100 % ee; $[\alpha]^{22}_D$ (*S*-**11**) = + 245.0° (*c* 0.015, $CHCl_3$).

General procedures for nitro group reduction[4]

Synthesis of (*S*)-*N*^{4}-allyl-10-amino-*N*^{1}-methyl-2-methyl-tetrahydro-1,4-benzodiapin-3-one (*S*-27)

To a mixture of (*S*)-**10** (829 mg, 3.01) and Fe powder (1.20 g, 21.4 mmol) was added CH_3OH (20 mL) and NH_4Cl (1.47g, 27.5 mmol) in 10.5 mL H_2O. The yellow suspension was heated to reflux for 3 hours under N_2. The hot reaction mixture with black precipitate was filtered off immediately and washed with hot CH_3OH (10 mL). The filtrate was evaporated to dryness and partitioned between CH_2Cl_2 (2 x 50 mL) and 10% $NaHCO_3$ (50 mL). The combined organic layers were dried over Na_2SO_4, filtered, and concentrated under vacuum to afford (*S*)-**27** as the light green solid (715 mg, 97% yield). The amine was immediately used next step without further purification.

Synthesis of (*S*)-N^4-allyl-10-amino-N^1-isopropyl-2-methyl-tetrahydro-1,4-benzodiapin-3-one (*S*-28)

(*S*)-**11** (109 mg, 0.37 mmol), Fe powder (141 mg, 2.52 mmol) and NH_4Cl (178 mg, 3.33 mmol) in 1.2 mL H_2O were treated as above to afford the desired amine (*S*)-**28** as green oil (93 mg, 92%). The amine was immediately used next step without further purification.

Synthesis of (*S*)-N^4-allyl-N^1-isopropyl-10-(*N,N*-dimethylamino)-2-methyl-tetrahydro-1,4-benzodiapin-3-one (*S*)-29[5]

To a mixture of formaldehyde (683 μL, 8.4 mmol) and first 2 equiv. of 3 M H_2SO_4 (0.7 mL, 2.1 mmol) at 0 °C was added a suspension of ***S*-28** (381 mg, 1.4 mmol) and $NaBH_4$ (370 mg, 9.77 mmol) dropwise. After the addition was complete, second 2 equiv. of 3 M H_2SO_4 (0.7 mL, 2.1 mmol) was added. The reaction mixture was stirred at 0 °C for 5 minutes. 10% NaOH was added to the reaction mixture until pH = 9. The reaction mixture was then partitioned between CH_2Cl_2 (2 x 30 mL) and H_2O (25 mL). The combined organic layers were dried over Na_2SO_4, filtered, and concentrated on vacuum to provide brown crude oil, which was then purified by flash column chromatography (CH_2Cl_2-CH_3OH: 98/2) on silica gel to afford the desired product **(*S*)-29** as yellow oil (394.7 mg, 94 %). ^{1}H NMR ($CDCl_3$): δ 1.04 (d, *J* = 6.4 Hz, 3 H), 1.10 (d, *J* = 7.2 Hz, 3 H), 1.25 (d, *J* = 6.4 Hz, 3 H), 2.90 (s, 6 H), 3.57 (7-let, *J* = 6.4 Hz, 1 H), 3.75 (d, *J* = 13.6 Hz, 1 H), 3.98 (dd, *J* = 6.0, 15.6 Hz, 1 H), 4.25 (q, *J* = 6.9 Hz, 1 H), 4.29 (dd, *J* = 5.4, 15.4 Hz, 1 H), 5.17-5.22 (m, 2 H), 5.75-5.85 (m, 1 H), 6.53 (d, *J* = 3.2 H, 1 H), 6.68 (d, *J* = 14.0 Hz, 1 H), 7.00 (d, J = 8.4 Hz, 1 H); ^{13}C NMR ($CDCl_3$): δ 16.45, 22.71,

22.76, 30.28, 41.06, 49.44, 51.44, 51.59, 58.37, 112.83, 112.88, 116.84, 125.06, 133.47, 133.59, 137.58, 146.80, 173.60. HRMS (FAB): calcd for $C_{18}H_{27}N_3O$ $[M+1]^+$ 301.2154, found 301.2145 (-3.0 ppm/-0.9 mmu); HPLC (5:95 *i*-PrOH:Hexane, CHIRALPAK AD, 4.6 x 250 mm: 1.0 mL/min; UV detection at 254 nM): 10.33 min., 99 % ee; $[\alpha]^{22}_D$ (*S*-**29**) = + 168.5° (*c* 0.015, $CHCl_3$).

Synthesis of (*S*)-N^4-allyl-N^1-isopropyl-10-phthalimido-2-methyl-tetrahydro-1,4-benzodiapin-3-one (*S*)-30[6]

Compound **27** (92.6 mg, 0.34 mmol) and phthalic anhydride (51 mg, 0.34 mmol) were combined in AcOH (3 mL), and heated to reflux for 1.5 hours. After cooling to room temperature, the reaction mixture was partitioned between CH_2Cl_2 (2 x 30 mL) and H_2O (25 mL). The combined organic layers were dried over Na_2SO_4, filtered, and evaporated to dryness to provide brown oily residue, which was then purified by flash column chromatography (CH_2Cl_2-EtOAc-Hexane: 7/2/1) on silica gel to afford the desired product (*S*)-**30** as yellow foamy solid (109.2 mg, 80 %). ^{1}H NMR ($CDCl_3$): δ 1.11 (d, *J* = 6.4 Hz, 3 H), 1.22 (d, *J* = 7.2 Hz, 3 H), 1.34 (d, *J* = 6.4 Hz, 3 H), 3.73 (7-let, *J* = 6.6 Hz, 1 H), 3.96-4.01 (m, 1 H), 4.00 (d, *J* = 14.8 Hz, 1 H), 4.24-4.27 (m, 1 H), 4.31 (q, *J* = 7.3 Hz, 1 H), 4.77 (d, *J* = 14.4 Hz, 1 H), 5.16-5.21 (m, 2 H), 5.73-5.82 (m, 1 H), 7.17-7.19 (m, 2 H), 7.31 (dd, *J* = 2.6, 8.6 Hz, 1 H), 7.76-7.80 (m, 1 H), 7.91-7.96 (m, 1 H); ^{13}C NMR ($CDCl_3$): δ 16.99, 22.40, 22.61, 50.27, 50.91, 50.98, 57.33, 117.48, 123.81, 123.64, 125.18, 126.36, 126.78, 130.91, 131.70, 133.10, 134.36, 147.90, 167.39, 172.73. HRMS (FAB): calcd for $C_{24}H_{26}N_3O_3$ $[M+1]^+$ 404.1974, found 404.1989 (+3.6 ppm/+1.4 mmu).

HPLC (2:8 *i*-PrOH:Hexane, CHIRALPAK AD, 4.6 x 250 mm: 1.0 mL/min; UV detection at 254 nM): 13.31 min., 98 % ee; $[\alpha]^{22}_{D}$ (*S*-**30**) = + 138.8° (*c* 0.020, $CHCl_3$).

General procedures for aromatic deamination[7]

Synthesis of (*S*)-*N*^{4}-allyl-*N*^{1}-methyl-2-methyl-tetrahydro-1,4-benzodiapin-3-one (*S*)-32

Compound **27** (192 mg, 0.78 mmol) was dissolved in a warm solution of H_2SO_4 (84 μL, 1.57 mmol) and AcOH (2 mL). After cooling to room temperature, $NaNO_2$ (81 mg, 1.17 mmol) in H_2O (1.2 mL) was added to in 15 minutes. After stirring at room temperature for additional 15 minutes, the reaction mixture was added to a suspension of Fe_2SO_4•$7H_2O$ (217 mg, 0.78 mmol) and DMF (11 mL). Gas evolution was observed and the reaction mixture was stirred at room temperature for 30 more minutes or until the cease of gas evolution. The reaction mixture was then partitioned between CH_2Cl_2 (3 x 30 mL) and NaOH (25 mL). The combined organic layers were dried over Na_2SO_4, filtered, and evaporated to dryness to provide brown oily residue, which was then purified by flash column chromatography (CH_2Cl_2-CH_3OH: 96/4) on silica gel to afford the desired product as brown oil (90 mg, 57%). ^{1}H NMR ($CDCl_3$): δ 1.30 (d, *J* = 7.2 Hz, 3 H), 2.85 (s, 3 H), 3.98-4.04 (m, 2 H), 4.01 (d, *J* = 15.2 Hz, 1 H), 4.20 (q, *J* = 6.9 Hz, 1 H), 4.79 (d, *J* = 15.2 Hz, 1 H), 5.16-5.22 (m, 2 H), 5.71-5.81 (m, 1 H), 6.89 (ddd, *J* = 0.9, 8.0, 7.6 Hz, 1 H), 6.99 (apparent dd, *J* = 1.0, 8.1 Hz, 1 H), 7.05 (apparent dd, *J* = 1.0, 7.4 Hz, 1 H), 7.25 (apparent ddd, *J* = 1.6, 7.6, 7.6 Hz, 1 H); ^{13}C NMR ($CDCl_3$): δ 14.82, 38.49, 50.33, 50.71, 60.67, 117.30, 120.77, 121.20, 128.42, 128.65, 128.72, 133.40,

150.10, 171.33. HRMS (FAB): calcd for $C_{14}H_{19}N_2O$ $[M+1]^+$ 231.1497, found 231.1490 (-3.2 ppm/-0.7 mmu); HPLC (3:97 *i*-PrOH:Hexane, CHIRALPAK AD, 4.6 x 250 mm: 1.0 mL/min; UV detection at 254 nM): 12.16 min., 100 % ee; $[\alpha]^{22}_D$ (*S*-**32**) = + 94.1° (*c* 0.005, $CHCl_3$).

Synthesis of (*S*)-*N*^{4}-allyl-*N*^{1}-isopropyl-2-methyl-tetrahydro-1,4-benzodiapin-3-one (*S*)-33

Compound **27** (350 mg, 1.28 mmol), H_2SO_4 (205 μL, 3.85 mmol) and AcOH (4 mL), $NaNO_2$ (132 mg, 1.92 mmol) and Fe_2SO_4•$7H_2O$ (354 mg, 1.28 mmol) in DMF (20 mL) were treated as above. The title compound was obtained as yellow solid (147 mg, 44%). ^{1}H NMR ($CDCl_3$): δ 1.08 (d, *J* = 6.4 Hz, 3 H), 1.14 (d, *J* = 7.2 Hz, 3 H), 1.32 (d, *J* = 6.4 Hz, 3 H), 3.69 (7-let, *J* = 6.5 Hz, 1 H), 3.89 (d, *J* = 14.4 Hz, 1 H), 3.95 (dd, J = 6.0, 15.6 Hz, 1 H), 4.30 (q, *J* = 6.5 Hz, 1 H), 4.30-4.35 (m, 1 H), 4.80 (d, *J* = 14.4 Hz, 1 H), 5.16-5.29 (m, 2 H), 5.74-5.84 (m, 1 H), 6.96 (apparent ddd, *J* = 1.1, 7.4, 7.4 Hz, 1 H), 7.09-7.13 (m, 1 H), 7.25 (apparent ddd, *J* = 1.6, 7.6, 7.8 Hz, 1 H); ^{13}C NMR ($CDCl_3$): δ 16.83, 22.59, 22.61, 49.89, 51.09, 51.11, 57.59, 117.07, 122.33, 123.28, 128.29, 128.75, 131.50, 133.29, 148.14, 172.98. HRMS (FAB): calcd for $C_{16}H_{23}N_2O$ $[M+1]^+$ 259.1810, found 259.1813 (+1.0 ppm/+0.3 mmu); HPLC (2:98 *i*-PrOH:Hexane, CHIRALPAK AD, 4.6 x 250 mm: 1.0 mL/min; UV detection at 254 nM) : 11.24 min., 99 % ee; $[\alpha]^{22}_D$ (*S*-**33**) = + 279.3° (*c* 0.006, $CHCl_3$).

Synthesis of (*S*)-N^1-isopropyl-N^4-propyl 2-methyl-tetrahydro-1,4-benzodiapin-3-one (*S*)-42[8]

Compound (*S*)-**33** (87 mg, 0.32 mmol) and 10% Pd/C (34 mg, 0.032 mmol) were combined in degassed CH_3OH (3 mL) and stirred under H_2 at room temperature for 2 hours. Pd/C was filtered off through celite. The filtrate was concentrated under reduced pressure to afford off-white solid as desired product (*S*)-**42** (87 mg, 100%). The desired product was pure by both NMR and TLC, no further purification step was required. ^{1}H NMR ($CDCl_3$): δ 0.90 (t, *J* = 7.2 Hz, 3 H), 1.06 (d, *J* = 6.8 Hz, 3 H), 1.13 (d, *J* = 6.8 Hz, 3 H), 1.31 (d, *J* = 6.4 Hz, 3 H), 1.60 (d, *J* = 7.1 Hz, 2 H), 3.33-3.40 (m, 1 H), 3.50-3.57 (m, 1 H), 3.68 (7-let, *J* = 6.5 Hz, 1 H), 3.90 (d, *J* = 14.4 Hz, 1 H), 4.26 (q, *J* = 6.9 Hz, 1 H), 4.86 (d, *J* = 14.0 Hz, 1 H), 6.9 (t, *J* = 7.4 Hz, 1 H), 7.08 (*J* = 7.4 Hz, 1 H), 7.25 (d, *J* = 7.2 Hz, 1 H), 7.22-7.26 (m, 1 H); ^{13}C NMR ($CDCl_3$): δ 11.27, 16.74, 21.06, 22.44, 22.76, 49.77, 50.71, 52.00, 57.40, 122.12, 123.21, 128.19, 128.53, 131.32, 148.05, 172.71. HRMS (FAB): calcd for $C_{16}H_{25}N_2O$ $[M+1]^+$ 261.1967, found 261.1979 (+4.7 ppm/+1.2 mmu); $[\alpha]^{22}_D$ (*S*-**42**) = + 207.9° (*c* 0.013, $CHCl_3$).

General procedures for Bundle's[9] oxidative deallylation

Synthesis of (*S*)-N^1-methyl-2-methyl-10-nitro-tetrahydro-1,4-benzodiapin-3-one (*S*-56)

To a solution of **10** (19.3 mg, 0.07 mmol) in dioxane (1 mL) and water (100 μL) was added a mixture of 4-methyl-morpholine *N*-oxide (24.6 mg, 0.21 mmol) and $K_2OsO_4 \bullet 2H_2O$ (2.06 mg, 0.0056 mmol) in *t*-BuOH (0.5 mL) followed by addition of a

suspension of $NaIO_4$ (44.9 mg, 0.21 mmol) in H_2O (0.5 mL). The mixture was stirred at 60 °C for 18 h and 90 °C for 6 h. After cooling to room temperature, the reaction mixture was diluted with brine (10 mL) and extracted with CH_2Cl_2 (2 x 15 mL). The combined organic layers were dried over Na_2SO_4, filtered and concentrated to provide brown liquid residue. Purification by preparative TLC (CH_2Cl_2-CH_3OH: 96/4) afforded the desired product as yellow solid (12.3 mg, 75%). ^{1}H NMR ($CDCl_3$): δ 1.43 (d, *J* = 6.8 Hz, 3 H), 3.01 (s, 3 H), 4.14 (dd, *J* = 7.2, 14.8 Hz, 1 H), 4.39 (q, *J* = 6.9 Hz, 1 H), 4.76 (dd, *J* = 4.0, 16.0 Hz, 1 H), 6.40 (s, br, 1 H), 6.92 (d, *J* = 9.2 Hz, 1 H), 7.96 (d, *J* = 2.8 Hz, 1 NH), 8.10 (dd, *J* = 3.2, 9.2 Hz, 1 H); ^{13}C NMR ($CDCl_3$): δ 14.51, 29.68, 37.68, 45.41, 58.50, 118.48, 124.67, 124.93, 125.73, 139.59, 155.29, 172.21. HRMS (FAB): calcd for $C_{11}H_{14}N_3O_3$ $[M+1]^+$ 236.1035, found 236.1053 (+7.6 ppm/+1.8 mmu).

Synthesis of (*S*)-*N*^{1}-isopropyl-10-(*N*,*N*-dimethylamino)-2-methyl-tetrahydro-1,4-benzodiapin-3-one (*S*-58)

Compound **29** (9.9 mg, 0.033 mmol), 4-methyl-morpholine *N*-oxide (12.0 mg, 0.099 mmol), K_2OsO_4•$2H_2O$ (1.2 mg, 0.0099 mmol in 0.5 mL *t*-BuOH) and $NaIO_4$ (21.2 mg, 0.099 mmol) were treated as above, except that the reaction mixture was heated to 60 °C for 6 h. The title compound was obtained as brown solid (5.5 mg, 64%). ^{1}H NMR ($CDCl_3$): δ 1.08 (d, *J* = 6.4 Hz, 6 H), 1.23 (d, *J* = 76.4 Hz, 3 H), 2.91 (s, 6 H), 3.58 (7-let, *J* = 6.3 Hz, 1 H), 3.67 (dd, *J* = 13.4 Hz, 1 H), 4.16 (q, *J* = 7.1 Hz, 1 H), 4.76 (d, *J* = 13.6 Hz, 1 H), 6.36 (apparent d, *J* = 6.4 Hz, 1 H), 6.57 (apparent d, *J* = 2.8 H, 1 H), 6.67 (d, *J* = 8.8 Hz, 1 H), 7.00 (d, J = 8.4 Hz, 1 H); ^{13}C NMR ($CDCl_3$): δ 16.15, 22.17, 23.36, 40.96, 46.07, 49.92, 58.13, 112.26, 112.54, 126.04, 135.88, 136.90, 147.32, 177.02.

HRMS (FAB): calcd for $C_{15}H_{23}N_3O$ $[M+1]^+$ 261.1841, found 261.1841 (-0.2 ppm/-0.1 mmu).

Synthesis of *N*-allyl-(2-fluoro-5-carbomethoxy)benzylamine (18)

4-Fluoro-3-methyl benzoic acid (1.01 mg, 6.56 mmol) and oxalyl chloride (700 μL, 7.87 mmol) with 2 drops of DMF were combined in CH_2Cl_2 (10 mL).[10] The suspension was stirred at room temperature under N_2 for 1 h, followed by addition of CH_3OH (2 mL). The resulting solution was stirred at room temperature for another 20 h. The reaction mixture was then partitioned between CH_2Cl_2 (50 mL) and H_2O (1 x 40 mL). The CH_2Cl_2 layer was dried over Na_2SO_4, filtered and concentrated under vacuum to afford 4-fluoro-3-methyl-methylbenzoate **14** as yellow solid (992 mg, 90 %), which was used immediately for NBS bromination without further purification. Compound **14** (combined from two separate reactions, 1.18 g, 7.01 mmol) and NBS (1.26 g, 7.01 mmol) were combined in CCl_4 (20 mL) and treated as in the synthesis of compound **2** to provide the crude product (1.52 g) as a mixture of mono-and di-brominated compounds. The % yield of compound 16 was calculated based on ^{1}H NMR integral. The desired compound 2-fluoro-5-carbomethoxybenzylbromide **16** was obtained as yellow oil (1.03 g, 59%). The crude mixture containing 1.03 g **16** (4.15 mmol) and allylamine (621 μL, 8.3 mmol) were combined in THF (20 mL) and treated as in the synthesis of compound **3**. The title compound **18** was obtained as yellow oil (748 mg, 81%). ^{1}H NMR ($CDCl_3$): δ 3.39 (d, J = 6.4 Hz, 2 H), 3.88 (s, 3H), 4.01 (s, 2H), 5.23-5.32 (m, 2H), 5.94-6.01 (m, 1H), 7.11, (t, J = 9.0 Hz, 1H), 7.96-8.00 (m, 1H), 8.19 (dd, J = 2.4, 7.2 Hz, 1H); ^{13}C NMR ($CDCl_3$): δ 44.59, 44.61, 50.43, 52.27, 115.62, 115.85, 119.55, 123.78, 123.94, 126.58, 126.61,

131.69, 131.79, 132.82, 133.04, 133.09, 162.80, 165.33, 165.90; HRMS (FAB): calcd for $C_{12}H_{15}FNO_2$ $[M+1]^+$ 224.1087, found 224.1093 (+2.8 ppm/+0.6 mmu).

Synthesis of (*S*)-N_α-Boc, *N*-allyl-*N*-(2-fluoro-5-carbomethoxybenzyl)alaninamide (*S*-20)

Compound **18** (748 mg, 3.35 mmol), DCC (830 mg, 4.02 mmol), HOBT (543 mg, 4.02 mmol)and Boc-(*S*)-Ala-OH (761 mg, 4.02mmol) were combined in CH_2Cl_2 (15 mL) and treated as in the synthesis of (*S*)-**6** to **8**. The title compound was obtained as yellow oil (1.26 g, 95%). ^{1}H NMR ($CDCl_3$): δ 1.30 (d, *J* = 6.4 Hz, 1 H), 1.35 (d, *J* = 6.8 Hz, 2 H), 1.43 (s, 9 H), 3.98 (apparent d, *J* = 4.8 Hz, 2 H), 4.50 (d, *J* = 15.2 Hz, 1 H), 4.59-4.70 (m, 1 H), 4.80 (d, *J* = 15.2 Hz, 1 H), 5.08-5.27 (m, 2 H), 5.38-5.46 (m, 1 H), 5.72-5.84 (m, 1 H), 7.09 (t, *J* = 9.0 Hz, 1 H), 7.84-8.01 (m, 2 H); ^{13}C NMR ($CDCl_3$): δ 19.34, 19.50, 28.26, 28.32, 42.36, 44.20, 46.21, 46.34, 48.03, 49.76, 52.24, 52.34, 77.20, 79.63, 115.51, 115.74, 115.84, 116.06, 117.84, 118.10, 124.28, 124.44, 126.66, 130.06, 131.09, 131.18, 131.52, 131.62, 131.73, 131.78, 131.86, 132.15, 155.07, 162.61, 165.14, 165.96, 173.70. HRMS (FAB): calcd for $C_{20}H_{28}FN_2O_5$ $[M+1]^+$ 395.1982, found 395.1963 (-4.9 ppm/- 1.9 mmu).

Ring closure of heterocyclic ring: (*S*)-N^4-allyl-10-carbomethoxy-2-methyl-tetrahydro-1,4-benzodiapin-3-one (*S*-21)

Compound **20** (1.26g, 3.19 mmol) was dissolved in CH_2Cl_2 (30 mL), followed by addition TFA (1 mL). The resulting mixture was stirred at room temperature for 1 h. Volatiles were evaporated under reduced pressure to provide brown liquid residue, which

was neturalized with 0.5 M NaOH (20 mL). The resulting free amine (884.8 mg, 3.01 mmol) that obtained after liquid-liquid partition was redissolved in DMSO (10 mL) and heated to 125 °C for 19 h. After cooling to room temperature, the reaction mixture was portioned between Et_2O (2 x 40 mL) and H_2O (30 mL). The combined organic layers were dried over Na_2SO_4, filtered and evaporated under reduced pressure to afford brown oily residue. Purification by column chromatography on silica gel, eluting with CH_2Cl_2-CH_3OH: 95/5 provided the title compound **21** as grey solid (178 mg, 22 %). ^{1}H NMR ($CDCl_3$): δ 1.42 (d, *J* = 6.4 Hz, 3 H), 3.82 (d, *J* = 14.8 Hz, 1 H), 3.84 (s, 3 H), 3.92 (apparent d, *J* = 3.2 Hz, 1 H), 4.31 (apparent dd, *J* = 5.6, 11.2 Hz, 1 H), 4.83-4.89 (m, 1 H), 5.15-5.21 (m, 2 H), 5.26 (d, *J* = 16.4 Hz, 1 H), 5.66-5.76 (m, 1 H), 6.44 (d, *J* = 7.6 Hz, 1 H), 7.58 (apparent d, *J* = 1.6 Hz, 1 NH), 7.69 (dd, *J* = 1.8, 8.2 Hz, 1 H); ^{13}C NMR ($CDCl_3$): δ 16.99, 42.62, 49.11, 49.67, 51.64, 115.31, 117.98, 118.02, 118.46, 130.80, 131.71, 133.01, 149.68, 166.79, 169.89; HRMS (FAB): calcd for $C_{15}H_{19}N_2O_3$ $[M+1]^+$ 275.1396, found 275.1393 (-0.7 ppm/- 0.3 mmu); HPLC (2:8 *i*-PrOH:Hexane, CHIRALPAK AD, 4.6 x 250 mm: 1.0 mL/min; UV detection at 254 nM): 9.08 min., 93 % ee.

General procedures for the formation of rearrangement products (40 and 46)

Formation of 40

To a solution of **33** (13.2 mg, 0.05 mmol) in dry THF (2 mL) at room temperature was added HMPA (54 μL, 0.31 mmol). The reaction mixture was then cooled to -78 °C,

followed by addition of LDA (1.5 M in cyclohexane, 68 μL, 0.102 mmol). The resulting orange mixture was stirred at -78 °C for 15 min. *n*-BuLi (2.5 M in hexanes, 41 μL, 0.102 mmol) was then added to it, and the reaction mixture was stirred at -78 °C for another 15 min. before the addition of EtI (42 μL, 0.51 mmol). The corresponding reaction mixture was stirred at -78 °C for further 1 h, followed by addition of $NH_4Cl_{(satd.)}$ (10 mL). The mixture was allowed to warm up to room temperature and diluted with CH_2Cl_2 (15 mL). The organic layer was dried over Na_2SO_4, filtered and evaporated under reduced pressure to afford brown oily residue. Purification on preparative TLC (EtOAc-CH_2Cl_2: 20/80) afforded the rearrangement product as yellow solid **40** (3.0 mg, 23 %). ^{1}H NMR ($CDCl_3$): δ 1.21 (d, *J* = 6.4 Hz, 6 H), 2.41 (s, 3 H), 3.63-3.68 (m, 1 H), 3.76 (apparent d, *J* = 6.0 Hz, 2 H), 4.50 (s, 2 H), 4.90 (s, br, 1 NH), 5.15-5.30 (m, 2 H), 5.68-5.77 (m, 1 H), 6.55-6.65 (m, 2 H), 7.00 (dd, *J* = 1.4, 7.4 Hz, 1 H), 7.19-7.23 (m, 1 H).

Formation of 46

Compound **42** (18.7 mg, 0.068 mmol), HMPA (71 μL, 0.41 mmol), LDA (227, μL, 0.34 mmol), *n*-BuLi (136 μL, 0.34 mmol) and EtI (55 μL, 0.68 mmol) were combined in THF (1 mL) and treated as above. The title compound **46** was obtained as yellow solid (3.1 mg, 17%). ^{1}H NMR ($CDCl_3$): δ 0.83 (t, *J* = 7.2 Hz, 3 H), 1.21 (d, *J* = 6.4 Hz, 6 H), 1.53-1.63 (m, 2 H), 2.43 (s, 3 H), 3.04-3.08 (m, 2 H), 3.65 (s, br, 1 H), 4.51 (s, 2 H), 4.83 (s, br, 1 NH), 6.56-6.65 (m, 2 H), 7.02 (dd, *J* = 1.4, 7.2 Hz, 1 H), 7.18-7.23 (m, 1 H); HRMS (FAB): calcd for $C_{16}H_{23}N_2O$ $[M]^+$ 259.1810, found 259.1823 (+6.0 ppm/+1.5 mmu);

6.2.2 (*S*)-Phenylalanine-derived tetrahydro-1,4-benzodiazepine-2-one project

(*S*)-Phenylalanine methyl ester hydrochloride was purchased from Aldrich. 2-Nitrobenzylbromide was obtained from ACROS. Both reagents were used without purification.

Synthesis of (*S*)-*N*-(2-nitrobenzylphenylalanine)methyl ester (*S*)-74[11]

To a solution of (*S*)-phenylalanine methyl ester hydrochloride (1.06 g, 4.90 mmol) and 2-nitrobenzylbromide **73** (1.06 g, 4.90 mmol) in DMF (10 mL) was added DIEA (1.75 mL, 9.80 mmol). The resulting reaction mixture was stirred at room temperature for 24 h. The volatiles were removed under reduced pressure to provide a yellow liquid residue, which was then partitioned between Et_2O (2 x 50 mL) and 10 % $NaHCO_3$ (1 x 50 mL). The combined Et_2O layers were dried over Na_2SO_4, filtered and evaporated under reduced pressure to afford yellow oily residue. Purification by column chromatography on silica gel, eluting with CH_2Cl_2-EtOAc-Hexane: 38/2/60 provided the title compound **74** as greenish yellow oil (1.31 g, 95 %). ^{1}H NMR ($CDCl_3$): δ 2.07 (s, br, 1 H), 2.91 (dd, *J* = 7.6, 13.6 Hz, 2 H), 2.99 (dd, *J* = 6.0, 13.6 Hz, 1 H), 3.48-3.51(m, 1 H), 3.66 (s, 3 H), 3.93 (d, *J* = 15.2 Hz, 1 H), 4.10 (d, *J* = 15.2 Hz, 1 H), 7.14-7.16 (m, 2 H), 7.20-7.30 (m, 3 H), 7.35-7.39 (m, 1 H), 7.44-7.51 (m, 2 H), 7.90 (dd, *J* = 1.2, 8.0 Hz, 1 H); ^{13}C NMR ($CDCl_3$): δ 39.73, 48.97, 51.76, 62.42, 124.67, 126.72, 127.88, 128.39, 129.19, 130.78, 133.01, 135.17, 137.13, 148.96, 174.65; HRMS (FAB): calcd for $C_{17}H_{19}N_2O_4$ $[M+1]^+$ 315.1345, found 315.1344 (-0.3 ppm/- 0.1 mmu).

General procedures for the preparation of (S)-75 and (S)-76

Synthesis of (*S*)-*N*-methyl-*N'*-(2-nitrobenzylphenylalanine)methyl ester (*S*)-75

To a solution of **74** (107 mg, 0.39 mmol) in DMF (5 mL) was added CH_3I (188 μl, 3.03 mmol) and DIEA (69 μl, 0.39 mmol). The resulting green reaction mixture was heated to 100 °C for 1.5 h. The volatiles were removed under reduced pressure to provide a brown liquid residue, which was then partitioned between Et_2O (2 x 40 mL) and 10 % $NaHCO_3$ (1 x 30 mL). The combined Et_2O layers were dried over Na_2SO_4, filtered and evaporated under reduced pressure to afford yellow oily residue. Purification by column chromatography on silica gel, eluting with CH_2Cl_2-EtOAc: 97/3 provided the title compound (*S*)-**75** as green oil (88 mg, 76 %). ^{1}H NMR ($CDCl_3$): δ 2.43 (s, 3 H), 2.89 (dd, *J* = 7.2, 14.0 Hz, 2 H), 3.11 (dd, *J* = 8.0, 13.6 Hz, 1 H), 3.55 (apparent t, *J* = 8.0 Hz, 1 H), 3.69 (s, 3 H), 4.03 (apparent d, *J* = 2.0 Hz, 1 H), 7.15-7.17 (m, 2 H), 7.19-7.29 (m, 3 H), 7.29-7.37 (m, 2 H), 7.40-7.45 (m, 1 H), 7.80-7.82 (m, 1 H); ^{13}C NMR ($CDCl_3$): δ 35.84, 37.54, 51.15, 55.96, 67.65, 124.36, 126.31, 127.75, 128.31, 129.14, 130.79, 132.46, 134.51, 138.24, 149.57, 171.98; HRMS (FAB): calcd for $C_{18}H_{21}N_2O_4$ $[M+1]^+$ 329.1501, found 329.1491 (-3.1 ppm/- 1.0 mmu).

Synthesis of (*S*)-*N*-allyl-*N'*-(2-nitrobenzylphenylalanine)methyl ester (*S*)-76

Compound **74** (132 mg, 0.49 mmol), allylbromide (342 μl, 3.92 mmol) and DIEA (86μl, 0.49 mmol) were combined in DMF (5 mL) and treated as above. The title compound (*S*)-**76** was obtained as green oil (118 mg, 75 %). ^{1}H NMR ($CDCl_3$): δ 2.94 (dd, *J* = 8.0, 14.0 Hz, 2 H), 3.10-3.18 (m, 2 H), 3.37-3.42 (m, 1H), 3.63 (t, *J* = 7.6 Hz, 1 H), 3.70 (s, 3 H), 4.03 (d, *J* = 16.4 Hz, 1 H), 4.22 (d, *J* = 16.4 Hz, 1 H), 5.09-5.19 (m, 2

H), 5.66-5.76 (m, 1 H), 7.12-7.14 (m, 2 H), 7.22-7.30 (m, 3 H), 7.32-7.41 (m, 3 H), 7.82-7.85 (m, 1 H); ^{13}C NMR ($CDCl_3$): δ 35.77, 51.27, 51.43, 54.04, 64.38, 117.80, 124.17, 126.35, 127.46, 128.25, 129.32, 130.67, 132.54, 134.99, 135.57, 138.19, 149.53, 172.45.

Synthesis of (*S*)-*N*^{4}-allyl-3-benzyl-tetrahydro-1,4-benzodiapin-2-one (*S*)-82

Compound (*S*)-**76** was reduced to corresponding primary amine by following the general procedures in the synthesis of (*S*)-**27**. Compound **76** (435 mg, 1.35 mmol), Fe powder (530 mg, 9.46 mmol), and NH_4Cl (650 mg, 12.16 mmol in 6.0 mL H_2O) were combined in CH_3OH (16 mL) and treated as described previously. The corresponding primary amine (*S*)-**80** was obtained as brown oil (385 mg, 98%). Compound (*S*)-**80** was used immediately in next step. To a solution of (*S*)-**80** (216 mg, 0.74 mmol) in CH_3CN (2.2 mL) was added 2 N NaOH (0.5 mL).[12] The resulting mixture was stirred at room temperature for 5 days. Volatiles were removed under reduced pressure to provide (*S*)-**81** as sodium salt (246 mg, 100%). No further purification was performed. Compound (*S*)-**81** (220 mg, 0.66 mmol), DCC (227 mg, 1.10 mmol) and HOBT (149 mg, 1.10 mmol) were combined in CH_2Cl_2 (10 mL) and treated as in the synthesis of (*S*)-**6** to **8**. The title compound (*S*)-**82** was obtained as yellow solid (148 mg, 77%). ^{1}H NMR ($CDCl_3$): δ 2.81 (dd, *J* = 7.6, 14.0 Hz, 2 H), 3.14-3.22 (m, 2 H), 3.31-3.36 (m, 1H), 3.70 (t, *J* = 7.6 Hz, 1 H), 3.87 (s, 3 H), 5.15-5.22 (m, 2 H), 5.72-5.82 (m, 1 H), 6.93 (d, *J* = 8.0 Hz, 1 H), 7.10-7.30 (m, 8 H), 8.42 (s, br, 1 H); ^{13}C NMR ($CDCl_3$): δ 36.65, 53.88, 55.93, 66.48, 118.07, 120.35, 124.71, 126.18, 128.13, 128.55, 129.10, 129.25, 130.26, 135.36, 137.12, 138.63, 173.33; HRMS (FAB): calcd for $C_{19}H_{21}N_2O$ $[M+1]^+$ 293.1654, found 293.1645 (-3.1 ppm/- 0.9 mmu).

Synthesis of (*S*)-N^4-allyl-3-benzyl-N^1-DAM-tetrahydro-1,4-benzodiapin-2-one (*S*)-83

Compound (*S*)-**82** (143 mg, 0.48 mmol) and NaH (60 wt% in oil, 23.2 mg, 0.58 mmol) were combined in THF (5 mL) and stirred at 0 °C for 30 min., followed by addition of DAM-Br (178 mg, 0.58 mmol) in THF (2 mL) dropwise. The resulting green suspension was stirred at 0 °C for 2 h. The excess NaH was quenched by H_2O (10 mL) at 0 °C. After the gas evolution was completed, the reaction mixture was partitioned between CH_2Cl_2 (2 x 30 mL) and H_2O (1 x 20 mL). The combined CH_2Cl_2 layers were dried over Na_2SO_4, filtered and evaporated under reduced pressure to afford yellow oily residue. Purification by column chromatography on silica gel, eluting with CH_2Cl_2-EtOAc: 9/1 provided the title compound (*S*)-**83** as yellow solid (181 mg, 72 %). ^{1}H NMR ($CDCl_3$): δ 2.75 (apparent d, *J* = 10.0 Hz, 1 H), 3.19-3.35 (m, 3 H), 3.46-3.48 (m, 2H), 3.65 –3.81 (m, 1 H), 3.71 (s, br, 3 H), 3.80 (s, br, 3 H), 6.62 (apparent d, *J* = 7.6 Hz, 2 H), 6.73 (apparent d, *J* = 7.6 Hz, 2 H), 6.83-6.93 (m, 5 H), 7.07-7.29 (m, 9 H); ^{13}C NMR ($CDCl_3$): δ 34.83, 54.22, 54.73, 55.08, 55.23, 63.04, 64.82, 113.23, 113.45, 113.77, 118.04, 123.67, 126.09, 127.71, 127.97, 128.21, 129.04, 129.54, 129.88, 130.76, 131.26, 135.85, 138.97, 141.11, 158.45, 158.55, 169.37; HRMS (FAB): calcd for $C_{34}H_{35}N_2O_3$ $[M+1]^+$ 519.2648, found 519.2661 (+2.6 ppm/+1.3 mmu).

6.2.3 (*S*)-Serine-derived 1,4-benzodiazepine-2-one project

Both Boc-(*S*)-serine and Boc-O-benzyl-(*S*)-serine were purchased from Advanced ChemTech, and used without purification. Boc-O-TBDMS-(*S*)-serine was synthesized from tert-butyldimethylsilyl chloride (TBDMSCl) and Boc-(*S*)-serine based on the

literature method.[13] 2-Amino-5-chloro-benzophenone was obtained from ACORS, and also used without purification.

Synthesis of N_α-Boc-O-benzyl-*N*-(2-benzoyl-4-chloro)phenyl serinamide (*S*-89)

To a solution of 2-amino-5-chlorobenzophenone **88** (1.74 g, 7.53 mmol) and Boc-O-benzyl-(*S*)-serine (2.02 g, 6.85 mmol) in THF (15 mL) was added DCC (1.55 g, 7.53 mmol) in 7.5 mL CH_2Cl_2 at 0 °C. The yellow mixture was allowed at warm up to room temperature at its own accord and stirred at room temperature for 18 h. White precipitate was filtered off and washed with cold CH_2Cl_2 (10 mL), and the filtrate was evaporated under reduced pressure to provide crude yellow oil. Purification by column chromatography on silica gel, eluting with CH_2Cl_2-EtOAc: 9/1 afforded the desired product as off-white solid (2.75 g, 79%). ^{1}H NMR ($CDCl_3$): δ 3.69 (dd, J = 4.4, 9.6 Hz, 1 H), 4.06 (apparent d, J = 7.2 Hz, 1 H), 4.43 (s, br, 1 H), 4.53 (apparent d, J = 4.2 Hz, 2 H), 5.56 (apparent d, J = 6.4 Hz, 1 H), 6.73 (apparent d, J = 7.6 Hz, 2 H), 7.24 (s, 5 H), 7.48-7.55 (m, 4 H), 7.63 (apparent tt J = 1.3, 7.4 Hz, 1 H), 7.68-7.70 (m, 2 H), 8.66 (d, J = 8.4 Hz, 1 H), 11.34 (s, 1 NH); ^{13}C NMR ($CDCl_3$): δ 28.24, 55.76, 69.52, 73.35, 80.56, 122.93, 125.17, 127.55, 127.64, 127.76, 128.35, 128.44, 128.57, 129.92, 132.42, 132.84, 133.67, 137.35, 137.77, 138.25, 169.83, 197.48; HRMS (FAB): calcd for $C_{28}H_{30}N_2O_5Cl$ $[M+1]^+$ 509.1843, found 5109.1828 (-3.0 ppm/-1.5 mmu).

Synthesis of N_α-Boc-O-(tert-butyldimethylsilyl)-*N*-(2-benzoyl-4-chloro)phenyl serinamide (*S*-97)

To make Boc-O-TBDMS-(*S*)-serine: to a solution of *N*-(tert-butoxycarbonyl)- (*S*)-serine (1.73 g, 8.44 mmol) in DMF (17 mL) under N_2 at 0 °C was added TBDMSCl (1.65 g, 10.97 mmol) and imidazole (1.72 g, 25.32 mmol). The reaction mixture was stirred at 0 °C for 1 h. The ice-bath was removed, and the reaction mixture was allowed to warm up to room temperature and stirred at room temperature for another 24 h. The reaction mixture was then partitioned between Et_2O (2 x 50 mL) and H_2O (1 x 40 mL). The combined Et_2O layers were dried over Na_2SO_4, filtered and evaporated under reduced pressure to afford pale yellow residue. Purification by column chromatography on silica gel, eluting with CH_2Cl_2-EtOAc: 4/1 (with 7 mL of AcOH per liter of solvent) provided Boc-O-TBDMS-(*S*)-serine as colorless oil (2.15 g, 92 %, lit. 85%). Boc-O-TBDMS-(*S*)-serine was used immediately in the next step. The general coupling procedures for the synthesis of *S*-**89** was followed for the preparation of *S*-**97**: 2-amino-5-chlorobenzophenone **88** (689 mg, 2.97 mmol) and Boc-O-TBDMS-(*S*)-serine (862.3 g, 2.70 mmol) and DCC (613 mg, 2.97 mmol in 4.0 mL CH_2Cl_2) in THF (9 mL) were combined and treated as described above. The title compound was obtained as white foamy solid (892 mg, 62%). ^{1}H NMR ($CDCl_3$): δ -0.022 (s, 3 H), 0.021 (s, 3 H), 0.78 (s, 9 H), 3.81 (dd, *J* = 4.2, 10.2 Hz, 1 H), 4.21 (apparent d, *J* = 4.8 Hz, 1 H), 4.30 (s, br, 1 H), 5.53 (apparent d, *J* = 4.2 Hz, 2 H), 5.56 (apparent d, *J* = 6.4 Hz, 1 H), 6.73 (apparent d, *J* = 5.2 Hz, 2 H), 7.24 (s, 5 H), 7.48-7.54 (m, 4 H), 7.59-7.63 (m, 1 H), 7.68 (d, *J* = 7.2 Hz, 2 H), 8.66 (d, *J* = 8.8 Hz, 1 H), 11.31 (s, 1 NH); ^{13}C NMR ($CDCl_3$): δ -5.57, -5.53, -0.026, 18.44, 25.58, 28.26, 57.55, 63.38, 80.50, 122.83, 125.01, 127.46, 128.41, 129.90,

132.47, 132.81, 133.73, 137.83, 138.28, 155.54, 170.19, 197.58; LRMS (FAB): calcd for $C_{27}H_{38}N_2O_5ClSi$ $[M+1]^+$ 533, found 533.

Synthesis of (*S*)-3-benzyloxymethyl)-10-chloro-5-phenyl-1,4-benzodiazepin-2-one (*S*-90)

To a solution of *S*-**89** (557 mg, 1.10 mmol) in CH_2Cl_2 (10 mL) was added TFA (1 mL). The resulting solution was stirred at room temperature for 1 h. Volatiles were removed under reduced pressure to provide yellow residue, which was immediately redissolved in CH_3OH-H_2O (10 mL: 5 mL), and the pH was adjusted to pH 8.5-9.0 with 10 % NaOH. The yellow mixture was stirred at room temperature for 65 h. Solvent was removed under reduced pressure and the yellow residue was partitioned between CH_2Cl_2 (2 x 50 mL) and H_2O (1 x 40 mL). The combined CH_2Cl_2 layers were dried over Na_2SO_4, filtered and evaporated under reduced pressure to afford yellow oil. Purification by column chromatography on silica gel, eluting with CH_2Cl_2-EtOAc: 9/1 provided the title compound as white foamy solid (328 mg, 76 %). ^{1}H NMR ($CDCl_3$): δ 3.86 (t, *J* = 6.4 Hz, 1 H), 4.21 (dd, *J* = 6.2, 9.4 Hz, 1 H), 4.45 (dd, *J* = 6.6, 9.4 Hz, 1 H), 4.71 (s, 2 H), 7.08 (d, *J* = 8.4 Hz, 1 H), 7.28-7.49 (m, 9 H), 7.53-7.55 (m, 2 H), 8.97 (s, 1 NH); ^{13}C NMR ($CDCl_3$): δ 63.41, 70.29, 73.69, 122.90, 126.94, 127.54, 127.63, 127.80, 128.33, 128.35, 128.47, 128.75, 128.82, 129.71, 130.39, 130.60, 131.75, 136.88, 138.41, 140.86, 168.62, 170.81; HRMS (FAB): calcd for $C_{23}H_{20}N_2O_2Cl$ $[M+1]^+$ 391.1213, found 391.1188 (-6.5 ppm/-2.5 mmu).

Synthesis of (*S*)-3-(tert-butyldimethylsilyloxymethyl)-10-chloro-5-phenyl-1,4-benzodiazepin-2-one (*S*-98)

To a solution of *S*-**97** (2.79 mg, 5.24 mmol) in CH_2Cl_2 (30 mL) was added TFA (4 mL). The resulting solution was stirred at room temperature for 1 h. Volatiles were removed under reduced pressure to provide yellow residue, which was immediately redissolved in CH_3OH-H_2O (30 mL: 15 mL), and the pH was adjusted to pH 7 with 10 % NaOH. The yellow mixture was heated to 40 °C for 22 h. Solvent was removed under reduced pressure and the yellow residue was partitioned between CH_2Cl_2 (2 x 50 mL) and H_2O (1 x 40 mL). The combined CH_2Cl_2 layers were dried over Na_2SO_4, filtered and evaporated under reduced pressure to afford yellow oil. Purification by column chromatography on silica gel, eluting with CH_2Cl_2-EtOAc: 9/1 (with 7 mL of AcOH per liter of solvent) provided the title compound as white foamy solid (1.30 g, 60 %). ^{1}H NMR ($CDCl_3$): δ 0.16 (s, 3 H), 0.18 (s, 3 H), 0.95 (s, 9 H), 3.74 (t, *J* = 6.6 Hz, 1 H), 4.29 (dd, *J* = 6.4, 10.0 Hz, 1 H), 4.58 (dd, *J* = 6.8, 10.4 Hz, 1 H), 7.13 (d, *J* = 8.4 Hz, 1 H), 7.31 (d, *J* = 2.0 Hz, 1 H), 7.36-7.40 (m, 2 H), 7.43-7.48 (m, 2 H), 7.51-7.53 (m, 2 H), 9.06 (s, 1 NH); ^{13}C NMR ($CDCl_3$): δ -5.25, -5.17, 18.48, 25.96, 63.30, 65.08, 123.05, 128.38, 128.77, 129.96, 130.63, 132.01, 137.16, 170.63; HRMS (FAB): calcd for $C_{22}H_{28}N_2O_2ClSi$ $[M+1]^+$ 415.1609, found 415.1629 (+4.9 ppm/+2.0 mmu).

Synthesis of (*S*)-3-benzyloxylmethyl-10-chloro-*N*^{1}-DAM-5-phenyl-1,4-benzodiazepin-2-one (*S*-99)

General procedures for the synthesis of (*S*)-**83** are followed: (*S*)-**90** (169 mg, 0.43 mmol), NaH (60 wt% in oil, 21 mg, 0.52 mmol) and DAM-Br (160 mg, 0.52 mmol) were

combined in THF (5 mL) and treated as described previously. The title compound (*S*)-**99** was obtained as off-white foamy solid (134 mg, 51 %). ^{1}H NMR ($CDCl_3$): δ 3.76 (s, 3 H), 3.84 (s, 3 H), 4.03 (t, *J* = 6.4 Hz, 1 H), 4.25 (dd, *J* = 6.4, 9.6 Hz, 1 H), 4.50 (dd, *J* = 6.4, 9.6 Hz, 1 H), 4.71 (d, *J* = 4.2 Hz, 2 H), 6.63 (d, *J* = 8.4 Hz, 2 H), 6.90 (d, *J* = 3.2 Hz, 2 H), 6.93 (d, *J* = 2.8 Hz, 2 H), 7.02 (s, br, 1 H), 7.04 (d, *J* = 2.0 Hz, 1 H), 7.13 (dd, *J* = 2.4, 8.8 Hz, 1 H), 7.18 (d, *J* = 9.2 Hz, 1 H), 7.25-7.30 (m, 8 H), 7.32-7.40 (m, 5 H), 7.45 (apparent t, *J* = 7.4 Hz, 1 H); ^{13}C NMR ($CDCl_3$): δ 55.16, 55.23, 55.30, 63.69, 64.24, 70.92, 73.87, 75.26, 113.57, 113.74, 113.85, 126.07, 127.59, 127.69, 127.95, 128.16, 128.34, 128.86, 129.05, 129.45, 129.93, 130.05, 130.20, 130.24, 130.59, 131.24, 133.03, 137.03, 137.60, 138.38, 139.35, 158.71, 158.95, 167.76, 168.73; HRMS (FAB): calcd for $C_{38}H_{34}N_2O_4Cl$ $[M+1]^+$ 617.2207, found 617.2222 (+2.5 ppm/+1.5 mmu).

Synthesis of (*S*)-3-(tert-butyldimethylsilyloxymethyl)-10-chloro-*N*^{1}-DAM-5-phenyl-1,4-benzodiazepin-2-one (*S*-100)

General procedures for the synthesis of (*S*)-**83** are followed: (*S*)-**98** (164 mg, 0.40 mmol), NaH (60 wt% in oil, 32 mg, 0.80 mmol) and DAM-Br (246 mg, 0.80 mmol) were combined in THF (5 mL) and treated as described previously. The title compound (*S*)-**100** was obtained as white foamy solid (133 mg, 52 %). ^{1}H NMR ($CDCl_3$): δ 0.15 (s, 3 H), 0.16 (s, 3 H), 0.92 (s, 9 H), 3.76 (s, 3 H), 3.84 (s, 3 H), 3.89 (s, 2 H), 3.93 (t, *J* = 6.4 Hz, 1 H), 4.29 (dd, *J* = 6.2, 10.4 Hz, 1 H), 4.66 (dd, *J* = 7.0, 9.8 Hz, 1 H), 4.71 (d, *J* = 4.2 Hz, 2 H), 6.63 (d, *J* = 8.4 Hz, 2 H), 6.91-6.93 (m, 3 H), 6.96 (d, *J* = 8.4 Hz, 2 H), 7.06-7.07 (m, 2 H), 7.13 (dd, *J* = 2.4, 8.8 Hz, 1 H), 7.20 (d, *J* = 8.8 Hz, 1 H), 7.24-7.29 (m, 4 H), 7.35 (t, *J* = 7.6 Hz, 2 H), 7.45 (apparent t, *J* = 7.4 Hz, 1 H), 7.79 (d, *J* = 7.6 Hz, 1 H);

^{13}C NMR ($CDCl_3$): δ -5.26, -5.18, 18.39, 25.93, 55.19, 55.33, 55.45, 63.23, 63.80, 66.16, 113.43, 113.54, 113.81, 126.01, 128.19, 128.85, 129.01, 129.41, 129.88, 130.08, 130.14, 130.54, 131.33, 132.22, 133.06, 137.78, 139.39, 140.61, 158.68, 158.92, 162.81, 167.67, 168.68; HRMS (FAB): calcd for $C_{37}H_{42}N_2O_4ClSi$ $[M+1]^+$ 641.2602, found 641.2601 (-0.3 ppm/-0.2 mmu).

Synthesis of (*S*)-*N*^{1}-isopropyl 3-(tert-butyldimethylsilyloxymethyl) -10-chloro- 5-phenyl-1,4-benzodiazepin-2-one (*S*-101)

To make isopropyl triflate (i-PrOTf): to a solution of isopropanol (500 μL, 6.33 mmol) and pyridine (520 μL, 6.33 mmol) in CH_2Cl_2 (10 mL) at 0 °C was added triflate anhydride (3.2 mL, 18.99 mmol). The resulting pink solution with white precipitate was stirred at 0 °C for 45 min. The white precipitate was filtered off and the volatile of filtrate was removed by rotary evaporator (water bath temperature < 40 °C). The pink solution of was used immediately in next step. General procedures for the synthesis of (*S*)-**83** are followed: (*S*)-**98** (417 mg, 1.01 mmol), NaH (60 wt% in oil, 202 mg, 5.04 mmol) and i-PrOTf (1.22 g, 6.33 mmol) were combined in THF (10 mL) and treated as described previously. The title compound (*S*)-**101** was obtained as yellow oil (310 mg, 67 %). ^{1}H NMR ($CDCl_3$): δ 0.14 (s, 3 H), 0.11 (s, 3 H), 0.92 (s, 9 H), 1.15 (d, *J* = 6.4 Hz, 1 H), 1.18 (d, *J* = 7.2 Hz, 3 H), 1.47 (d, *J* = 6.8 Hz, 3 H), 3.67 (t, *J* = 6.4 Hz, 1 H), 4.30 (dd, *J* = 7.2, 10.4 Hz, 1 H), 4.55 (7-let, *J* = 7.0 Hz, 1 H), 4.53 (dd, *J* = 6.2, 10.2 Hz, 1 H), 7.27 (d, *J* = 2.4 Hz, 1 H), 7.36-7.49 (m, 5 H), 7.59-7.62 (m, 2 H); ^{13}C NMR ($CDCl_3$): δ -5.30, -5.16, 18.49, 20.51, 22.15, 22.28, 25.97, 26.61, 29.62, 50.95, 63.08, 64.03, 66.39, 67.99, 125.42, 128.46, 129.28, 129.33, 130.31, 130.55, 132.86, 138.03, 140.18, 167.17,

168.80; HRMS (FAB): calcd for $C_{25}H_{34}N_2O_2ClSi$ $[M+1]^+$ 457.2078, found 457.2062 (-3.5 ppm/-1.6 mmu).

Synthesis of (*S*)-10-chloro-*N*^{1}-DAM-3-(hydroxymethyl)-5-phenyl-1,4-benzodiazepin-2-one (*S*-104)

To a solution of (*S*)-**100** (677 mg, 1.06 mmol) in THF (10.6 mL) under N_2 at room temperature was added tetrabutylammonium fluoride[14] (5.3 mL, 5.29 mmol) dropwise. The resulting orange mixture was stirred at room temperature under N_2 for 1 h. The volatile was removed under reduced pressure and the brown residue was partitioned between CH_2Cl_2 (2 x 40 mL) and H_2O (1 x 30 mL). The combined CH_2Cl_2 layers were dried over Na_2SO_4, filtered and evaporated under reduced pressure to afford brown oil. Purification by column chromatography on silica gel, eluting with CH_2Cl_2-EtOAc: 9/1 (with 7 mL of AcOH per liter of solvent) provided the title compound as yellow foamy solid (511mg, 92 %). ^{1}H NMR ($CDCl_3$): δ 2.87 (t, *J* = 7.2 Hz, 1 H), 4.30 (dd, *J* = 7.2, 10.4 Hz, 1 H), 3.76 (s, 3 H), 3.84 (s, 3 H), 3.96 (dd, *J* = 4.2, 7.6 Hz, 1 H), 4.19-4.25 (m, 1 H), 4.48-4.54 (m, 1 H), 6.63-6.67 (m, 1 H), 6.64 (d, *J* = 8.8 Hz, 1 H), 6.90-6.96 (m, 2 H), 6.94 (d, *J* = 8.8 Hz, 1 H), 6.98 (s, br, 1 H), 7.15 (dd, *J* = 2.6, 9.0 Hz, 1 H), 7.20 (s, 1 H), 7.22-7.30 (m, 4 H), 7.36 (apparent t, *J* = 7.6 Hz, 2 H), 7.47 (dd, *J* = 1.5, 7.4 Hz, 1 H); ^{13}C NMR ($CDCl_3$): δ 55.20, 55.33, 63.03, 63.99, 64.59, 113.63, 113.95, 126.09, 128.25, 128.78, 129.05, 129.42, 129.88, 129.91, 130.09, 130.45, 130.77, 131.25, 133.06, 137.53, 139.04, 158.80, 159.03, 168.31, 170.41; HRMS (FAB): calcd for $C_{31}H_{28}N_2O_4Cl$ $[M+1]^+$ 527.1738, found 527.1735 (-0.5 ppm/-0.2 mmu).

Synthesis of (*S*)-10-chloro-N^1-DAM-5-phenyl-3-(tosylatemethyl)-1,4-benzodiazepin-2-one (*S*-105)

To a solution of (*S*)-**104** (491 mg, 0.93 mmol), DMAP (137 mg, 1.12 mmol), and TsCl (1.06 g, 5.58 mmol) in CH_2Cl_2 (10 mL) at 0 °C was added Et_3N (790 μL, 5.58 mmol).[15] The ice-bath was removed and the resulting mixture was then stirred at room temperature for 1 h. The volatile was removed under reduced pressure and the brown residue was partitioned between CH_2Cl_2 (2 x 40 mL) and H_2O (1 x 30 mL). The combined CH_2Cl_2 layers were dried over Na_2SO_4, filtered and evaporated under reduced pressure to afford brown oil. Purification by column chromatography on silica gel, eluting with CH_2Cl_2-EtOAc: 97/3 provided the title compound (*S*)-**105** as yellow foamy solid (555mg, 88 %). ^{1}H NMR ($CDCl_3$): δ 2.41 (s, 3 H), 3.75 (s, 3 H), 3.85 (s, 3 H), 4.11 (dd, *J* = 5.6, 11.2 Hz, 1 H), 4.77 (dd, *J* = 7.2, 10.0 Hz, 1 H), 4.89 (dd, *J* = 5.6, 10.4 Hz, 1 H), 6.60-6.63 (m, 1 H), 6.62 (d, *J* = 8.8 Hz, 1 H), 6.86 (d, *J* = 8.8 Hz, 2 H), 6.92-6.95 (m, 1 H), 6.93 (d, *J* = 8.8 Hz, 2 H), 7.04 (apparent d, *J* = 1.2 Hz, 1 H), 7.18-7.23 (m, 5 H), 7.32-7.36 (m, 4 H), 7.46 (apparent t, *J* = 7.2 Hz, 1 H), 7.86 (d, *J* = 8.8 Hz, 2 H); ^{13}C NMR ($CDCl_3$): δ 21.66, 29.68, 55.18, 55.33, 62.75, 63.96, 70.46, 113.64, 113.92, 126.20, 128.12, 128.21, 128.82, 129.17, 129.48, 129.69, 129.83, 129.89, 130.33, 130.74, 130.91, 131.21, 132.76, 137.16, 138.94, 144.79, 158.82, 159.07, 167.62, 168.27; HRMS (FAB): calcd for $C_{38}H_{34}N_2O_6ClS$ $[M+1]^+$ 681.1826, found 681.1807 (-2.8 ppm/-1.9 mmu).

Synthesis of N^1-isopropyl-10-chloro-3-methylene-5-phenyl-1,4-benzodiazepin-2-one (103)

To a solution of (*S*)-**101** (19.7 mg, 0.043 mmol) and HMPA (46 μL, 0.26 mmol) in THF (1 mL) at -78 °C was added KHMDS (350 μL, 0.17 mmol). The resulting orange mixture was then stirred at -78 °C for 30 min. The reaction was then quenched by saturated NH_4Cl (10 mL) and partitioned between CH_2Cl_2 (2 x 10 mL) and H_2O (1 x 10 mL). The combined CH_2Cl_2 layers were dried over Na_2SO_4, filtered and evaporated under reduced pressure to afford brown oil. Purification by preparative TLC (CH_2Cl_2-EtOAc-Hexane: 50/49/1 provided the title compound **103** as yellow solid (7.7mg, 55 %). ^{1}H NMR ($CDCl_3$): δ 1.28 (d, *J* = 6.8 Hz, 3 H), 1.57 (d, *J* = 6.8 Hz, 3 H), 4.49 (7-let, *J* = 7.0 Hz, 1 H), 4.82 (s, 1 H), 5.09 (s, 1 H), 7.26 (apparent t, *J* = 2.0 Hz, 1 H), 7.37 (d, *J* = 8.4 Hz, 1 H), 7.42-7.47 (m, 3 H), 7.52 (apparent tt, *J* = 1.6, 7.2 Hz, 1 H), 7.71-7.73 (m, 2 H); ^{13}C NMR ($CDCl_3$): δ 20.60, 22.35, 51.72, 104.46, 125.44, 128.52, 129.29, 129.45, 130.16, 130.62, 131.18, 133.08, 137.04, 139.51, 149.70, 165.43, 169.60; HRMS (FAB): calcd for $C_{19}H_{18}N_2OCl$ $[M+1]^+$ 325.1108, found 325.1093 (-4.5 ppm/-1.5 mmu).

Synthesis of 10-chloro-N^1-DAM-3-methylene-5-phenyl-1,4-benzodiazepin-2-one (106)

To a solution of (*S*)-**105** (22.1 mg, 0.033 mmol) and HMPA (34 μL, 0.20 mmol) in THF (2 mL) at -45 °C was added KHMDS (163 μL, 0.081 mmol). The resulting orange mixture was then stirred at -45 °C for 2 h. The reaction was then quenched by saturated NH_4Cl (10 mL) and partitioned between CH_2Cl_2 (2 x 10 mL) and H_2O (1 x 10 mL). The combined CH_2Cl_2 layers were dried over Na_2SO_4, filtered and evaporated

under reduced pressure to afford brown oil. Purification by column chromatography on silica gel, eluting with CH_2Cl_2-EtOAc: 9/1 provided the title compound **106** as yellow solid (13.1mg, 79 %). ^{1}H NMR ($CDCl_3$): δ 3.77 (s, 3 H), 3.85 (s, 3 H), 4.91 (s, 1 H), 5.22 (s, 1 H), 6.67 (d, *J* = 8.4 Hz, 2 H), 6.87 (s, br, 1 H), 6.94 (d, *J* = 8.4 Hz, 2 H), 7.01 (d, *J* = 8.8 Hz, 2 H), 7.04 (d, *J* = 2.4 Hz, 1 H), 7.10 (dd, *J* = 2.8, 8.8 Hz, 1 H), 7.19 (d, *J* = 8.8 Hz, 1 H), 7.26 (d, *J* = 8.4 Hz, 2H), 7.40-7.43 (m, 4 H), 7.49-7.61 (m, 1 H); ^{13}C NMR ($CDCl_3$): δ 55.21, 55.33, 64.91, 104.91, 113.61, 113.83, 126.44, 128.33, 128.95, 129.05, 129.55, 129.93, 130.01, 130.11, 131.12, 131.17, 133.44, 137.03, 138.71, 149.19, 158.73, 159.00, 165.96, 169.41; HRMS (FAB): calcd for $C_{31}H_{26}N_2O_3Cl$ $[M+1]^+$ 509.1632, found 509.1602 (-5.9 ppm/-3.0 mmu).

References for chapter 6

1 Schutkowski, M.; Mrestani-Klaus, C.; Neubert, K. Synthesis of dipeptide 4-nitroanilides containing non-proteinogenic amino acids. *Int. J. Pept. Protein Res.* **1995,** *45,* 257-265.

2 Ohfune, Y.; Kurokawa, N.; Higuchi, N.; Saito. M.; Hashimoto, M.; Tanaka, T. An efficient one-step reductive *N*-monoalkylation of α-amino acids. *Chem. Lett.* **1984,** 441-444.

3 Hart, B. R.; Rush, D. J.; Shea, K. J. Discrimination between Enantiomers of Structurally Related Molecules: Separation of Benzodiazepines by Molecularly Imprinted Polymers. *J. Am. Chem. Soc.* **2000,** *122,* 460-465.

4 Wissner, A.; Overbeek, E.; Reich, M. F.; Floyd, M. B.; Johnson, B. D.; Mamuya, N.; Rosfjord, E. C.; Discafani, C.; Shi, X.-Q.; Rabindran, S. K.; Gruber, B. C.; Ye, F.; Hallett, W. A.; Nilakantan, R.; Shen, R.; Wang, Y.-F.; Greenberger, L. M.; Tsou, H.-R. Synthesis and Structure-Activity Relationship of 6,7-Disubstituted 4-Anilinoquinoline-3carbonitriles. The design of an Orally Active, Irreversible Inhibitor of the Tyrosine Kinase Activity of the Epidermal Growth Factor Receptor (EGFR) and the Human Epidermal Growth Factor Receptor-2 (HER-2) *J. Med. Chem*. **2003**, *46*, 49-63.

5 Giumanini, A. G.; Chiavari, G.; Gusiani, M. M.; Rossi, P. *N*-Permethylation of Primary and Secondary Aromatic Amines. *Synthesis*, **1980**, 743-746.

6 Perry, C. J.; Parveen, Z. The cyclisation of substituted phthalanilic acids in acetic acid solution. A kinetic study of substituted N-phenylphthalimide formation. *J. Chem. Soc., Perkin Trans*. **2001**, *2*, 512-521.

7 Wassmundt, F. M.; Kiesman, W. F. Efficient Catalytic of Hydrodediazoniations in Dimethylformamide. *J. Org. Chem.* **1995,** *60,* 1713-1719.

8 Lubell, W.; Rapoport, H. Surrogates for Chiral Aminomalondialdehyde. Synthesis of *N*-(9-Phenylfluoren-9-yl) and *N*-(9-Phenylfluoren-9-yl)vinylglycianl. *J. Org. Chem.* **1989,** *54,* 3824-3831.

9 Kitov, P. I.; Bundle, D. R. Mild Oxidative One-Pot Allyl Group Cleavage. *Org. Lett.* **2001,** *3,* 2835-2838.

10 Petersen, L.; Jensen, K. J. A New, Efficient Glycosylation Method for Oligosaccharide Synthesis under Neutral Conditions: Preparation and Use of New DISAL Donors.*J. Org. Chem.* **2001,** *66,* 6268-6275.

11 Wu. Z.; Ercole, F.; FitzGerald, M.; Perera, S.; Riley, P.; Campbell, R.; Pham, Y.; Rea, P.; Sandanayake, S.; Mathieu, M. N.; Bray, A. M.; Ede, N. J. Synthesis of Tetrahydro-1,4-benzodiazepine-2-ones on Hydrophilic Polyamide SynPhase Lanterns *J. Com. Chem.* **2003**, *5,* 166-171.

12 Cheguillaume, A.; Salaün, A.; Sinbandhit, S.; Potel, M.; Gall, P.; Gaudy-Floćh, M.; Le Grel, P. Solution synthesis and characterization of aza-beta(3)-peptides (N(alpha)-substituted hydrazino acetic acid oligomers). *J. Org. Chem.* **2001,** *66,* 4923-4929.

13 Yoo, D.-W.; Oh, J. S.; Lee, D. -W.; Kim, Y.-G. Efficient Synthesis of a Configurationally Stable L-Serinal Derivatives. *J. Org. Chem***. 2003,** *68,* 2979-2982.

14 Scheidt, K. A.; Chen, H.; Fellows, B. C.; Chemler, S. R.; Coffey, D. S.; Roush, W. R. Tris(dimethylamino)sulfonium Difluorotrimethylsilicate (TAS-F), a Mild Reagent for the Removal of Silicon Protecting Groups. *J. Org. Chem.* **1998,** *63,* 6436.

15 Langenhan, J. M.; Gellman, S. H. Preparation of Protected syn-α,β-Dialkyl-β-Amino Acids That Contain Polar Side Chain Functionality. *J. Org. Chem.* **2003**, *68,* 6440-6443.